AN ABSTRACT OF THE THESIS OF

Brian D. Jones for the degree of Doctor of Philosophy in Chemistry presented on April 30, 1999.

Title: Applications of Redox Indicators for Evaluating Redox Conditions in Environmental Samples

Redacted for privacy

Abstract approved: _____

James D. Ingle, Jr.

Redox sensors based on immobilized redox indicators have been developed and characterized as to their applicability for evaluating environmental redox conditions. Unique methodology was developed to immobilize indicators to both agarose films and cellulose filter papers, allowing contact of the indicator with both dissolved and adsorbed redox-active species and microbes in environmental samples. The agarose films are placed in a novel flow cell allowing the absorbance of the indicator to be monitored continually while an environmental sample (e.g., groundwater or wastewater slurry) is pumped through the cell with minimal filtering. The absorbance of a given indicator decreases when conditions become sufficiently reducing and can be used to define a "redox potential". The immobilized redox indicators are reversibly reduced and oxidized by reductants and oxidants in the sample.

Three primary redox indicators with quite different formal reduction potentials at pH 7 ($E_7^{0'}$), thionine, cresyl violet, and phenosafranine, establish a redox scale and were

shown to couple to reductants produced under distinct microbial redox conditions. Thionine ($E_7^{0'}$ = +52 mV on agarose) is reduced by Fe(II) (at Fe(II) levels > 100 μM and pH 7 or greater) and is useful for identifying Fe(III)-reducing conditions, and cresyl violet ($E_7^{0'}$ = -81 mV on agarose) couples to sulfide ([S(-II)] of 1 - 100 μM at pH 6-8) and is useful for identifying sulfate-reducing conditions. Phenosafranine ($E_7^{0'}$ = -267 mV on agarose) is reduced under methanogenic conditions. Indicators can be used in pairs to delineate different types of reduction conditions (e.g., Fe(III)- from sulfate-reducing). Moreover, the degree of reduction of thionine or cresyl violet by a given level of Fe(II) or sulfide in simple solutions corresponds reasonably well with that predicted by equilibrium models in most cases. It was demonstrated that reduction of redox indicators can be used to predict the onset of redox transformations of As(V) to As(III) and trichloroethylene to *cis*-dichloroethylene.

The effect of different redox species on the Pt electrode potential (E_{Pt}) and determination of hydrogen with redox indicators were also investigated. In soil slurries under anaerobic conditions, no evidence was found that E_{Pt} is controlled by inorganic redox couples. The feasibility of determining H_2 by its reduction of a redox indicator in the presence of palladium catalyst was demonstrated. H_2 levels as low as 0.0002 atm (160 nM in solution) were detected with thionine. Although adsorption of thionine on Pd prevented achieving detection limits suitable for environmental samples, criteria were established for attaining this goal in future studies.

Applications of Redox Indicators for Evaluating Redox Conditions in Environmental Samples

by

Brian D. Jones

A THESIS

submitted to

Oregon State University

in partial fulfillment of
the requirements for the
degree of

Doctor of Philosophy

Completed April 30, 1999
Commencement June 2000

Doctor of Philosophy thesis of Brian D. Jones presented on April 30, 1999

APPROVED:

Redacted for privacy

Major Professor, representing Chemistry

Redacted for privacy

Chair of Department of Chemistry

Redacted for privacy

Dean of Graduate School

I understand that my thesis will become part of the permanent collection of Oregon State University libraries. My signature below authorizes release of my thesis to any reader upon request.

Redacted for privacy

Brian D. Jones, Author

ACKNOWLEDGEMENTS

TABLE OF CONTENTS

TABLE OF CONTENTS (Continued)

TABLE OF CONTENTS (Continued)

TABLE OF CONTENTS (Continued)

TABLE OF CONTENTS (Continued)

TABLE OF CONTENTS (Continued)

LIST OF FIGURES

Figure **Page**

LIST OF FIGURES (Continued)

Figure **Page**

LIST OF FIGURES (Continued)

Figure **Page**

LIST OF FIGURES (Continued)

LIST OF FIGURES (Continued)

LIST OF FIGURES (Continued)

Figure **Page**

LIST OF TABLES

LIST OF TABLES (Continued)

LIST OF APPENDICES

LIST OF APPENDIX FIGURES

APPLICATIONS OF REDOX INDICATORS FOR EVALUATING REDOX CONDITIONS IN ENVIRONMENTAL SAMPLES

CHAPTER 1: INTRODUCTION

Redox reactions are of primary importance in environmental systems as they i) are responsible for life-giving energy conversion reactions and production of ATP in living organisms and ii) are responsible for redox transformations of organic and inorganic environmental species including many contaminants (e.g., As, trichloroethene (TCE)). Furthermore, the redox level (tendency of a system to be oxidizing or reducing) of a system is a critical factor in determining if a given redox transformation can occur. In terms of human health and safety, the persistence, mobility and biological effects of a contaminant are of primary concern and intimately related to its redox state and the redox level of the system (1). For example, Cr(VI) is known to be very soluble and quite toxic, while Cr(III) is very insoluble and not very toxic. Furthermore, dehalogenation of aromatic compounds occurs most readily under anoxic conditions, while ring cleavage and conversion to CO_2 occur most readily under oxic conditions.

For the environmental engineer or scientist, a clear understanding of the redox status of the system is necessary to make predictions of redox transformations of contaminants or intrinsic redox species. The direct determination of the redox state of a particular inorganic contaminant or the conversion products of an organic contaminant can be expensive, time consuming, and, in some cases, very difficult. For example, potential problems include oxidation of the sample upon exposure to air or the need for separation of certain redox-active species based on their redox state (e.g.,

As(V) and As(III) separation based on ion-exchange resins (2)). Therefore, a simple, qualitative and accurate in-field redox sensor would be of great help for initial assessment of environmental sites. Several methods have already been proposed for making qualitative measures of the redox status of a system (e.g., potential of a Pt electrode, GC determination of H_2 concentration (3)). However, these methods have limitations and are perhaps not the "best" way to measure the redox status of a system. These issues are explored in more detail in Chapter 2.

Recently, Lemmon et al. (4) reported the development of a redox sensing approach based on immobilized redox indicators. This approach is described in more detail in Chapter 2. Colored in their oxidized form and colorless when reduced and with a distinct formal potential, redox indicators couple to many oxidants and reductants in groundwater and, when immobilized on beads and packed into a flow cell, can be monitored spectrophotometrically. From the absorbance of the indicator, the fraction of the indicator oxidized can be estimated and the redox potential of the indicator can be calculated based on the Nernst equation, giving an estimate of the redox potential of the system. Lemmon also developed a chemostat reactor system for studying redox transformations of redox species in both environmental matrices and simple electrolyte solutions. Filtered solution can be pumped through the flow cell, providing contact between the soluble redox-active species and immobilized redox indicators.

The work presented here builds on the initial work by Lemmon. Overall, the research was conducted to better understand how redox sensors (Pt electrodes, redox indicators) couple to environmental systems, which methods for redox analysis are

more convenient, and which methods are more accurate. The focus has been to: 1) understand which species in environmental systems control or contribute to poising of the Pt electrode, 2) determine if redox indicator speciation can be used to estimate the redox level of a system and when redox transformations of inorganic and organic contaminants (e.g., As, TCE) are occurring, and 3) develop simple, field-useable redox sensors based on immobilized redox indicators. The five major chapters of this thesis are presented in the chronological order of this study.

In Chapter 3, the effects of various redox species on the Pt electrode potential (E_{Pt}) are discussed. The experimental design for determining which species affect(s) E_{Pt} employed the strategy of "testing by addition" in which a known quantity of an environmentally relevant "redox-active" species (either initially present or not) was added to simple solutions or soil or wastewater slurries and E_{Pt} was monitored. When possible and convenient, concentrations of the redox species added were monitored before and after addition.

A major focus of this research has been to determine under what conditions redox transformations of redox indicators take place in groundwaters, soil and wastewater slurries and microbial cultures. These results are presented in Chapters 4, 5 and 6. The approach taken was based on observing and comparing the speciation of a given immobilized redox indicator in contact with a sample (e.g., groundwater, soil or wastewater slurry) to E_{Pt}, concentrations of important environmental reductants (e.g., Fe(II), HS^-) in the sample, and the *microbial redox level* (i.e., defined by the dominant microbial process under which a given *terminal electron acceptor* (TEA) is reduced).

This concept of microbial redox level is explored more thoroughly in Chapter 2 and throughout Chapters 4, 5 and 6.

In this thesis, immobilized redox indicators were tested in soil and wastewater slurries under Fe(III)-reducing (Chapter 4), sulfate-reducing (Chapters 5 and 6), and methanogenic conditions (Chapters 5 and 6). In some cases, experiments were conducted to determine (by chelation or precipitation of the reductive species) which species in groundwater and soil or wastewater slurries were responsible for the reduction of the indicators. Fe(II) and HS^-, which are products of Fe(III)- and sulfate-reducing conditions, respectively, were identified as important environmental reductants. Titrations of the indicators (free and immobilized) with Fe(II) and HS^- were conducted to determine how indicator speciation (degree of reduction) depends on Fe(II) and sulfide levels, pH, and immobilized indicator concentration. Experimental results are compared to values predicted by equilibrium models.

A single redox indicator by itself is a rather limited redox sensor as its redox range (reduction potential range corresponding from about 90% oxidized to about 10% oxidized based on the Nernst equation) is about 60 mV. In the environment, the redox range can vary between about +400 mV (oxidizing, aerobic) to -300 mV (reducing, anaerobic), at pH 7. Therefore, several indicators spanning this redox range would be necessary to assess different environmental systems and to establish a basis to monitor continuously the redox level of groundwater, soils or microbial cultures in transition from oxidizing to reducing conditions. Based on spectrophotometric (or visual) analysis, several different redox indicators spanning this redox range could possibly be used to define a redox scale or ladder.

In previous work, Lemmon et al. (4) successfully immobilized the redox indicators thionine ($E_7^{0'}$ = +52 mV) and phenosafranine ($E_7^{0'}$ = -286 mV) to 60-μm agarose beads which could then be packed into a flow cell for spectrophotometric analysis. This reaction involved the covalent coupling of amine groups on the redox indicators to aldehyde groups on the agarose beads via a reductive amination reaction. In this thesis, the redox indicators, toluidine blue ($E_7^{0'}$ = +36 mV), azure A ($E_7^{0'}$ = +13 mV) and cresyl violet ($E_7^{0'}$ = -81 mV), were immobilized to agarose beads which further fills in gaps in the redox window scale.

One focus of this study has been to determine if redox indicator speciation can be used to determine when redox transformations of inorganic and organic contaminants are occurring. In previous research, Lemmon (5) performed the concurrent titration of thionine and Cr(VI) with Fe(II) in the reactor system and found that Cr(VI) was reduced to Cr(III) before the onset of reduction of thionine. In this research, redox indicator speciation was monitored in a Bashaw soil slurry during transformation of As(V) to As(III) (Chapter 4) and in a groundwater sample as reductive dechlorination of trichloroethylene (TCE) to cis-dichloroethylene (cis-DCE) was occurring (Chapter 5).

Another major focus of this research was to immobilize redox indicators in a film form, amenable to field analysis. Solutions with particulate matter must be filtered to prevent clogging of the flow cell packed with indicator-immobilized agarose beads (4, 5). With the chemostat reactor system, a cross-flow filter system (4, 5) is suitable for providing continuously filtered solution to the flow cell. In field use (presented in Chapter 5), this "packed bed" configuration clogged easily. Simple filtering of the

sample in the field tended to expose the sample to O_2 and the current cross-flow filter system is too bulky and complex for field use.

In this thesis, three different immobilization matrices were evaluated: silicon sol-gels, polyacrylamide gels and agarose gels. Agarose films proved to be the most suitable for this function and the redox indicators thionine (Thi), azure A (AA), cresyl violet (CV), nile blue (NB) and phenosafranine (PSaf) were successfully immobilized to these films. Procedures were developed for preparing and modifying thin agarose films with aldehyde groups for covalent immobilization. These results are presented in Chapter 6. The coupling chemistry is equivalent to that used for the agarose beads.

To accomodate the films, a specially designed spectrophotometric flow cell with removable windows was developed. Films approximately 3 x 3 mm in size, with a thickness of 0.3 - 0.5 mm, were placed in the cell from which the absorbance of the immobilized indicator was monitored with a spectrophotometer. Solution from the reactor was then pumped through the flow cell, allowing contact between the immobilized indicator and the sample. This configuration allows solution to be pumped across the immobilized indicators with less demanding filtering (a pore size of 30-μm compared to 0.6 μm for the bead-immobilized form). With a larger filter pore size, higher flow rates (10 - 50 mL/min compared to 0.5 - 1 mL/min with the beads) can also be used which improves the response time. Overall, the film form provides for more direct contact between the indicators and microbes and particulates in the sample.

Immobilization of redox indicators to cellulose filter membranes is also discussed in Chapter 6. These membranes can be used in a spectrophotometric flow cell (like the agarose films) or pressure-fitted to the surface of a Pt electrode. In the

latter case, the Pt electrode responds to the immobilized indicator, becoming poised in the region of the formal potential of the indicator when the indicator is partially reduced. Tests of this technology were performed in the reactor system in wastewater slurries under sulfate-reducing and methanogenic conditions.

Lovley (3) has made strong arguments in support of the notion that H_2 concentrations provide the best estimate of the redox status of a system. Furthermore, H_2 is known to be a major substrate for dechlorinators in the dechlorination of such aliphatic chlorinated compounds as TCE (6, 7). In the presence of Pd or Pt, redox indicators are reduced by H_2, and, forseeably, this reaction may be used as the basis for a low-level H_2 sensor. In chapter 7, the use of organic (e.g., Thi) and chelated inorganic redox indicators (e.g., Fe(III)-(orthophenanthroline)$_3$) for quantifying H_2 are discussed.

References

1. McBride, Murray B., *Environmental Chemistry of Soils*, Oxford University Press, Inc., 1994.

2. Bos, Mark, *Part I: Development and Application of an Arsenic Speciation Technique Using Ion-Exchange Solid Phase Extraction Coupled with GFAAS, Part II: Investigation of Zinc Amalgam as a Reductant*, M. S. Thesis, Oregon State University, Corvallis, 1996.

3. Lovley, Derek R.; Chapelle, Francis H., *Environ. Sci. Technol.*, **1994**, *28*, 1205-1210.

4. Lemmon, T. L.; Westall, J. C.; Ingle, J. D., Jr. *Anal. Chem.*, **1996**, *68*, 947-953.

5. Lemmon, Teresa, *Development of Chemostats and Use of Redox Indicators for Studying Transformations in Biogeochemical Matrices*, **1995**, Ph.D. Thesis, Oregon State University.

6. Vancheeswaran, Sanjay, *Abiotic and Biological Transformation of TBOS and TKEBS, and their Role in the Biological Transformation of TCE and c-DCE*, **1998**, M.S. Thesis, Oregon State University.

7. Vancheeswaran, Sanjay; Halden, Rolf U.; Semprini, Lewis; Williamson, Kenneth J.; Ingle, James D. Jr., "Abiotic and Biological Transformation of Tetraalkoxysilanes and Trichloroethene/cis-1,2-Dichloroethene Cometabolism Driven by Tetrabutoxysilane-Degrading Microorganisms", *Environ. Sci. Technol.*, in press.

CHAPTER 2: HISTORICAL

2.1 Overview of redox reactions in the environment

Oxidation/reduction (redox) reactions involve the transfer of electrons from one chemical species to the other:

$$red_1 + ox_2 \rightleftharpoons red_2 + ox_1 \qquad (2\text{-}1)$$

where red is the reduced form of a species, ox is the oxidized form, and the subscripts 1 and 2 denote the species. One species is oxidized ($red_1 \rightleftharpoons ox_1 + ne^-$) and loses electrons while one species is reduced ($ox_2 + ne^- \rightleftharpoons red_2$) and gains electrons, where n is the number of electrons (e^-) transferred.

The tendency of a species to lose or gain electrons can be determined with the Nernst equation:

$$E_H = E^{0'} - \frac{RT}{nF} \ln \left(\frac{a_{red}}{a_{ox}}\right) \qquad (2\text{-}2)$$

where E_H is the reduction potential for the redox half-reaction (V), $E^{0'}$ is the formal reduction potential of the redox half-reaction (V), R is the molar gas constant (J/mol K), T is the temperature (K), F is Faraday's constant (96,500 C/eq), a_{red} is the activity of the reduced species and a_{ox} is the activity of the oxidized species (in many cases, the concentrations of the reduced and oxidized species can be substituted for the activities without significant error (1)). Standard and formal reduction potentials (in the standard state and corrected for ionic strength and other effects) are relative to the standard hydrogen electrode (SHE, defined as 0 V for 1 atm hydrogen pressure and pH 0).

The Nernst equation can be used to predict if one chemical species will be reduced or oxidized by another by comparing the reduction potentials calculated from Eq. 2-2 for each half-reaction. The oxidized species of the couple with the more positive E_H will act as the oxidizing agent (acquiring electrons) in the overall reaction. Because the Nernst equation is based on thermodynamics, not on the kinetics, the equilibrium concentrations of redox species calculated with the Nernst equation may not be realized in redox systems with slow (or very slow) kinetics. However, microbial activity in aquatic and soil water systems increases the rates of many redox reactions which would only occur very slowly otherwise. Microbial mediation of redox reactions is a very important factor in environmental systems and will be discussed in more detail shortly.

A variety of common chemical species in environmental systems undergo redox reactions and can exist in a variety of redox states. These include oxygen (O_2, H_2O_2, H_2O), hydrogen (H_2, H^+), nitrogen (NO_3^-, NO_2^-, N_2, NH_4^+), sulfur (SO_4^{2-}, SO_3^{2-}, S^0, HS^-), iron ($Fe(OH)_3$ and other Fe(III)-oxides and hydroxides, Fe(II)), manganese (MnO_2, Mn(II)) and organic carbon species (acids, aldehydes, alcohols, sugars)(1, 2, 3). Additionally, a variety of inorganic contaminant species (As, Cr, Se, Hg) are redox-active and can exist in more than one redox state. In many cases, these reactions are microbially mediated and do not (generally) occur without enzymatic catalysis.

2.2 Concept of microbial redox level

Because most redox reactions in the environment are microbially mediated, the system is not in equilibrium and a true system E_H does not exist; the Nernst equation does not apply. Many microbiologists, soil scientists and environmental engineers have adopted a more practical scale for redox level based on microbial activity and the dominant *terminal electron acceptor* (TEA) process.

Microbes utilize redox reactions to produce adenosine triphosphate (ATP) for energy (2, 3). To catalyze redox reactions, microbes employ enzymes which lower the activation energy for the reaction. Through oxidation of a substrate (usually an organic acid, alcohol, sugar or H_2), electrons can be "shuttled" through an electron transport mechanism, creating ATP, ADP and other important biochemical species (2, 3). The electrons are eventually transferred to another available chemical species, termed the TEA. Important TEA's include O_2, NO_3^-, Fe(III) (from Fe(III)-oxides), Mn(IV) (from Mn(IV)-oxides), SO_4^{2-} and CO_2. It is this dominant TEA process which defines the microbial redox level.

The dominant TEA processes, along with the reactants (TEA's) and products, are presented in Table 2.1. Some of these products, such as Fe(II) and HS^-, can further act as reducing agents directly in the environment, without the need for microbial mediation (1).

Microbial redox levels can further be delineated between aerobic (oxic) and anaerobic (anoxic) conditions. Under aerobic conditions, O_2 is the dominant TEA and generally this redox level occurs when surface and subsurface soils are drier and O_2 can

Table 2.1 Important microbial redox levels in environmental systems.

redox level	TEA	product of TEA process	comments on redox level
O_2-reducing	O_2	H_2O	aerobic, most oxidizing redox level
nitrate-reducing	NO_3^-	NO_2^-, N_2	aerobic or anaerobic; products of TEA process; N_2 is inert[a]
Mn(IV)-reducing	Mn(IV) (usually as MnO_2)	Mn(II)	anaerobic, very close to Fe(III)-reducing redox level and not considered as important; Mn(II) is generally inert[a]
Fe(III)-reducing	Fe(III) (usually as Fe_2O_3 or other Fe(III)-oxides or hydroxides	Fe(II)	anaerobic, important redox level; Fe(II) acts as reductant itself
sulfate-reducing	SO_4^{2-}	S^{2-} (or HS^-) or sometimes SO_3^{2-}	very anaerobic, very reducing; HS^- an important reducing species in environmental systems
methanogenic	CO_2	CH_4	very anaerobic, most reducing level; CH_4 inert[a]
reductive dechlorination	chlorinated species (e.g., TCE, *cis*-DCE)	dechlorinated species (e.g., *cis*-DCE, VC)	often occurs under sulfate-reducing or methanogenic conditions

[a] inert implies that the species produced does not tend to react with other environmental species under normal temperatures and pressures.

easily diffuse into the system (4). The next TEA process is NO_3^- reduction, occurring after O_2 has been depleted (the activity of nitrate reductase, an enzyme responsible for the reduction of nitrate to nitrite, is inhibited by O_2 (3)). As the system becomes more reducing (generally as the soil or aquifer becomes waterlogged and O_2 diffusion is very slow), the dominant TEA processes become Mn(IV)- or Fe(III)-reduction (in this order (5); Patrick (6) has noted Mn(IV) reduction before Fe(III) reduction in flooded soil systems), sulfate reduction, and finally CO_2-reduction (or otherwise known as methane production, termed methanogenesis). Furthermore, chlorinated compounds (e.g., TCE) can be used as a TEA by certain microbes, defining a microbial redox level.

In all, roughly five or six distinct microbial redox levels exist. In some situations, two TEA processes can occur concurrently (e.g., during the transition from one redox level to another), and no particular TEA process dominates. In these cases, the most reducing TEA process in the system may be considered to define the overall reduction level of a system. For example, if the *effective* reduction potential of the system is low enough to reduce CO_2 to methane, it is also low enough to reduce Fe(III) or SO_4^{2-} (or other TEA's) if the right enzymes and substrates are present.

2.3 Current methods and problems in measuring redox status

Important methods for characterizing the redox status of an environmental system include:

1) chemical analysis for all relevant redox-active species in a sample

2) potential of a Pt electrode

3) H_2 activity of the system

4) redox indicator speciation

Method 1 is the most direct and accurate, but it is expensive and time-consuming. In practice, the determined redox-active species are the TEA's or reduced products of TEA's that are soluble, and contaminants (e.g., As(V) and As(III), Cr(VI) and Cr(III), TCE, *cis*-DCE and VC) of interest. This method also requires sampling of the system and extensive laboratory analysis.

In the process of sampling or sample storage before analysis, several processes can influence the redox state or cause loss of a chemical species including oxidation by O_2, precipitation, or volatilization. Moreover, many analytical methods for inorganic species cannot distinguish between the redox states of a species (e.g., GFAA and ICP spectrophotometry) and separation of the different redox states of a species (e.g., As(V) and As(III)) before determination is necessary (7).

Measuring the concentrations of TEA's or the products of TEA processes, does not necessarily provide a complete picture. The nature of the dominant TEA process cannot always be based solely on the presence or consumption of a TEA or the appearance of a product, due to factors such as precipitation, adsorption, zone

transport and replacement of a species (e.g., SO_4^{2-}) by mineral sources (3). For example, sulfides readily precipitate Fe(II) and other ions (e.g., Hg_2^{2+}, Cu(II)) so that lack of an increase in soluble sulfide concentrations does not mean that sulfate-reduction is not occurring (8). Fe(II) commonly adsorbs on Fe(III)-oxyhydroxides and as little as 2% of the total Fe(II) in a soil or groundwater aquifer may be in solution (9). Transport of gases such as H_2S and CH_4 across environmental zones is common (9), and these products may be detected in regions where sulfate-reduction and methanogenesis are not actually occurring.

The Pt electrode is probably the most used and convenient sensor for measuring the redox status of a system. An *in situ* method, it appears to give useful results under some conditions (10). There have been some attempts to correlate Pt electrode potentials to the TEA process, with some success (6). However, interpretation of E_{Pt} in soil or groundwater aquifer systems to determine microbial redox processes or redox speciation of redox-active species (e.g., As(V) and As(III)) suffers from the disequilibria of environmental systems, solid coatings on the surface which affects potential (11), and the fact that no one is really sure what species the Pt electrode is responding to in environmental systems.

Measurement of H_2 activity has recently been proposed by Lovley and Chapelle (8, 12) as an alternative to these methods for redox analysis. Hydrogen is the most ubiquitous intermediate product of anaerobic microbial metabolism, and the activity of H_2 is argued to be indicative of a given TEA process (12). The rates of H_2 exchange are rapid compared to overall rates of TEA consumption and the steady state concentration of H_2 is determined by its rate of production and rate of consumption. If

H_2 diffuses to a less reducing zone, its concentration will rapidly decrease, unlike for transport of other gases such as CH_4 and H_2S, because the rate of H_2 consumption increases (microbes responsible for less reducing conditions have a greater affinity for H_2).

Determination of H_2 activity, although theoretically simple, does suffer from the complexity and expense of the analysis. H_2 levels are normally very low in environmental systems (for groundwaters, between less than 0.05 nM for NO_3^--reduction to about 10 nM for methane production) (12). The analytical technique involves a complex and labor-intensive measurement based on a gas stripping/GC method with a special reduction gas detector (12). A GC equipped with the special detector can cost over $20,000 (13).

2.4 Previous work in the use of redox indicators for environmental analysis

Historically, used as end point indicators in redox titrations (14), redox indicators are generally colored in their oxidized form and colorless when reduced and can poise the Pt electrode (14, 15, 16). Redox indicators (In) undergo the general redox reaction

$$In_{ox} + ne^- \rightleftharpoons In_{red}$$

(2-3) which can be monitored spectrophotometrically from the change in absorbance (or fluorescence) of one or both species in the couple (normally the oxidized form). The indicator potential (E_{ind}) can be calculated with the known concentrations (activities) of oxidized and reduced indicator species and the Nernst equation

$$E_{ind} = E_m^{0'} - RT/nF \ln [In_{red}]/[In_{ox}]$$

(2-4)

where $E_m^{0'}$ is the formal potential of the indicator at a specified pH. The formal potential can be determined with a Pt electrode as the potential where the indicator is half reduced. Ideally, a redox indicator in contact with an environmental system will interact with all natural redox couples (oxidants and reductants) in an equilibrium fashion and the ratio of the redox forms of the indicator will reflect the "effective" E_H of the system. This effective E_H can be determined by the spectrophotometric analysis of the indicator. In reality the indicator can only provide information about certain natural redox couples that react with the indicator.

Zobell (17) pioneered early work in environmental redox analysis with redox indicators by using redox indicators to probe the redox properties of marine sediments.

Later, Tratnyek and Wolfe (18) investigated the reduction potential and reducing capacity of anaerobic sediment slurries with redox indicators. However, they found that only negatively-charged redox indicators (indicators with sulfonate groups) could be used effectively, as the positively-charged indicators would adsorb to the negatively-charged soil surfaces.

Problems involving indicator adsorption to particulate matter (due to electrostatic or hydrophobic interactions) and the difficulty in separating redox indicators from the solid phase (for spectrophotometric measurements) without disturbing the redox status of the system have limited the applicability of redox indicators to environmental redox analysis (18). In fact, Hesse (19), commenting about the use of redox indicators for determination of soil redox potentials stated that their use for this purpose is "unsatisfactory" and "not recommended". However, McBride (5) has pointed out that "clever experimental designs might circumvent the known drawbacks".

In more recent work involving identification of reversible (i.e., redox indicators which can be reduced and reoxidized) redox indicators, Mobley (21) tested 17 indicators and found that 9 of these indicators reacted reversibly with a variety of reductants (Fe(II), dithionite, ascorbic acid) and oxidants (Ce(IV), O_2, Cr(III), Fe(III)). More recently, Lemmon et al. (15, 20) developed an immobilization scheme for redox indicators. Five of the indicators initially identified by Mobley contained amine groups which could (theoretically) be coupled to aldehyde groups through a reaction known as reductive amination. Employing 40 - 60 μm, cross-linked (4%) agarose beads (Spectrum, Spectra/Gel MAS Beads Macroflow) containing monoaldehyde surface

groups, Lemmon (15) successfully immobilized four of the amine-containing indicators to the beads. These indicator-immobilized beads were packed into a flow cell (Hellma, 170.700-QS) for spectrophotometric analysis (15). Two of the immobilized indicators, thionine (Thi) and phenosafranine (PSaf), were reduced and reoxidized reversibly and functioned well in the flow cell configuration. One of the indicators, nile blue (NB) was found to be too hydrophobic for this configuration such that the pressure in the flow cell increased to 70 psi with normal flow rates.

To characterize these immobilized redox indicators and to study their behavior in "real" (environmental) systems, Lemmon et al. (15, 20) constructed a sophisticated, air-tight, 2-L chemostat reactor system with ports for Pt, pH and reference electrodes, dispensing pumps, and a gas control system. The details of this reactor system are described in the experimental sections of Chapters 3 through 6. The pH and E_{Pt} of reactor samples (soil slurries or simple electrolyte solutions) could be maintained at an operator-chosen level with the use of a computer. Furthermore, a special cross-flow filter system was developed to separate reactor solution from particulate matter in the bulk matrix which allowed filtered reactor solution to be pumped through the flow cell and contact of soluble reductants/oxidants in the sample with the immobilized indicators.

To determine the formal potentials (at pH 7) of immobilized Thi and PSaf, Lemmon et al. (15) titrated both the free indicator and the immobilized indicator concurrently (as outlined in Appendix I) with Ti(III)-citrate while monitoring the absorbance of both forms spectrophotometrically. Immobilization decreased the formal potential by 15 - 30 mV for either indicator. In other reactor experiments, Lemmon

titrated both free Thi and Cr(VI) together in solution with Fe(II) and determined that the onset of reduction of free Thi occurred only after complete reduction of Cr(VI) to Cr(III) (20). In bioreactor experiments, Lemmon (20) demonstrated the first use of immobilized indicators to assess redox status of soil (a soil slurry). Significant reduction of immobilized thionine occurred when Fe(II) concentrations in anaerobic Bashaw soil slurry at pH 6.0 increased to about 0.6 mM (20). The recent accomplishments by Lemmon illustrate two important breakthroughs in environmental redox analysis with redox indicators: 1) the immobilization of redox indicators to a sensor surface which helps to facilitate redox analysis in environmental systems and 2) application of redox indicators to determining when the onset of a redox transformation of an important priority contaminant (Cr) are occurring. These breakthroughs have significantly influenced the direction of this thesis research and have led to many new significant results and breakthroughs which are presented in the following chapters.

2.5 References

1. Snoeyink, Vernon L.; Jenkins, David, *Water Chemistry*; John Wiley & Sons, Inc., 1980.

2. Brock, Thomas D.; Madigan, Michael T.; Martinko, John M.; Parker, Jack, *Biology of Microorganisms, Seventh Edition*; Prentice Hall: Englewood Cliffs, New Jersey, 1994.

3. Chapelle, Francis H., *Groundwater Microbiology and Geochemistry;* John Wiley & Sons, Inc., 1993.

4. Baham, John, Private communication, Oregon State University, June 3, 1994.

5. McBride, Murray B., *Environmental Chemistry of Soils*, Oxford University Press, Inc., 1994.

6. Patrick, W. H., Jr.; Jugsujinda A., *Soil Sci. Soc. Am. J.*, **1992**, *56*, 1071-1073.

7. Bos, Mark, *Part I: Development and Application of an Arsenic Speciation Technique Using Ion-Exchange Solid Phase Extraction Coupled with GFAAS, Part II: Investigation of Zinc Amalgam as a Reductant,* M. S. Thesis, Oregon State University, Corvallis, 1996.

8. Chapelle, Francis H.; McMahon, Peter B.; Dubrovsky, Neil M.; Fujii, Roger F.; Oaksford, Edward T.; Vroblesky, Don A., *Water Resour. Res.*, **1995**, *31*, 359-371.

9. Bodek, Itamar, *Environmental Inorganic Chemistry: Properties, Processes, Estimation Methods*, Pergamon Press, Elmsford, N.Y., 1988.

10. Berner, Robert A., *Geochim. Comochim. Acta*, **1962**, *27*, 563-575.

11. Whitfield, M., *Limnol. Oceanogr.*, **1974**, *19*, 857-865.

12. Lovley, Derek R.; Chapelle, Francis H. Chapelle; Woodward, Joan C., *Environ. Sci. Technol.*, **1994**, *28*, 1205-1210.

13. Ingle, James D. Jr., Private communication, Oregon State University, January 11, 1997.

14. *Indicators*, Bishop, E., Ed., Pergamon Press: Oxford, 1972.

15. Lemmon, T. L.; Westall, J. C.; Ingle, J. D. Jr., *Anal. Chem.*, **1996**, *68*, 947-953.

16. Clark, W. Mansfield, *Oxidation-Reduction Potentials of Organic Systems*; Williams & Wilkins Company: Baltimore, 1960.

17. Zobell, Claude E., *Bull. Am. Assoc. Petroleum. Geol.*, **1946**, *30*, 477.

18. Traytnek, Paul G.; Wolfe, N. Lee, *Environ. Toxicol. Chem.*, **1990**, *9*, 289.

19. Hesse, P. R., *A Textbook of Soil Chemical Analysis*; Chemical Publishing Co., Inc.: 1971.

20. Lemmon, Teresa, *Development of Chemostats and Use of Redox Indicators for Studying Transformations in Biogeochemical Matrices*, **1995,** Ph.D. thesis, Oregon State University.

21. Mobley, James, Oregon State University, unpublished report, **1992**.

CHAPTER 3: EVALUATION OF THE EFFECT OF VARIOUS REDOX SPECIES ON THE PT ELECTRODE POTENTIAL

3.1 Introduction

The Pt electrode is currently the most commonly used sensor for estimating redox conditions in the field and in environmental samples. This is largely due to its ease of use and relatively low cost. In practice, the Pt electrode is placed in a sample along with a reference electrode (usually Ag/AgCl or SCE, whose potential is known relative to the standard hydrogen electrode (SHE)) and the potential difference between the two electrodes is measured with a voltmeter. This measured potential is termed E_{meas} (or E_m), or often, E_{Pt}. Often, E_{Pt} is then referenced to the SHE. This corrected potential is termed the "measured E_H" of the system. In principle, the E_{Pt} of the system correlates to the true thermodynamic E_H of the system defined by the Nernst equation:

$$E_H = E^0 - \frac{RT}{nF} \ln \prod_i^m \left(\frac{a_{red}}{a_{ox}}\right)_i \qquad (3\text{-}1)$$

In real systems (e.g., soil or ground water), the formal potential, $E^{0'}$, is substituted for E^0, and the bulk concentrations of the species are generally substituted for the activities, a_i.

A few studies suggest E_{Pt} is a useful measure of redox status in environmentally-relevant systems and can be used to estimate the concentration or the redox state of certain redox-active species. In studies of anaerobic marine sediments and artificial sulfide systems, Berner (1) found a Nernstian response between Pt electrode potential and S^{2-} concentration in the range of 10^{-8} to 10^{-16} M S^{2-} and pH range of 10 to 7 (at pH 10, 10^{-8} M S^{2-} corresponds to 100 μM total S(-II) and at pH 7, 10^{-16} M S^{2-} corresponds

to 0.002 μM total S(-II) by eq. H-8 of Appendix H). In controlled laboratory studies with a Pt electrode with a thin layer of Fe(III)-oxide deposited on the surface and under oxygen-free conditions, Doyle (2) demonstrated that the potential can be predicted from the Nernst equation, the Fe(II) concentration, and the Fe(III)-oxide solid phase (believed to be lepidocrocite) for Fe(II) concentrations in the range 0.008 to 2 mM.

There are serious limitations to the use of a Pt electrode for determining the concentrations of redox species (3). In studies of environmental systems, Lindberg and Runnels (4) report that concentrations of most redox couples (e.g., NO_3^-/NO_2^-, SO_4^{2-}/SO_3^{2-}) cannot be estimated from measured values of E_{Pt} and the Nernst equation. This lack of correlation is ascribed to slow kinetics of electron transfer for most redox couples at the Pt surface and non-equilibrium conditions in the system (4). This lack of equilibrium between redox species in real systems limits the possibility of measuring the speciation of a given redox couple in order to predict the behavior of other redox species.

Many redox couples which influence E_{Pt} in a Nernstian fashion at significant concentrations (~ 1 mM) do not influence E_{Pt} in natural systems due to their relatively low concentrations. For instance, in studies of the kinetics of various redox couples at the surface of a Pt electrode in electrolyte systems, Kempton (5) determined that the Fe(II)/Fe(III) system at pH 3 and the H^+/H_2 system at pH 3 influence E_{Pt} in a Nernstian fashion. However, at pH 6, soluble Fe(III) and H^+ are at such low concentrations that these couples no longer influenced E_{Pt} in a Nernstian fashion (5). Additionally, Kempton suggests H_2 must be at concentrations of 10^{-5} M (or greater) and the pH 5 or less to poise the Pt electrode and these H_2 and pH levels are uncommon in environmental

systems (3). Moreover, Kempton makes the comment "platinum E_H measurements are likely to have very restricted quantitative applications in natural aqueous systems" (5).

Some research has been directed towards the use of E_{Pt} as a *qualitative* measure of redox status rather than as a quantitative predictor of redox species concentrations in environmental systems. Attempts have been made to correlate certain ranges of E_{Pt} to specific microbial redox levels (e.g., Fe(III)-reducing, sulfate-reducing) by monitoring E_{Pt} concurrently along with the disappearance of specific terminal electron acceptors (TEA's) or the appearance of the products of those reactions in biologically-active environmental systems. Patrick et al. (6), using a soil slurry in an anaerobic bioreactor in which E_{Pt} could be maintained constant (statted) by addition of O_2, determined that E_{Pt} qualitatively tracked the disappearance of various TEA's such as NO_3^- and SO_4^{2-} and the appearance of products such as HS^- and Fe(II). However, many researchers using E_{Pt} to measure the redox status of environmental systems undergoing different microbial processes find that the onset and range for reduction of a given TEA can vary 200 mV or more (3). The correlation between the absolute value of E_{Pt} and microbial level may be strongly dependent on then system being measured.

In most studies as described above, the relationship between measured concentrations of certain redox-active species or the disappearance of TEA's and E_{Pt} was emphasized. Relatively little work has been directed to determine those species in environmental systems that *actually affect* E_{Pt}. Obviously, most field research does not allow one to directly test which species affect the electrode potential (e.g., by varying the concentration of a given species *already in that system* and noting its effect on E_{Pt}). This research is best conducted with a representative field sample such as a soil or

groundwater sample which can be placed in a laboratory bioreactor in which many variables (e.g., pH, temperature) can be held constant.

In this thesis, the effects of various environmentally relevant redox-active species or couples on E_{Pt} in soil slurries or other environmental media under controlled conditions were investigated. This required the use of a sophisticated bioreactor system, developed previously (7), which could maintain anaerobic conditions and allowed the systematic control of pH, temperature, and measured E_{Pt} of environmental samples. A strategy of "testing by addition" was employed in which one or more redox-active species were added to the bioreactor sample in known amounts with continual monitoring of E_{Pt}. When feasible, the concentration of that species was monitored before and after addition. If a change in E_{Pt} occurred, that species or couple was tested in more detail to further evaluate its effect on E_{Pt} was Nernstian or if it affected E_{Pt} by some other mechanism (e.g., oxidizing or reducing other species, adsorbing at the Pt surface). Additionally, the effects of some redox species on E_{Pt} in simple electrolyte systems were compared to their effect on E_{Pt} in environmental samples. The effects of ionic strength and exposing the Pt surface to oxygen in air on E_{Pt} were also studied.

3.2 Background

3.2.1 Theory

In general, redox sensors must interact with redox-active species in a system to illicit a meaningful signal response. The platinum electrode, in particular, develops a potential, E_{Pt}, based on *exchange currents* generated by the transfer of electrons from one redox species to another at the platinum surface. Under equilibrium conditions, if a redox couple at the Pt surface produces a large enough exchange current, E_{Pt} can be predicted by the known concentrations of the redox species and application of the Nernst equation (Eq. 3-1).

There are two current components. The cathodic current is generated by the transformation of oxidized species to reduced species at the Pt surface, which is given by (8):

$$I_c = nFAk_c[O] \qquad (3\text{-}2)$$

where I_c is the cathodic current, A; n is the number of electrons transferred in the half-reaction; F is Faraday's constant of 96,500 C/eq; A is the surface area of the Pt, cm^2; [O] is the oxidant concentration at the Pt surface (in a well-stirred system this should be the concentration in the bulk of the solution), M; and k_c is the cathodic heterogeneous rate constant, cm/s. The anodic current is generated by the transformation of reduced species at the Pt surface (8):

$$I_a = nFAk_a[R] \qquad (3\text{-}3)$$

where [R] is the reductant concentration, M, and k_a is the anodic rate constant. The cathodic and anodic rate constants are given by equations 3-4 and 3-5, respectively (8)

$$k_c = k_0 \exp[-\alpha_c nF(E - E^{0'})/RT] \quad (3\text{-}4)$$

$$k_a = k_0 \exp[\alpha_a nF(E - E^{0'})/RT] \quad (3\text{-}5)$$

where k_0 is the standard rate constant, cm/s; α_c is the cathodic charge transfer coefficient, α_a is the anodic charge transfer coefficient, E is the potential, V; $E^{0\prime}$ is the formal potential at standard state, V; and T is the absolute temperature, K. In potentiometric measurements with the Pt electrode, the potential, E, at which the exchange currents sum to zero, ($I = I_c - I_a$) is theoretically the measured Pt electrode potential, E_{Pt}.

In terms of the redox reaction at its surface, platinum itself is usually considered inert and does not take part in the redox reaction. However, there is some evidence that certain species (e.g., Cl, S and O) do form a surface film on the electrode, affecting E_{Pt} (9).

3.2.2 "Poising" of the Pt electrode

Under equilibrium conditions in which the electron transfer kinetics of a redox couple at a Pt electrode surface are sufficiently rapid and the concentration of both species in the couple are great enough and similar (within a factor of about 1000 (10)), the Pt electrode can be *poised in a Nernstian fashion* and the measured potential, E_{Pt}, has real relevance. The term *poised* is often defined operationally and implies that the redox system has a sufficient *redox buffer capacity* that the redox potential does not drift

upon small additions of oxidants or reductants (11). As an example of a redox couple which poises the Pt electrode in a Nernstian fashion, the $Fe(CN)_3^{4-}/Fe(CN)_3^{3-}$ redox couple has a standard rate constant (k_0) of about 0.014 cm/s and easily poises the Pt electrode in a Nernstian fashion at species concentrations of 100 μM each (5). Under these conditions, the ratio of concentrations (more precisely, activities) of the redox species can be determined directly from the Nernst equation and the measured E_{Pt}.

A distinction must be made between *equilibrium* (Nernstian) poising and *non-equilibrium* (non-Nernstian) poising. In a non-equilibrium system (although perhaps at steady-state), the Pt electrode can be *poised in a non-Nernstian fashion* by several redox species which, although not in equilibrium with each other or the system, poise the electrode by virtue of the sum of the exchange currents being zero. In this case though, E_{Pt} is simply the potential at which I = 0 and cannot be predicted from the Nernst equation. Because the measured potential is a function of the exchange currents of a variety of redox species, the E_{Pt} is termed a *mixed potential* (12).

Considering these possibilities, there are two limiting cases in which the Pt electrode can be poised by soluble redox-active species in an environmental system:

Case 1): the Pt electrode is poised by one or more redox couple(s) in equilibrium with each other and the Nernst equation applies, and

Case 2): the Pt electrode is poised by two or more redox couples not in equilibrium with each other and the Nernst equation does not apply

If case 1 were true, it would be possible to calculate concentrations of some redox species from the Nernst equation and the measured potential. For case 2, the Nernst equation would not apply and no simple relationship between the concentrations of the redox species and E_{Pt} exists. Furthermore, any number of redox species could influence E_{Pt} and it would be very difficult to predict the behavior of the Pt electrode under a given set of conditions or make qualitative judgements of the redox conditions based on Pt electrode potentials.

In environmental systems, the transition from oxidizing (aerobic) to reducing (anaerobic) conditions corresponds to a large range of E_{Pt} values (about +400 to -300 mV) (10). Many different couples would likely be responsible for poising the Pt electrode over this range because any one couple can only poise the electrode over a modest potential range. If the ratio of oxidized to reduced species becomes too low or high, one of the exchange current components becomes too small and poising is lost (10). A normal Nernstian slope is 29 or 59 mV per decade, depending on the number of electrons transferred in the reaction, so that a given couple could poise the electrode over a range of about 60 to 120 mV.

To observe poising in an environmental system, the following conditions are proposed:

1) the concentrations of redox-active species must be great enough to affect E_{Pt}

2) the kinetics of electron transfer for the couple at the electrode surface must be rapid enough to create a large enough exchange current to affect the potential

3) at least one oxidized and one reduced species must be in contact with the Pt surface (generally soluble, although a solid layer at the Pt surface can exist), generating an anodic and cathodic current, respectively

Morris and Stumm (13) propose that the minimum exchange current density (I_a/A or I_c /A) necessary to poise a Pt electrode is about 0.1 $\mu A/cm^2$. More recently, Kempton (5) suggests that the minimum exchange current density necessary for poising is 10 $\mu A/cm^2$, two orders of magnitude greater. Kempton measured exchange currents and determined heterogeneous rate constants at a Pt electrode for several species. For the very reversible $Fe(CN)_3^{4-}/Fe(CN)_3^{3-}$ redox couple, the electrode was poised down to a concentration of about 7 μM of each species where the current density was calculated to be about 8 $\mu A/cm^2$. It was better poised (E_{Pt} was independent of stirring) at about twice this concentration and exchange current. It appears redox species at low concentration (below 5 μM) or with slow electrode kinetics can effectively be eliminated as poising the Pt electrode.

In studies of the Fe(II)/Fe(III) couple at pH 3.0, Kempton (5) found that the Pt electrode was poised as total Fe concentration reached about 13 μM (about 6 μM each in Fe(II) and Fe(III)). As the Fe(II)/Fe(III) couple at low pH (pH < 4) is a common example of a redox system which poises the Pt electrode in a Nernstian manner, one would expect that other environmental species must be at similar concentrations or greater (> ~5 μM) to affect E_{Pt} or ultimately poise the Pt electrode. Additionally, many environmental redox-active species have one redox state which exists as a solid under most environmental conditions (e.g., Fe(III)-oxides, Mn(IV)-oxides). In this case, an

appreciable exchange current can only be generated if the solid redox species is in contact with the electrode (e.g., coating the electrode or particles bombarding the electrode). In laboratory experiments, Doyle (2) observed such behavior with the Fe(II)/FeOOH couple under O_2 free conditions. A Nernstian response was observed over an Fe(II) concentration range of 0.008 to 2 mM and a pH range of 4.5 to 7.0 when a layer of Fe(III)-oxyhydroxide (believed to be lepidocrocite) was deposited on the Pt surface.

3.2.3 Soluble environmental species which may directly poise the Pt electrode

Either inorganic and organic components can potentially poise a Pt electrode in environmental systems. Because the possibilities are more limited, it is easier to concentrate first on inorganic species that affect E_{Pt} and address organic species later.

The periodic table can be used as an initial guide to determine which inorganic redox couples which might affect E_{Pt} in a Nernstian fashion and which could be eliminated. Rare earths, lanthanides, or actinides are normally at relatively low concentrations in natural systems as to never influence E_{Pt} (except possibly at some nuclear waste sites). Similarly, even high levels of many elements such as halogens, alkali metals, alkaline earths, and soil silicate and aluminate compounds do not influence the electrode potential because they are essentially not redox-active in a typical system (i.e., they exhibit a single redox state under normal conditions). In addition, many natural silicate and aluminate compounds are very insoluble in water. The elements left to consider are redox-active inorganic species which are present at relatively high

concentrations ($\geq$ 1 μM) in the environmental system, are soluble (at least one of the redox states), and which commonly exhibit more than one redox state.

These restrictive conditions leave a handful of transition metal species and a small assortment of non-metal (and metalloid) species to consider. Metals or metalloids exhibiting different redox states include Cr (III and VI), Mn (II and IV), Fe (0, II and III), Cu (0, I and II), Ag (0 and I), Hg (0, I and II), Pb (0 and II), Se(0, IV and VI) and As (III and V). However, the priority pollutant elements (Cr, Ag, Hg, Pb, Se and As) and soluble Cu are normally found at such low concentrations (generally << 1 μM) as to never significantly affect E_{Pt}. Additionally, the heterogeneous kinetics of these couples at the Pt surface are generally slow (5, 14). Therefore, Cr, Ag, Hg, Pb, Se, As and Cu are unlikely candidates for poising the Pt electrode.

Fe(II) and Fe(III) compounds are important in environmental systems and are commonly transformed microbially (15). In terms of microbial processes, Fe(III) compounds (hydroxides, oxides and oxyhydroxides) are very important as terminal electron acceptors (TEA's) in microbial processes (16), and the Fe(II)/Fe(III) system defines an important microbial redox level (i.e., the Fe(III)-reducing level). In addition, soluble Fe(II) concentrations can be quite high in groundwater (16) and soil systems (> 100 μM) (17, 18) and Fe(III)-oxides are often a large component of soil solids (12). At normal pH values in natural soil and water systems (pH > 5), free Fe(III) is at very low concentrations because it forms insoluble Fe(III)-hydroxides (12). Poising of a Pt electrode would only be expected if a solid oxide layer formed at the surface or the Pt is in direct contact with Fe(III)-hydroxides or Fe(III)-oxides as observed by Doyle (2) in laboratory studies. It is not known if Fe(III)-oxide layers commonly form on Pt

electrodes during field measurements. However, there is enough evidence to suggest that the Fe(II)/Fe(III) system should be considered as a couple that could affect E_{Pt}.

Mn, like Fe, is commonly transformed microbially and defines a distinct microbial redox level (Mn-reducing conditions) (12). Mn is transformed from the (IV) state as the oxide MnO_2 to the reduced species Mn(II) and can be at reasonably high concentrations in soil solutions (as high as 1 mM) (19). However, the kinetics of electron transfer between the two states is slow at the Pt surface and it is unlikely that the MnO_2/Mn(II) couple affects the Pt electrode potential (14). Also, even if the rate constants were sufficiently large, a layer of Mn(IV)-oxide must be formed at the Pt surface to poise the electrode. Therefore, Mn is predicted not to be important in influencing E_{Pt}, but should still be considered as it is important in microbial transformations.

Nonmetals which exhibit different redox states under normal conditions include N, O, H and S compounds. Nitrogen in the compounds such NO_3^-, NO_2^-, N_2 and NH_4^+ exhibits a number of different redox states (ranging from +5 to -3) and these compounds are commonly at significant concentrations in sub-surface water. However, nearly all redox reactions involving nitrogen of environmental relevance are microbially mediated (16) and the N couples exhibit very slow electron transfer kinetics at the Pt surface (20). These facts suggest that is unlikely that nitrogen species directly influence E_{Pt}.

The effect of oxygen on the Pt electrode potential has been a hotly disputed subject. Although O_2 is known to exhibit slow electron transfer kinetics at the Pt electrode surface (10), formation of $Pt(OH)_2$, PtO or Pt-O (chemisorbed O) at the surface may control E_{Pt} under many conditions (9). Some researchers consider that the Pt electrode potential may be controlled by formation of $Pt(OH)_2 \cdot xH_2O$ phases (9).

Whitfield (9), comparing E_H/pH data from several sources, notes that Pt electrode measurements fall within about 50 mV of the E_H/pH curve for the Pt/Pt-O couple under oxidizing conditions (E_{Pt} > +200 mV). In this case, the Pt electrode is essentially responding to pH (9). However, under anaerobic (reducing) conditions, this direct relationship between E_{Pt} and pH is no longer observed, a Pt-O layer may not be formed, and the Pt electrode is likely responding to other redox couples (9).

When O_2 is added to a complex real system, it would be difficult to determine if it directly affects the Pt electrode (by directly poising the electrode or by forming an oxide layer) or simply oxidizes an existing species which affects E_{Pt}. To add to the complexity, O_2 can react with H^+ (5) to form H_2O_2 which Lemmon (17) used as an oxidant to maintain or raise E_{Pt} in Bashaw soil slurries.

H_2 gas is a common byproduct of microbial reactions such as fermentation and must be considered. At 1 atm pressure (about 0.8 mM in water, calculated with a Henry's Law constant of 0.00079 mol L^{-1} atm^{-1} (21)) and a pH of 0, H_2 poises the Pt electrode and is the basis for the E_H scale. In most environmental systems, concentrations of H^+ and H_2 are substantially lower (in anaerobic samples, dissolved H_2 typically ranges from 0.01 to 10 nM (22) but can be as high as 100 nM for some areas contaminated by chlorinated organics (23)), and in fact probably too low to affect E_{Pt}. Therefore, it is possible that H_2 may have an effect on E_{Pt}, but its low levels in environmental systems suggest that a direct effect is unlikely.

Sulfur in sulfur compounds can exhibit many redox states (e.g., the charge for S ranges from +6 for SO_4^{2-} to -2 for HS^-) and these compounds can be at significant concentration in groundwaters, soils and sediments as to affect the Pt electrode potential.

Berner (1) has conducted experiments in marine sediments which tend to suggest that the sulfur species S^{2-} (or HS^-) in the presence of oxidized S^{2-} (to form polysulfides, e.g., S_5^{2-}) may be responsible for poising the Pt electrode under certain circumstances. The sulfur system is important in microbial transformations, much like iron and manganese, so investigation of sulfur compounds in terms of their effect on E_{Pt} is fully warranted.

In summary, few inorganic species can be identified that could realistically influence the Pt electrode potential in environmental systems based on several facts:

1) low concentrations of inorganic redox-active species

2) low solubility of one species in the redox couple

3) many elements (e.g., important soil species Si(IV) and Al(III)) are found predominately in a single redox state under normal conditions

4) slow electron exchange kinetics at the Pt surface

Carbon species (organic and/or biochemical) are prevalent in a multitude of forms. Carbon compounds are ubiquitous to environmental systems and microbes commonly use them as substrates or electron donors. Many redox-active organic species have been shown to poise the Pt electrode. These species include many different quinones and several thiazine, oxazine and azine compounds (heterocyclic colored compounds referred to as redox indicators) (24). Additionally, microbes use biochemical oxidants and reductants in transformations of environmental redox-active species. Flavin mononucleotide (FMN), for example, can poise the Pt electrode (25). These biochemical species may or may not reach high enough steady-state concentrations

(extra-cellular) to affect E_{Pt}. These species may act as mediators and indirectly affect E_{Pt}.

Of the inorganic species listed, the Fe(II)/Fe(III) system and the S(-II)/S^0 (or polysulfide) systems are the most likely inorganic species to affect E_{Pt} while the N (e.g., NO_3^-, NO_2^-), O (e.g., O_2, H_2O_2), H (e.g., H_2, H^+) and Mn (e.g., Mn(II)) systems must still be considered because of their great relevance in microbial transformations and redox processes. Obviously, carbon (C) species are very numerous in environmental systems. Identification and determination of specific species influencing E_{Pt} would also be a challenging problem.

3.3 Experimental

3.3.1 Instrumentation

Studies were carried out in two different systems. The first system was an open beaker system which contained an unbuffered electrolyte. The second system was an air-tight (anaerobic) bioreactor system which had been developed previously (7, 17) for studies of redox transformations in anaerobic systems. In some cases, pH buffers were used. In both systems, the effects of several different redox species were tested as to their influence on E_{Pt}.

The first test system, the "open system" consisted of a 250-mL Pyrex beaker open to the atmosphere. Typically, about 100 mL of an electrolyte solution and the redox species of interest were added to the beaker. Two Pt-button electrodes (Orion 967800) and a Ag/AgCl double-junction reference electrode (Orion 900200), modified to give the same potential as an SCE electrode, were used to make E_{Pt} measurements. E_{Pt} measurements were taken with a digital voltmeter (DVM) (Fluke Model 8024 B Multimeter). The pH of the system was measured with an OAKTON WD-35615-Series pH/mV/Temperature meter. Only manual stirring was used to homogenize the solution. In experiments with Zobell's solution (Appendix C) in the open beaker system, two Pt-ring electrodes (ORP Pt electrodes, Analytical Sensors, Inc.) were used along with a single Pt-button electrode.

The second system, the bioreactor system illustrated in Figure 3.1, consisted of a 2-L glass bioreactor (Applikon) fitted with a Delrin lid. The Delrin lid had eight

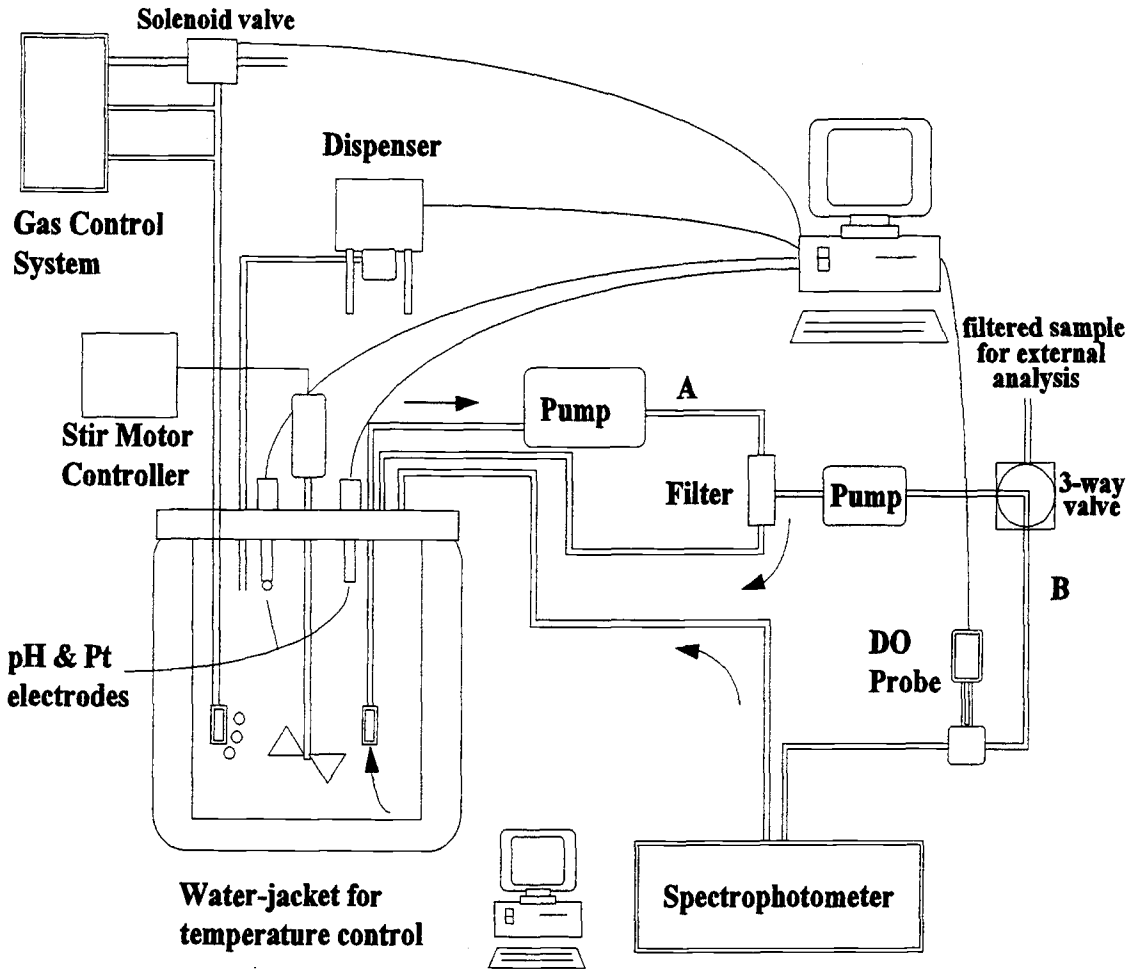

Figure 3.1 Bioreactor system for controlling and maintaining redox conditions, pH and anaerobic integrity. Loop A above refers to the primary loop and loop B above refers to the secondary loop, from which the samples are taken for analysis.

inlet/outlet ports for liquid and gas tubing connections, five electrode ports, and a stirrer shaft port. The bioreactor was equipped with a water jacket and temperature controller bath (Haake FJ temperature controller water bath circulator) which maintained the temperature of the bioreactor solution constant at 25°C.

Under normal operating conditions, the bioreactor system was configured with one or two Pt button electrodes (Orion 967800), a glass pH electrode (Orion 9101BN), a Ag/AgCl double junction reference electrode (Orion 900200), a mechanical stirring system (the motor, Applikon P100; the controller, Applikon ADI 1012) with a plastic propeller, and acid and base dispensing pumps (Fluid Metering, Inc. Micro II-Petter) for pH-statting. When testing the effects of S(-II) on E_{Pt} in the bioreactor, a sulfide electrode (ORION Model 94-16 silver/sulfide electrode) was substituted for one of the Pt electrodes. The stirring shaft was coated with Teflon heat shrink to eliminate contact between the electrolyte (or soil) solution and the metal of the stirring shaft.

In one experiment, a Pt electrode, covered with a filter membrane, was placed in the reactor which allowed only smaller particles and dissolved species to interact with the Pt surface. A 0.65-μm filter membrane (Millipore type DV), cut into a circle approximately 1.5-cm in diameter, was press-fit against the Pt surface by means of a cap-like device (made from a plastic screw cap for a Fisherbrand 7.4-mL vial; a 1-cm i.d. hole was drilled through the middle) which fit over the end of the Pt electrode.

A sophisticated dual pumping system was used to obtain filtered samples from the reactor for analysis of redox species. The system contained a primary and a secondary loop (see A and B in Figure 3.1), which were connected through a cross-flow filter to separate solution from particulate matter in the bulk matrix. The primary loop

consisted of a peristaltic pump (Masterflex speed controller, Easy load pump head 7518-50, Tygon tubing size 14 (1.6-mm id, 5-mm od), 20-30 mL/min) and the cross-flow filter. Solution or slurry was pumped from the reactor, through the cross-flow filter, and back to the reactor in a continuous cycle. The filtered reactor solution was pumped by a secondary pump (FMI Model RHV) from the outlet of the cross-flow filter through a four-way switching valve (Upchurch Scientific, model V•100D) from which a reactor sample could be taken. The filtered solution was then pumped back to the bioreactor. With the exception of a 20-cm section of Tygon tubing in the primary loop, all tubing was PEEK (polyetheretherketone) tubing which was selected because of its low oxygen permeability. For the primary loop, 1/8"-OD tubing was used and 1/16"-OD tubing was used in the secondary loop. All tubing connections were made with Upchurch fittings (normally 1/4-28).

For some studies, a Clark polarographic electrode (Orion 970800) for determination of dissolved oxygen concentration and a Pt electrode with an internal reference electrode (Analytical Sensors, Model OR101431-03-B) for redox measurements were placed in-line in the secondary loop. Both electrodes were placed in specially made flow-through electrode holders to allow interaction with the filtered solution.

The cross-flow filter consisted of a two-piece Delrin casing, which sandwiched a series of filters and meshes, and was held together by bolts (Figure 3.2 a). A conceptual schematic of its function is shown in Figure 3.2 b. A Durapore filter (Millipore, 0.65 μm) was used as the primary filter, which itself was sandwiched between two mesh

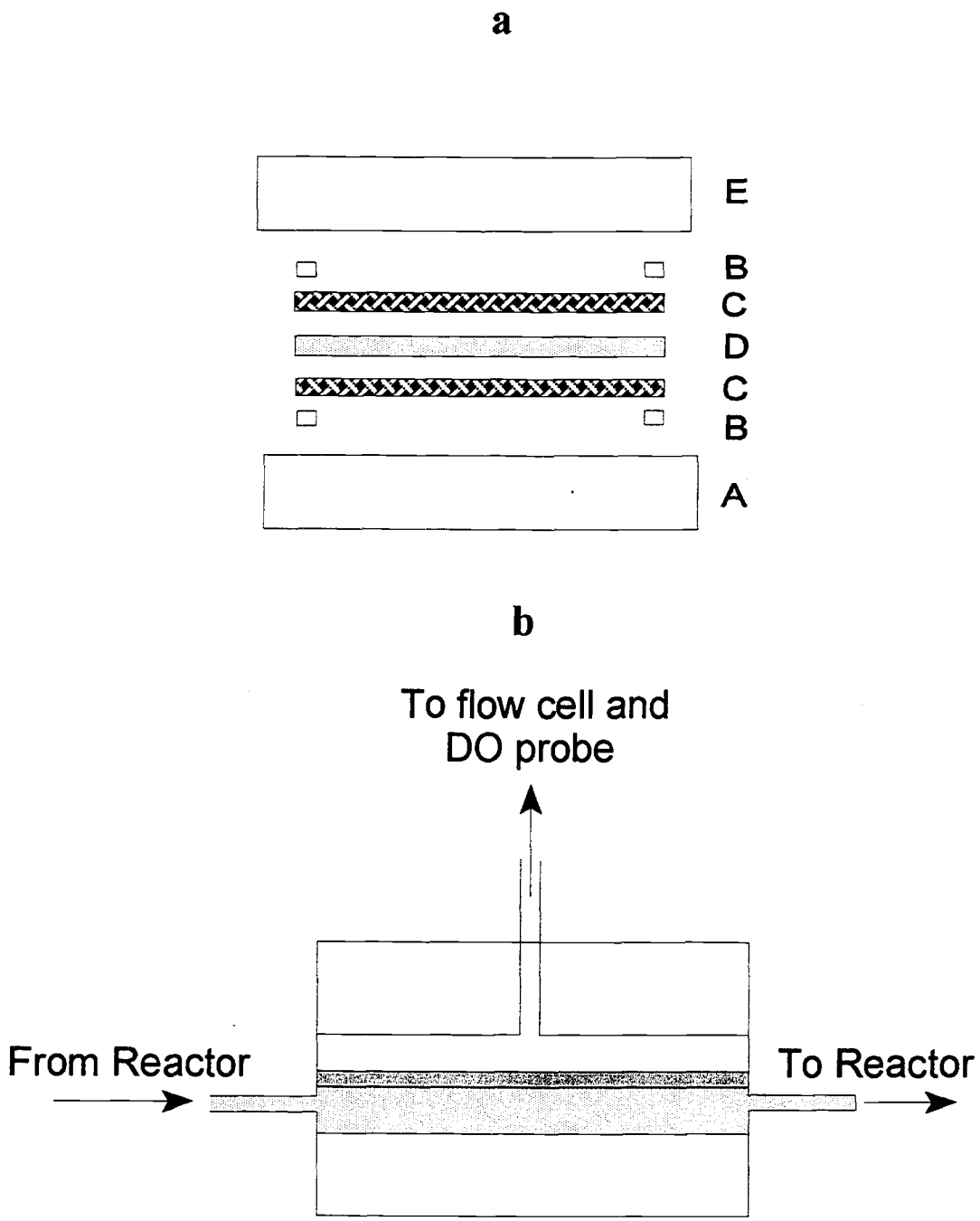

Figure 3.2 Assembly of cross-flow filter (a) and conceptual design (b). (a): (A) filter holder inlet side; (B) Teflon ring; (C) fluorocarbon mesh; (D) Durapore filter; (E) filter holder outlet side; (b) conceptual diagram of cross-flow filter which separates solution from soil particles in the biogeochemical matrix.

filters (Spectra-Mesh fluorocarbon, 70 μm). Additionally, Teflon rings (PTFE, 0.005" thick) were placed between the mesh filters and the Delrin casing to minimize solution leakage.

The cross-flow filter module was placed in a sonicator bath (Bransonic 52) which was turned on for 15 min and off for 15 min at regular intervals. This helped to prevent clogging by soil particulates in the cross-flow filter. A computer-controlled solid-state relay switch was used to turn the sonicator on and off. The details of its construction are located in Appendix A.

Normally pre-purified N_2 gas was used to purge O_2 from bioreactor samples and to maintain the anaerobic integrity of the system. The gas control portion of the system consisted of a Tylan RO-28 readout and control box and three Tylan FC280 mass flow controllers. In previous studies, CO_2 and O_2 were used as input gases. An oxygen trap (Alltech Oxy-Trap 4001) and an indicating O_2 trap (Alltech 4004) were placed in the N_2 flow line between the gas cylinder and the mass flow controller to eliminate any residual O_2. At the outlet for the N_2 gas system, a 10-μm filter (Upchurch Scientific UHMWPE solvent filter, A•426) was used for gas sparging.

Samples were drawn from the external loop for determination of Fe(II) and Mn(II). Spectrophotometric measurements for Fe(II) (with the 1,10-orthophenanthroline (OP) method, Appendix B) were made with a Hewlett Packard 8452A diode array spectrophotometer. Mn was measured with a Buck Scientific flame atomic absorption spectrophotometer under standard conditions. About 10 μL of HCl(c) was added to 2 mL of sample to preserve samples until analysis.

3.3.2 Interfacing and software

The bioreactor system was interfaced to a 386 PC equipped with a multiplexed ADC and I/O board (Computer Boards Inc., CIO-AD08-PGA), which includes eight differential A/D channels and four digital output ports. The differential channels were used to take potentiometric measurements and the output ports controlled the acid/base dispensers via solid-state relays. The electrodes and dispensers were connected to the computer board with a custom made interface box via BNC or banana connectors (15). The pH and reference electrodes were first connected to a pH meter (Chemtrix Type 60A) and from there to the interface box. The original system was modified by the addition of a computer I/O board (Computer Boards Inc., CIO-DIO24) to allow for control of the sonicator. An output line from the board was connected directly to a solid-state relay (Appendix A) which turned the sonicator on and off at computer-controlled timed intervals.

The computer program which controls the bioreactor functions is written in QuickBASIC 4.5. It primarily controls the rate of addition of acid/base or oxidant/reductant to maintain or change the pH and/or E_{Pt} to a given level, calculates the buffer capacities, takes electrode readings at predetermined time intervals (normally every 15 min, but this can be varied) and allows the user general control of these parameters. Additionally, it allocates this information to a series of data files which can be retrieved for later use. All reported potentials are corrected for the potential of the reference electrode (0.242 V). Modifications of the original computer program (26) included a subroutine for control of the sonicator and a subroutine for E_{Pt} measurements

with a second Pt electrode. The sonicator subroutine controls the solid-state relay switch which turns the sonicator on and off. The on/off times for the sonicator are operator-defined at the start of the program. The subroutine for the second Pt electrode is nearly identical to that of the first, except that it sends this information to a separate file and displays the E_{Pt} readings on a different part of the computer screen.

3.3.3 Chemicals and solution preparation

A 0.05 M Fe(II) solution in 0.1 M $HClO_4$ was prepared from hydrated ferrous perchlorate crystals ($Fe(ClO_4)_2 \cdot 6H_2O$, G. Frederick Smith Chemical Co.) and 70% $HClO_4$ solution (Mallinckrodt, Inc.). Fe(II) measurements were made with the 1,10-phenanthroline (OP) method (see Appendix B) and based on a calibration with a blank and a 50 mg/L (89.5 μM) Fe(II) standard. Hydroxylamine hydrochloride (10% w/v in water) and the 50 mg/L Fe(III) standard were prepared by Dean Johnson of Oregon State Department of Chemistry. A 0.5 % (w/v) OP solution in water was prepared by Dean Johnson, although eventually a 0.5% standard was made in-house with solid OP (Aldrich). $FeCl_3 \cdot 6H_2O$ (Mallinckrodt, Inc.) was used as an Fe(III) source.

For sulfur species, $Na_2SO_4 \cdot 10H_2O$ (Baker & Adamson) was used as a sulfate source, anhydrous Na_2SO_3 (Mallinckrodt, Inc.) as a sulfite source, and sodium sulfide, $Na_2S \cdot 9H_2O$ (Manckrodt, Inc.), as a sulfide source. Elemental sulfur, S^0, was also obtained from Mallinckrodt, Inc. Sodium hydrosulfite (dithionite), $Na_2S_2O_4$ (Sigma, 80% pure), was used as a $S_2O_4^{2-}$ source. In one particular experiment, $Cu(NO_3)_3 \cdot 2.5H_2O$ (Mallinckrodt) was used to precipitate S^{2-}.

A variety of other redox species were tested as to their effect on E_{Pt}. These are presented in Table 3-1.

Chemicals used to prepare buffers for various experiments included sodium phosphate dibasic heptahydrate, $Na_2HPO_4 \cdot 7H_2O$, and sodium phosphate monobasic, NaH_2PO_4, (Mallinckrodt, Inc.), or TRIZMA hydrochloride (Sigma). Concentrated HCl (Mallinckrodt, Inc.) and 6 M NaOH to adjust the pH, generally after dilution with DI water to 1 or 0.1 M. KCl and NaCl (both Mallinckrodt), or $CaCl_2 \cdot 2H_2O$ (Baker) were used to adjust the ionic strength. Zobell's solution (0.0033 M in each (27)) was prepared from $K_3Fe(CN)_6$, $K_4Fe(CN)_6$, and KCl, all obtained from Mallinckrodt, Inc., as outlined in Appendix C.

3.3.4 Bashaw soil samples

Soil samples were taken from the Jackson Frazer Wetlands north of Corvallis, OR. and processed as described by Lemmon (17). The type of soil used was a Bashaw A1 type soil which was high in clay content (52% w/w), high in organic carbon content (12.5 % w/w), and had a dithionite-citrate extractable Fe and Mn concentrations of 1.7 and 0.2 %(w/w), respectively. This particular sample of soil had been subject to a variety of natural reducing and oxidizing conditions in the field, characteristic of the seasonal flooding and redox cycling in the area.

As described by Lemmon (17), the soil samples were air dried, crushed with a rolling pin, sieved through a 2-mm mesh, and later pulverized with a mortar and pestle. The pulverized soil was then re-sieved once with a 0.5-mm mesh and then twice with a

Table 3.1 Some other redox species tested as to their effect on E_{Pt}

species tested	chemical	source	comments
NO_3^-	$NaNO_3$(s)	Mallinckrodt	added as solid
NO_2^-	$NaNO_2$(s)	Baker & Adamson	added as solid
NH_4^+	NH_4Cl(s)	EM Science	added as solid
Mn(II)	$MnSO_4 \cdot H_2O$(s)	Mallinckrodt	added as solid
O_2	dissolved O_2 in DI water	equilibrated with atmospheric O_2	added in 1-5 mL aliquots
H_2O_2	30% H_2O_2 in water	Mallinckrodt	OB[a] ; estimated to be 9.79 M[b]
formaldehyde	formalin (37% (w/w) in H_2O/methanol)	Mallinckrodt	added as solution
hydroquinone	(same)	Eastman	added as solid
anthraquinone 2,6-disulfonic acid	(same)	Aldrich	added as solid
ubiquinone	(same)	Aldrich	OB; added as solid; AR[c]
glutathione	(same)	Sigma	OB; added as solid; AO[d]
humic acid	(same)	Aldrich	added as solid; AR
NAD	(same)	Sigma	OB; added as solid
NADH	(same)	Sigma	OB; added as solid
pyruvic acid	(same)	Mallinckrodt	OB; added as solid
L-lactic acid	(same)	Mallinckrodt	OB; added as solid
fumaric acid	(same)	Aldrich	OB; added as solid
succinic acid	(same)	Aldrich	OB; added as solid

[a] tested in open beaker system only
[b] also used as statting oxidant for bioreactor experiments (diluted to 1.0 M)
[c] attempted to produce reduced form of compound by reduction with Fe(II) for ubiquinone or 100% $H_{2(g)}$ (Industrial Welding Supply) and Pd catalyst (coated on alumina, Sigma) for humic acid
[d] attempted to produce oxidized component with H_2O_2

0.25-mm mesh. The very fine consistency of the final sample was necessary to prevent clogging of the primary loop of the reactor, which tended to occur when larger particles and organic roots were not eliminated.

For the reactor experiments, 50 g of this sieved Bashaw soil sample were added to 1 L of DI water with 10 mmol of $CaCl_2$ to increase the ionic strength. The final soil/water ratio was 1:20 (w/w). Also, 2 mmol of NH_4Cl were added as a nitrogen source. Because several reactor experiments were performed over a long period of time, two different Bashaw soil samples were taken from the field.

3.3.5 Evaluation of effects of individual redox species and couples on E_{Pt}

Several redox-active species were first tested in the "open beaker" system to determine if they had any obvious effect on E_{Pt}. Species were added directly to an electrolyte solution (50 to 100 mM $CaCl_2$ or KCl in DI water) and E_{Pt} readings were taken before and after the additions. The pH was adjusted manually by addition of 1.0 M HCl or 1.0 M NaOH. All redox species which had a significant effect on E_{Pt} were later tested in the bioreactor system under deareated conditions.

In the bioreactor, the system was closed to the atmosphere and purged of O_2. E_{Pt} readings were taken before and after addition of a given species, at intervals varying from every 30 s to every 15 min, often for well over a 2-hr time period. Solution additions to the bioreactor were made via a syringe through the septum of a Mininert valve (Alltech model 95246) which was screwed into an input port of the Delrin reactor lid. To make additions of solid redox species, this valve was momentarily unscrewed

and species were added directly to the reactor solution. The valve was then immediately refitted into the port to maintain the anaerobic integrity of the system. In general, the solution was sparged with N_2 gas at a rate of 50 - 100 mL/min, unless a particular species was expected to partition strongly into the gas phase (e.g., S(-II) lost as H_2S). All experiments of this type were performed at pH 7.0 with a 0.1 M phosphate buffer or a 50 mM TRIZMA buffer.

To simulate natural redox conditions in the environment, the soil slurry described was used as the matrix. The soil slurry was placed in the bioreactor, closed to the atmosphere by fitting of the reactor lid, and purged of O_2. Computerized addition of 1.0 M HCl and 1.0 M NaOH was used to control the pH at 7.0, unless otherwise stated. In general, E_{Pt} fell naturally due to the purging of O_2 and microbial activity, achieving reducing conditions similar to that which would be found in a field or a soil pore water system. Redox species were added during periods when E_{Pt} appeared poised (unchanging) and at test E_{Pt} levels at which a change in concentration of that species should affect E_{Pt} (in some cases, E_H-statting with H_2O_2 was used to establish a given E_{Pt}. Often, the test species was already at appreciable concentrations in the soil solution (e.g., Fe(II) or Mn(II) under reducing conditions). If possible, the concentration of a given redox-active species was monitored before and after the addition of that species.

In conjunction with soil E_{Pt} experiments, a separate Pt electrode was occasionally placed in the external loop of the reactor to interact with filtered solution. In some other experiments, the Pt electrode covered with a membrane or the effect of stirring in the bioreactor on E_{Pt} was also evaluated.

3.3.6 Iron system

Several experiments were performed in a variety of simple electrolyte and soil slurries to note the effect of the Fe(II)/Fe(III) couple on the Pt electrode response. In open system studies (i.e., "beaker" studies), 1 mL of a 0.5 M Fe(II) in 0.1 M $HClO_4$ was combined with 4.5 g of NaCl in the beaker and diluted with DI water to approximately 100 mL, forming an Fe(II) solution of approximately 5 mM. A 26-μL aliquot of 30% H_2O_2 solution was added to the Fe(II) solution with an automatic 1000-μL pipet (Rainin EDP-2 electronic digital pipette) to oxidize approximately half of the Fe(II) to Fe(III), creating an Fe(II)/Fe(III) couple. The pH was measured to be ~3. E_{Pt} measurements were taken and the pH was subsequently raised to ~ 7 by additions of 1.0 M NaOH with the same pipet.

In several bioreactor experiments, the test solution consisted of 0.05 M KCl as an electrolyte and ~0.05 M TRIZMA buffer to at pH 7.0 unless stated otherwise. Phosphate buffer could not be used as it tended to precipitate out the Fe(II) as $Fe_3(PO_4)_2$. The Fe(II) was added over time with a 100-μL syringe (Hamilton, GASTIGHT #1801) from a deaerated solution of 0.5 M Fe(II) in 0.1 M $HClO_4$, in increments ranging from 50 to 500 μmol. E_{Pt} measurements were taken throughout these experiments usually at intervals ranging from 1 to 15 min. Fe(II) samples were taken from the external loop and quantified with the OP method. In general, significant time (hours) was allowed for the Fe(II) level to stabilize before the Fe(II) was measured.

In one particular experiment, OP was added to an Fe(II)-electrolyte solution in the bioreactor to determine the effect of complexing the Fe(II) in solution. In this

complexation reaction, three OP molecules complex one Fe(II) ion. Approximately 1000 μmol of OP were added to the reactor to completely complex the Fe(II). Subsequent additions of Fe(II) and then OP were made as E_{Pt} was monitored throughout the experiment.

To deposit a layer of Fe(III)-hydroxide on a Pt surface, a flat-bottomed Pt electrode was placed overnight in a 100-mL plastic beaker containing 25 mL of a 0.1 M Fe(II) solution made from $Fe(ClO_4)_2 \cdot 6H_2O$. The pH of this solution was neither adjusted nor measured. By the next day, a brownish-yellowish solid film, believed to be lepidocrocite (2), was deposited on the Pt surface. This Pt electrode was then placed into an electrode holder of the bioreactor in a deaerated 1-L solution of pH 7.0 buffer. At this point, Fe(II) additions were made to the solution to note the effect on E_{Pt}. Fe(II) was quantified periodically with the OP method. In a separate experiment, approximately 300 μmol of Fe(III) were added as solid $FeCl_3 \cdot 6H_2O$ to a deaerated solution of about 300 μM Fe(II) in a pH 7.0 buffer in the bioreactor as E_{Pt} was monitored.

The effects of Fe(II) and Fe(III) additions on Pt electrode potential in Bashaw soil slurries were investigated in the bioreactor under anaerobic conditions, a controlled pH of 7.0, and constant E_{Pt} (poised) or falling or rising E_{Pt}. In a series of separate experiments, involving different Bashaw soil fractions (from the same original sample), Fe(II) was added (in aliquots ranging from 0.1 to 2.5 mmol) at reducing soil slurry E_{Pt} values ranging from -160 to +200 mV (all values reported vs. SHE). In general, Fe(II) was quantified with the OP method before and after addition of the Fe(II). Approximately 1 mmol Fe(III) was added at +65 mV and at -60 mV as solid

$FeCl_3 \cdot 6H_2O$. In some cases, computerized E_H-control was used to maintain the potential of the Pt electrode at a given value before addition of Fe(II) or Fe(III).

3.3.7 Sulfur system

The effects of several sulfur species including sulfate, sulfite, dithionite and sulfide on Pt electrode potentials were tested in both the open system and bioreactor system. In both the open beaker studies and in the bioreactor studies, the concentrations of sulfur species were not determined before or after additions.

In open beaker studies, a pH 7, 0.1 M phosphate buffer in DI water containing 4.5 g of NaCl was used. To test the SO_4^{2-}/SO_3^{2-} couple, the concentrations of SO_4^{2-} and SO_3^{2-} were adjusted to 1 mM each. The concentration of each species for evaluating the $SO_3^{2-}/S_2O_4^{2-}$ and $S_2O_4^{2-}$/S(-II) couples was 5 mM for all species except S(-II). The S(-II) was added from a saturated S(-II) solution in contact with solid $Na_2S \cdot 9H_2O$, which had saturated with water over time. The total concentration of reduced sulfur species (i.e., S^{2-}, HS^-, $S_2O_3^{2-}$ and $S_2O_4^{2-}$) in this solution was estimated to be 2.5 M, from an iodine endpoint titration method (see Appendix D). (However, later evidence indicated that only a very small proportion of the solution remained as sulfide species (28), most likely from oxidation by O_2 over time). For the experiment with the $S_2O_4^{2-}$/S(-II) couple, 1 mL of this solution was added to the 100 mL sample to yield nominally 25 mM of total reduced sulfur species. Stirring was done manually by gently swishing the contents of the beaker.

In bioreactor experiments (deaerated, buffered to pH 7 with 50 mM phosphate buffer in DI water), the effect of S(-II) on E_{Pt} was monitored. In this particular experiment, the sulfide electrode (ORION Model 94-16 silver/sulfide electrode) was substituted for one of the Pt electrodes. A 25 mL solution of 0.1 M total sulfide was made in a volumetric flask from 0.6 g (0.025 moles) of $Na_2S \cdot 9H_2O$ and DI water. Next, 1 mL of this sulfide solution (100 μmol) was then added to the deaerated reactor solution, and both E_{Pt} and E_{S2-} (the potential of the sulfide electrode) were monitored over time. After approximately 5 hr, 100 μmol of Cu(II), as $Cu(NO_3)_2$, were added to precipitate the S(-II) as CuS.

Sulfur compounds were tested in bioreactor soil slurries at a variety of steady-state potentials. Additions of 1 mmol SO_4^{2-} (as solid Na_2SO_4) were assumed to greatly increase the soluble sulfate in the system because sulfate concentrations are normally in a range of 0.1 - 1 mM in most soil systems (29). For sulfite tests, 1.5 mL of a deaerated solution of 0.5 M Na_2SO_3 in DI water were added (approximately 0.75 mmol SO_3^{2-}). A 0.1 M dithionite stock solution was made from 1.741 g of solid $Na_2S_2O_4$ diluted to 100 mL in a volumetric flask with DI water. The solution was then deaerated with N_2. With a 10 mL syringe (B-D), 10 mL of this solution (1 mmol dithionite) were then injected into the bioreactor via the septum. After 2 hr, 9 mL of the solution was injected into the bioreactor. Sulfide was added to the reactor as the saturated sulfide solution previously described, at four different E_{Pt}'s ranging from +43 to -250 mV.

3.3.8 Oxygen system

A series of O_2 additions were made to the reduced soil slurries at potentials ranging from -78 to -75 mV by adding 10 to 30 mL of O_2-saturated DI water (approximately 2 μmol O_2/10 mL DI water). Dissolved O_2 was not directly measured during these experiments.

H_2O_2 was tested in the open beaker system by making 100 μL additions of 30% (v/v) H_2O_2 solution (9.79 M) to an electrolyte solution containing 4.5 g of NaCl and 100 mL of DI water. In previous work with bioreactor soil slurries, H_2O_2 was used as an oxidant for E_H control and a typical response will be discussed.

3.3.9 Nitrogen and Manganese systems

Other inorganic species tested in soil slurries in the bioreactor under anaerobic conditions at pH 7 were nitrate (1 mmol added), ammonium ion (1 mmol added) and Mn(II) (1 mmol added). For Mn(II), duplicate samples were collected 1 hr prior to the addition of 0.169 g of $MnSO_4 \cdot H_2O$ the Mn(II), and every hour for 5 hr thereafter. Mn in the samples was then quantified with flame AAS.

3.3.10 Organic systems

Various organic species were tested as to their effect on E_{Pt}, both in the bioreactor and open beaker systems. In open beaker experiments at pH 7, NAD/NADH (0.5 mM each), pyruvic acid/L-lactic acid (5 mM each) and fumaric/succinic acid (5 mM

each) couples were tested. Humic acid (0.2 g each, oxidized and reduced species), ubiquinone (1 mM each) and glutathione (1 mM each) were also tested.

In soil reactor experiments, additions were made at E_{Pt} values ranging from -75 to +290 mV. For additions at E_{Pt} values of 0 mV or above, E_{Pt}-statting with H_2O_2 was used. Species added included humic acid (oxidized, 0.5 g), ubiquinone (oxidized, 0.5 mmol), formaldehyde (added as Formalin, approximately 0.2 mL, 2.7 mmol), anthraquinone 2,6-disulfonic acid (0.206 g, 0.5 mmol), and hydroquinone (0.5 and 1 mmol).

3.3.11 Effect of physical properties on E_{Pt}

Several additional Pt electrode experiments were performed to evaluate the effects of a membrane at the Pt surface, filtering the soil slurry, stirring, and cleaning the electrode surface. The potential of a membrane-covered Pt electrode was monitored along with the E_{Pt} of the uncovered Pt electrode with a soil slurry sample.

In a series of experiments, an uncovered Pt electrode was taken out of the reactor containing a reduced soil slurry, cleaned with Alkonox detergent, rinsed in DI water, soaked in 1 M HCl for 10-15 min, and re-rinsed with DI water. At this point, the Pt electrode was either placed immediately back in the reactor, or allowed to sit out in the open air for 1, 2 or 12 hr before returning it to the reactor. In one case, the Pt electrode was placed in a solution of 0.5 M Na_2SO_3, a reducing agent, for 1 min immediately after cleaning, rinsed with DI water, and placed immediately back in the reactor. In all cases, E_{Pt} was then monitored in 1-min intervals for roughly 1 hr.

To evaluate if the oxide layer on a Pt electrode can be removed by the physical effect of particulate "bombardment" of the Pt surface, two equivalent Pt electrodes were cleaned in 3% H_2O_2 solution for 10 min, rinsed with DI water, and allowed to sit in open air for 24 hr, to develop an oxide layer on the surface of the Pt. Then 1 L of 50 mM phosphate buffer at pH 7 was purged in the bioreactor with N_2 to remove O_2. The stirring rate was ~100 rev/min. The Pt electrodes were then fitted into the bioreactor lid and E_{Pt} was monitored for 3 days. After 3 days, 50 g of bath sand (assumed to be non-redox active) used in sonicators were added to the bioreactor. E_{Pt} was monitored for the next 4 days at which point the reactor was opened to the atmosphere to allow O_2 saturation of the water (the N_2 purge was then turned off). E_{Pt} was then monitored for approximately 1 more day.

3.3.12 Experiments with Zobell's solution

Two separate experiments were conducted with Zobell's solution to determine the effect of the concentration of the redox-active species and the ionic strength on E_{Pt}. In the first experiment, E_{Pt} was monitored while a given quantity of Zobell's solution was diluted sequentially. First, 100 mL of a 3.3 mM Zobell's solution (see Appendix C) were placed in an 800-mL beaker along with three Pt electrodes and a Ag/AgCl reference electrode (the one used in reactor experiments). One electrode had been used previously in reactor experiments and was an Orion Model flat-bottomed combination redox electrode. The other two Pt electrodes were single ORP Pt-ring electrodes (Analytical Sensors, Inc., of which one had been used only recently for beaker experiments and the

other had never been used). Initial E_{Pt} readings were taken and the solution was diluted by sequential addition of 20 mL increments with DI water until the beaker was full. At this point, the excess solution was poured out until 100 mL of the solution was left in the beaker and the dilution was repeated. During this time, E_{Pt} readings were taken every minute, allowing for equilibration of the reading. This process was repeated until the Pt electrodes

in the beaker were no longer poised. Concentrations of the ferric and ferrous cyano species and the ionic strength were then calculated to find lower limits for poising of the electrodes.

A Zobell's solution 0.1 M in both Fe species was prepared for the second experiment. Next, 10 μL aliquots of this solution were added to 1 L of a deaerated, 0.1 M NaCl solution into the bioreactor while monitoring E_{Pt} until poising of the two Pt electrodes occurred. The ionic strength was maintained at 0.1 M.

3.4 Results and Discussion

3.4.1 Effect of iron species on E_{Pt}

At low pH, Fe(III) is soluble and the Fe(II)/Fe(III) equilibrium potential is +0.71 V for an equimolar composition and is theoretically independent of pH. However, at higher pH (roughly above pH 3 and Fe(III) concentrations > 100 μM (30)), Fe(III) begins to precipitate as amorphous $Fe(OH)_3$ and the activity of the Fe(III) species in the Nernst equation becomes unity. When Fe(III) is predominantly in the solid phase, the equilibrium potential becomes a function of the Fe(II) concentration, pH, and the type of Fe(III)-solid phase which coexists with the Fe(II). Information about some common Fe(III)-oxides is summarized in Table 3.2.

Table 3.2 Summary of Fe(III)-solid/Fe(II) redox reactions

solid name	chemical formula	redox reaction	E^0 (V) (ref)
ferrihydrite	$Fe(OH)_3$(am)	$Fe(III)(OH)_3 + 3\ H^+ + e^- \rightleftharpoons Fe(II) + 3\ H_2O$	1.057 (12)
lepidocrocite	γ-FeOOH	$Fe(III)OOH + 3\ H^+ + e^- \rightleftharpoons Fe(II) + 2\ H_2O$	0.965 (2)
geothite	α-FeOOH	$Fe(III)OOH + 3\ H^+ + e^- \rightleftharpoons Fe(II) + 2\ H_2O$	0.80 (31)
hematite	α-Fe_2O_3	$Fe(III)_2O_3 + 6\ H^+ + 2\ e^- \rightleftharpoons 2\ Fe(II) + 3\ H_2O$	0.728 (2)

The amorphous Fe(III)-hydroxide phase known as ferrihydrite is an immediate product of oxidation of Fe(II) to Fe(III) at moderate pH. Lepidocrocite can also be formed by oxidation of Fe(III) by O_2 (2). Over time, Fe(III) solids form more ordered

states, including the geothite and hematite. The standard potential (E^0) is different for each solid phase. The potential for the Fe(II)/Fe(III)$(OH)_3$ couple at a given pH is given by

$$E_{Fe(II)/Fe(III)-solid} = E^0 - 0.177pH - 0.059\log a_{Fe^{2+}} \qquad (3\text{-}6)$$

for a temperature of 298 K (Appendix F). For calculations in this chapter, Fe(II) concentration will be substituted for Fe(II) activity. The sum of the first two terms is the formal potential ($E^{0'}$) at a given pH, and at pH 7, $E^{0'}$ is -0.182 V for ferrihydrite and -0.274 V for lepidocrocite. Application of the Nernst equation to calculate the redox potentials of these Fe(II)/Fe(III) systems is complicated by the possibility that more than one phase may be present. The value of $E^{0'}$ and even the pH dependence may be a function of more than one phase.

In open beaker studies at pH 3, both Pt electrodes placed in the ~0.25 mM/~0.25 mM Fe(II)/Fe(III) solution were well poised at +609 mV (a value different from the standard potential of +0.71 V was expected because the concentrations were approximate and the ionic strength was significant). When the pH was increased by subsequent additions of NaOH, the Pt electrodes were no longer poised and E_{Pt} decreased as solid $Fe(OH)_3$ particles were observed to flocculate and gradually settle out at the bottom of the beaker. At pH 7, E_{Pt} for both electrodes drifted between +100 to +150 mV.

Several studies were conducted to determine the effect of Fe(II) and Fe(III) on E_{Pt} in deaerated electrolyte solutions in the bioreactor. When 50 μmol of Fe(II) was added to a deaerated electrolyte solution, E_{Pt} fell rapidly from about +225 to +25 mV, as shown in Figure 3.3A. Comparatively, additions of 100 μmol Fe(II) at 16 hr and 300 μmol Fe(II) at 35 hr had a far less dramatic effect. In Figure 3.3B, the effects of additions of Fe(II) on

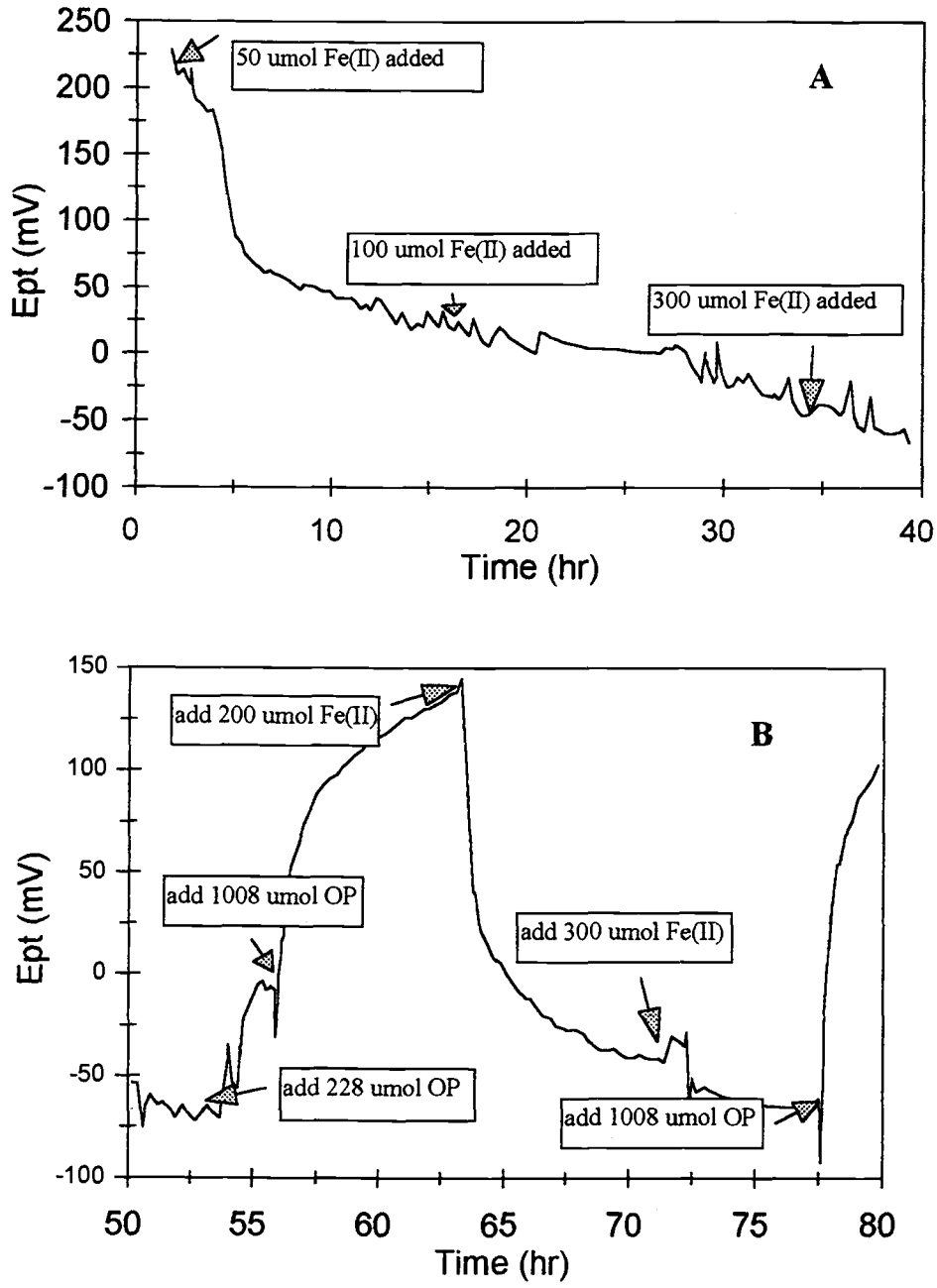

Figure 3.3 Effect of additions of Fe(II) (A) and orthophenanthroline (B) on E_{Pt} in anaerobic bioreactor solutions at pH 7. Initially, additions of Fe(II) to the reactor solution cause E_{Pt} to fall rapidly. Complexation of the Fe(II) with the orthophenanthroline (OP) gives rise to a reversal of this effect.

E_{Pt} were reversed by the addition of the Fe(II)-complexing agent, orthophenanthroline (OP). OP added at 52.5 and 55 hr (a total of over 1200 μmol) completely complexed the Fe(II) and the potential increased back up to about 140 mV. A subsequent addition of 200 μmol Fe(II) again lowered E_{Pt} to about -50 mV. Consistent with the results in Figure 3.3A, addition of 300 μmol Fe(II) near -50 mV had little effect on E_{Pt}. At 75.5 hr, addition of 1008 μmol OP again reverses the effect of Fe(II) on E_{Pt}. These results demonstrate that Fe(II) has a substantial and direct effect on E_{Pt} in the absence of other redox species, and this effect can be reversed by the addition of a complexing agent.

Figure 3.4 illustrates the effect of higher Fe(II) concentrations (> 350 μM) on the potentials of two Pt electrodes in a deaerated bioreactor solution. Between 350 μM (~ log 2.6) and 630 μM (~ log 2.8) Fe(II), E_{Pt} decreased by over 75 mV to about -150 mV. With further increases in Fe(II) levels, the potential remained relatively constant between -125 and -175 mV. Throughout the experiment, the two potentials tracked one another, but they always differed significantly. At Fe(II) concentrations less than 500 μM, the difference in potential was approximately 50 mV, but at higher Fe(II) concentrations this difference decreased to approximately 25 mV. The observed recovery of 60 - 70 % (OP method) may be due to adsorption of some of the added Fe(II) adsorbs on the walls of the bioreactor or on previously formed Fe(III)-hydroxides.

The equilibrium potentials corresponding to the Fe(II)/ferrihydrite couple and Fe(II)/lepidocrocite couple are also shown in Figure 3.4. Neither model fits the data well although the lepidocrocite model predicted E_{Pt} values closer to observed values. No obvious sign of an Fe(III)-oxide layer was observed on the two electrodes after the experiment.

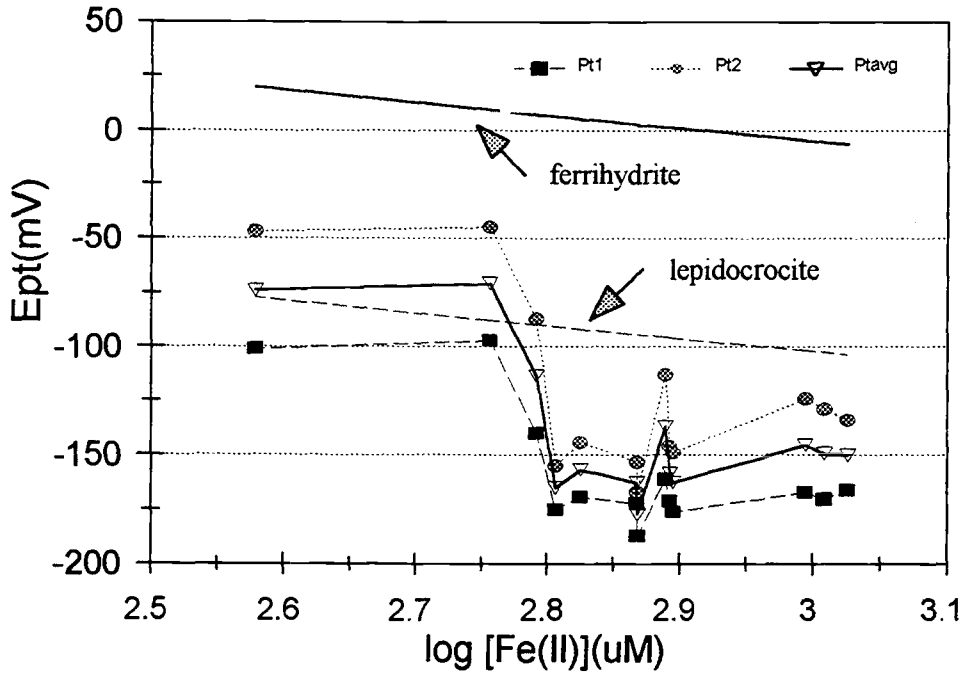

Figure 3.4 Dependence of E_{Pt} on Fe(II) concentration in a purged bioreactor at pH 7. Fe(II) was quantified with the 1,10-phenanthroline method. There is little correlation between measured E_{Pt} and E_H values calculated based on the ferrihydrite or lepidocrocite Fe(III)-solid phases and the known Fe(II) concentration (equation 3-6 with $E^{0'}$ values specified in Table 3-2). The electrolyte was 0.05 M KCl and 0.05 M TRIZMA buffer at pH 7.

Figure 3.5 shows that the potential of a Pt electrode covered with a yellowish layer of $Fe(OH)_3$ at pH 7.0 varied little (-70 to -85 mV) with Fe(II) concentration in the range of 0.030 to 3 mM. As shown by the theoretical plots based on the ferrihydrite and lepidocrocite Fe(III)-solid models, E_{Pt} should have changed by about 120 mV over the two orders of magnitude in Fe(II) concentration if equilibrium models applied. Doyle (2) observed a Nernstian response (correlating to the lepidocrocite model) under similar conditions. The reason for the lack of agreement with Doyle's results is not known. One possibility is that a significant amount of Fe(II) was adsorbed into the Fe(III)-coating as it was forming, creating an effective "buffer" for Fe(II) at the Pt surface. Under these conditions the Pt electrode would respond only very slowly to changes in the bulk concentration of Fe(II) in solution, as the Fe(II) at the Pt surface came to equilibrium with that in the bulk. To test this hypothesis, one might vary the stirring rate in the reactor to note how quickly E_{Pt} changes (it would be expected that E_{Pt} would change more rapidly at higher stirring because of the greater mass transfer rate of Fe(II) to the Pt surface.

Additions of $FeCl_3 \cdot 6H_2O$ to a deaerated solution of 300 μM Fe(II) in the bioreactor ($E_{Pt} \approx$ -130 mV) did not bring about deposition of a visible layer of $Fe(OH)_3$ on the surface of the Pt or change E_{Pt} substantially. However, the Pt electrode was only left in the bioreactor for about 10 min after the addition.

Most additions of Fe(II) to Bashaw soil slurries at a variety of E_{Pt} values had little permanent effect on E_{Pt}. These results are summarized in Table 3.3. As shown in Figure 3.6A, the addition of 2.5 mmol of Fe(II) to a soil slurry at -163 mV and pH 7.0 resulted in a large momentary increase in E_{Pt}. However, this change is attributed to the rapid

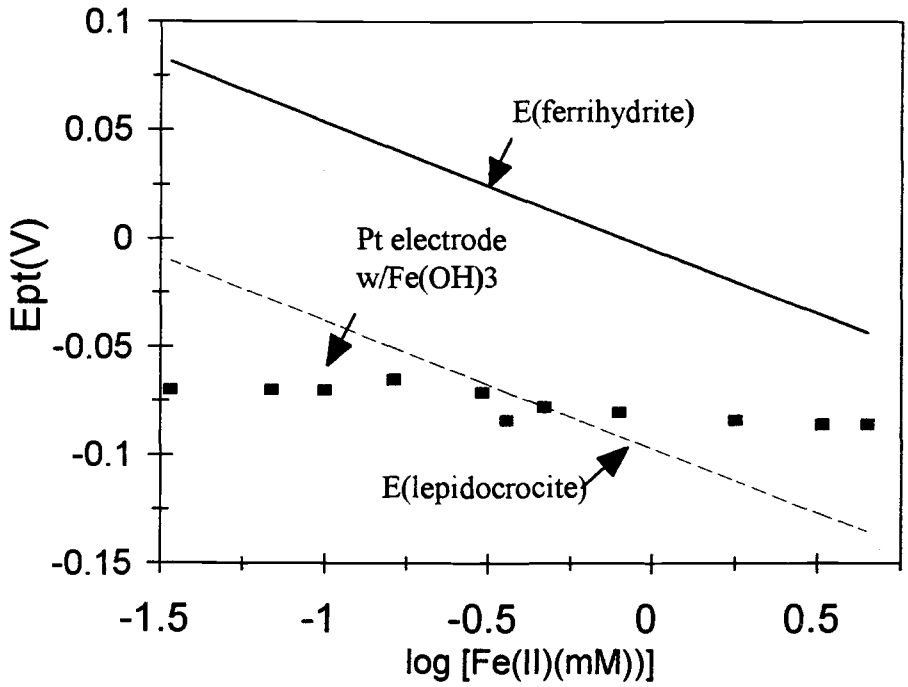

Figure 3.5 Pt electrode response to Fe(II) when the Pt surface is covered with an $Fe(OH)_3$ layer. The pH is buffered at 7.0 and the Fe(II) concentration was determined with the 1,10-orthophenanthroline method. The theoretical lines are based on equation 3-6 and the measured [Fe(II)].

Table 3.3 Summary of effect of Fe(II) additions to soil slurries

E_{Pt} (mV) prior to addition	measured [Fe(II)] (mM) before addition	amount of Fe(II) added (mmol)	measured [Fe(II)] (mM) after addition	effect on E_{Pt}
-163	0.6	2.5	1.6	none
-175	0.8	0.5	1.2	none
0	0.3	1	NM[a]	none
+100	0.1	0.1	0.15	none
+200	0.115	0.25	0.225	rapidly decreased to +75 mV

[a] NM. = not measured

decrease in pH caused by the acid in the Fe(II) solution (0.1 M $HClO_4$). The pH-stat system of the bioreactor brought the pH back to 7.0 within a few minutes. The addition increased the actual Fe(II) concentration from 0.6 to 1.6 mM (Figure 3.6B). After several hours, E_{Pt} leveled out at approximately -158 mV, within about 5 mV of the initial value. The rapid change in pH could have affected many characteristics of the soil slurry such as microbial activity or soluble concentrations of metal-oxides, causing the small overall change in E_{Pt}. In terms of the Nernst equation, E_{Pt} should have been lowered by about 25 mV for this change in [Fe(II)].

The calculated potentials based on eq. 3-6 based on both ferrihydrite or lepidocrocite Fe(III)-solid phases and the initial Fe(II) concentration (0.6 mM) are +8 and -84 mV, respectively. Clearly, these potentials are considerably higher than the measured

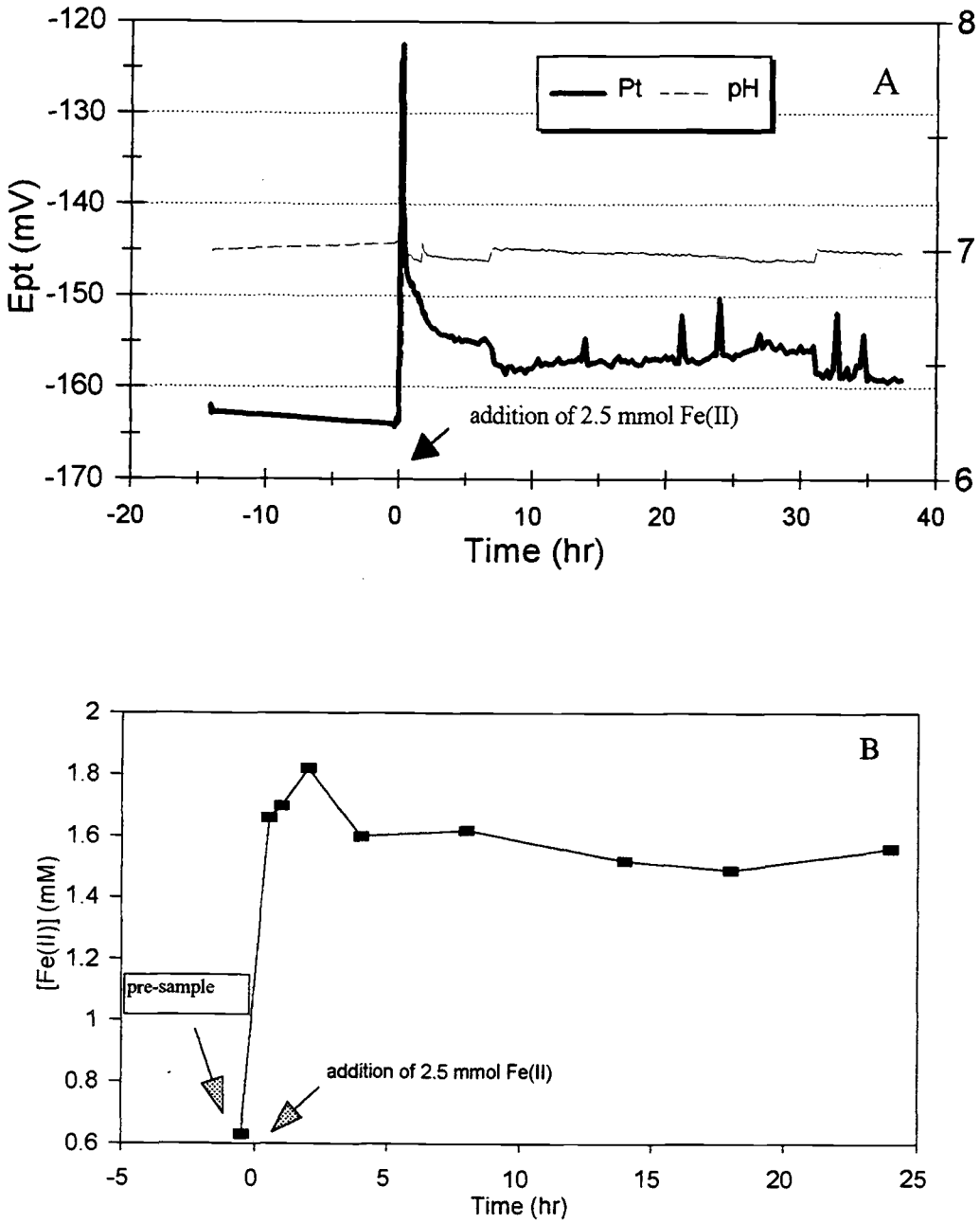

Figure 3.6 Response of the Pt electrode to addition of 2.5 mmol Fe(II) to an anaerobic soil slurry at pH 7. Prior to addition the Fe(II) concentration was about 0.6 mM. In (A), the sharp spike in E_{Pt} is due to the pH change that occurs from the addition of 0.1 M $HClO_4$ acid in the Fe(II) solution. The pH statting system of the bioreactor subsequently brought the pH of the soil slurry back to 7. The Fe(II) concentration in the reactor increased from about 0.6 mM to 1.6 mM upon addition (B). The soil slurry had been in the bioreactor about 460 hr before the addition.

E_{Pt} of -160 mV. When Fe(II) was added to a deaerated electrolyte solution (Figure 3.4) with 0.6 mM [Fe(II)] (~log 2.8), the average E_{Pt} value was also about -160 mV and further additions of Fe(II) caused essentially no change in E_{Pt}. Therefore, the behavior observed with additions of Fe(II) to a simple electrolyte solution or a soil slurry are consistent. In a similar soil experiment with $E_{Pt} \approx$ -175 mV, addition of 0.5 mmol Fe(II) to a soil slurry with 0.8 mM Fe(II) had no effect on E_{Pt} initially or several hours after addition, although the Fe(II) concentration increased to 1.2 mM and remained at this concentration for more than 10 hr. Again, this is consistent with the previous results.

In another Fe(II) addition experiment at +100 mV (the E_H-stat had been used to maintain this potential, but was disabled about 15 min before the Fe(II) addition), 0.1 mmol of Fe(II) was added to a soil slurry with ~0.1 mM Fe(II). Although the Fe(II) level rose to 0.15 mM (sampled 45 min later), no effect on E_{Pt} was observed. A 1 mmol addition of Fe(II) at 0 mV also had no effect on E_{Pt}.

At +200 mV, however, Fe(II) additions did have a substantial effect on E_{Pt} as shown in Figure 3.7A. After several days during which E_{Pt} was maintained at +200 mV by addition of H_2O_2, the E_H-stat system was turned off and, ~ 15 min later, 0.25 mmol of Fe(II) was added. The Fe(II) addition caused E_{Pt} to drop immediately to about +80 mV. A subsequent addition of 0.125 mmol Fe(II) further lowered the Pt electrode potential to approximately +65 mV. Addition of 0.3 mmol of Fe(III) (as the solid form of $FeCl_3 \cdot 6H_2O$) at +65 mV did not affect E_{Pt}.

Figure 3.7B shows how the Fe(II) concentration changes over time. The low level of Fe(II) measured initially (after addition) is most likely due to the lag time required for a well-mixed, representative Fe(II) sample to reach the external loop of the bioreactor.

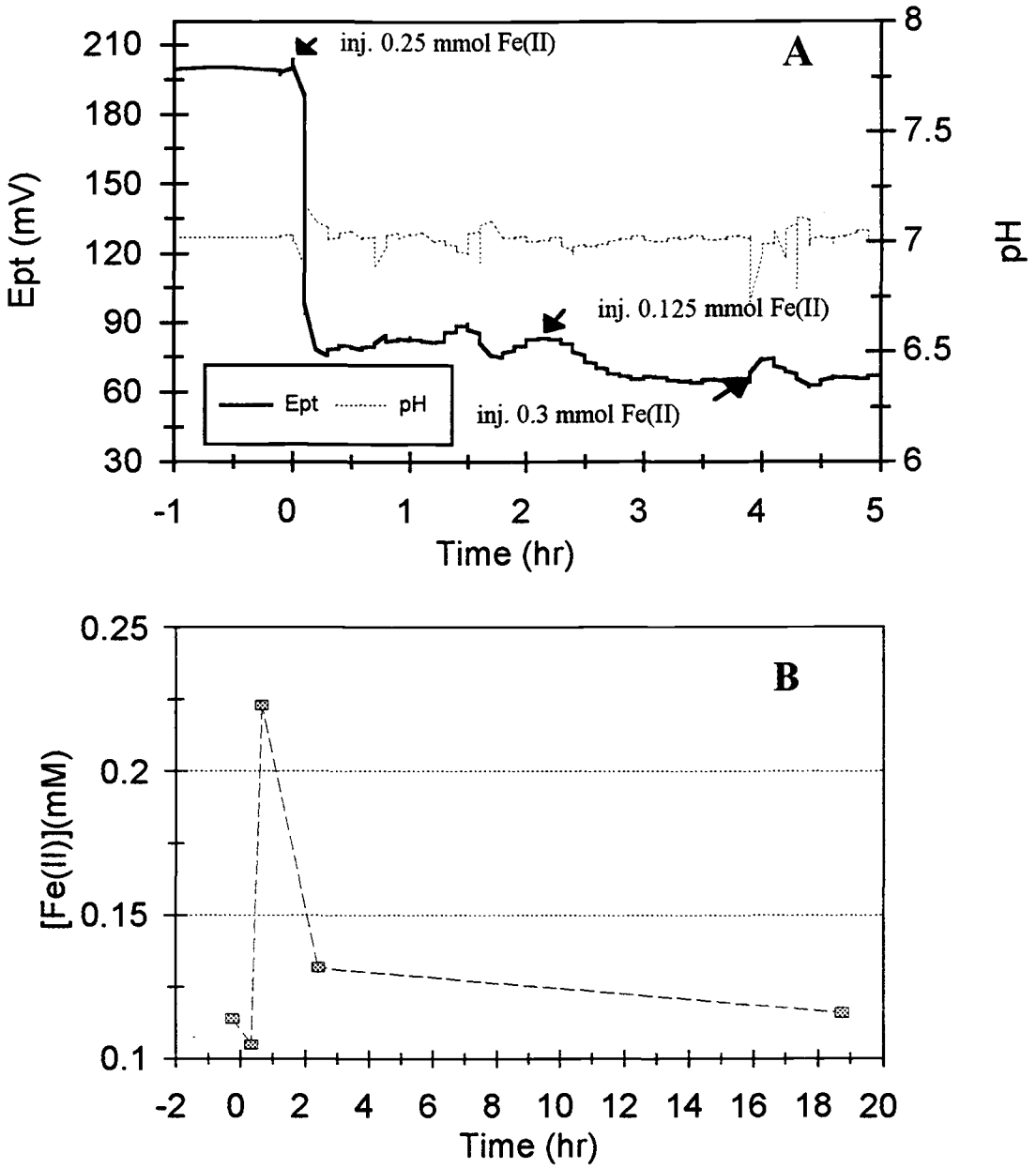

Figure 3.7 Effect of additions of Fe(II) and Fe(III) on E_{Pt} in a soil slurry in the bioreactor at +200 mV and pH 7 (A) and measured Fe(II) concentration (B). The soil slurry had been maintained at +200 mV by H_2O_2 addition with the E_H-stat which was turned off prior to the first Fe(II) addition. After the initial addition of 0.25 mmol, [Fe(II)] rose to about 0.22 mM. The addition of 0.125 mmol Fe(II) at approximately 2 hr did not increase the soluble Fe(II) concentration.

Addition of 0.25 mmol of Fe(II) increased the Fe(II) concentration by only approximately half of what it should (0.22 mM as opposed to 0.36 mM). Possibly some of the Fe(II) reacted with a species involved in poising the Pt electrode such as the residual H_2O_2 from E_H-statting. The decrease in E_{Pt} of about 80 mV is much greater than predicted from the Nernst equation (about 18 mV) if Fe(II) controlled the potential. Over the course of several hours, the Fe(II) level returned to ~0.12 mM, about the same as before the additions, indicating that the added Fe(II) was eventually adsorbed or reacted with other species. Considering that the Fe(II) level went back down over time but E_{Pt} remained at the lower potential suggests that Fe(II) could not have been poising the Pt electrode. If this were true, E_{Pt} would have returned to its previous potential.

Addition of 1 mmol of Fe(III) to a soil slurry at -60 mV had a pronounced effect on E_{Pt} (Figure 3.8). After the system stabilized at about +5 mV following the pH drop caused by the addition, E_{Pt} was about +65 mV above the initial potential. It appears that Fe(III) may have oxidized some species that affected E_{Pt}. It is also possible that Fe(III)-hydroxides formed may have adsorbed Fe(II) (Fe(II) concentrations were not measured) or other species that affect E_{Pt}. About 3 hr after the addition of Fe(III), 1 mmol of Fe(II) was added (at +10 mV), but it did not affect E_{Pt} as it did previously when added at +200 mV.

The results of the tests of Fe(II) in deaerated electrolyte solutions at pH 7 show that Fe(II) definitely affects E_{Pt}, although not in a Nernstian fashion, and only for E_{Pt} values above about -100 mV. It also appears that E_{Pt} becomes independent of [Fe(II)] for concentrations above ~ 0.6 mM (at which point E_{Pt} was about -160 mV). In contrast to simple electrolyte solutions, the effect of Fe(II) on E_{Pt} in anaerobic soil slurries is less

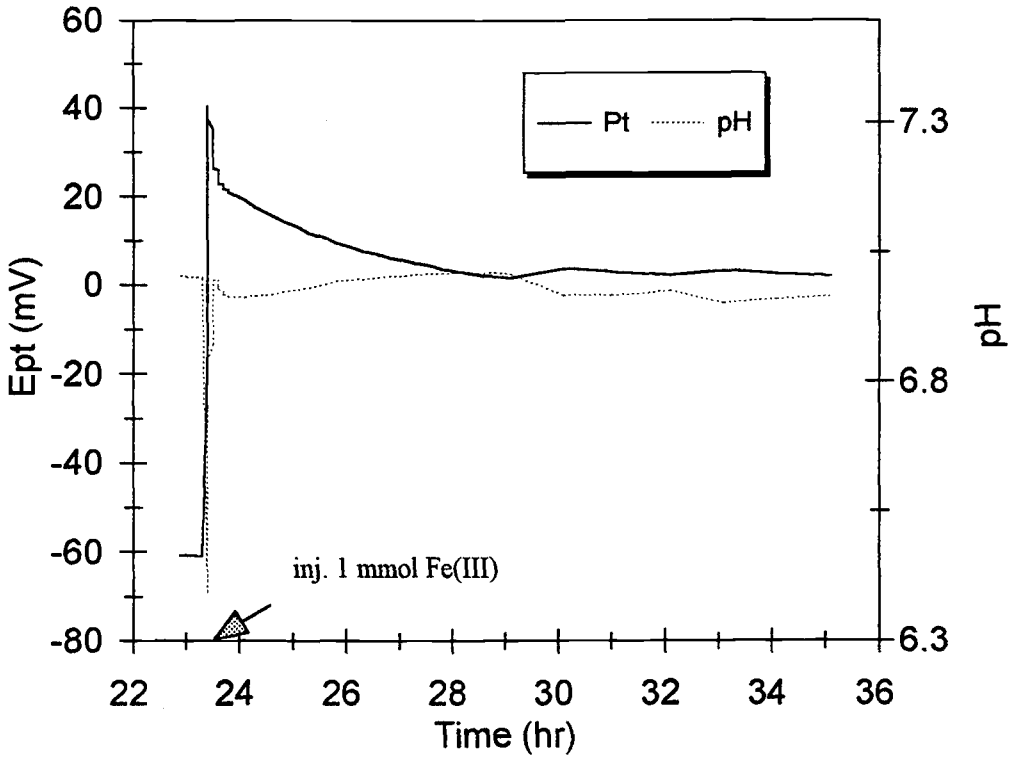

Figure 3.8 Effect of Fe(III) addition on a reduced soil slurry at -60 mV. The Fe(III) added at 23.5 hr appears to act as an oxidant to some species currently affecting E_{Pt}. The subsequent addition of 1 mmol of Fe(II) at +10 mV (~26.5 hr) did not change E_{Pt}.

obvious. At low E_{Pt} (< -100 mV), additions of Fe(II) to bioreactor soil slurries had no effect on E_{Pt}, which might be expected considering thermodynamic potentials (a potential of -100 mV for the Fe(II)/ferrihydrite couple corresponds to an Fe(II) concentration of 41 mM which is nearly two orders of magnitude greater than that found in the Bashaw soil experiments) and the results shown in simple electrolyte systems. On the other hand, Fe(II) additions to soil slurries at potentials between -100 and +100 mV had no effect on E_{Pt}, which differs from results obtained in simple solutions (although the E_{Pt} change for subsequent Fe(II) additions to deaerated electrolyte systems was notably less pronounced than the initial Fe(II) addition). Addition of Fe(II) to the soil slurry at +200 mV, did decrease E_{Pt} and it appears Fe(II) most likely acted as a reducing agent for some species which was poising the Pt electrode (perhaps H_2O_2) rather than affecting it directly. Fe(III) only appears to affect E_{Pt} directly at low pH (< 4) when it is soluble. At higher pH, Fe(III) can act indirectly as an oxidizing agent in soil slurries for E_{Pt} values below about 0 mV.

3.4.2 Effect of sulfur on E_{Pt}

Sulfur species have a complex chemistry and the sulfur atom exists in a variety of oxidation states, ranging from -2 to +6 in natural systems. Most sulfur species (except S° itself) and are generally quite soluble in soil systems, unless precipitated with a metal cation (e.g., S(-II) as FeS). Table 3.3 lists some sulfur redox reactions along with their standard potentials.

Table 3.4 Summary of relevant environmental sulfur redox reactions

sulfur species	chemical formulas	redox reaction	$E_7^{0'}$ (V)[a] (ref)
sulfate/sulfite	SO_4^{2-}/SO_3^{2-}	$SO_4^{2-} + H_2O + 2e^- \rightleftharpoons SO_3^{2-} + 2OH^-$	-0.53 (31)
sulfate/dithionate	$SO_4^{2-}/S_2O_6^{2-}$	$2SO_4^{2-} + 4H^+ + 2e^- \rightleftharpoons S_2O_6^{2-} + 2H_2O$	-1.08 (32)
sulfate/hydrogen sulfide	SO_4^{2-}/H_2S	$SO_4^{2-} + 10H^+ + 8e^- \rightleftharpoons H_2S + 4H_2O$	-0.21 (12)
sulfite/dithionite	$SO_3^{2-}/S_2O_4^{2-}$	$2SO_3^{2-} + 2H_2O + 2e^- \rightleftharpoons S_2O_4^{2-} + 4OH^-$	-0.30 (32)
sulfur(rhombic)/ sulfide ion	$S_{(0,\ rhomb)}/S^{2-}$	$S_0 + 2e^- \rightleftharpoons S^{2-}$	-0.475 (1)

[a] $E_7^{0'}$ was calculated from the reaction equations and $E^{0'}$ values given in the references.

In open beaker studies of various sulfur couples, only S(-II) species affected E_{Pt}. The SO_4^{2-}/SO_3^{2-} and $SO_3^{2-}/S_2O_4^{2-}$ mixtures had no effect on E_{Pt}, which remained in the range of +300 - 400 mV of the O_2-saturated solution. The $S_2O_4^{2-}$/S(-II) mixture did not poise the Pt electrode but lowered E_{Pt} significantly to an unsteady value between -50 and -100 mV. The decrease in E_{Pt} is attributed to S(-II).

In closed system bioreactor experiments in deaerated electrolyte solutions, S(-II) was shown to have a direct and reversible effect on E_{Pt} (Figure 3.9). Addition of 100 µmol of S(-II) caused an immediate drop in E_{Pt} from ~300 mV to less than -100 mV and a sharp drop in sulfide electrode potential (E_{S2-}), which poised at approximately -350 mV. After about 20 min, E_{Pt} fluctuated around -185 mV, although E_{Pt} was not constant enough to be considered poised. The effect of S(-II) on E_{Pt} and E_{S2-} was subsequently reversed by the addition of 100 µmol of Cu(II), which precipitated the S(-II), resulting in a final E_{Pt} of about +200 mV. This suggests that the S(-II) affects E_{Pt} directly in solution, rather than

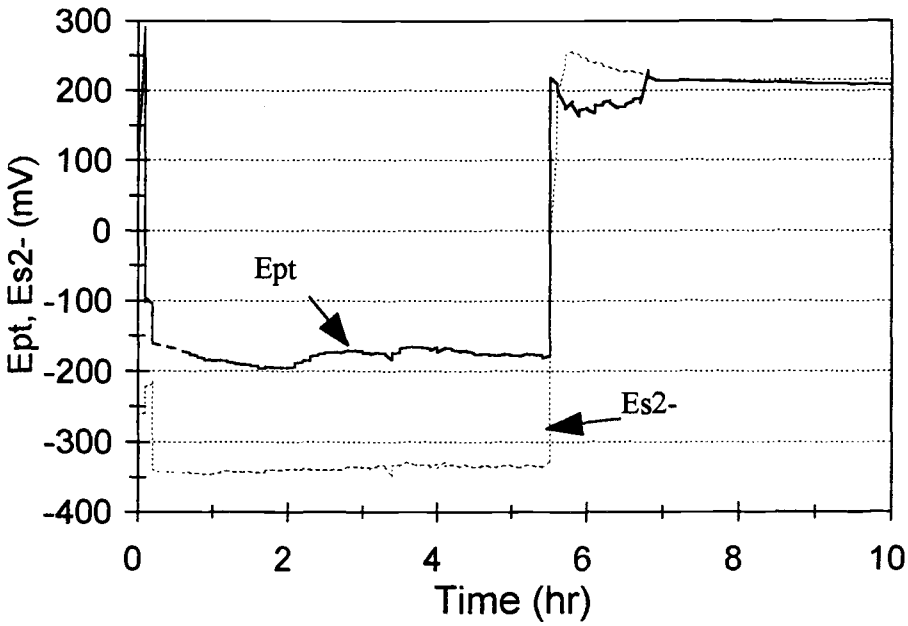

Figure 3.9 Effect of sulfide addition on electrode potentials in a deaerated electrolyte solution in reactor at pH 7. Similar to the Fe(II) addition experiment in a simple electrolyte solution (Figure 3.6), sulfide has a notable effect on E_{Pt} and which can be reversed by precipitation with Cu(II). Interestingly, the sulfide electrode used (E_{S2-}) responds in a similar fashion to the addition of sulfide and its subsequent precipitation.

simply by adsorption of S(-II) on Pt (9). However, Cu(II) might have desorbed S(-II) from the Pt surface.

In another experiment, sulfide was added incrementally (ranging from 1 - 100 μmol total sulfide) to a deaerated electrolyte solution at pH 7 as E_{Pt} and E_{S2-} were monitored (Figure 3.10). E_{S2-} decreased substantially immediately after each addition but then slowly rose about 30 mV. It is hypothesized that sulfide leaked out of the reactor over time as H_2S gas, which should be nearly equimolar with HS^- at this pH ($pK_a \approx 7.1$ (30)). However, throughout the experiment, E_{Pt} was only affected by the initial addition of sulfide, and no evidence of a Nernstian response ($E_{Pt} \propto -\log$ [S(-II)(tot)]) or poising was observed.

In bioreactor soil slurries, only S(-II) additions affected E_{Pt}. Additions of 1 mmol SO_4^{2-} (at -80 and -23 mV), 0.75 mmol SO_3^{2-} (at -75 mV) and 1 mmol $S_2O_4^{2-}$ (at -75 mV) had no effect on E_{Pt}, which was not surprising, considering that they had no effect E_{Pt} in open beaker experiments. Addition of 0.25 mL of saturated S(-II) solution (nominally 2.5 M in total reduced sulfur species, but partially oxidized such that only a fraction was sulfide species) resulted in a sudden decrease in E_{Pt} from +43 mV to well below -20 mV (Figure 3.11). After ~30 min, E_{Pt} leveled out at about 0 mV. After many hours had passed, E_{Pt} again rose back to near initial levels (about +40 mV). If S(-II) affected E_{Pt} directly, the latter increase in E_{Pt} may have been due to precipitation of S(-II) with Fe(II), initially in the bioreactor (~0.3 mM). However, no Fe(II) samples were taken and E_{S2-} was not monitored to substantiate this hypothesis.

Additions of saturated sulfide solution to soil slurries at more negative redox potentials also decreased E_{Pt}. When 0.6 mL of saturated S(-II) solution (15 mmol total

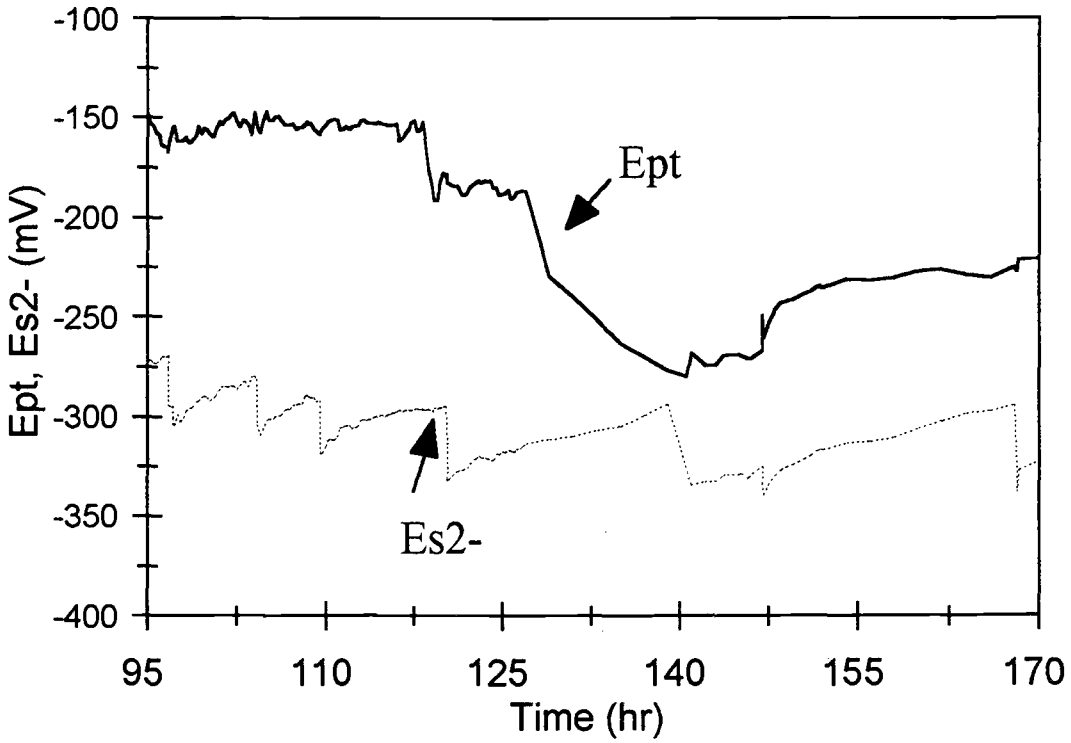

Figure 3.10 Sequential additions of sulfide to a deaerated electrolyte solution at pH 7. The sulfide electrode responds as expected. Although E_{Pt} decreased significantly after one addition, overall E_{Pt} does not change in a predictable manner (i.e., Nernstian).

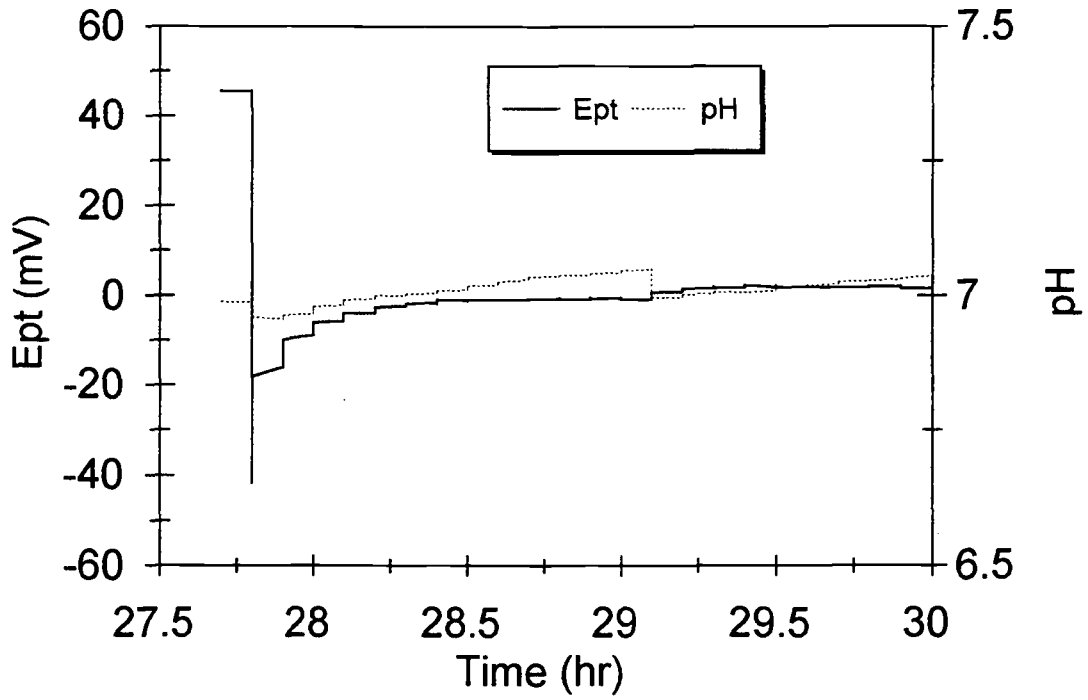

Figure 3.11 Effect of sulfide addition on E_{Pt} in an anaerobic soil slurry.

sulfur species) was added at -185 mV, E_{Pt} decreased about -5 mV, and then eventually rose back to pre-addition levels. Addition of 4 mL of this solution (100 mmol) to the soil slurry 2 days later resulted in a more substantial decrease in E_{Pt} from -180 mV to a steady-state value of -205 mV after several hours. At -250 mV, however, addition of sulfide did not affect E_{Pt}. S(-II) was not quantified during any of these experiments. However, no sulfide smell could be detected prior to addition of sulfide into the reactor.

Of the sulfur species tested, only S(-II) had an effect on E_{Pt}. In deaerated electrolyte solutions, S(-II) had a direct and reversible effect on E_{Pt}. Because sulfide was not directly measured, it is unknown whether the response was Nernstian or not. However, evidence presented with Pt electrode and sulfide electrode measurements (Figure 3.10) suggest that the Pt electrode does not respond to changes in [S(-II)] in a Nernstian manner. In anaerobic soil slurries, sulfide also has an effect on E_{Pt} down to potentials of about -250 mV. Without sulfide measurements, it is difficult to determine if the effect was direct, or if sulfide acted as a reductant

3.4.3. Effect of oxygen and hydrogen peroxide on E_{Pt}

The formal reduction potential for O_2 reduction to H_2O ($\frac{1}{2}O_2 + 2H^+ + 2e^- \rightleftharpoons H_2O$) is quite high, +0.82 V at pH 7. Oxygen is also reduced to H_2O_2, in a two electron transfer reduction ($O_2 + 2H^+ + 2e^- \rightleftharpoons H_2O_2$) with a formal potential of +0.27 V at pH 7 (calculated from data in reference 33). Hydrogen peroxide, a strong oxidizing agent and an oxygen containing compound normally has a short lived existence in the presence of

ions (33), particularly under reducing conditions. For the reduction of H_2O_2 to water ($H_2O_2 + 2H^+ + 2e^- \rightleftharpoons 2H_2O$), the standard potential is +1.36 V at pH 7 (calculated from data in reference 33).

Oxygen additions to reducing soil slurries abruptly raised the E_{Pt} of the system. As shown in Figure 3.12, addition of 20 mL of aerated DI water (about 4 μmol O_2) immediately raised E_{Pt} about 3 mV from -78 to -75 mV. After 2 hr at this potential, 10 mL more aerated DI water (~ 2 μmol O_2) were added and E_{Pt} jumped to -73 mV, and eventually leveled out at -74 mV. In a similar experiment two days later, with E_{Pt} at -75 mV, a 30 mL addition (~ 6 μmol) of the aerated DI water caused E_{Pt} to increase abruptly by 5 mV. Because O_2 is reported not to directly affect E_{Pt} (3), it most likely oxidized an unknown species affecting E_{Pt}.

In an open beaker/electrolyte system saturated with O_2, addition of 300 μL of 30% (v/v) H_2O_2 solution (~ 300 μmol) raised E_{Pt} from about +350 mV to between +450 and +500 mV. Although there was a definite effect on E_{Pt}, there was no sign of poising of the Pt electrode potential.

Addition of H_2O_2 to soil slurries under reducing conditions ($E_{Pt} < +200$ mV or so) always increases E_{Pt}. Figure 3.13 shows an example of how the E_H-stat system controls E_{Pt} in anaerobic soil slurries in the bioreactor by addition of H_2O_2. The computer program calculates the amount of H_2O_2 necessary to add to achieve and maintain a given E_{Pt}.

The mechanism by which H_2O_2 affects E_{Pt}, both in simple electrolyte systems and in biologically-active soil slurries, is unknown. H_2O_2 may interact with the Pt surface in a manner similar to O_2. For anaerobic soil slurries, the rapid increase of E_{Pt} following H_2O_2 addition suggests that H_2O_2 oxidizes species that affect E_{Pt}. Even at a moderately

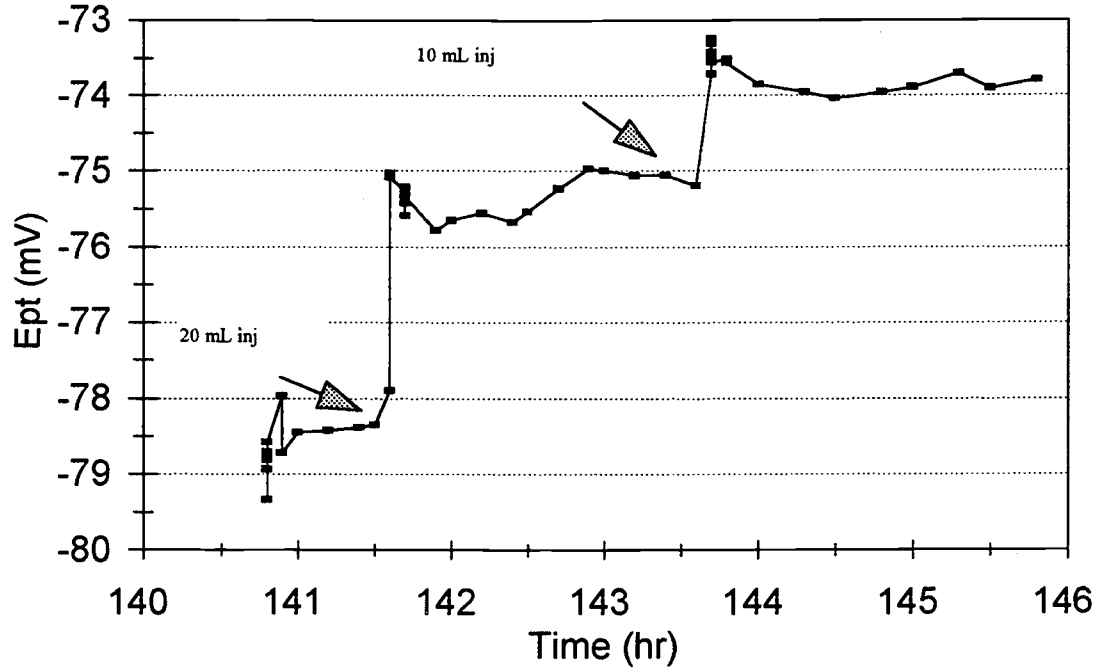

Figure 3.12 Effect on E_{Pt} of additions of DI water, equilibrated with atmospheric O_2, to an anaerobic soil slurry in the bioreactor. For saturated water, 10 mL contains about 2 μmol O_2.

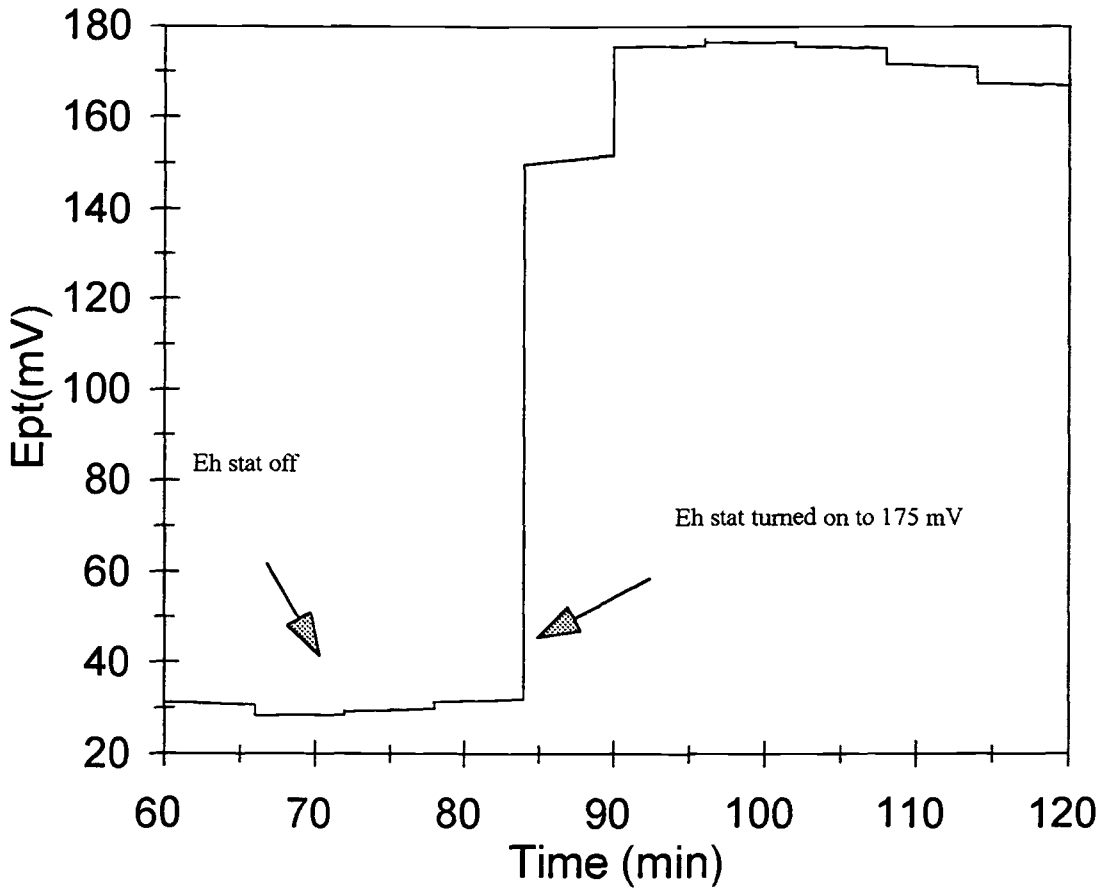

Figure 3.13 Example of E_H-statting of E_{Pt} with H_2O_2. At 84 hr, the E_{Pt}-stat system was turned on to increase E_{Pt} from +30 to +175 mV. Approximately 350 μmol of H_2O_2 were added to raise the E_{Pt} to the new level.

reducing potential (E_{Pt} = 0 V), both O_2 and H_2O_2 concentrations should be incredibly low (calculated with the Nernst equation to be about 8 x 10^{-55} M O_2 and 2 x 10^{-43} M H_2O_2 from their formal potentials (+0.82 and 1.36 V at pH 7)). Therefore, neither O_2 or H_2O_2 should be present in groundwater or soil systems at reducing potentials.

3.4.4 Effect of other species on E_{Pt}

Table 3.4 summarizes experiments conducted with other species and formal potentials of the redox couples at pH 7. In open beaker studies, none of the organic and biochemical species or couples tested affected E_{Pt}. With humic acid and ubiquinone (both attained in the oxidized form) or glutathione (attained in the reduced form) it was not determined if the procedures to make the reduced or oxidized forms, respectively, of these couples were successful.

In reactor experiments with a soil slurry, addition of the nitrogen species (NO_3^- or NH_4^+) or Mn(II) also had no effect on E_{Pt}. In the Mn experiment, the addition of 1 mmol Mn(II) increased the Mn(II) concentration from 0.45 to 0.8 mM. Additions of formaldehyde, anthraquinone 2,6-disulfonic acid, or ubiquinone also did not influence E_{Pt} in reduced soil slurries.

Quinone and hydroquinone (the reduced form) are often used as a redox couple to calibrate Pt electrodes (34) (formal potential of 390 mV at pH 7). When 1 mmol of hydroquinone was added to a soil slurry with E_{Pt} at about +290 mV (which had been controlled at +300 mV for several hours at which point the E_H-stat had been turned off), E_{Pt} immediately fell to +230 mV. After remaining poised at this potential for ~2 hr,

Table 3.5 Summary of formal redox potentials at pH 7 for redox reactions of various inorganic and organic species.

redox couple	$E_7^{0'}$ (V)(ref)	species added (amount)	E_{Pt} at addition (mV)
NO_3^-/N_2	+0.74 (15)	NO_3^- (1 mmol)	-100
NO_3^-/NO_2^-	+0.42 (15)		
N_2/NH_4^+	-0.27[a] (31)	NH_4^+ (1 mmol)	-100
MnO_2/Mn(II)	+0.38[a] (35)	Mn(II) (1 mmol)	-23
MnOOH/Mn(II)	+0.21[a] (12)		
humic acid (ox)/(red)	+0.7[b] (36)	both, 0.2 g each OB[c]; (ox) (0.5 g)	-75
fumarate/succinate	+0.03 (15)	both, 5 mM each OB	
pyruvate/lactate	-0.19 (15)	both, 5 mM each OB	
NAD^+/NADH	-0.32 (15)	both, 0.5 mM each OB	
formaldehyde (ox)/(red)	?	formaldehyde (red?) 2.7 mmol	-100
anthraquinone 2,6-disulfonic acid	-0.184 (11)	(ox), 0.5 mmol	-140
quinone/ hydroquinone	+0.29 (35)	hydroquinone (1 and 0.5 mmol)	+290 0
glutathione (ox)/(red)	+0.04 (11)	both 1 mM OB	
ubiquinone (CoQ) (ox)/(red)	+0.12 (15)	both 1 mM OB; (ox)(0.5 mmol)	+170

[a] calculated from standard potentials
[b] redox potential at pH = 0
[c] OB = open beaker study

E_{Pt} began to fall again and was no longer poised. It is hypothesized that initially enough of the hydroquinone was oxidized to quinone by residual H_2O_2 (left in the bioreactor from E_H-statting) to poise the Pt electrode. Eventually, it appears that the quinone was then reduced by some unknown species in the bioreactor, due to microbial activity, and poising was lost. When 0.5 mmol of hydroquinone was later added at 0 mV, E_{Pt} was not affected. As expected, addition of one species in a redox couple which poises the Pt electrode will not influence the potential if added at a potential where it is already the dominant form of the redox couple.

When 0.5 g of humic acid was added to the bioreactor soil slurry at -75 mV, the E_{Pt} of the soil system increased 10 mV. This increase is attributed to the Fe(III)-oxides in the humic material. Approximately 1% by weight of the humic acid is known to be Fe (12), and most likely in the form of Fe(III)-oxides. In previous experiments of this study, additions of Fe(III) to the soil slurry (with E_{Pt} at about -60 mV) increased E_{Pt}, most likely by oxidation of other species.

3.4.5 Transport or surface effects on the Pt electrode potential

During the course of many studies of soil slurries, it was noted that the potential difference between two "identical" Pt electrodes varied with E_{Pt}. At higher E_{Pt} (above 0 mV), the two E_{Pt}'s often differed by a relatively constant value of as much as 50 mV. As the system became more reducing, this difference tended to decrease, and for E_{Pt} values below -150 mV, the difference was as little as 10 mV. In fact, at E_{Pt} values around -250 mV (very reducing conditions), the E_{Pt} values were often within 5 mV of one

another. This general trend suggests that the Pt electrode is better poised under more reducing conditions than under more oxidizing conditions.

In a soil slurry, the potential of the Pt electrode with a 0.65-μm filter membrane pressed against its surface was consistently lower (as much as 200 mV) than that for a bare Pt electrode and sometimes decreased below -250 mV. The membrane-covered Pt electrode often appeared less poised (more drift) and was less affected by changes in concentrations of redox species (e.g., S(-II)) than the bare electrode. Interestingly, turning off the stirrer motor of the bioreactor resulted in an immediate (within 1 min) decrease in E_{Pt} for a bare electrode by as much as 100 mV (e.g., from -150 mV).

These two phenomena may be related for several reasons. First, the membrane or lack of stirring might allow a microbial biolayer to build up on the surface, which otherwise would be displaced by vigorous stirring. It is more likely that the membrane affords more protection for undisturbed region for microbial growth. Second, the membrane or stirring might affect the transport and nature or concentration of redox species and the double-layer at or near the electrode surface. Third, a membrane on the Pt surface or the lack of stirring would allow less interaction of particles with the Pt surface. However, it is unknown how this should affect E_{Pt}.

In contrast, the value of E_{Pt} for a Pt electrode placed in the external flow loop of the reactor was consistently higher than that of the bare Pt electrode in the reactor. The electrode surface in the external loop experiences low flow rates and a filtered solution (0.65-μm membrane filter in the cross-flow filter module) which minimizes contact of the electrode surface with larger particles and exposure to many microbes. Except for filtering out many microbes from the external loop, these conditions might encourage

microbial growth as proposed for the membrane-covered electrode in the bioreactor. However, the trend in E_{Pt} for the Pt electrode in the external loop and the Pt electrode in the reactor covered with the membrane are opposite, suggesting some other reason for this difference. The higher value of E_{Pt} for the Pt electrode in the external loop is hypothesized to be due to trace levels of O_2 leaking into external loop (below the detection limit of the DO probe).

Figure 3.14 shows the effects of leaving a cleaned Pt electrode out in open air for a period of time, before use. The lowest potentials were obtained when the Pt electrode was taken out of the reactor, cleaned, treated with the reductant sulfite, and immediately placed back in the reactor. After ~1 hr, E_{Pt} for this electrode fell below -50 mV, but had not yet reached a steady-state (the soil slurry had previously been measured to be about -80 mV with the same electrode). The E_{Pt} values of the electrodes that were cleaned and then allowed to sit out in open air for 0, 1, or 2 hr were very similar, approximately -10 mV after 30 min, about 20 mV higher than that of the electrode treated with reductant. When the Pt electrode was cleaned and exposed to air longer (12 hr), E_{Pt} was significantly higher (about +15 mV after 30 min and about -5 mV after 1 hr). For the Pt electrode which was not cleaned and allowed to sit out for 12 hr before placement back in the reactor, the E_{Pt} value was highest (about +15 mV after 1 hr). Interestingly, the rate at which E_{Pt} decreased for each condition was about the same such that the difference between potentials was often a nearly constant.

Figure 3.15 illustrates some of the effects of bombardment of the Pt surface of two electrodes with bath sand. For 60 hr with continual purging with N_2, the potentials

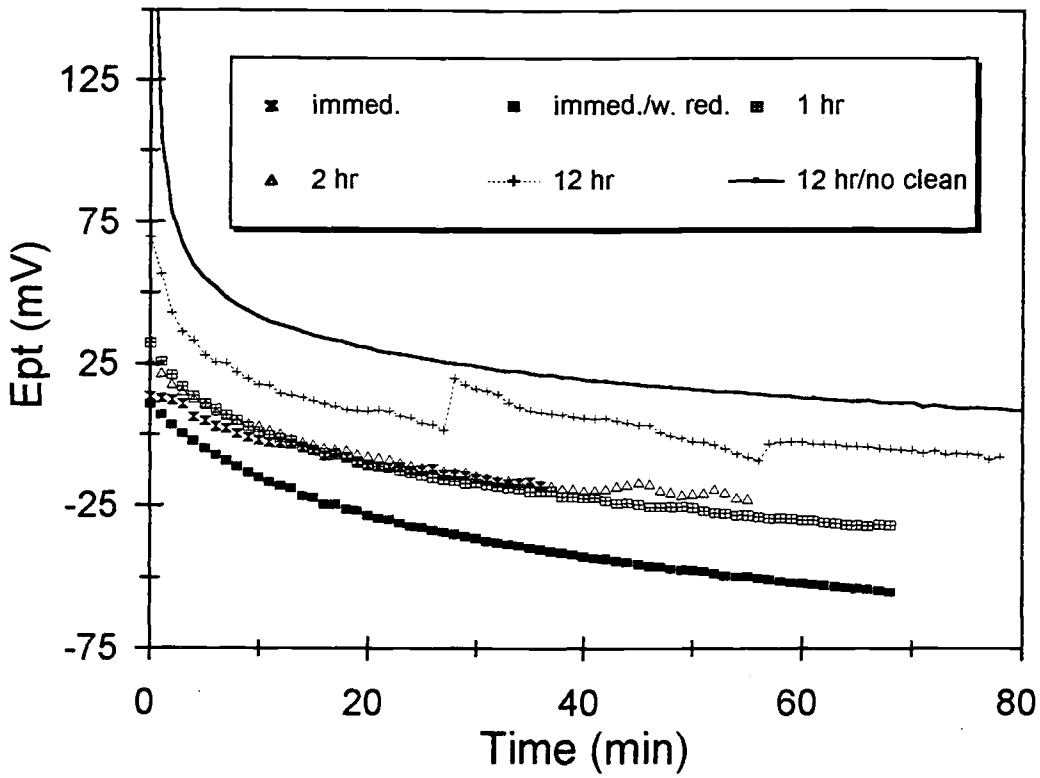

Figure 3.14 Dependence of the potential of a Pt electrode on the time it is exposed to air after cleaning before insertion into an anaerobic soil slurry. No reductant was used after cleaning except for one case (w red.). For one run (12 hr/no clean), the electrode was not cleaned.

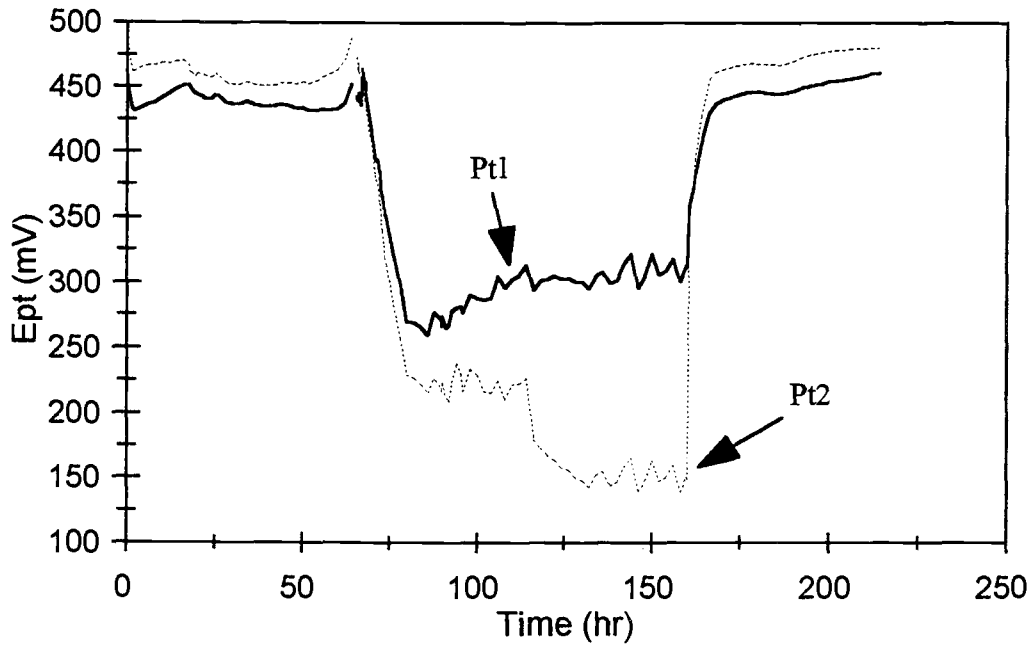

Figure 3.15 Effect of adding bath sand to a deaerated, pH 7 buffer in the bioreactor. The Pt electrode had been cleaned and then exposed to air for 24 hr before it was inserted into the reactor solution. After 3 days, 50 g of sand was added.

of the two Pt electrodes remained around +450 mV. Within about 10 hr after the addition of bath sand, the potentials of the two electrodes decreased significantly to about +275 and +225 mV. After about another day, $E_{Pt,2}$ fell further to +150 mV, while $E_{Pt,1}$ increased slightly. The reactor was then opened to the air at which point the Pt electrode potentials returned to near their original values.

These results suggest that the surface of the Pt electrodes is altered by bombardment of sand. Possibly, physical removal of adsorbed O_2 or a PtO layer occurs. The fact that the potentials of the two electrodes returned to about their initial values after the reactor was opened to the atmosphere suggests that O_2 is somehow involved in this effect. Interestingly, there no longer appeared to be a relatively constant difference in potential between the two Pt electrode potentials after the sand was added. After the reactor was reopened to the air, the two potentials of the Pt electrodes not only returned to about the initial values, but the potential difference became approximately constant. This behavior may relate to differences in the surfaces of the two Pt electrodes and their affinity for O_2 or perhaps differences in surface concentrations of other adsorbed species (e.g., S and Cl).

3.4.6 Poising with Zobell's solution

Zobell's solution is equimolar in both $Fe(CN)_6^{3-}$ and $Fe(CN)_6^{4-}$ at a concentration of 3.33 mM (each), with a KCl concentration of 0.1 M. Neglecting the ionic effects of the Fe species (which, because of their high charge, give an unrealistic value for the ionic strength of 0.14 (37)), the ionic strength of the solution is 0.1 M. Figure 3.16 illustrates

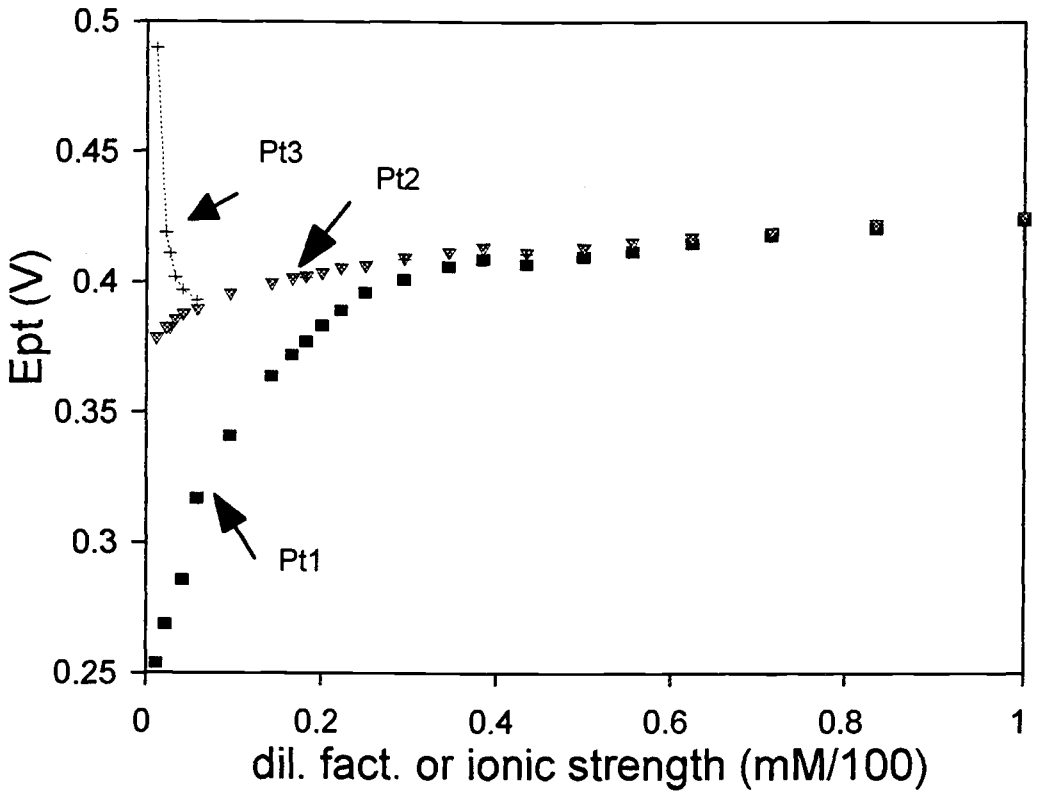

Figure 3.16 Dependence of Pt electrode poising on dilution factor and ionic strength in Zobell's solution. Initial E_{Pt} values were 424 and 425 mV for Pt1 and Pt2, respectively, compared to the nominal value of 428 mV. Pt1 denotes a well used Pt electrode which loses its poise most quickly. In contrast Pt2 had been used only once previously, and Pt3 had not been used at all.

how the potentials of three Pt electrodes vary as the solution is diluted with DI water. Up to a dilution factor of about 0.5 (50 mM ionic strength), E_{Pt} for all three Pt electrodes decreased slightly (about 10 mV). The potentials of electrodes Pt1 and Pt2 began to deviate significantly when the molarity of the Fe species approached 1 mM and the ionic strength was approximately 33 mM (dilution factor of 0.33). By the time the test solution had been diluted to the point that the concentration of each Fe species was 0.5 mM and the ionic strength was about 20 mM, E_{Pt} of Pt1 had plummeted greatly and the electrode was no longer poised. When the solution was diluted even further to Fe species concentrations just below 0.2 mM and an ionic strength of 10 mM (dilution factor of 0.1), the value of E_{Pt} of the third Pt electrode suddenly increased towards +500 mV. The second Pt electrode, even at this dilution, appeared weakly poised.

A "Zobell's" solution, 0.1 M in both Fe species, was added to a 0.1 M, deaerated NaCl solution in the bioreactor. Even after only 10 μL of the test solution was added (making a solution 1 μM in both Fe species), E_{Pt} changed significantly (from about 450 mV to about 430 mV). After 50 μL were added (5 μM in both species), both electrodes were well poised at +424 mV, the same E_{Pt} they reach in the 3.3 mM Zobell's solution. The reactor was subsequently opened to the atmosphere and no effect due to O_2 was observed after two days (E_{Pt} of the two Pt electrodes remained constant).

The results of the second test with Zobell's solution suggest that the loss of poise of the Pt electrodes in the first test was in fact related to the low ionic strength rather than the low concentrations of the Fe species. In the first experiment, poising of a *well used* Pt

electrode was lost when the ionic strength decreased below 30 mM, even though the concentration of a reversible couple was 0.75 mM (750 μM), well above the ~5 μM which poised the electrode with an ionic strength of 0.1 M. For a new Pt electrode, poising was lost at ionic strengths below 10 mM.

If the ionic strength must be about 10 mM or higher for proper poising of the Pt electrode, field measurements with the Pt electrode are questionable. An ionic strength of 10 mM is often an upper limit for soil ground water (38). In addition, it was shown that the concentrations of species in a reversible couple must be above 1 μM to significantly poise the Pt electrode.

3.5 Conclusions

Due to its ease of use, the Pt electrode is a convenient sensor for measuring the redox status of environmental systems. However, the measured E_{Pt} cannot generally be correlated to concentrations of redox-active species of interest. From the work in this thesis, E_{Pt} has been found to be a function of a number of different factors including the presence and/or concentrations of certain redox species, a variety of Pt surface and species transfer effects (oxide coatings, cleaning of the Pt surface, stirring of the system), and ionic strength. Due to this variety of factors, it is not surprising that we and other researchers (22) have observed many inconsistencies in the use of E_{Pt} (e.g., [Fe(II)] in soil slurries can differ by nearly two orders of magnitude at a given measured E_{Pt}). Therefore, from the experiments we have conducted, it is difficult to determine precisely to what the Pt electrode is responding.

Of the redox species tested, the only species which affect E_{Pt} directly or indirectly were Fe(II), Fe(III), S(-II), O_2, H_2O_2, and hydroquinone (not an environmentally-significant species). Additions of Fe(II) and Fe(III) to reactor soil slurries appear to indirectly affect E_{Pt} by oxidizing or reducing species currently in solution that affect E_{Pt}. Addition of Fe(II) to soil slurries with E_{Pt} values above +100 mV generally lowered E_{Pt}. In the case of the electrolyte system, Fe(II) had a direct effect on E_{Pt}. When Fe(II) was added to simple electrolyte solutions (E_{Pt} values initially about +350 mV), the E_{Pt} values were clearly lowered by over 50 mV by even small amounts of Fe(II) ($<<$ 100 μmol). This effect was reversed by complexing the Fe(II) added. However, no evidence of a

Nernstian response ($E_{Pt} \propto$ - log [Fe(II)]) was observed in electrolyte solutions or soil slurries.

At pH 7 and 25°C and with a ferrihydrite Fe(III) solid-phase, equation 3-6 simplifies to:

$$E_{Fe(OH)_3/Fe(II)} = -0.182 - 0.059 \log [Fe^{2+}] \quad (3\text{-}7)$$

At Fe(II) concentrations of 10 μM, 100 μM and 1 mM (environmentally relevant and measurable concentrations), the corresponding calculated potentials are +113, +54 and -5 mV, respectively, which suggest that Fe(II) in this range of concentrations should have an effect on E_{Pt} in this region. However, no consistent relationship between E_{Pt} and [Fe(II)] was observed. In Bashaw soil slurries, it appears that another redox couple or several redox couples (mixed potential) is poising the Pt electrode. Under reducing conditions in these soil slurries, E_{Pt} consistently fell to very low values (-100 to -250 mV) with or without a significant concentration of Fe(II) present.

The quinone/hydroquinone couple clearly poised the Pt electrode. However, when hydroquinone was added at a potential (0 mV) significantly below its formal potential (+290 mV), no effect on E_{Pt} was observed. This result suggests that addition of one species of a redox couple (which can poise the Pt electrode) will not change E_{Pt} if that species is added at a potential at which it should already be the predominant form.

Sulfide had a more dramatic effect on E_{Pt} than Fe(II) and was the only sulfur species which affected E_{Pt}. In electrolyte solutions, addition of sulfide immediately decreased the potential from about +200 mV to nearly -200 mV, at which point the effect could be reversed by addition of Cu(II). Like Fe(II), sulfide affects E_{Pt} in a direct and nearly reversible manner in simple, deaerated electrolyte solutions. However, sulfide

addition causes E_{Pt} to decrease more rapidly and to lower potentials than addition of Fe(II). This may be in part due to the greater reducing power of sulfide compared to Fe(II). However, there is also no indication of a Nernstian response on E_{Pt}.

Addition of sulfide to soil slurries had a less dramatic effect on E_{Pt} than in the electrolyte solution. However, sulfide additions consistently lowered Pt electrode potentials even at E_{Pt} values as low as -180 mV. Usually E_{Pt} eventually increased after the initial decrease, suggesting that sulfide was subsequently precipitated (e.g., as FeS) or was oxidized by some species.

For the $S^0_{(s,\ rhmb)}/S^{2-}$ half-reaction (Table 3-3), the redox potential at pH 7 and 25°C, based on the Nernst equation and a formal potential used by Berner (1) is given by

$$E_{S/S2-} = -0.475 - 0.0295 \log [S^{2-}] \qquad (3\text{-}8)$$

At 0.01, 0.1 and 1 mM *total* sulfide, the corresponding potentials are -111, -140, and -170 mV, respectively (based on eq. H-9 in Appendix H).

From the experimental results, sulfide most likely affects E_{Pt} directly (but might also act as a reductant). Very low E_{Pt} values are often measured under sulfate-reducing conditions (1, 22). However, sulfate-reducing conditions (i.e., sulfide production) were not observed in the Bashaw soil slurry studied even though E_{Pt} naturally decreased to very low potentials (occasionally below -200 mV). It appears that some species other than sulfide controlled E_{Pt} at lower potentials in the soil slurries studied, although sulfide might have had some effect on E_{Pt} if it had been present.

Addition of O_2 or H_2O_2 to reducing soil slurries (E_{Pt} ~ 100 mV or less) consistently and dramatically increased E_{Pt}. However, the O_2/H_2O couple does not

couple well to the Pt electrode because of slow electrode kinetics (9). Therefore, O_2 most likely affected E_{Pt} indirectly, by oxidizing a species currently involved in poising E_{Pt}. H_2O_2, which we have used as an oxidant in E_H-statting of soil slurries (17), also affects E_{Pt}, probably indirectly, by oxidizing species in the system. However, because H_2O_2 also increased E_{Pt} substantially (by about 100 - 150 mV) in aerated electrolytes in beaker experiments, it apparently can also have a direct effect.

Several brief studies demonstrated that transport and surface effects can greatly influence E_{Pt} for a given test solution. In anaerobic soil slurries, compared to the potential of an uncovered Pt electrode in a well-stirred slurry, E_{Pt} decreases dramatically when the Pt surface is covered with a membrane or when the slurry is no longer stirred. These differences appear to be due to transport phenomena that affect the micro-environment near or at the electrode surface (e.g., less interaction with larger particles or a major change in the electric double-layer), or an electrode surface effect (e.g., development of a microbial biofilm).

For a given Pt electrode, E_{Pt} values varied significantly with the period of time that a cleaned electrode was exposed to air before use. Also, E_{Pt} decreased significantly in the reactor when bath sand was added and allowed to bombard the Pt surface. Both results are consistent with the hypothesis that an oxide layer forms on the Pt surface which can be removed physically or chemically (with acid cleaning and/or a reductant).

In the course of experiments with two Pt electrodes in either soil slurries or electrolyte solutions, the potentials often differed by a relatively constant value (typically 25 - 50 mV), but the *dynamics* of the response were often similar (i.e., the direction and rate of change of potential). The difference between the two potentials became less

pronounced as the system became more reducing which suggests that the Pt electrode is better poised under more reducing conditions, although the species controlling the potential of the Pt electrode remains unknown.

These observations also suggest that two (or more) Pt electrodes should be used routinely when redox potentials are to be determined with a Pt electrode as a type of quality control. Presumably, differences in the surfaces of the Pt electrodes (e.g., differences in extent of oxide, Cl or S layers) cause this difference in measured E_{Pt} values of the same sample. If the redox buffering capacity of the system increases (resulting in better "poising" of the Pt electrodes), the two E_{Pt} values converge, giving the user evidence that potential measured is a better reflection of a property of the systems rather than of the particular Pt electrode used. If E_{Pt} values of two "equivalent" electrodes differed by 50 mV or more, the measured potential has much less relevance.

In the experiments with the reversible ferrous/ferric hexacyano couple, good poising was observed when the concentration of both forms of the redox couple were about 5 μM. This lower limit is in agreement with the findings of Kempton (5) and provides a guideline to assess the potential of any redox couple poising the Pt electrode.

With the same Fe couple, it was found that the electrode poise was lost when the ionic strength fell below about 10 mM which is higher than is often found in groundwater. This behavior suggests one factor that limits the applicability and reproducibility of potential measurements with Pt electrodes in environmental systems. Clearly, there are some redox species affecting E_{Pt} in environmental systems, but low ionic strength may be a major contributing factor in the many inconsistencies in redox measurements with Pt electrodes.

In further studies, measurement of exchange current densities in environmental systems may help complement these results and help better evaluate the true nature of the Pt electrode potential. An interesting question is if and how the exchange current density changes as E_{Pt} in an environmental system (e.g., groundwater, soil slurry or microbial culture) decreases in the transition from oxidizing to more reducing potentials. The better poising of Pt electrodes in samples with lower redox levels (i.e., the potential of two electrodes converge) suggests that the exchange current density would be higher than that at more oxidizing potentials. It would also be interesting to measure the exchange current densities at different microbial redox levels (e.g., Fe(III)-, sulfate-reducing and methanogenic systems) to confirm this hypothesis, to provide insight into what types of redox species may be affecting E_{Pt}, and to find out if microbial activity produces species that directly determine the measured E_{Pt}.

3.6 References:

1. Berner, R. A., *Geochim. Comochim. Acta.*, **1962**, *27*, 563-575.

2. Doyle, Roger W., *American Journal of Sci.*, **1968**, 840-859.

3. Lovley, Derek R.; Goodwin, Steve, *Geochim. Cosmochim. Acta*, **1988**, *52*, 2993-3003.

4. Lindberg, R. D.; Runnels, D. D., *Science*, **1984**, *225*, 925-927.

5. Kempton, J. H., *Heterogenous Electron Transfer Kinetics and Measurement of* E_H, **1982**, M.S. Thesis, University of Colorado.

6. Patrick, W. H., Jr.; Jugsujinda A., *Soil Sci. Soc. Am. J.*, **1992**, *56*, 1071-1073.

7. Lemmon, T. L.; Westall, J. C.; Ingle, J. D. Jr., *Anal. Chem.*, **1996**, *68*, 947-953.

8. Brett, Christopher M. A., Brett, Ana Maria Oliveira, *Electrochemistry: Principles, Methods and Applications*, Oxford Science Publications, 1993.

9. Whitfield, M., *Limnol. Oceanogr.*, **1974**, *19*, 857-865.

10. Bohn, Hinrich L., *Soil Science*, **1971**, *112*, 39-45.

11. Clark, W. Mansfield, *Oxidation-Reduction Potentials of Organic Systems*, Williams & Wilkins Company: Baltimore, 1960.

12. McBride, Murray B., *Environmental Chemistry of Soils*, Oxford University Press, Inc., 1994.

13. *Equilibrium Concepts in Natural Water Systems*, Stumm, Werner, Ed., Chapter 13, 270-285, American Chemical Society: 1967.

14. Ingle, James D. Jr., Private communication, Oregon State University, November 18, 1995.

15. Brock, Thomas D.; Madigan, Michael T.; Martinko, John M.; Parker, Jack, *Biology of Microorganisms, Seventh Edition*, Prentice Hall: Englewood Cliffs, New Jersey, 1994.

16. Chapelle, Francis H., *Groundwater Microbiology and Geochemistry*, John Wiley & Sons, Inc., 1993.

17. Lemmon, Teresa, *Development of Chemostats and Use of Redox Indicators for Studying Transformations in Biogeochemical Matrices,* **1995,** Ph.D. Thesis, Oregon State University.

18. Jones, Brian, Laboratory notebook #1, 1995, Oregon State University.

19. Bohn, Hinrick L.; McNeal, Brian L.; O'Connor, George A., *Soil Chemistry, 2nd Ed.*, John Wiley & Sons, 1985.

20. David, Renate, *Radiat. Environ. Biophys.*, **1986**, *25*, 219-229.

21. Hand, Clifford W., *General Chemistry*, Saunders College Publishing, 1996.

22. Lovley, Derek R.; Chapelle, Francis H.; Woodward, Joan C., *Environ. Sci. Technol.*, **1994**, *28*, 1205-1210.

23. Vancheeswaran, Sanjay, Private communication, Oregon State University, October 22, 1997.

24. *Indicators*, Bishop, E., Ed., Pergamon Press: Oxford, 1972.

25. Lowe, H. J.; Clark, W. Mansfield, *J. Biol. Chem.*, **1956**, *221*, 983-992.

26. Laboratory notebook: BASIC computer program for bioreactor.

27. *Standard Methods for the Examination of Water and Wastewater;* American Public Health Association: Washington, D. C., 1995.

28. Jones, Brian; Chapter 5 of this thesis.

29. Baham, John, Private communication, Oregon State University, December 6, 1994.

30. Stumm, Werner; Morgan, James J., *Aquatic Chemistry*, John Wiley & Sons: 1981.

31. Pankow, James F., *Aquatic Chemistry Concepts*, Lewis Publishers, Inc.: 1991.

32. *Standard Potentials in Aqueous Solution*, Bard, Allen J.; Parsons, Roger; Jordan, Joseph, Eds., Marcel Dekker, Inc.: 1985.

33. Shriver, Duward F.; Atkins, Peter; Langford, Cooper H., *Inorganic Chemistry,* Second Edition, W. H . Freeman and Co.: 1994.

34. *Instructions for ORP Electrode Use*, Analytical Sensors, Inc.: Houston.

35. Bard, Allen J.; Faulkner, Larry R., *Electrochemical Methods: Fundamentals and Applications*, John Wiley & Sons: 1980.

36. Thurman, E. M., *Organic Geochemistry of Natural Waters*, Kluwer Academic, Dordrecht: 1985.

37. Westall, John C., Private communication, Oregon State University, August 18, 1995.

38. Baham, John, Private communication, Oregon State University, August 26, 1995.

CHAPTER 4: EVALUATION OF THE REDOX INDICATORS FOR DETERMINING FE(III)-REDUCING CONDITIONS

4.1 Introduction

The Fe(III)-reducing redox level is considered one of the most important microbial redox levels in terms of its effects on the biogeochemistry of the environment. High Fe(II) concentrations in groundwater cause major problems in drinking water (e.g., discoloration) and are an important concern of water treatment facilities (1). Also, Fe(III) reduction is coupled with the oxidation of various organic substrates, some introduced by anthropogenic sources (2). Nearly all facultative anaerobes are capable of using Fe(III) compounds as terminal electron acceptors (TEA's) (3) and iron (in various forms) is a major component of freshwater and oceanic sediments, constituting between 1 to 9% of the overall bulk (4).

In addition to microbially-mediated reactions, Fe(III)-oxyhydroxides are often responsible for the direct oxidation of man-made pollutants such as benzidine and phenols (2). Chemisorption of various charged species on Fe(III)-oxides is also well known. For example, arsenate ($As(V)O_4^{3-}$), the common oxidized form of arsenic near neutral pH, chemisorbs to Fe(III)-oxides (2). Dissolution of Fe(III)-oxyhydroxides during microbial reduction releases the arsenate into solution (5), and the byproduct, Fe(II), can (thermodynamically) reduce arsenate (+5) to arsenite (+3) if Fe(II) levels are high enough ([Fe(II)] > 100 μM at pH 7 or greater) (6). Ions of other trace metals, including Zn, Pb, Mn, Ni, Cu, Co, V, Mo and Cr, are also known to concentrate on Fe(III)-oxides (4) and are released upon dissolution of the Fe(III)-oxide. Therefore, a

significant concentration of Fe(II) in natural waters can be a redox marker for particular redox transformations and also the release of certain trace metals into solution. Determining the presence of Fe(II) in environmental media may allow one to ascertain the redox state of a given species or the likelihood that a given species may be in a soluble form without having to directly monitor the species of interest.

The colorimetric determination of Fe(II) is commonly based on the Fe(II)-chelating agent 1,10-orthophenanthroline (OP) (7) and can be adapted for field measurements. However, this colorimetric method requires that a sample must be taken from the system being investigated. *In situ* sensors based on OP have been proposed (sol-gels) but not proven for field use. The OP method is selective for Fe(II) but does not directly measure the redox characteristics of the system (i.e., the system may also have other soluble reductants which the OP method cannot detect). The reaction of OP with Fe(II) is essentially irreversible which makes it difficult to develop a convenient sensor for Fe(II) that can monitor increases and decreases of [Fe(II)] over time.

Commonly, the Pt electrode potential, E_{Pt}, has been used as a measure of "redox level" (8, 9). Fe(III)-reducing conditions have been observed over a wide range of E_{Pt} values (generally +100 to -100 mV (8), although as high as +600 mV and as low as -200 mV (9)) by different researchers. Hence, E_{Pt} does not provide an unambiguous measure of the onset of Fe(III)-reducing conditions or the transition to another microbial level.

In anaerobic Bashaw soil slurries at pH 6.0, Lemmon (10) observed measurable Fe(II) levels (about 50 μM) when E_{Pt} dropped to +100 mV. Over time, E_{Pt} decreased further to a minimum of about -130 mV due to microbial activity as Fe(II) levels reached nearly 3 mM. Upon addition of H_2O_2 to the soil slurry to incrementally raise E_{Pt} back up

to +200 mV, Fe(II) levels did not begin to decrease until E_{Pt} increased to about -30 mV. Values of E_{Pt} under conditions in which H_2O_2 was used to maintain the potential were 100 mV higher for the same levels of Fe(II) as E_{Pt} values measured in the natural state at the same Fe(II) levels. Plots of E_{Pt} vs -ln [Fe(II)] were very nonlinear and E_{Pt} changed about 160 mV for a factor of 10 change in [Fe(II)] (compared to a 59 mV change predicted by the Nernst equation).

In other experiments, addition of Fe(II) to reducing Bashaw soil slurries had little effect on E_{Pt} (11). When 2.5 mmol Fe(II) was added to a soil slurry with an Fe(II) concentration of about 0.6 mM and E_{Pt} = -160 mV, the Fe(II) level in the reactor increased to 1.6 mM without a substantial (greater than 5 mV) permanent effect on E_{Pt}. Furthermore, additions of Fe(II) to soil slurries (with measured [Fe(II)] > 0.1 mM) at E_{Pt} values of +100, 0 and -175 mV had no effect on E_{Pt}. In these instances, the $Fe(II)/Fe(OH)_3$ couple clearly does not control the value of E_{Pt} and, most likely, E_{Pt} cannot be used to directly determine when Fe(III)-reducing conditions exist.

Redox indicators which react with Fe(II) present a possible means of determining when Fe(III)-reducing conditions exist. Normally, colored in their oxidized form and colorless when reduced, the absorbance of the indicator can be monitored with a spectrophotometer. As the oxidized species reacts with a reductant (e.g., Fe(II)), the absorbance decreases and a relative measure of the "reducing power" of the system can be estimated. The redox half-couple of a redox indicator can be described by

$$Ind_{ox} + ne^- + mH^+ \rightleftharpoons Ind_{red} \qquad (4\text{-}1)$$

where n, the number of electrons transferred, is typically 1 or 2, and m, the number of protons transferred, is typically 0, 1 or 2 and dependent on the pH (12). Many redox indicators are reversible and couple to the Pt electrode (10, 13, 14).

The redox potential for an indicator (E_{ind}) is determined by the relative concentrations (activities) of the oxidized and reduced species and the Nernst equation,

$$E_{ind} = E^{0'}_{ind,m} - \frac{RT}{nF} \ln \left(\frac{[Ind_{red}]}{[Ind_{ox}]} \right) \qquad (4\text{-}2)$$

where $E_{ind,m}^{0'}$ is the formal potential of the indicator and m indicates the pH. This formal potential is different for different indicators and is often a complex function of pH because many indicators have groups such as amines which can be protonated or unprotonated. Experimentally, the concentration ratio in equation 4-2 is evaluated by measuring the absorbance of one of the species, normally the colored oxidized form (see Appendix I for details). In this case, the concentration ratio equals $(1 - f_{ox})/f_{ox}$ where f_{ox} is the *fraction of indicator oxidized*, determined from the absorbance of the indicator. Equation 4-2 can be rewritten as

$$E_{ind} = E^{0'}_{ind,m} - \frac{RT}{nF} \ln \left(\frac{1 - f_{ox}}{f_{ox}} \right) \qquad (4\text{-}3)$$

An indicator with a formal potential very near that of the dominant Fe(II)/Fe(III)-solid couple could be reduced by Fe(II) at an environmentally-relevant pH if the Fe(II) levels are high enough. The speciation of the indicator (fraction oxidized) could be monitored spectrophotometrically. Furthermore, if an indicator/Fe(II) equilibrium existed and a known model could be applied, the absorbance (and f_{ox}) might be useful for determining (or estimating) Fe(II) levels in a system.

In initial studies of redox indicators, Fe(II) was shown to reversibly reduce the oxidized form of various redox indicators (e.g., thionine, methylene blue) near neutral pH (14). Furthermore, Lemmon (10, 13) developed an immobilization scheme for several redox indicators including thionine. In bioreactor experiments with anaerobic Bashaw soil slurries at pH 6.0, significant reduction of immobilized thionine occurred when Fe(II) concentrations increased to about 0.6 mM (10). The direct coupling of Fe(II) to thionine (and other indicators) might present a basis for the development of a sensor which is better suited than the Pt electrode to determining when Fe(III)-reducing conditions exist in sub-surface water or soil.

In this chapter, the relationship of the redox speciation of the redox indicators thionine, toluidine blue O, and cresyl violet acetate to Fe(II) concentration and pH, in both simple solutions and complex environmental systems, is examined. All experiments were performed in a 2-L, deaerated, bioreactor system. Free (non-immobilized) and immobilized indicators were titrated with Fe(II) at various environmentally-relevant pH values in simple electrolyte solutions in the bioreactor system. The absorbance of the indicator, Fe(II) concentration, and Pt electrode potential (E_{Pt}) were measured during the titrations. The dependence of redox indicator speciation on Fe(II) concentration was compared to thermodynamic models. In addition, soil and wastewater slurries were used to confirm that Fe(II), at naturally occurring levels, reduces the redox indicators at about the same levels as in simple titration experiments. In these experiments, the pH was either controlled at 7.0 or allowed to assume its natural value.

Additionally, experiments were conducted to evaluate if redox indicator speciation could be used to predict the prevalent redox state of As in a Bashaw soil

slurry. In previous studies, Cr(VI) was shown to be completely reduced to Cr(III) before the onset of the reduction of thionine (10). In this chapter, results are presented which attempt to correlate immobilized thionine redox speciation to the onset of reduction of As(V) to As(III).

4.2 Experimental

4.2.1 Instrumentation

Studies of the effects of Fe(II) concentration on redox indicator speciation were conducted in an air-tight bioreactor system, shown in Figure 4.1, which has been described previously in detail (11). The bioreactor was used to achieve and maintain anaerobic conditions for both simple electrolyte solutions or soil/wastewater slurries. A Pt-button electrode (Orion 967800) was used for E_{Pt} measurements and a glass pH electrode (Orion 9101BN) was used to measure the pH. One reference electrode (Orion 900200 Ag/AgCl double junction, modified to give the same potential as an SCE) was used for all indicator electrodes. Occasionally another, similar, Pt electrode was used to compare E_{Pt} readings, or a sulfide electrode (Orion 9416BN) was used to measure or determine if sulfide was being produced in the bioreactor when soil or wastewater slurries were present. Dispensing pumps (FMI Micro II-Petter) were used to add acid or base to control the pH. Readings of E_{Pt}, pH and E_{S2-} were taken at operator-chosen time intervals with a 386 PC and a QuickBASIC program developed to take electrode readings automatically, control the pH, and to calculate various parameters associated with control such as the pH buffer capacity. The pH electrode was calibrated with pH buffer solutions made from commercially available METREPAK pH capsules. To maintain anaerobic conditions, the bioreactor was purged with N_2 gas (pre-purified grade), at a rate ranging between 10 and 50 mL/min as maintained by a mass flow

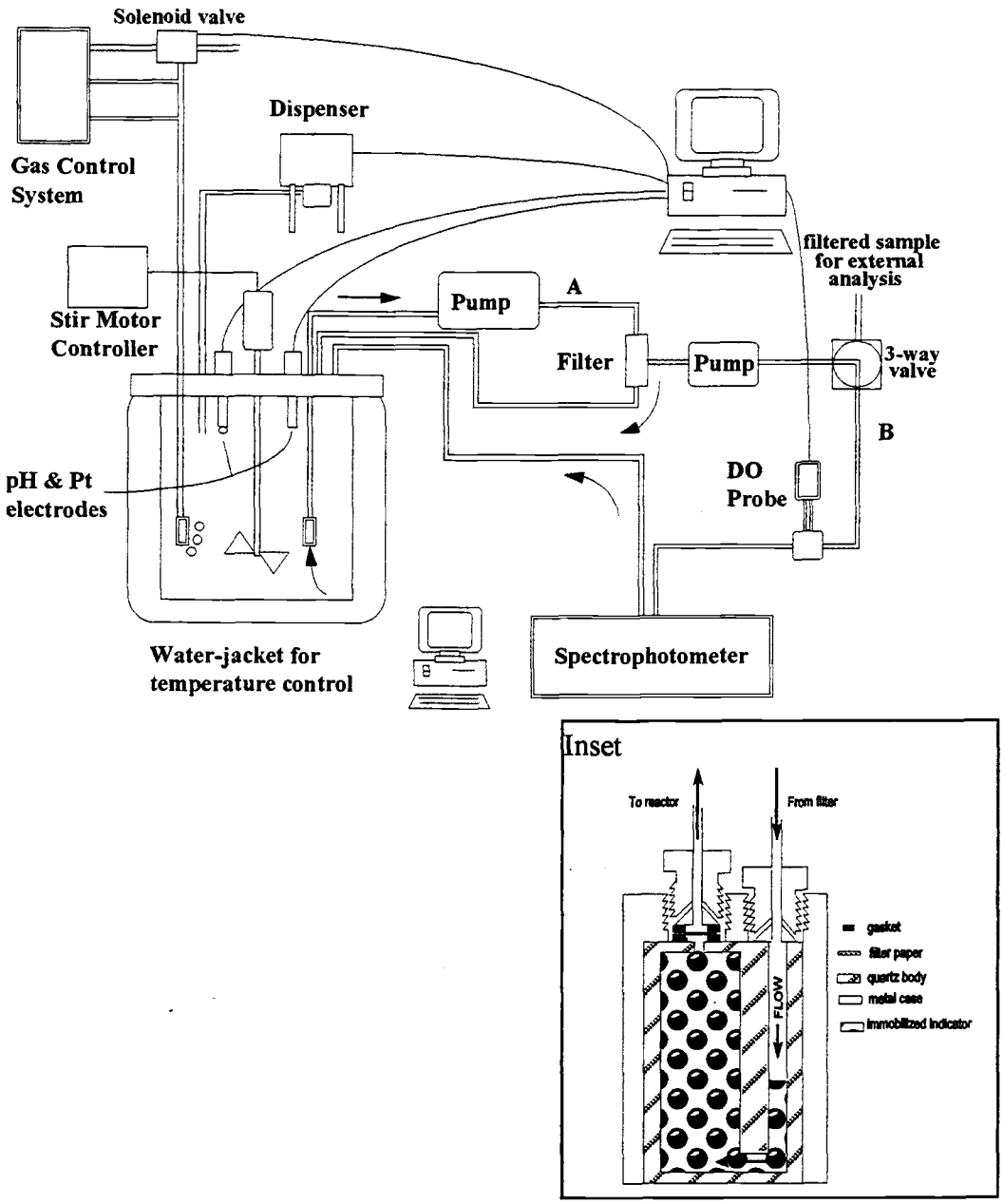

Figure 4.1 Bioreactor system for controlling and maintaining redox conditions, pH and anaerobic integrity. Loop A above refers to the primary external loop and loop B above refers to the secondary external loop, from which samples are taken for analysis. The bioreactor has a 2-L volume and normally contained 1 L of solution or slurry. The DO probe in loop B was not used for these experiments. The flow cell (inset) is packed with beads containing immobilized indicator, plumbed into loop B, and placed in the spectrophotometer sample compartment.

controller (Tylan FC280 with a Tylan RO-28 readout box). Residual O_2 in the tank was removed with an oxygen trap (Alltech Oxy-Trap 4001).

A sophisticated cross-flow filter system provided the continuous separation of liquid from solids in the reactor slurry and direct interaction of soluble redox species with the immobilized redox indicator (10, 11, 13). The primary and loop (A) includes the cross-flow filter and a peristaltic pump (Masterflex speed controller, Easy load pump head 7518-50). In the secondary loop, a persitaltic pump (Pharmacia Peristaltic Pump P-3) pumps filtered solution from the filter through a spectrophotometric flow cell and then back to the reactor. A peristaltic pump was chosen for the secondary loop because buildup of Fe(II) and Fe(III)-solids tended to clog and destroy the O-rings in the pump (FMI Model RHV) previously used by Lemmon (10, 13). Filtered bioreactor samples were taken from the external loop. To minimize residual O_2 leakage in the external loop, both pumps were encased in two large, plastic containers (Rubbermaid) which are purged continuously with N_2. With the exception of the tubing used with the two pumps (Tygon tubing size 14, 1.6-mm id, 5-mm od, Masterflex® from Cole-Parmer Instrument Co.), PEEK tubing (UPCHURCH type 1533, 1/16" od, 0.030" id, which has low O_2 permeability) was used throughout both primary and secondary loops. An oxygen probe (Orion 970800) was located in external loop B to measure dissolved O_2 and determine when the reactor system had achieved anaerobic conditions.

For titration experiments of immobilized indicators with Fe(II), the affinity beads with immobilized redox indicators were packed in a flow cell (Hellma 170.700-QS, 1-mm pathlength) and allowed to interact with filtered bioreactor solution pumped through the external loop. A schematic of the flow cell is shown in the inset in in Figure 4.1.

Sometimes two or more such packed flow cells were used in series. During titrations of free dissolved indicators, the indicator solution in the reactor was pumped through a 1-cm pathlength flow cell (Hellma 176.730-QS) in the external loop for absorbance measurements.

For absorbance measurements of Fe(II) in solutions and for the thionine/ orthophenanthroline (OP) experiment, a UV-Vis spectrophotometer cuvette with a screw cap was used (Spectrocell RF-0010-T, 10-mm, vol., 3.7 mL). All absorbance measurements were made with a Hewlett Packard 8452A diode array spectrophotometer. Soluble Fe(II) was quantified with the OP method, described in Appendix B.

For the arsenic experiment, samples were obtained from the reactor and quantified by Mark Bos (15). A separation scheme devised by Bos allows separation of arsenate (As(V)) from arsenite (As(III)) based on anion-extraction disks. Arsenite, a neutral species near neutral pH, passes unretained through the disks while arsenate, an anionic species, is retained in the disk. The water sample containing arsenic is pulled through the disk by vacuum suction, and the arsenite fraction is first collected. Arsenate is then eluted with 0.1 M HCl and collected. The As in each fraction was quantified with an electrothermal atomic absorption spectrophotometer (Perkin Elmer Zeeman/3030).

4.2.2 Chemicals

All solutions and bioreactor slurries were prepared from deionized water obtained from a Millipore Milli-Q water system. The redox indicators thionine (Thi) and cresyl violet acetate (CV) were obtained from Aldrich. Toluidine blue O (TB) was obtained

from Sigma. Redox indicators were immobilized on 60-μm, cross-linked agarose (4%), affinity beads (Sterogene ALD beads) by a procedure developed by Lemmon (10, 13), which is described in detail in Appendix E. The immobilization scheme involves a coupling of the amine groups on the redox indicators to aldehyde groups on the affinity beads (40-50 μmol/mL of gel), forming an imine. A 1.0 M $NaCNBH_3$ solution (coupling buffer), obtained from Sterogene, is used to reduce the imine bond to a more stable secondary amine. Lemmon (10, 13) had immobilized Thi and phenosafranine previously. CV and TB, which had not been previously immobilized (to our knowledge), were immobilized to the affinity beads in a similar manner. However, the pH needed to couple CV was lower than that normally used (3-4 rather than 5-7). TB was immobilized at a pH of approximately 6.

Two Fe(II) solutions, 0.5 and 0.05 M in 0.1 M $HClO_4$, were prepared with hydrated ferrous perchlorate crystals ($Fe(ClO_4)\bullet 2H_2O$, G. Frederick Smith Chemical Co.) and 70% $HClO_4$ (Mallinckrodt, Inc.). Hydroxylamine hydrochloride (10% (w/v) in water), a 0.5% (w/v) OP solution in water, and a 50 mg/L Fe(III) solution in 0.006 M HCl were obtained from Dean Johnson of the OSU Department of Chemistry.

Buffers were occasionally used to adjust the pH of simple electrolyte systems in the bioreactor. Phosphate buffer was prepared with $Na_2HPO_4\bullet 7H_2O$ and sodium phosphate monobasic, NaH_2PO_4 (both from Mallinckrodt, Inc.). In some cases, TRIZMA hydrochloride (Sigma) was also used as a pH buffer. When the computerized pH-stat was used, 12 M HCl (Mallinckrodt, Inc.) or 6 M NaOH were added to adjust the pH (after dilution). Nitrogen gas (pre-purified) in 230 ft^3 tanks was used.

$CaCl_2 \cdot 2H_2O$ (Baker) and NH_4Cl (EM Science) were added to soil and wastewater slurries to increase ionic strength and to provide a microbial nitrogen source, respectively. In simple electrolyte solution experiments, KCl (Mallinckrodt) was used as an electrolyte, at concentrations of 0.05 or 0.1 M. $FeCl_3 \cdot 6H_2O$ was used as an Fe(III) source (Mallinckrodt, Inc.). Sodium acetate ($NaC_2H_3O_2 \cdot 3H_2O$) and sodium bicarbonate ($NaHCO_3$) were obtained from Mallinckrodt, Inc. NaCl was obtained from EM Science. Arsenic standards and Ti(III) citrate (10% (w/v)) were prepared by Mark Bos (15).

4.2.3 Simple electrolyte solutions and Bashaw soil samples

For titration of redox indicators (immobilized and free in simple electrolyte solutions), KCl (0.1 or 0.05 mol) was added to 1 L of deionized (Millipore) water to adjust the ionic strength. Experiments were performed both with buffers and with the pH-stat system of the bioreactor. In experiments where the electrolyte was pH buffered, phosphate buffer (0.05 M) or TRIZMA buffer (0.05 M) was used.

Soil samples were taken from a location near Corvallis, OR in the Jackson Frazier Wetlands. The physical and chemical structure of the soil have been described in more detail (10, 11). The air-dried soil was first crushed, with roots and leaves removed, and then sifted through a 0.5-mm mesh twice and then through a 0.25-mm mesh once until a very fine consistency was obtained. For soil bioreactor experiments, 50 g of this soil sample were added to the bioreactor along with 10 mmol of $CaCl_2$ and 2 mmol of NH_4Cl. Next, DI water was added up to the 1 L mark and then the slurry was purged with N_2.

The stirring motor speed was maintained in a range between 50 and 100 rpm. In most experiments, the pH of the soil slurry was maintained at 7.0.

4.2.4 Wastewater slurry samples

Wastewater sludge samples were obtained in 1-L plastic bottles from the City of Corvallis Wastewater Reclamation Plant and contained significant numbers of anaerobic, reducing microbes (methanogens and sulfate-reducers). The samples were stored in a refrigerator for subsequent use. For reactor experiments, approximately 300 mL of this material was placed in the reactor along with 700 mL of deaerated, DI water, and 10 mmol of $CaCl_2$. The slurry was immediately purged with N_2 to maintain the anaerobic integrity of the system and prevent unnecessary exposure of the microbes to O_2.

During initial attempts to pump reactor solution through the primary and secondary loops, significant clogging occurred in the cross-flow filter in the primary loop due to debris in the slurry. To offset this effect, the stirrer controller was turned down so that the stirrer rotated at only 5 to 10 rpm, allowing larger debris to settle at the bottom of the reactor. The solution pumped through the primary loop was taken from approximately 1-2 in from the top of the wastewater solution rather than near the bottom.

4.2.5 Iron(II) as an important reductant in soil slurries

The effect of OP on the reduction of free Thi by Fe(II) and Ti(III) was tested. First, 1 mL of 20 μM Thi (0.2 μmol) was added to a spectrophotometer cuvette along

with 1 mL of a 0.1 M, pH 7.0 phosphate buffer. The pH of this solution was not measured. At this point, the vial was capped and purged with N_2 and the absorbance spectrum of the Thi mixture was measured (λ_{max} = 600 nm). Then, 2 µL of 0.5 M Fe(II) solution (1 µmol) was injected into the cuvette and a second spectrum was acquired. The second experiment was identical to the first, except OP was also added to the reaction mixture (1 mL of 20 µM Thi, 200 µL of 10% (w/v) OP, and 800 µL of phosphate buffer). The second spectrum was taken about 5 min after the Fe(II) was added. The third experiment was identical to the second experiment except 20 µL of a 10% (w/v) Ti(III) citrate solution were injected, allowed to react, and another absorbance measurement was taken.

To determine if soluble Fe(II) was a significant reductant of the immobilized Thi in a Bashaw soil slurry under Fe(III)-reducing conditions, an experiment was devised to mix reactor solution with OP. A Bashaw soil slurry, under anaerobic conditions in the bioreactor for several weeks, had a measured soil E_{Pt} of about -250 mV (all E_{Pt} values reported vs. SHE) and a pH of 7.6 (no pH stat was used). Filtered solution from the reactor had been pumped continually through the flow cell packed with immobilized Thi and no dissolved oxygen was detected in the external loop. Soluble Fe(II) levels were measured to be about 130 µM and f_{ox} of Thi was determined to be approximately 0.2 (or about 80 % reduced).

To evaluate the soil slurry, 1 mL aliquots of free reactor solution were mixed with 1 mL aliquots of free Thi, with and without OP. In the capped spectrophotometer cuvette, 1 mL of 20 µM Thi was purged and 1 mL of filtered reactor solution was added directly to the spectrophotometer cuvette via a needle attached directly to PEEK tubing

in the external loop. The cuvette was shaken slightly and allowed to equilibrate for approximately 5 min, at which time an absorption spectrum was acquired. This procedure was again repeated, except this time 80 μL (it was calculated that 200 μL were far more than necessary) of the 10% (w/v) OP solution were added to 1 mL of 20 μM Thi as the Fe(II)-complexing agent. Other reductants were not employed.

4.2.6 Titrations of free and immobilized indicators with Fe(II)

In several experiments, various free and immobilized redox indicators were titrated with Fe(II) at several different pH's. Free (i.e., non-immobilized) indicator solutions of Thi (λ_{max} = 600 nm), TB (λ_{max} = 632 nm) and CV (λ_{max} = 586 nm) were titrated with Fe(II) at pH values of 6.3, 7.0 and 7.5. In the case of free indicator titrations, the computer-based pH stat was used to maintain the pH at the desired value, without a buffer. For these experiments, 1 L of a 20 μM solution of the indicator was prepared by adding 10 mL of a 2 mM indicator solution to the bioreactor along with 0.05-0.1 mol KCl to adjust ionic strength. For Thi, an indicator concentration of 40 μM was also titrated. The reactor was purged with N_2 for ~3 hr until the O_2 level measured with the DO probe was below the detection limit (<0.6 ppm).

An initial absorbance spectrum of the free indicator was acquired to determine the absorbance peak height of the indicator when it was fully oxidized. A 0.05 M Fe(II) solution in 0.1 M $HClO_4$ was used as the Fe(II) stock solution. A 100 μL syringe (Hamilton) was used to inject the Fe(II) solution (10 - 100 μL, 0.5 - 5 μmol increments) through the septum port in the lid of the bioreactor. Because the Fe(II) solution was

quite acidic, the pH of the reactor solution dropped dramatically upon injection, but then quickly returned back to the desired level within about 2 min due to the action of the pH-stat. The reactor solution was continually pumped through a 1 cm-path length flow cell in the secondary loop so that absorbance of the indicator and Fe(II) samples could be acquired and measured at any time. In general, absorbance measurements were taken 0.5 - 1 hr after injection after allowing sufficient time for the system to come to steady-state. Only one Fe(II) sample was taken per addition. The wavelength maximum of the OP-Fe(II) complex (510 nm) was sufficiently separated from the wavelength maxima of the redox indicators to allow accurate measurements of Fe(II). Pt electrode measurements were taken throughout the experiment, normally with a 15-min interval.

For titrations of the immobilized redox indicators with Fe(II), a 0.05 M TRIZMA buffer was used in the reactor solution to maintain constant pH. Phosphate buffer could not be used during long-term titration experiments because Fe(II) tended to precipitate out as $Fe_3(PO_4)_2$. No free redox indicator or additional electrolyte was used.

Immobilized indicator beads were packed into the 1 mm-path length cell (inset of Figure 4.1) and an initial absorbance spectrum was taken. Fe(II) was added in the same manner as described for the free indicator. Because of the slower mass transfer rates of Fe(II) to the immobilized indicator and overall slower reaction times, more time was allowed for equilibration, typically 2 to 4 hr between additions. For experiments with both the free and immobilized indicators, data points were taken only after the absorbance of the indicator and the Fe(II) level became constant.

Titrations of immobilized TB were conducted at three different concentrations. The effective concentration on the agarose beads can be varied with the pH or time

allowed for the coupling reaction (10). Batches of TB were coupled for 2, 3 and 4 hr time periods, giving three batches of differing color densities (concentrations) of the indicator on the agarose beads. Titration experiments were conducted at pH 7.0 as previously described.

In one particular experiment with immobilized TB, the reversibility of the Fe(II)/indicator equilibrium was tested. Portions of the Fe(II)-buffer reactor solution were removed and then deaerated buffer solution with no Fe(II) was added to bring the volume back to the initial value (to decrease the Fe(II) concentration by 25 - 100%). When Fe(II) levels dropped below about 100 μM, Fe(II) additions were again made to the reactor to reverse the effect.

To test mixtures of free redox indicators, titrations were conducted at pH 7.0 with 10 μM each of Thi and TB and then 10 μM TB and 20 μM CV. A higher concentration of the CV relative to other indicators was necessary, because of its lower molar absorptivity (16). Although the absorption bands of the two redox indicators in the mixture in both experiments tended to overlap (particularly in the Thi/TB experiments), baseline subtraction techniques were used to resolve the absorbance contributions from the two bands. Experiments were conducted as previously described for the single free indicator.

To test simultaneously two immobilized redox indicators, two flow cells (each packed with a different immobilized indicator) were placed in series in external loop B. First, immobilized Thi and TB were titrated with Fe(II) at pH 7.0 in the same manner described previously. Absorbance measurements of the immobilized redox indicators were taken consecutively and a single sample was taken to determine Fe(II). When Thi

was significantly reduced (before TB), its cell was replaced with one packed with immobilized CV.

4.2.7 Reactor experiments with soil and wastewater slurries under Fe(III)-reducing conditions

To determine the Fe(II) levels, generated by Fe(III)-reducing activity, necessary for the reduction of indicators in actual soil or wastewater media, Bashaw soil slurries and wastewater slurries were studied in the bioreactor. In previous studies with Bashaw soils, Lemmon (10) observed that natural microbial activity under reducing conditions at pH 6.0 generated soluble Fe(II) levels greater than 2 mM that reduced Thi. For work in this thesis, bioreactor experiments were conducted at pH 7.0. Generally, Fe(II) levels reached as high as 800 μM, completely reducing the immobilized indicator Thi. However, in later experiments with a second batch of Bashaw soil taken one year later from the same region, Fe(II) levels never increased much above 25 μM and were not high enough to reduce the redox indicators. It is not known why Fe(II) levels did not reach their previous levels. Possibly, the Fe(III)-reducing microbes in the soil were damaged or a greater fraction of the Fe(II) generated was adsorbed on soil surfaces.

To generate soluble Fe(II), nutrients were added to wastewater slurries to stimulate Fe(III)-reducing conditions. Wastewater sludge was added to the bioreactor and the pH was controlled at 7.0 by addition of acid. To stimulate Fe(III)-reducing conditions, an Fe(III) source, and a variety of nutrients and sodium acetate as a substrate were added as described by Chapelle (1). To the wastewater slurry, 13.5 g (50 mmol) of $FeCl_3 \cdot 6H_2O$ were added as an Fe(III) source along with 6.8 g of sodium acetate as a

substrate. Also, 1.5 g of NH_4Cl, 0.6 g of NaH_2PO_4, 0.1 g of KCl, 2.5 g of $NaHCO_3$, and 1.0 g of NaCl were added as additional nutrients. Immobilized Thi and CV were packed into separate flow cells and placed in the external loop of the bioreactor system. Absorbance measurements of the two indicators were taken along with Fe(II) samples throughout the course of the experiment.

4.2.8 Arsenic speciation experiment

An experiment was conducted with a reducing Bashaw soil slurry in the bioreactor to determine if immobilized Thi speciation could be used to predict the prevalent form of arsenic in the soil slurry (15). For this experiment, a Bashaw soil slurry (50 g) was treated as described previously, except that half the amounts of $CaCl_2$ and NH_4Cl (5 mmol $CaCl_2$ and 1 mmol NH_4Cl) were added as ionic and nitrogen sources and 500 µL of a 1000 mg/L (6.7 µmol) As(V) solution were injected. The pH stat was not used because the Cl^- from the HCl tended to interfere with the As separation scheme. Thi redox indicator speciation, Fe(II) levels, As(V) and As(III) levels, and E_{Pt} and pH were monitored throughout the duration of the experiment.

4.3 Results and Discussion

4.3.1 Iron(II) as a reductant of thionine in soil slurries

Orthophenanthroline (OP) rapidly chelates Fe(II), forming an orange-red complex with a λ_{max} of 510 nm. Three OP molecules react with one Fe(II) ion resulting in the colored complex. The calibration curve is linear in the range of 0 to 200 μM and the calibration slope is independent of pH in the range of 3 to 9 (7). Additional details are given in Appendix B.

The results of initial tests of the effect of OP on the reduction of Thi by Fe(II) are shown in Figure 4.2. The reduction of Thi by Fe(II) is indicated by the eradication of the Thi absorbance band at 600 nm (Figure 4.2A). When OP is added to the reaction mixture (Figure 4.2B), Thi is not reduced. The spectrum taken after the Fe(II) addition is a superposition of the tail of the absorption band of the Fe(II)-OP complex (maximum at 510 nm) and the band of unreduced Thi. From the spectrum in Figure 4.2C, it is clear that Ti(III) citrate reduces Thi even in the presence of OP. These data support the hypothesis that OP in the solution impedes the reduction of Thi by complexing the Fe(II) before it can react with Thi rather than by chemically interacting with the Thi directly so that it cannot be reduced.

When a filtered aliquot of anaerobic soil slurry from the bioreactor with 130 μM Fe(II) was mixed with Thi, the Thi was reduced immediately. The elimination of the Thi absorbance band observed in Figure 4.3A is similar to that seen in Figure 4.2A. With OP present to complex the Fe(II), the Thi band remains (Figure 4.3B).

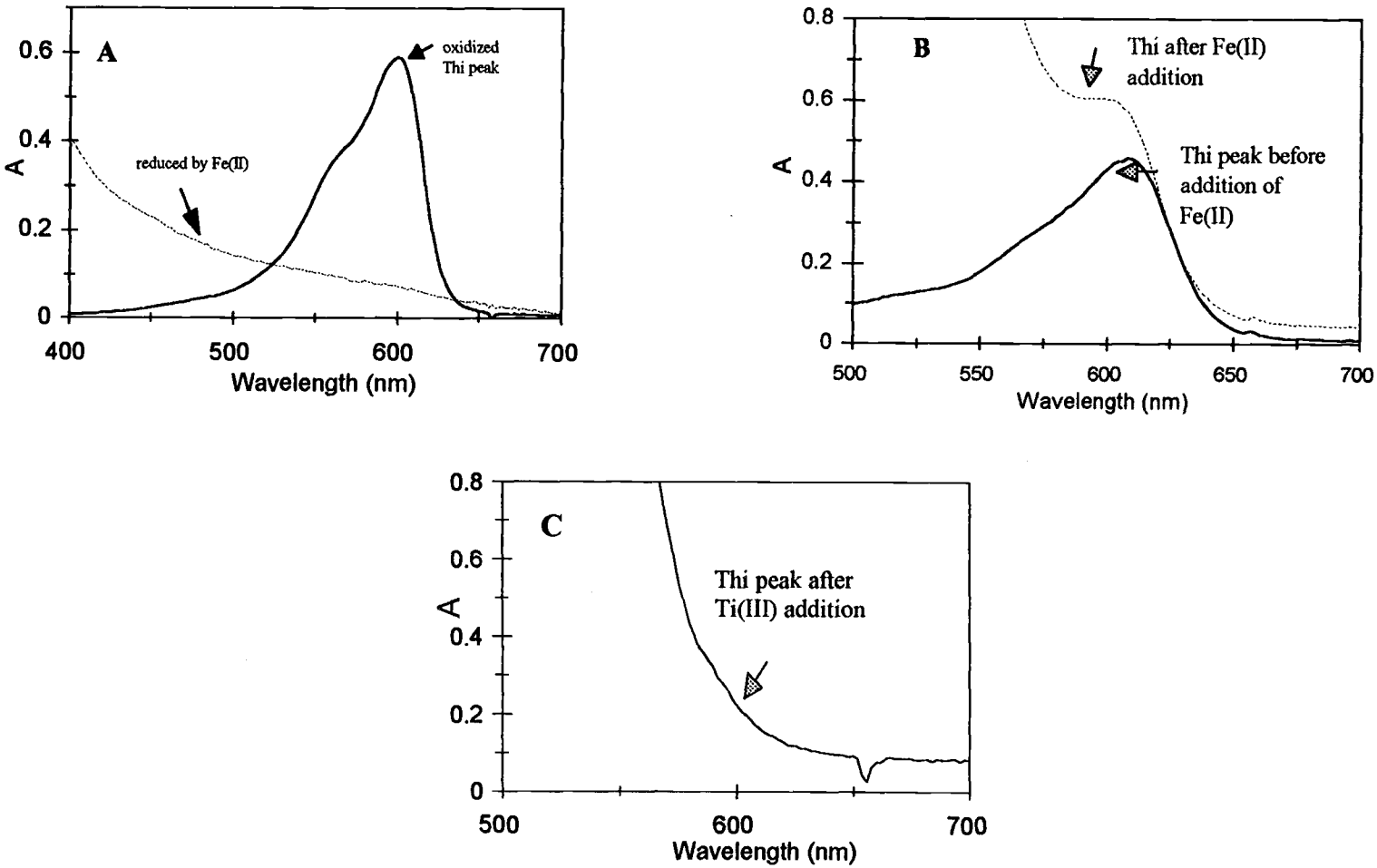

Figure 4.2 Effect of orthophenanthroline (OP) on the reduction of thionine (Thi) by Fe(II) and Ti(III). (A) Spectrum of oxidized Thi (10 μM) without OP, before and after addition of 1 μmol Fe(II). In the presence of OP (55 mM), Fe(II) does not reduce the thionine (B). Addition of 200 μL of 10% (w/v) titanium citrate reduces the Thi (C).

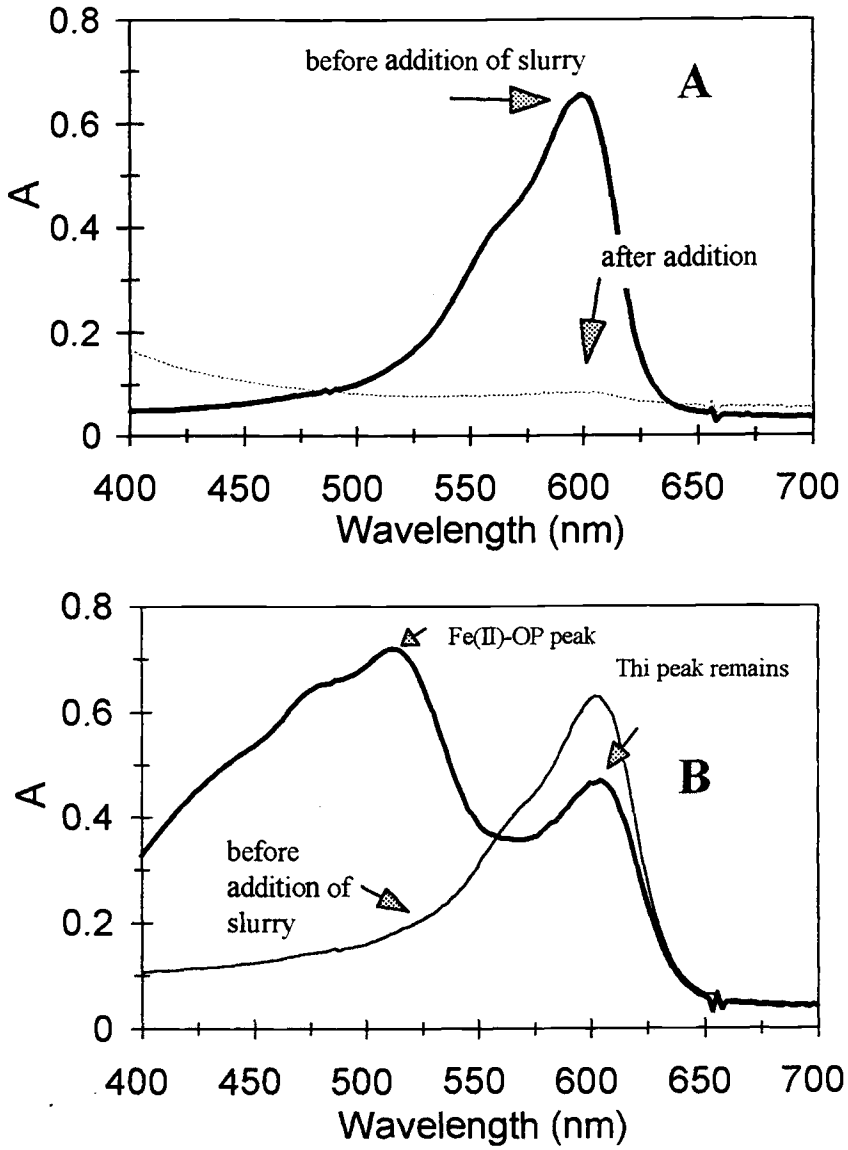

Figure 4.3 Effect of orthophenanthroline (OP) on the reduction of thionine (Thi) by a soil slurry containing Fe(II). Spectrum of 1 mL of 20 μM Thi before and after addition of one mL of bioreactor solution, with a measured Fe(II) concentration of 130 μM, without (A) and with (B) OP. The absorbance band at 600 nm is due to oxidized Thi and the absorbance band at 510 nm is from the Fe(II)-OP complex.

The decrease in the absorbance of the Thi band is attributed to the 50% dilution of the Thi solution with 1 mL of reactor solution, rather than the partial reduction of the indicator.

The results of this study strongly support the hypothesis that the soluble Fe(II) in the soil slurry is a major reductant of the redox indicator Thi and perhaps the *primary* reductant of Thi in soil slurries under Fe(III)-reducing conditions. However, Fe(II) may not be the *only* reductant of redox indicators under Fe(III)-reducing conditions. Other significant reductants may be present at lower concentrations or may have slower reaction kinetics with the redox indicator.

4.3.2 Titrations of free indicators with Fe(II) at pH 7

TB and CV, unlike Thi, had not been previously characterized by Lemmon (10) or Mobley (14). TB (tolonium chloride), a thiazine molecule that is colored blue in its oxidized form and colorless when reduced, is similar in structure to Thi. CV (5,9-diaminobenzo[a]- phenoxazonium acetate), is an oxazine-type compound with a structure similar to that of Nile blue (16). The structures of the indicators are shown in Figure 4.4.

The reduction of the redox indicators Thi, TB, or CV requires the transfer of two electrons and two protons (Eq. 4-1 with n = 2 and m =2). Fe(II), acting as a the reductant, transfers one electron for every Fe(II) atom. This half-reaction is

$$Fe(OH)_{3(s)} + e^- + 3H^+ \rightleftharpoons Fe(II) + 3H_2O \qquad (4\text{-}4)$$

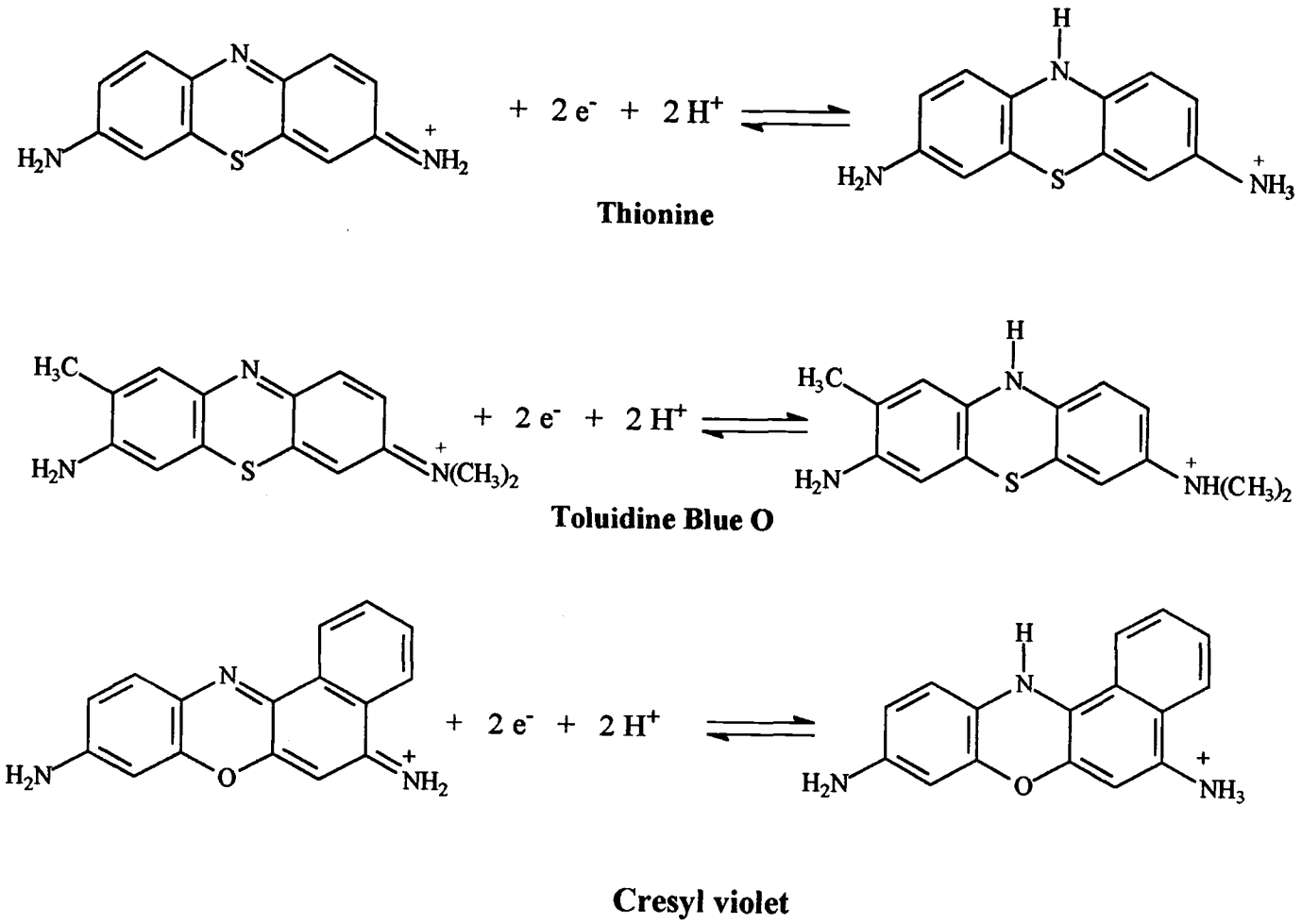

Figure 4.4 Structures of thionine (Thi), toluidine blue O (TB) and cresyl violet (CV).

where, at relevant environmental pH's (5-8), the Fe(III) form is an insoluble solid (17). The coupling of the two half reactions (eq. 4-1 and 4-4) yields

$$Ind_{(ox)} + 2\ Fe(II) + 6H_2O \rightleftharpoons Ind_{(red)} + 2\ Fe(OH)_3 + 4H^+ \qquad (4\text{-}5)$$

assuming that an Fe(III)-solid phase forms. The potential of the $Fe(II)/Fe(OH)_3$ couple can be calculated with the Nernst equation

$$E_{Fe(OH)_3/Fe(II)} = E_m^{0'} - \frac{RT}{nF} \ln [Fe(II)] \qquad (4\text{-}6)$$

where $E_m^{0'}$ is the formal potential of the Fe couple at a given pH. The likely Fe(III) products, ferrihydrite or lepidocrocite, have $E_7^{0'}$ (formal potential at pH 7) values of -0.182 and -0.274 V, respectively. For an Fe(II)/indicator system at equilibrium, the potentials would be equal (the indicator potential is given by equation 4-2 or 4-3).

Titration data for the three free indicators with Fe(II) at pH 7.0 are shown in Figure 4.5. In Figure 4.5A it is clear that the order of reduction is Thi, TB and CV. For CV, reduction occurred at a considerably lower potential and required a much greater amount (and concentration) of Fe(II) (Figure 4.5B).

Formal potentials at pH 7 are compared in Table 4.1 and the values measured for Thi and TB in this work correspond well with literature values (except for one literature value for TB (18)) and values previously measured in this laboratory. However, the formal potential measured for CV differs significantly from the single literature value found (18). The method for determination of the formal potentials at pH 7 of TB ($E_7^{0'}$ = +31 mV) and CV ($E_7^{0'}$ = -75 mV) by Ti(III) citrate titration are presented in Appendix I.

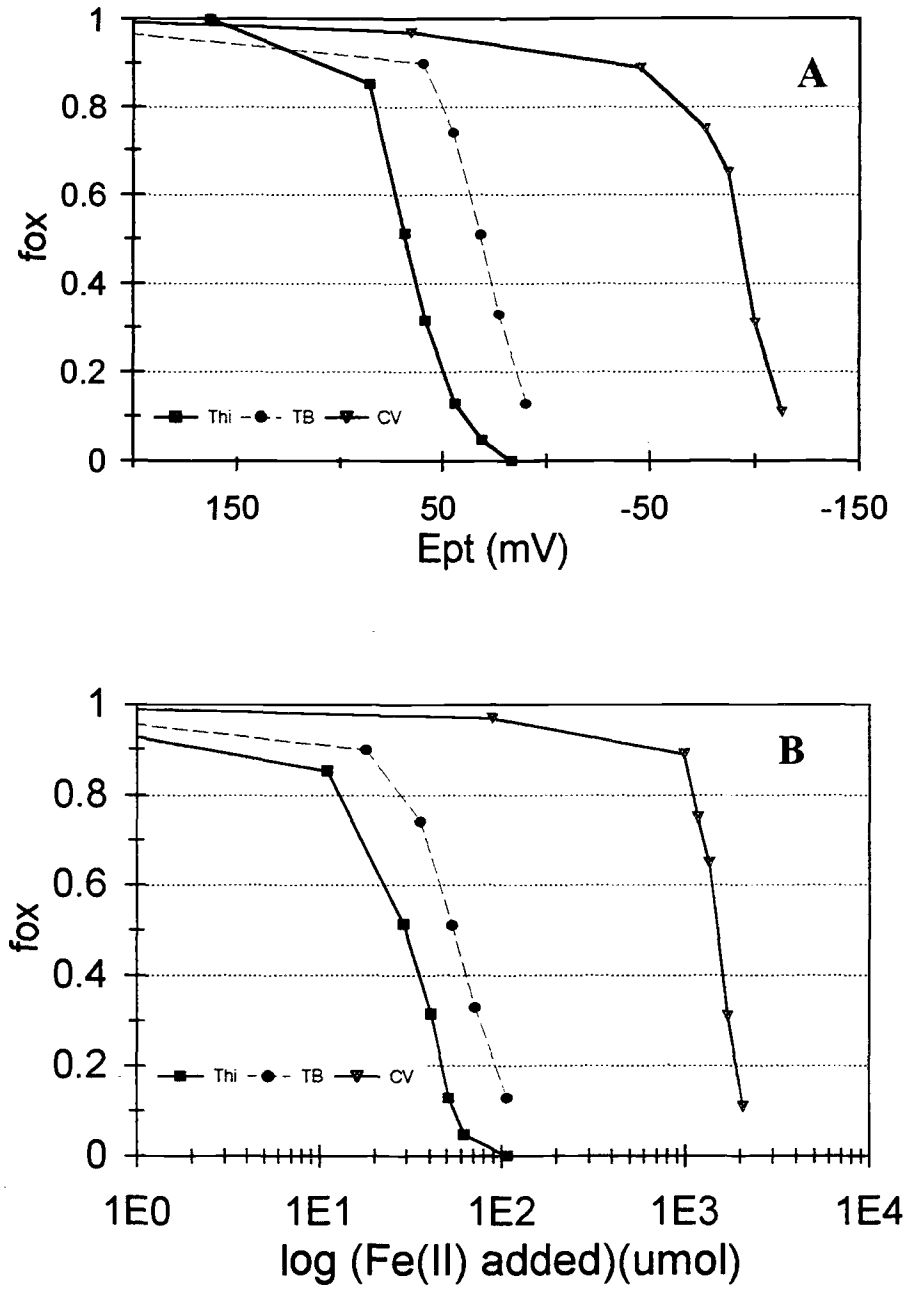

Figure 4.5 Comparison of results for titrations of 20 μM thionine, toluidine blue O and cresyl violet with Fe(II) at pH 7 in terms of E_{Pt} (A) and total Fe(II) added (B). The indicators poise the Pt electrode as they are reduced. Cresyl violet, with the much lower formal potential, requires far more Fe(II) for reduction than the other two indicators.

Table 4.1 Formal potentials of indicators at pH 7.

Indicator	$E_7^{0'}$(mV)[a]	$E_7^{0'}$(mV)[b]	$E_7^{0'}$(mV)[c]	$E_7^{0'}$(mV)[d]	$E_7^{0'}$(mV)[e] (this work)	$E_7^{0'}$(mV)[f] (this work)
thionine	+64	+62	+66	NT[g]	+66	+75
toluidine blue	+34	-11	NT	+31	+31	+36, +23
cresyl violet	not found	-167	NT	-75	-92	-77

[a] From Bishop (12).
[b] From Jacob (18).
[c] From Ti(III) citrate titration(10, 13).
[d] From Ti(III) citrate titration, Jones (Appendix I).
[e] From this work, Fe(II) titration of single indicators (data from Figure 4.6).
[f] From this work, Fe(II) titration of two indicators in solution; two values for TB based on titrations with Thi and CV, respectively (data from Figure 4.8).
[g] NT, not tested.

$E_7^{0'}$ values for d, e, f, determined by interpolation of graphical results.

Titration data for 20 μM of free Thi, TB and CV at pH 7 are shown in separate graphs in Figure 4.6 (same data as in Figure 4.5), along with the measured Fe(II) concentration. Note that Fe(II) was detected only after the last addition when Thi was nearly completely reduced. In contrast, for TB and CV, significant soluble Fe(II) was measured before complete reduction and more total Fe(II) was required to completely reduce these indicators. This behavior is consistent with the lower reduction potentials of these indicators and demonstrates the equilibrium between the indicator and Fe couples. For the titration of TB, the Fe(II) concentration was estimated to be ~30 μM at half-reduction ($f_{ox} = 0.5$) and ~65 μM at complete reduction. For CV, the indicator with the lowest reduction potential, about 1100 μM Fe(II) was required to achieve half-reduction, over an order of magnitude greater than for Thi or TB.

From the titration data, Fe(II) mass balances were evaluated by calculating the fraction Fe(II) recovered [f(Fe(II))] from

$$f(Fe(II)) = \frac{(2*[Ind]*(1-f_{ox}) + [Fe(II)]_{meas})*V}{N_{Fe(II)}} \quad (4\text{-}7)$$

where [Ind] is the initial indicator concentration (μM) (each indicator molecule is assumed to react with two Fe(II) ions), f_{ox} is the fraction of oxidized indicator, $[Fe(II)]_{meas}$ is the measured Fe(II) concentration (μM), V is the volume of indicator solution in the reactor (1 L), and $N_{Fe(II)}$ is the amount of Fe(II) added (μmol). For titrations of Thi and TB (Figure 4.7A), there was considerable variability in the fraction of Fe(II) recovered (50 - 90 % for Thi and 20 - 95% for TB). For TB, notably, the measured concentration of Fe(II) and f_{ox} of the indicator did not change with the last

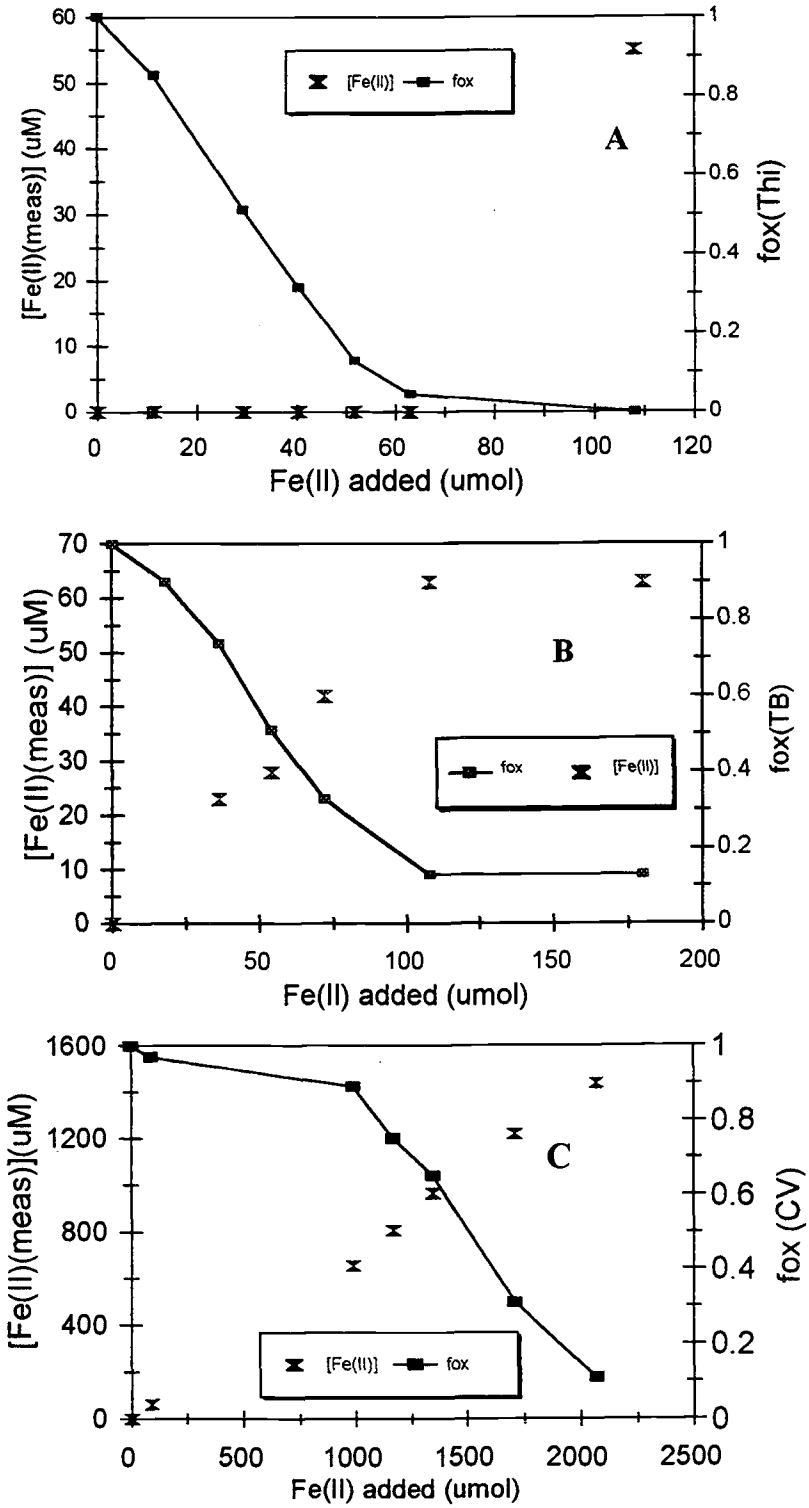

Figure 4.6 Results from titrations of 20 μM thionine (A), toluidine blue O (B) and cresyl violet acetate (C) with Fe(II) at pH 7. Fe(II) could only be measured after Thi was completely reduced. Cresyl violet (CV) required over 2000 μmol of total Fe(II) for complete reduction compared to about 60 and 110 μmol Fe(II) for Thi and TB, respectively.

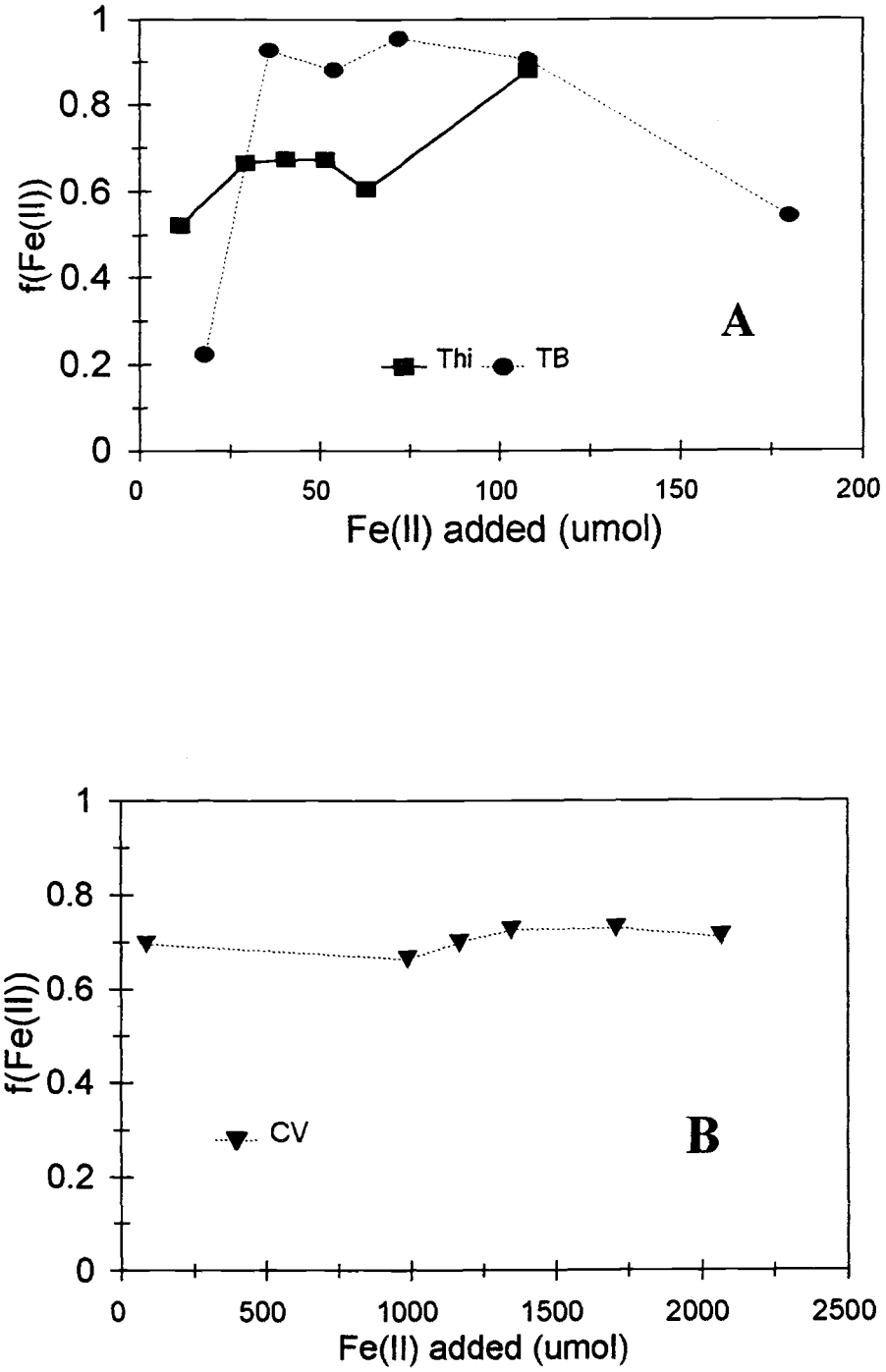

Figure 4.7 Variation of fraction of Fe(II) recovered (f(Fe(II)) with Fe(II) added for thionine (Thi) and toluidine blue O (TB) (A) and cresyl violet (CV) (B).

addition of Fe(II). For the titration of CV, however, Fe(II) recovery remained nearly constant at 75% (Figure 4.7B).

The low recovery of Fe(II) may be due to different causes. As Fe(II) reduces an indicator molecule, it forms Fe(III)-hydroxide which subsequently precipitates and can adsorb Fe(II) (4). It is hypothesized that a fraction of the Fe(II) added may have been adsorbed to Fe(III)-solids formed during reduction of the indicator. Also, a small fraction of the Fe(II) standard solution may have been oxidized to Fe(III) by O_2 during preparation (no measurements were made to determine this) or residual O_2 in the reactor solution. For Thi or TB, which have a considerably higher formal potential than that of CV, the rate of reduction was faster (for CV, it took about twice as long for the potential and absorbance to stabilize after each Fe(II) addition). The lower variability in the fraction of Fe(II) recovered for the Fe(II)/CV system, relative to the Fe(II)/Thi and Fe(II)/TB systems, may be due to the longer equilibration time for Fe(II) adsorption to stabilize or the high molar ratio of Fe(II) relative to $Fe(OH)_3$ or the indicator.

Results of titrations of mixed indicator systems with Fe(II) at pH 7.0 (Figure 4.8) proved to be similar to those for titrations of the single indicator species, except for CV. Formal potentials and Fe(II) levels required to reduce a given fraction of indicator for both single and mixed indicator systems are summarized in Tables 4.1 and 4.2, respectively. For titrations of 10 μM Thi and TB (Figures 4.8A and B), Fe(II) levels were not measurable until Thi was nearly completely reduced. TB was about half reduced when the Fe(II) concentration was ~30 μM as observed with TB by itself. Measured formal potentials differed by 9 mV for Thi and 5 mV for CV in the single and

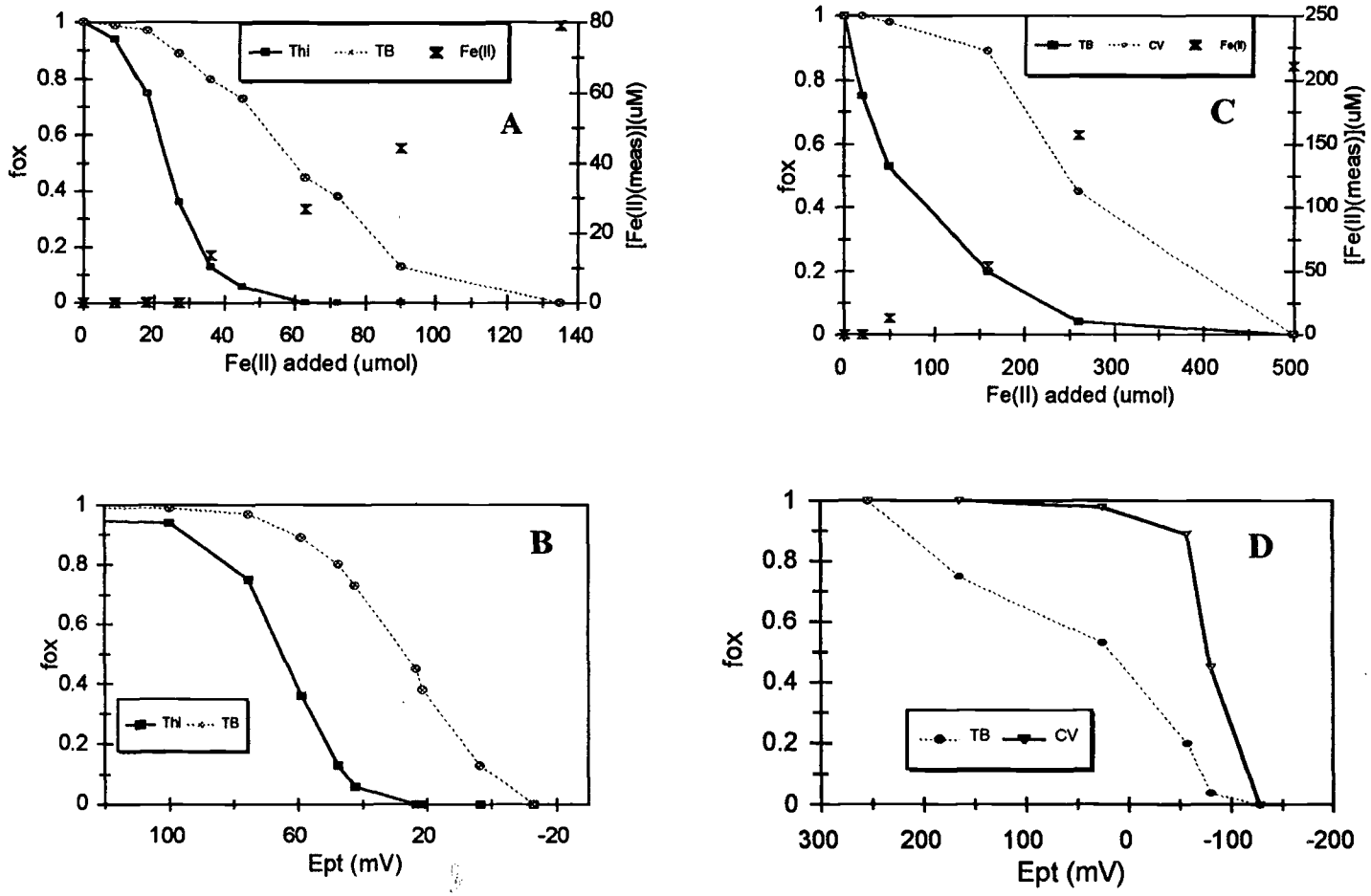

Figure 4.8 Reduction of mixtures of 10 μM each thionine and toluidine blue O at pH 7 (A,B) or 10 μM toluidine blue O and 20 μM cresyl violet (C,D). Cresyl violet is reduced at much lower concentrations of Fe(II) in the mixture than when by itself (~200 μmol compared to ~2000 μmol).

Table 4.2 Comparison of Fe(II) levels measured at pH 7 for given f_{ox} values for indicators.

Indicator	[Fe(II)][a](μM): f_{ox} = 0.5 (stoichiometry)[c] (single indicator)	[Fe(II)][a](μM): f_{ox} < 0.1 (stoichiometry)[c] (single indicator)	[Fe(II)][b](μM): f_{ox} = 0.5 (mixed indicators)	[Fe(II)][b](μM): f_{ox} < 0.1 (mixed indicators)
Thi	NM[e] (1:1)	NM (1:1)	NM	20
TB[d]	28 (1:2.8)	65 (1:3.3)	27, 15	45, 80
CV	1100 (1:8)	1450 (1:6)	130	200

[a] From titrations of single indicators (data from Figure 4.6).
[b] From titrations of mixed indicators (data from Figure 4.8).
[c] "Corrected" stoichiometry based on amount of indicator titrated compared to one-half of amount of Fe(II) added (stoichiometry based on eq. 4-5).
[d] Data based on $f_{ox} \approx 0.15$ rather than $f_{ox} < 0.1$.
[e] NM, not measurable.

mixed indicator solutions. Small differences in measured formal potentials could be due to small differences in pH between test solutions (a change of as little as ±0.2 pH units would alter the potential about 12 mV for the indicators near pH 7).

For the mixture of 10 μM TB and 20 μM CV (Figures 4.8C & D), the amount of Fe(II) required (equilibrium concentration) to reduce one-half of TB is within a factor of 2 observed in the Thi/TB mixture (Table 4.2) or TB by itself. However, CV was reduced with much less total Fe(II) than observed in the single-indicator experiment (f_{ox} = 0.5 with an Fe(II) level about one-eighth that observed with CV by itself (130 vs 1100 μM)).

Analysis of the E_{Pt} data (Table 4.1) shows that the measured formal potential (i.e., at half-reduction) for TB in a mixture of TB and CV is within 7 mV of the single indicator value. For CV in the mixture, the measured formal potential is significantly less (15 mV) than that derived from Fe(II) titration data of the single indicator, but it differs by only 2 mV from the formal potential measured by titration with Ti(III) citrate. The high levels of Fe(II) (> 1000 μM) in the reactor necessary to reduce CV (by itself) might have affected the response of the Pt electrode (mixed potential) or of the pH or reference electrode. In another study with deaerated electrolyte in the reactor, Fe(II) levels in excess of 1 mM drove E_{Pt} values below -100 mV (11).

In Table 4.3, measured Fe(II) levels for f_{ox} = 0.5 for Thi, TB and CV (for both single indicator and mixed indicator experiments) are compared to Fe(II) levels expected based on Fe(II)/ferrihydrite and Fe(II)/lepidocrocite models, based on mass balance, and based on total Fe(II) added. The thermodynamic model is derived by equating the redox potentials of the indicator and $Fe(OH)_3$/Fe(II) couples (equations 4-3 and 4-6,

Table 4.3 Comparison of measured and calculated Fe(II) levels for $f_{ox} = 0.5$ for Thi, TB and CV at pH 7.

Indicator	$E_7^{0'}$ (mV)[a]	[Fe(II)](μM) measured total Fe(II) added[b] based on mass balance[c] (single indicator)	[Fe(II)](μM) measured total Fe(II) added[b] based on mass balance[c] (mixed indicator)	[Fe(II)](μM)[d] calculated with Fe(II)/ferrihydrite model	[Fe(II)](μM)[d] calculated with Fe(II)/lepidocrocite model
Thi	+66	NM[e] 30 10	NM 25 13	60	2
TB	+31	28 55 30	27 15 60 60 30 43	250	7
CV	-75	1100 1500 1480	130 250 210	15,000	420

[a] From Ti(III) citrate titration measurements (Appendix I).

[b] Total moles of Fe(II) added to achieve half reduction ($f_{ox} = 0.5$) of a given indicator (interpolated from graphs).

[c] Based on total Fe(II) added and assumed stoichiometric reaction of Fe(II) with redox indicator as specified in equation 4-8

$$[Fe(II)]_{mb} = [\{\text{moles Fe(II) added}\} - 2*(\{\text{moles of indicator reduced}\}/\{\text{volume of reactor solution}\})] \quad (4\text{-}8)$$

[d] Based on solving eq. 4-9 (in text) for [Fe(II)] with $f_{ox} = 0.5$

$$[Fe(II)](M) = \text{antilog}\,((-1/0.059)*(E_{ind,m}^{o'} - E_{Fe,m}^{o'})) \quad (4\text{-}10)$$

where $E_{Fe,m}^{o'}$ is the formal potential for the Fe(II)/Fe(III)-solid couple at pH m, and at pH 7 is -0.182 V for ferrihydrite and -0.274 V for the lepidocrocite solid phases.

[e] NM, not measured.

respectively) from which the fraction of indicator oxidized can be calculated as shown in equation 4-9.

$$f_{ox} = \frac{1}{\left(10^{\left[\frac{2}{0.059}\left(E^{0'}_{ind,m} - E^{0'}_{Fe(OH)3/Fe(II),m}\right) + \log\,[Fe(II)]^2\right]} + 1\right)} \qquad (4\text{-}9)$$

Details of the derivation are presented in Appendix F.

For the single indicator titrations, the measured Fe(II) levels lie between those predicted from the ferrihydrite and lepidocrocite models (although the lepidocrocite model more closely predicts the levels). For Thi, the lepidocrocite model predicts that Fe(II) levels would be nearly unmeasurable at half-reduction (the detection limit with the OP method is 2 - 5 μM (19)) which is consistent with the results obtained. For TB in the single and mixed indicator systems, the (calculated) Fe(II) levels based on a mass balance necessary to achieve half-reduction are comparable (between 30 and 45 μM), as are the measured levels (between 15 and 30 μM). However, this overall range (15 - 45 μM) differs significantly from levels calculated with either model.

Interestingly, the Fe(II) level (measured or based on a mass balance) for half-reduction of CV in the mixture TB/CV is somewhat lower than that predicted by the lepidocrocite model. Furthermore, the great difference between Fe(II) levels (measured or based on a mass balance) for reduction of the CV by itself and CV in the mixture (about a factor of 7) is quite remarkable and puzzling. Possibly the hydrophobic nature of CV promotes association with other similar species. For instance, oxidized CV may associate with TB, somehow affecting its interaction with Fe(II). A different Fe(III) product, with a lower formal potential may have been formed, but the measured potential at half-reduction for CV in the mixture is very close to that obtained from the Ti(III)

citrate titration, suggesting that the basic chemistry of CV was not altered too significantly (there was also no obvious change in the wavelength maximum during the titration).

4.3.3 pH dependence of reduction of free thionine with Fe(II)

The equilibrium reaction between Fe(II) and an indicator to form an iron hydroxide solid phase (Eq. 4-5), such as ferrihydrite or lepidocrocite, is very pH dependent, and the concentration of Fe(II) required to reduce a given concentration of indicator decreases with increasing pH. The E_H/pH dependence of the half-reaction for the redox indicator is not obvious in equation 4-2 because it is incorporated in the formal potential.

For thiazine type indicators (e.g., thionine), $E_m^{0\prime}$, the formal potential at a specified pH, is given by Bishop (12) as

$$E_m^{0'} = E^{0'} + \frac{RT}{nF}\ln\left(\frac{[H^+]^4 + K_{r1}[H^+]^3 + K_{r1}K_{r2}[H^+]^2}{[H^+] + K_{O1}}\right) \qquad (4\text{-}11)$$

where K_{r1} and K_{r2} are acid dissociation constants of the reduced form of the indicator and K_{O1} is the acid dissociation constant for the oxidized form of the indicator. For Thi, K_{r1}, K_{r2} and K_{O1} are $10^{-4.38}$, $10^{-5.3}$ and $10^{-11.0}$, respectively (12) ($E^{0\prime}$ was calculated by substitution of the measured $E_7^{0\prime}$ of +0.066 V and $[H^+] = 10^{-7}$ into eq. 4-11 and solving gave $E^{0\prime} = 0.558$ V). However, for pH values from 6 to 8 (relevant environmental pH values) some terms are negligible and eq. 4-11 simplifies to

$$E_m^{0'} \approx E^{0'} + \frac{RT}{nF}\ln(K_{r1}[H^+]^2 + K_{r1}K_{r2}[H^+]) \qquad (4\text{-}12)$$

In Figure 4.9, the theoretical E_H/pH dependence of the free indicator Thi is compared to that for a ferrihydrite Fe(III)-solid phase at three different Fe(II) concentrations. The Thi potential is not nearly as dependent on pH (about 29 mV/pH unit in region of pH 6 - 8) as the Fe(II)/ferrihydrite potential, which exhibits a slope of 177 mV per unit pH. At a pH of about 6.5 and below, the Fe(II)/ferrihydrite equilibrium lines are above (at a higher potential) than that of the Thi line (Fe(II) is stable relative to Thi and Thi remains oxidized). Significantly below pH 7, only very high levels (>> 1 mM) of Fe(II) would significantly reduce Thi. Near pH 7, Fe(II) (> 100 μM) has the ability to reduce Thi, and above pH 7, ferrihydrite would be the predominant form of the Fe couple ([Fe(II)] > 10 μM). Significantly above pH 7, even sub-micromolar levels of Fe(II) should completely reduce Thi.

Clearly, pH is by far the more important factor in the Thi/Fe(II) equilibrium compared to the Fe(II) concentration. In the region of pH 6.5 - 7.5, Thi indicator speciation might be used to predict approximate Fe(II) levels in environmental systems under Fe(III)-reducing conditions if the pH were accurately known and the solid Fe(III) phase formed was known and homogenous (i.e., the Fe(III)-solid formed is not a mixed phase).

The results of titrations of 20 μM free Thi at pH values of 6.3 and 7.5 are shown in Figure 4.10. In the figure, the Thi redox potential (E(thi)) calculated from the indicator speciation corresponds closely to the measured E_{Pt} during the titration. The

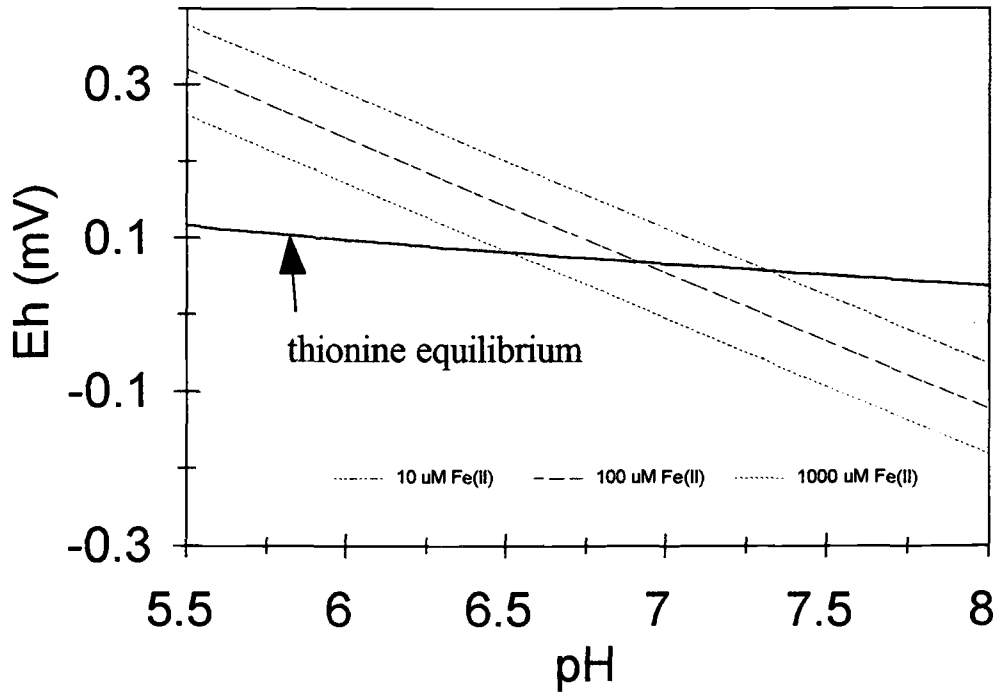

Figure 4.9 Dependence of E_H of the free Thi couple (E_{ind}) and the Fe(II)/ferrihydrite couple on pH. The Thi line is based on equations 4-3 and 4-12 with f_{ox} = 0.5 (half-reduced). The three Fe lines are based on Fe(II) concentrations of 10, 100 and 1000 μM and equation 4-6. For pH 6, 7 and 8, the theoretical Fe(II) concentration (based on the ferrihydrite model) to reduce half the Thi is 18 mM, 63 μM and 0.2 μM, respectively.

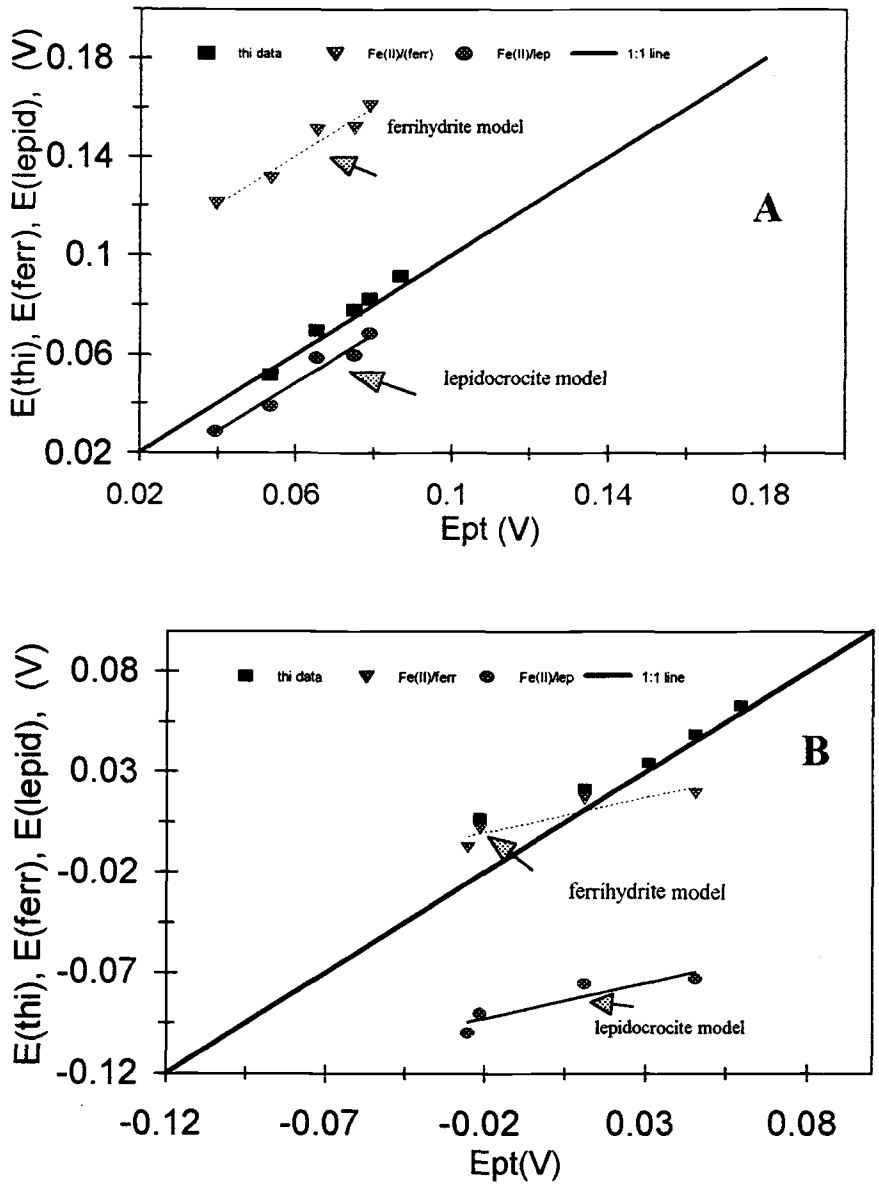

Figure 4.10 Comparison of redox potentials for the titration of 20 μM free Thi with Fe(II) at pH 6.3 (A) and 7.5 (B). The redox potential of the indicator (E(thi)) is calculated from equations 4-3 and 4-12 and the measured speciation. The redox potentials based on the Fe(II)/lepidocrocite and Fe(II)/ferrihydrite equilibrium models and the measured Fe(II) concentration are calculated with equation 4-6 and the appropriate formal potential. Data for the titration of Thi at pH 7.0 are not shown. At pH 6.3, the data fit more closely to the Fe(II)/lepidocrocite equilibrium model. However, at pH 7.5, the data fit more closely to the Fe(II)/ferrihydrite equilibrium model.

corresponding least-squares fits based on equilibrium models for two Fe(III) oxides and the measured Fe(II) concentration are also shown. At pH 6.3, the calculated Fe(II) potentials (in the figure, E(ferr) and E(lep), respectively) lie significantly closer to the lepidocrocite equilibrium line than the ferrihydrite equilibrium line. However, at pH 7.5, the Fe(II) data appear closer to the ferrihydrite line (at pH 7.0, only one data point for Fe(II) concentration was measured so no figure is shown). From the data, it cannot be stated that the Fe(II)/free Thi system is in true thermodynamic equilibrium. Possibly, more than one solid Fe(III) phase was formed.

Fe(II) levels necessary to achieve a given level of reduction of free Thi at pH 6.3, 7, and 7.5 are summarized in Table 4.4. At pH 6.3, much more Fe(II) was required to reduce the Thi than at pH 7 or 7.5, following the expected pattern. However, more Fe(II) was measured (and added) at pH 7.5 than at 7, a result opposite to that predicted from the Thi/Fe(II) equilibrium (Fig. 4.9). The nature of the Fe(III)-hydroxide phase formed may change with pH as supported by the data in Figure 4.10. Because the formal potential of the Fe(II)/ferrihydrite couple is greater than that of the Fe(II)/ lepidocrocite couple by nearly 100 mV ($E_7^{0'}$ = -0.182 vs -0.274 V, respectively), Fe(II) would be a weaker reductant if ferrihydrite were the Fe(III)-product formed at pH 7.5.

4.3.4 Titrations of immobilized indicators with Fe(II)

Data for the titrations of immobilized Thi, TB and CV with Fe(II) at pH 7 are shown in Figure 4.11 and the results are summarized in Table 4.5. As with the corresponding free indicators, Fe(II) concentrations about two orders of magnitude

Table 4.4 Comparison of Fe(II) titration data of 20 μM Thi at pH 6.3, 7 and 7.5.

pH	[Fe(II)](μM) (for observable reduction)	[Fe(II)](μM) f_{ox} = 0.5 measured (added)[a]	[Fe(II)](μM) f_{ox} < 0.1 measured (added)	stoichiometry[b]	[Fe(II)](μM)[c] f_{ox} = 0.5 or (0.1) calculated ferrihydrite model	[Fe(II)](μM)[c] f_{ox} = 0.5 or (0.1) calculated lepidocrocite model
6.3	>100	200 (270)	500 (600)	~20:1	3300 (27,000)	92 (760)
7	NM[d]	NM (25)	NM (60)	~3:1	63 (188)	2 (5)
7.5	NM	NM (30)	35 (75)	~3.8:1	4 (8)	0.1 (0.2)

[a] μmol added to 1 L.
[b] Based on total Fe(II) added to completely reduce 20 μM Thi; 2:1 is expected by balanced reaction equation.
[c] Based on eq. 4-10 or eq. 4-9 with f_{ox} = 0.1 and $E_{ind,m}^{0'}$ given by eq. 4-12.
[d] NM, not measurable.

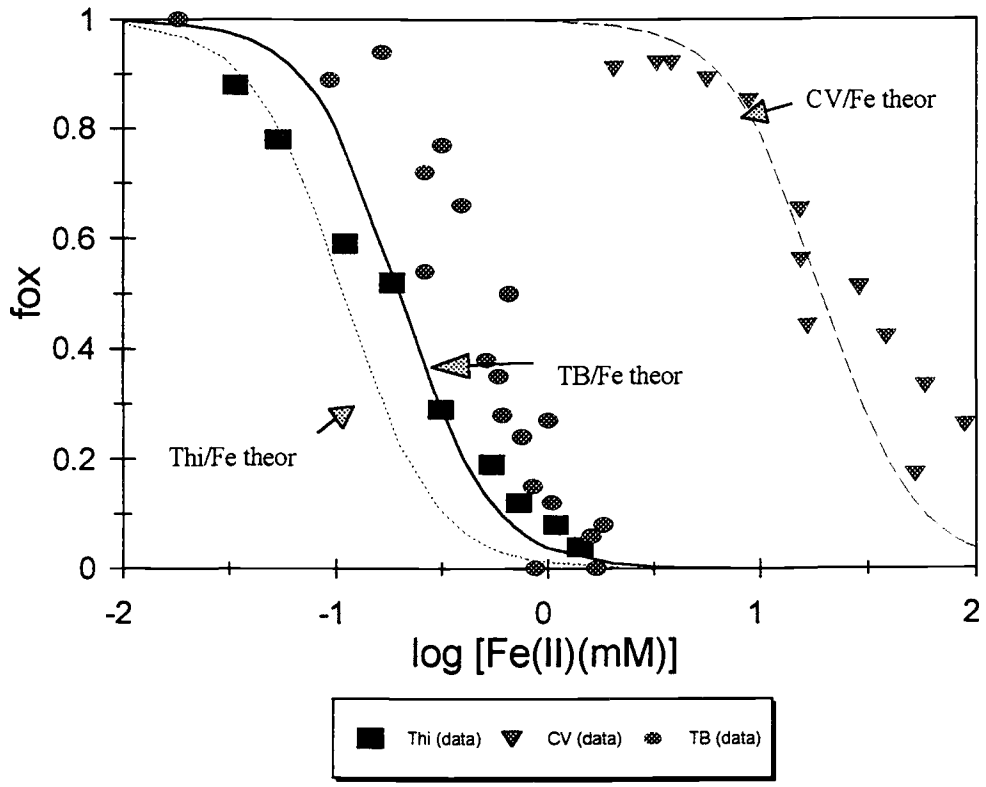

Figure 4.11 Comparison of titration data of immobilized Thi, TB and CV with Fe(II) to results predicted from equilibrium models based on ferrihydrite as the Fe(III)-solid phase at pH 7. The theoretical sigmoidal-shaped curves are based on calculations for the equilibrium between a given indicator couple and the ferrihydrite/Fe(II) couple (equation 4-9) and the measured Fe(II) concentration.

Table 4.5 Summary of results of titrations of immobilized indicators with Fe(II) at pH 7.

redox indicator	$E_7^{0'}$ (mV) free	$E_7^{0'}$ (mV) immobilized	[Fe(II)](μM) $f_{ox} \approx 0.8$ immobilized (free)	[Fe(II)](μM) $f_{ox} = 0.5$ immobilized (free)	[Fe(II)](μM) $f_{ox} < 0.1$ immobilized (free)	[Fe(II)](μM) $f_{ox} = 0.5$ immobilized based on lepidocrocite model[c]	[Fe(II)](μM) $f_{ox} = 0.5$ immobilized based on ferrihydrite model[c]
Thi	+66	+52	60 (NM[a])	200 (NM)	650 (NM)	3	100
TB	+31	+36	200 (NM)	400 (28)	1000 (65)	6	200
CV	-75	-81	10,000 (800)	16,000 (1100)	ND[b] (1500)	540	19,000

[a] NM, not measured.
[b] ND, not determined.
[c] based on eq. 4-10.

greater were required to reduce a given fraction of CV relative to Thi. About 10 mM Fe(II) was needed to observe significant reduction ($f_{ox} \approx 0.8$) of CV. Upon immobilization, the formal potentials of Thi and CV decreased by 5-15 mV, making the (equilibrium) concentration of Fe(II) necessary to reduce a given fraction of immobilized Thi or CV higher than that for the free indicator. For TB, immobilization increased the formal potential about 5 mV.

Much more Fe(II) (by an order of magnitude) is required to achieve a given level of reduction (Table 4.5) of immobilized TB relative to free TB. This behavior may be due to the formation of a different Fe(III) product (with a much higher formal potential) or non-equilibrium conditions at the times indicator absorbance and [Fe(II)] were measured. It takes some time for Fe(II) to be pumped from the reactor to the flow cell, diffuse into the agarose beads, and reach all immobilized indicator molecules.

The experimental titration data shown in Figure 4.11 agree more closely with the equilibrium line predicted by the Fe(II)/ferrihydrite model than the Fe(II)/lepidocrocite model (which better matched titration data of the free indicators (Tables 4.3, 4.4)). Similar S-shaped curves calculated with lepidocrocite as the Fe(III)-solid phase (not shown) were shifted about two orders of magnitude toward lower [Fe(II)] compared to the curves shown.

It is clear from Figure 4.11 that more Fe(II) is required to reduce Thi or TB than expected from the equilibrium model based on ferrihydrite and there is significant scatter in the experimental data for all three indicators. This scatter may be due to kinetic factors (i.e., not allowing enough time for the system to come to equilibrium), small pH

variations, or inaccurate absorbance values due to light scattering from the buildup of Fe(III)-solids in the flow cell over time.

Titration data at pH 8 are summarized in Table 4.6. Relative to pH 7, substantially less Fe(II) was required to reduce the immobilized indicators. With either indicator, more Fe(II) was added to achieve half reduction than predicted by equilibrium models with ferrihydrite or lepidocrocite as the solid phase. No attempt was made to reduce the immobilized indicators at pH values lower than 7.

Figure 4.12 shows the effects of raising and lowering (by dilution) the Fe(II) concentration on the speciation of immobilized TB at pH 7. Note that the redox speciation of the TB tracks Fe(II) concentration during both addition and dilution stages. These data provides strong evidence of the reversibility of the indicator/Fe(II) redox reaction.

In many experiments involving titrations of the immobilized indicators with Fe(II), a buildup of a brownish layer (believed to be Fe(III)-oxides and/or Fe(II)-hydroxides) on the agarose beads in the flow cell coincided with the initial reduction of the indicators. It is hypothesized that as Fe(II) concentrations decrease in the reactor solution, the Fe(III)-oxides coated on the beads are responsible for the reoxidation of the indicator. Possibly, the Fe(III)-solids provide a catalytic surface or provide a high localized Fe(II) concentration that enhances the rate of reduction of the indicator by Fe(II).

During titrations of free indicators, Fe(III)-oxide buildup was not observed. Oxide buildup is more obvious in the packed flow cell because it is indicated

Table 4.6 Comparison of fraction of immobilized Thi and CV reduced at pH 7 and 8.

indicator	[Fe(II)](μM) pH 7[a] for $f_{ox} \approx 0.8$ $f_{ox} = 0.5$ $f_{ox} < 0.1$	[Fe(II)](μM) pH 8 for $f_{ox} \approx 0.8$ $f_{ox} = 0.5$ $f_{ox} < 0.1$	[Fe(II)](μM) pH 8 for $f_{ox} = 0.5$ based on lepidocrocite model[b]	[Fe(II)](μM) pH 8 for $f_{ox} = 0.5$ based on ferrihydrite model[b]
Thi	60 200 650	NM[c] 40 150	0.01	0.3
CV	10,000 16,000 ND[d]	600 ND ND	2	60

[a] Same data as in Table 4.5.

[b] Based on eq. 4-10 and $E_{ind,m}^{0'}$ given by eq. 4-12; assumptions: 1) that pH dependence of formal potential of immobilized indicator is similar to that of the free indicator; 2) the pH dependence of formal potential of CV is similar to that of Thi (~30 mV/pH unit).

[c] NM, not measured.

[d] ND, not determined.

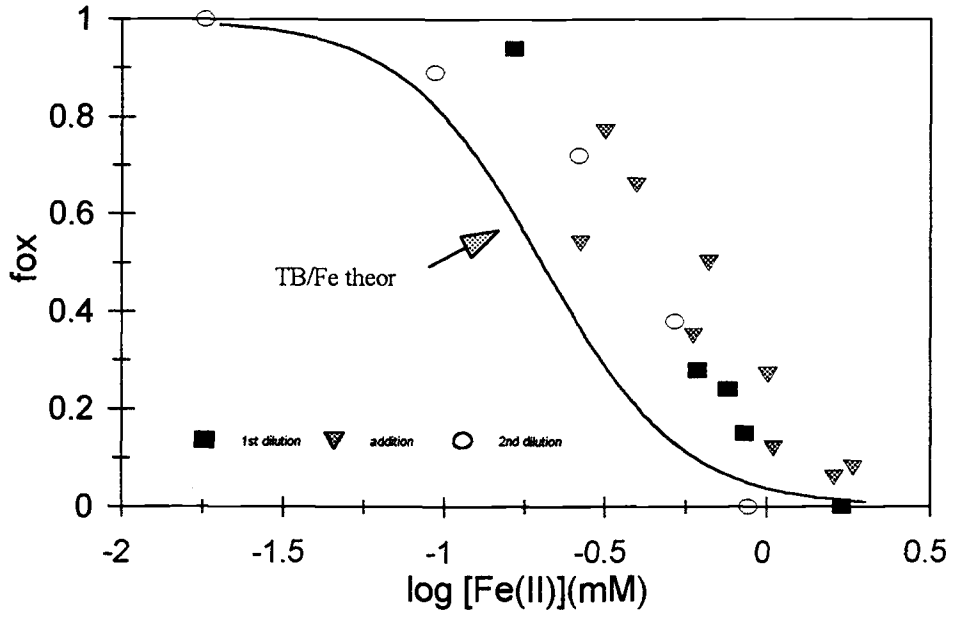

Figure 4.12 Dependence of speciation of TB on Fe(II) concentration at pH 7, showing reversibility of Fe(II)-TB equilibrium. Fe(II) was first added to the reactor to completely reduce TB. The solution was then diluted, more Fe(II) was added, and the solution was diluted again.

spectrophotometrically by an increasing baseline absorbance and the confinement of the indicator and Fe(III) oxides to a small volume. Also with free indicators, it is not possible to decrease the Fe(II) concentration by dilution without also decreasing the concentration of indicator.

Algebraic manipulation of the equations describing the indicator/Fe equilibrium (see Appendix F) shows that the concentration ratio of the reduced to oxidized forms is given by

$$[\text{Ind(red)}]/[\text{Ind(ox)}] = (1 - f_{ox})/f_{ox} = k\,[\text{Fe(II)}]^2 \qquad (4\text{-}13)$$

where

$$k = \exp[((nF/RT)(E_{ind,m}^{0\prime} - E_{Fe,m}^{0\prime})] \qquad (4\text{-}14)$$

Therefore, a plot of the square of the concentration of Fe(II) vs. $(1 - f_{ox})/f_{ox}$ should be linear with a slope related to the difference in formal potentials of the indicator and Fe couples. Such a plot is shown in Figure 4.13 for data acquired during titrations of TB and Thi at pH 7 (different data than presented in Figure 4.11). Although there is considerable scatter, the data for TB and Thi are consistent with the prediction of the linear model, suggesting that indicator absorbance might be used as a qualitative measure of Fe(II) levels over the range of 100 to 1000 μM.

Note that the relative scatter in the data (possibly due to making measurements before equilibrium is reached, pH variations, or random error in the measurements) is enhanced (compared to sigmoidal equilibrium plots) by squaring the [Fe(II)] (compared to taking the log) and by taking the ratio of $(1 - f_{ox})/f_{ox}$ (compared to f_{ox} by itself). Furthermore, the scatter in the data makes a more detailed statistical analysis of the results difficult, and therefore, the results should be interpreted qualitatively rather than

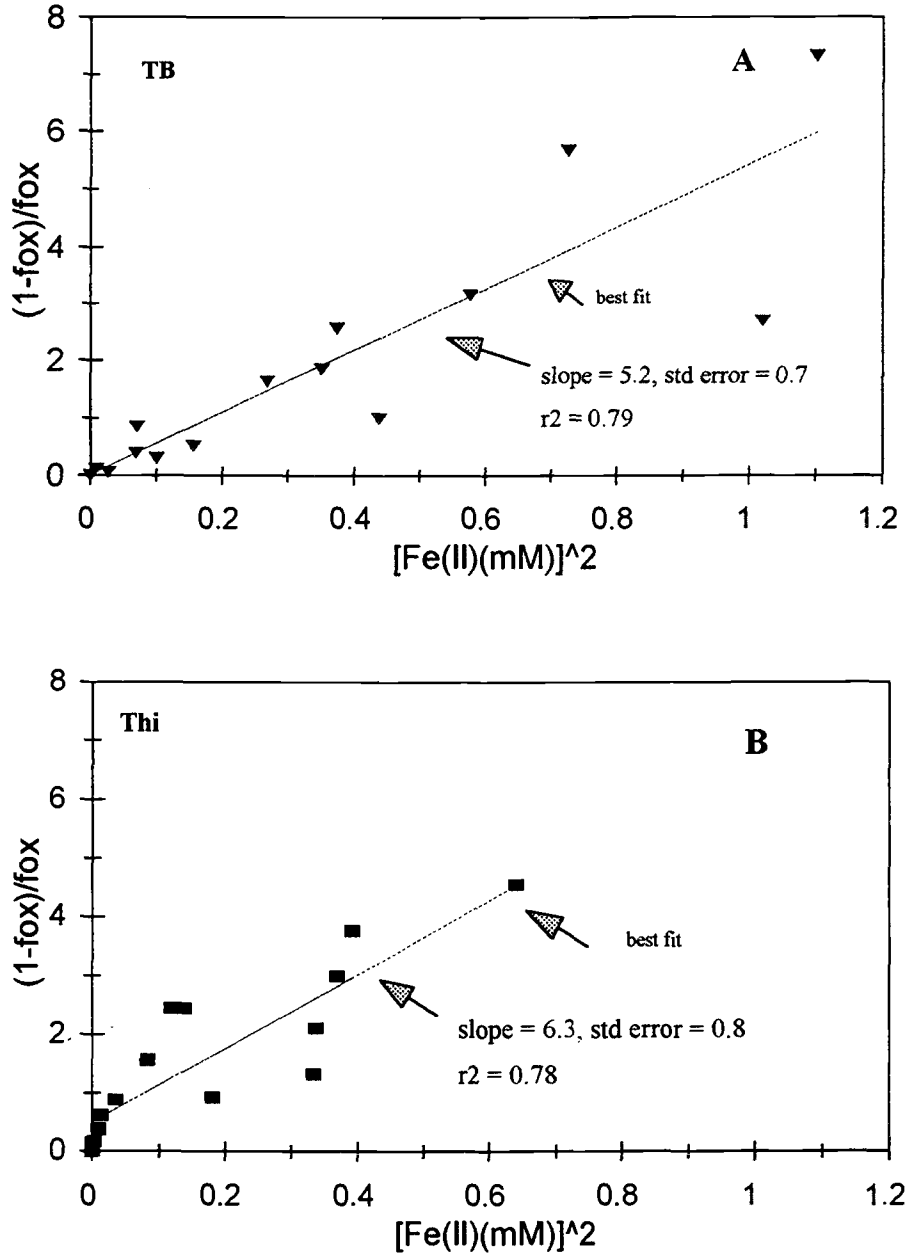

Figure 4.13 Linearized plots of Fe(II) titrations of immobilized TB (A) and immobilized Thi (B) at pH 7. Lines shown are least squares fits. For TB, the intercept of the best fit was 0.03 with a standard error of 0.33. For Thi, the intercept of the best fit was 0.5 with a standard error of 0.2.

quantitatively. Initially plots of $(1 - f_{ox})/f_{ox}$ vs [Fe(II)] for TB and Thi were made and found to be quite non-linear (correlation coefficients for the linear least squares fit of 0.3 and 0.08, respectively).

The effect of the concentration of immobilized indicator on titrations with Fe(II) are shown in Figure 4.14. The relative concentration of the immobilized TB varied about a factor of 4 as indicated by the absorbance of the fully oxidized indicator. With a higher TB concentration, the Fe(II) level necessary for reduction of a given fraction of TB increased and the slope of the curve in Figure 4.14 decreased (31, 4.2 and 1.7 $(mM)^{-2}$, respectively).

Similar behavior was observed for titrations of free Thi (20 and 40 μM) with Fe(II) at pH 7 as discussed in more detail in Appendix J. With 20 μM Thi, essentially no Fe(II) was measurable in solution until after complete reduction of Thi (data presented in Figure 4.6). With 40 μM Thi, Fe(II) levels ranged from 45 μM for $f_{ox} = 0.75$ to 170 μM for $f_{ox} = 0.30$.

The equilibrium model used to describe the reaction between a redox indicator couple and the Fe(II)/ferrihydrite (or lepidocrocite) couple reaction does not predict that the equilibrium concentration of Fe(II) to reduce a given fraction of indicator is dependent on the indicator concentration. A change is formal potential of the indicator or Fe couple with indicator concentration could cause the observed effect. One possibility is that Fe(II) adsorbed on Fe(III)-oxides, or Fe(II)-hydroxides themselves, may be partially or primarily responsible for the reduction of the immobilized indicators.

These results indicate that semi-quantitative measurements of Fe(II) levels with immobilized redox indicators would require calibration of a particular batch of the

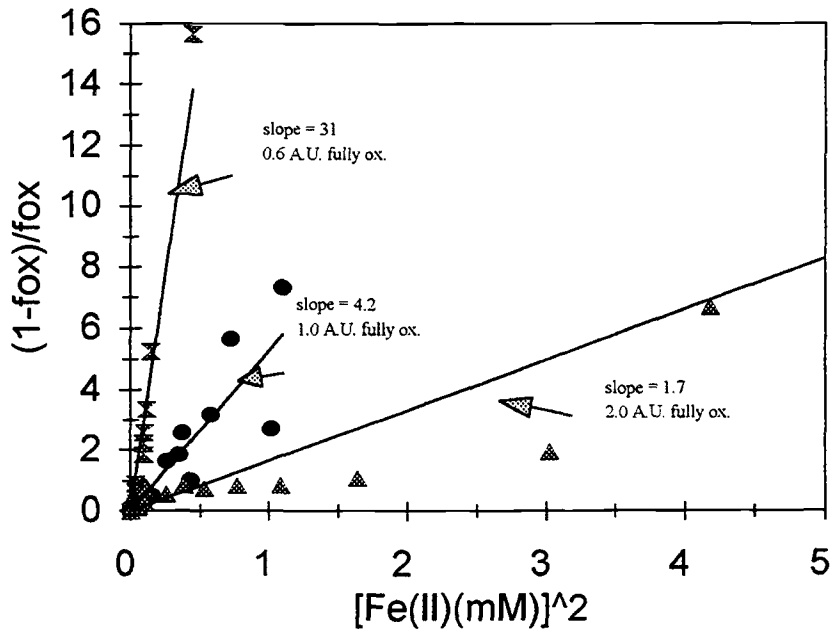

Figure 4.14 Dependence of the speciation of immobilized TB on its concentration and the concentration of Fe(II) at pH 7. Lines shown are linear least squares fits. The effective concentration of the TB is proportional to the absorbance of the fully oxidized indicator shown. The Fe(II) concentration required to reduce half the indicator (calculated with the eq. 4-3 and the slope of the linear least squares fit) is 0.18, 0.49 and 0.77 mM for absorbances of 0.6, 1.0 and 2.0 A.U.

immobilized indicator (i.e., the fraction of indicator reduced may depend on its effective concentration). A lower level of immobilization might be utilized to detect lower concentrations of Fe(II) with immobilized indicators.

Results for the concurrent titration of Thi, TB and CV with Fe(II) at pH 7.0 are shown in Figure 4.15. The redox potential calculated from the measured [Fe(II)] (based on ferrihydrite as the solid phase) is plotted on the x-axis and the redox potential calculated from speciation of the redox indicators is plotted on the y-axis. For a system at equilibrium, all data should fall along the diagonal. Thionine data lie closer to the diagonal near its formal potential (52 mV), but at lower potentials (higher Fe(II) levels), the data deviate more above the diagonal, possibly due to the difficulty in accurately measuring f_{ox} when $Fe(OH)_3$ builds up in the flow cell.

TB data are noticeably further from the diagonal while CV data lie closest to the diagonal. Inconsistencies may be due to non-equilibrium conditions or differences in the effective concentration of immobilized indicators on the beads.

4.3.5 Evaluation of immobilized thionine and cresyl violet in wastewater slurries

Figure 4.16A shows the time dependence of Fe(II) levels and the speciation of immobilized Thi and CV in contact with a wastewater slurry under Fe(III)-reducing conditions at pH 7. The Fe(II) levels in the wastewater slurry rose to just over 400 μM, which was sufficient to reduce ~75% of the Thi ($f_{ox} = 0.25$). The absorbance of CV decreased slightly (to $f_{ox} = 0.8$), but changes this small can be due to changes in the packing density of the beads. The Pt electrode remained poised at about -260 mV for

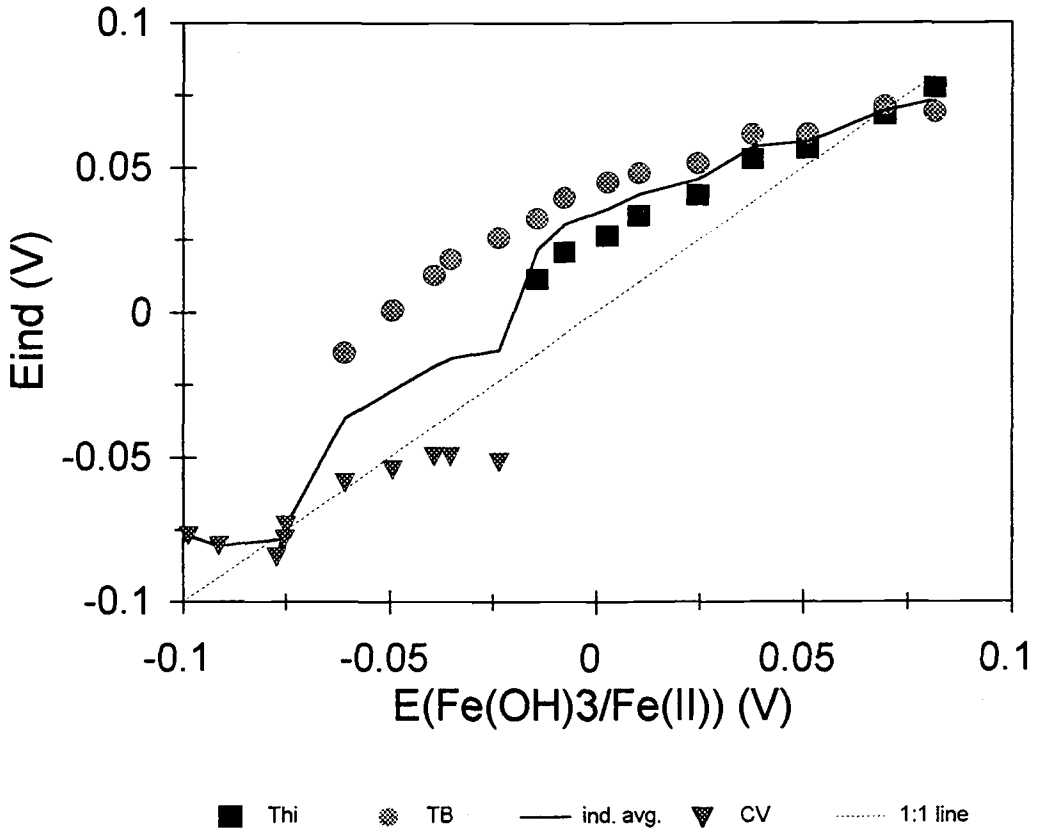

Figure 4.15 Comparison of the redox potentials calculated from the speciation of immobilized indicators to the redox potential calculated for the Fe(II)/ferrihydrite couple. Data were acquired during the concurrent titration of thionine (Thi), toluidine blue (TB), and cresyl violet (CV) measured with Fe(II) at pH 7. The 1:1 line on the figure is the equilibrium line based on measured Fe(II) concentrations and eq. 4-6. The redox potential for the indicator (E_{ind}) is calculated from eq. 4-3. The formal potentials for Thi, TB, and CV are 52, 36, and -81 mV, respectively.

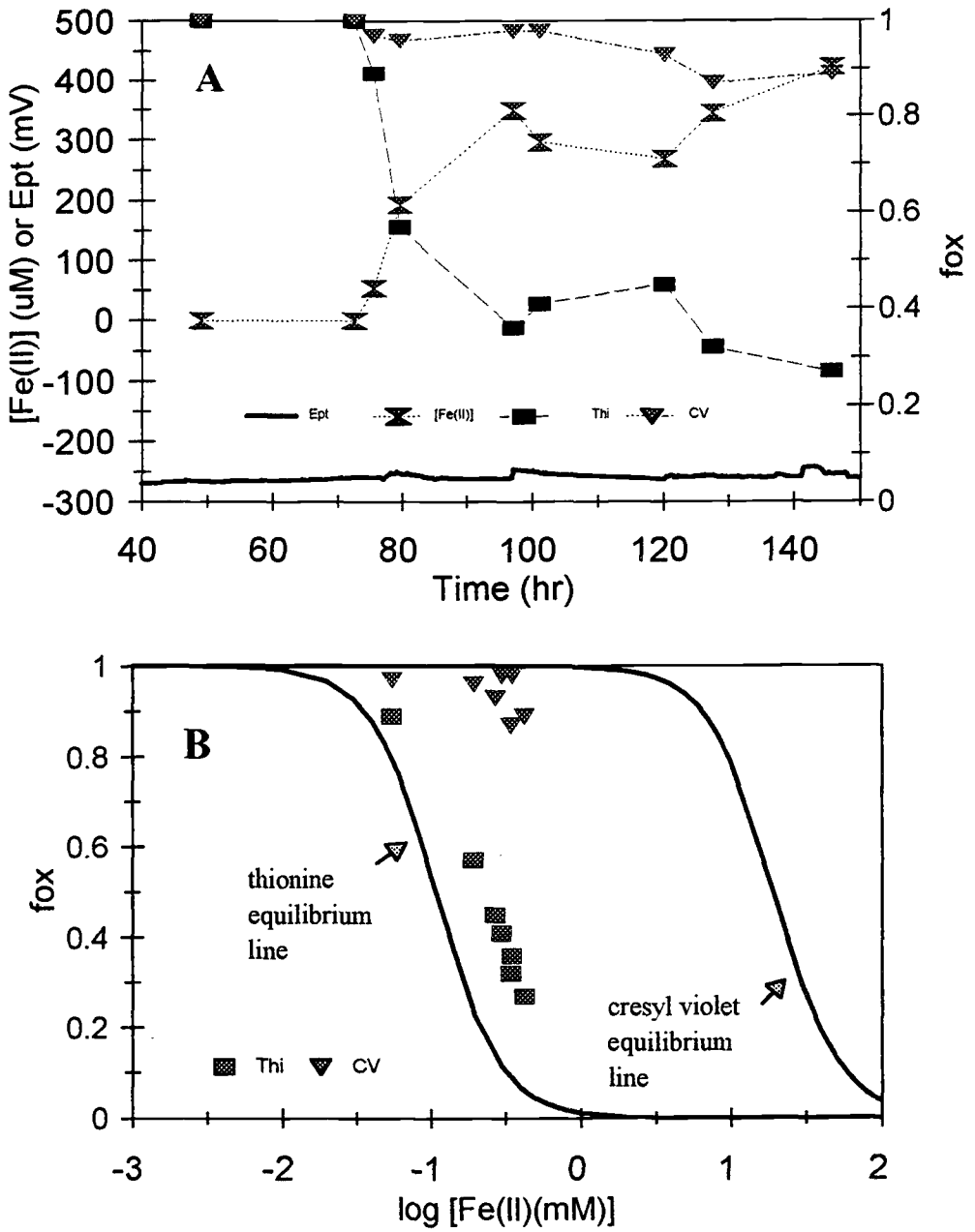

Figure 4.16 Correlation of the redox speciation of immobilized thionine (Thi) and cresyl violet (CV) to Fe(II) levels in a wastewater slurry (A) and comparison to equilibrium models (B) at pH 7. The equilibrium model is based on ferrihydrite as the Fe(III)-solid phase (eq. 4-9).

the duration of the experiment. Often a value of E_{Pt} this negative is indicative of the sulfate-reducers and methanogens in the slurry. However, no sulfide was detected (with CHEMetrics vials, the detection limit is about 0.5 μM total sulfide).

About 0.1 - 0.2 mM more Fe(II) was required to achieve the level of reduction of Thi than predicted by the equilibrium model based on ferrihydrite as the solid. Similar results were previously obtained for titrations of immobilized Thi with Fe(II) in a simple buffer solution (Figure 4.11). In both wastewater and simple solutions, more than 0.4 mM Fe(II) was necessary for significant reduction of CV ($f_{ox} < 0.8$) .

4.3.6 Application of redox indicators to evaluation of arsenic transformations

In soils, As(V) is known to adsorb strongly on the surface of Fe(III)-oxides and is subsequently released upon reduction of the Fe(III) (5). Figure 4.17A shows how Fe(II) levels and speciation of immobilized Thi correlate to redox transformations of As in a Bashaw soil slurry to which As(V) had been added and strongly adsorbed (at 0 hr). The time dependence of Pt electrode potential and pH is presented in Figure 4.17B. After ~100 hr under microbially-mediated, Fe(III)-reducing conditions (E_{Pt} = +80 mV), Fe(II) levels rose to nearly 300 μM, at which point soluble As(III) was detected. After about 175 hr (E_{Pt} = -100 mV), reduction of Thi began. By 300 hr, Thi was completely reduced.

At ~460 hr, about 400 mL of reactor solution leaked out through the flow cell in the external loop. When the reactor was subsequently refilled to the 1-L level with a deaerated DI water solution (2.5 mM $CaCl_2$ and 0.5 mM NH_4Cl), unexpectedly, the

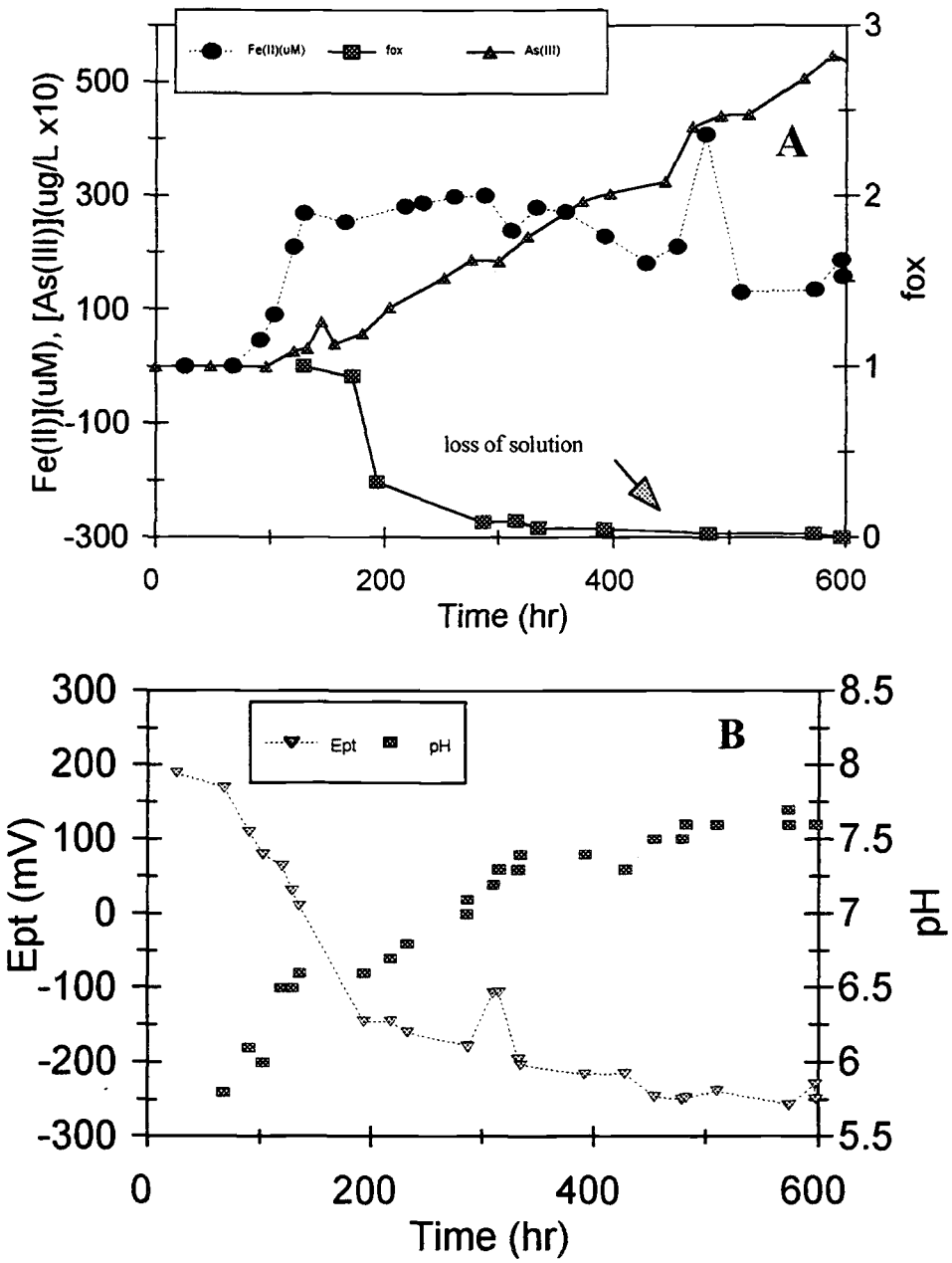

Figure 4.17 Time dependence of indicator speciation, arsenic speciation, and Fe(II) level in a Bashaw soil slurry under Fe(III)-reducing conditions. As Fe(II) levels rose to ~300 μM (A), As(III) was first observed in solution, and soon reduction of the immobilized indicator Thi commenced. In (B) the variation of Pt electrode potential and pH is shown.

measured Fe(II) level rose to ~400 μM but then eventually decreased. Eventually, E_{Pt} of the slurry decreased to about -250 mV.

Overall, there is a clear relationship between the appearance of Fe(II) in solution, the rising levels of As(III), and the reduction of Thi. The lag time between the appearance of significant Fe(II) levels (>100 μM) and reduction of Thi (~300 μM) appears to be related to the pH which rose from an initial value of 5.2 to about 7.6. Partial reduction ($f_{ox} \approx 0.3$) of Thi (~ 195 hr) occurred when the pH was measured to be ~6.6 with [Fe(II)] ≈ 0.3 mM. Based on equilibrium calculations at pH 6.6, the calculated [Fe(II)] to achieve $f_{ox} = 0.3$ is 1.1 and 0.03 mM with ferrihydrite and lepidocrocite as the Fe(III)-solid phase, respectively. It is possible that the Fe(III)-solid formed at the lower pH was a mixed phase of ferrihydrite and lepidocrocite. The results previously obtained by titrations of Thi with Fe(II) suggest that the solid-phase formed may vary with pH and that at lower pH, the lepidocrocite model provides a better prediction of the experimental results (i.e., less Fe(II) is required to reduce a given fraction of Thi than predicted by the ferrihydrite model). As the pH of the slurry rose above 7 (around 300 hr), Thi was almost completely reduced.

4.4 Conclusions

In the soil and wastewater slurries studied, Fe(II) appears to be a major reductant of the redox indicator Thi under Fe(III)-reducing conditions. In simple test solutions containing Fe(II) and in wastewater slurries, the presence of the OP, an Fe(II) complexing agent, impeded the reduction of Thi. Although there is no proof that Fe(II) is the *only* reductant of Thi under Fe(III)-reducing conditions, the data do support the notion that Fe(II) is indeed an *important* reductant. It is possible that other reductants or mediators are involved in the actual reduction of the indicator.

Increases in Fe(II) levels appear to be a "redox marker" for the transformation of As(V) to As(III). The immobilized indicator Thi, coupling to Fe(II) in solution, provides a convenient means to sense the onset of this transformation. Previously, Lemmon (10) demonstrated that the onset of Thi reduction indicates complete reduction of soluble Cr(VI) to Cr(III). There is good evidence to suggest that Thi speciation could be used in the field to determine when redox transformations of both Fe(III) and As(V) are occurring and if the transformation of Cr(VI) to Cr(III) has occurred.

Thi and TB have shown to couple well to Fe(II) at pH values greater than about 6.5 and Fe(II) levels greater than 100 μM. TB, with a formal potential ~15 mV below that of Thi, requires Fe(II) levels about 50 - 200 μM greater than those for Thi to achieve the same level of reduction (f_{ox}) of Thi. For field monitoring, the use of both indicators is limited to samples above pH of ~6.5 because otherwise much higher Fe(II) levels are required for reduction at lower pH values (e.g., ~10 mM for Thi at $f_{ox} = 0.5$ and pH 6 based on ferrihydrite as the solid phase). Based on experimental evidence and

equilibrium models, even low levels of Fe(II) (~10 μM and less) can substantially reduce Thi and TB, at pH values greater than ~7.5. Overall, Thi or TB speciation appear to be useful for sensing Fe(III)-reducing conditions and estimating Fe(II) levels under these conditions in the pH range of ~6.5 to ~7.5. To make good estimates of Fe(II) concentrations, pH would have to be measured to within 0.1 pH unit.

Under normal field conditions, CV would not be reduced by Fe(II) because its formal (immobilized) potential is too low (-81 mV). For field measurements, monitoring the speciation of Thi and TB concurrently (along with pH), would provide a means of qualitatively estimating Fe(II) level in the range of 0.1 - 0.8 mM (at pH 7). If CV were also monitored concurrently, this region could be extended up to 5 mM or higher (if Fe(II) levels were ever to rise that high).

In terms of the development of a field sensor for estimating [Fe(II)], the Fe(II)/indicator equilibrium is reversible (i.e., reduced indicator is re-oxidized when the Fe(II) level is lowered). It is hypothesized that a buildup of Fe(III)-hydroxides in the flow cell (observed as a brownish discoloration and increase in background absorbance) is a critical aspect of this reversibility. Interestingly, initial reduction of the indicator did not occur until some discoloration was observed. Fe(III)-solid particles may be involved in catalysis of indicator reduction.

Comparison of data from Fe(II)/indicator titrations to predictions from equilibrium models do not confirm any distinct Fe(III)-solid phase. With immobilized indicators, the fraction of indicator oxidized can be better predicted with a model based on the Fe(III)-solid ferrihydrite. For free Thi, experimental results are better predicted at pH 6.3 with a Fe(II)/lepidocrocite couple and at pH 7.5 by the Fe(II)/ferrihydrite model.

These results suggest that pH, and probably other factors, influence the nature of the actual Fe(III) product(s) formed. This uncertainty in nature of the Fe(III)-solid phase (e.g. formal potential) leads to difficulties in estimating Fe(II) levels with an Fe(II) sensor based on immobilized redox indicators.

According to simple equilibrium models with any one Fe(III)-solid phase, the speciation of the indicator at a specific pH should be identical for a given level of Fe(II), regardless of the total concentration of the redox indicator. Experimentally, with either free or immobilized indicators, the concentration of Fe(II) required to reduce a given fraction of indicator increased when the total redox indicator concentration was increased. It is difficult to determine if the Fe(II)/indicator system *does not* achieve equilibrium, or if the system *does* achieve equilibrium but an inappropriate equilibrium model or parameter (e.g., formal potential) is being applied. A more sophisticated model would have to consider both soluble Fe(II) and Fe(II) adsorbed on the Fe(III)-hydroxides as reductants.

Immobilized and free redox indicators couple to Fe(II) in much the same manner and their redox characteristics are affected similarly by pH and indicator concentration. However, there are important differences, especially in terms of their applicability to environmental field analysis. An immobilized indicator is fixed to a sensor surface, will not be adsorbed to particles in ground water or soils, and can be retracted from the sample (allowing for multiple analyses). A free indicator, once mixed with the sample, cannot be extracted easily for later use. Nevertheless, free indicator tends to react and come to equilibrium more quickly with Fe(II) (15 - 30 min) than does immobilized indicator (1 - 2 hr). The slower response for immobilized indicators is due in part to the

need for filtering and pumping (0.5 - 1.0 mL/min) the sample to a flow cell and the low rates of mass transfer through the beads in the flow cell.

As an indicator of Fe(III)-reducing conditions, Thi ($E^{0\prime}_7$ = +52 mV) is perhaps the best choice as it reacts to the lowest levels of Fe(II). TB ($E^{0\prime}_7$ = +36 mV) is not as useful for detection of Fe(II) because a higher level is required to achieve a given level of reduction. However, TB may be useful for semi-quantitative analysis of Fe(II) because it has a surprisingly linear response to Fe(II) for plots of $((1 - f_{ox})/f_{ox})$ vs. $[Fe(II)]^2$ (Figure 4.13A). TB may have a formal potential too similar to Thi to provide any unique information about redox levels or redox transformations. CV ($E^{0\prime}_7$ = -81 mV), with the lowest potential, may find application to lower redox potential regions (i.e., sulfate-reducing or methanogenic conditions).

For further development of field sensors for Fe(III)-reducing conditions, research should be directed at finding and characterizing a redox indicator which reacts with trace levels of Fe(II) (< 10 μM). Such an indicator should have a significantly higher formal potential (perhaps 150 - 250 mV) and an amine group for immobilization. Unfortunately, none of the redox indicators that have been immobilized during this thesis research or known from the literature meet these criteria.

It may be necessary to try different immobilization schemes and/or to use a chelated-inorganic redox indicator. One possible organic redox indicator with a formal potential in this range is 2,6-dichloroindophenol ($E_7^{0\prime}$ = +217 mV) (10), but unfortunately it is not reversible (14). It does not have an amine group, but does have a phenolic component which might be immobilized to an amine group via a Mannich reaction (20). This scheme involves the reaction of a hydrogen group *cis* to the -OH

group on the phenol with an amine group via formaldehyde as the crosslinker. This reaction has been used to immobilize phenol red to amine groups on agarose affinity beads (20).

A second option is the use of Fe(III)- or Cu(II)-chelates with formal potentials in the range of 150 to 1200 mV. Bishop (12) describes a variety of organic chelating agents (ligands) which form colored complexes with both Fe(II)/Fe(III) or Cu(I)/(II) for which the reduced species normally has a higher molar absorptivity. A well-known example is the inorganic chelate, Fe(II)/Fe(III)-$(OP)_3$ (ferroin), which has a formal potential of +1.12 V (10, 14). In general, Cu chelates have a lower formal potential than the Fe chelates (by 300 - 400 mV lower) (12). Use of these chelates would also require a sophisticated immobilization scheme, as none of the chelates have amine groups.

4.5 References

1. Chapelle, Francis H., *Groundwater Microbiology and Geochemistry,* John Wiley & Sons, Inc., 1993.

2. McBride, Murray B., *Environmental Chemistry of Soils*, Oxford University Press, Inc., 1994.

3. *Proceedings of Symposium on Paddy Soil*, Okazaki, Masanori; Wada, Hidenori; Takai, Yasuo, Science Press, Springer-Verlag: Beijing, China, 1981.

4. Bodek, Itamar, *Environmental Inorganic Chemistry: Properties, Processes, Estimation Methods*, Pergamon Press, Elmsford, N.Y., 1988.

5. Masscheleyn, Patrick H.; Delaune, Ronald D.; Patrick, William H. Jr., *J. Environ. Qual.*, **1991**, *20*, 522-527.

6. Masscheleyn, Patrick H.; Delaune, Ronald D.; Patrick, William H. Jr., *Environ. Sci. Technol.*, **1991**, *25*, 1414-1419.

7. *Standard Methods for the Examination of Water and Wastewater;* American Public Health Association: Washington, D. C., 1995.

8. Patrick, W. H., Jr.; Jugsujinda A., *Soil Sci. Soc. Am. J.*, **1992**, *56*, 1071-1073.

9. Lovley, Derek R.; Chapelle, Francis H.; Woodward, Joan C., *Environ. Sci. Technol.*, **1994**, *28*, 1205-1210.

10. Lemmon, Teresa, *Development of Chemostats and Use of Redox Indicators for Studying Transformations in Biogeochemical Matrices,* **1995,** Ph.D. Thesis, Oregon State University.

11. Jones, Brian; Chapter 3 of this thesis.

12. *Indicators*, Bishop, E., Ed., Pergamon Press: Oxford, 1972.

13. Lemmon, T. L.; Westall, J. C.; Ingle, J. D. Jr., *Anal. Chem.*, **1996**, *68*, 947-953.

14. Mobley, James, Oregon State University, unpublished report, **1992**.

15. Bos, Mark, *Part I: Development and Application of an Arsenic Speciation Technique Using Ion-Exchange Solid Phase Extraction Coupled with GFAAS, Part II: Investigation of Zinc Amalgam as a Reductant,* **1996**, M.S. Thesis, Oregon State University.

16. Green, Floyd J., *The Sigma Aldrich Handbook of Stains, Dyes and Indicators*, Aldrich Chemical Company, Inc.: Milwaukee, WI, 1990.

17. Snoeyink, Vernon L.; Jenkins, David, *Water Chemistry*, John Wiley & Sons, Inc., 1980.

18. Jacob, H. E., *Redox Potential,* p. 92-123, from *Methods in Microbiology, Vol. 2*, Norris, J. R.; Ribbons, D. W., Eds., Academic Press, Inc., New York: 1970.

19. Jones, Brian, personal research experience, 1993-1999, Oregon State University.

20. Hermanson, Greg T.; Mallia, A. Krishna; Smith, Paul K., *Immobilized Affinity Ligand Techniques*, Academic Press, Inc., 1992.

CHAPTER 5: EVALUATION OF REDOX INDICATORS FOR DETERMINING SULFATE-REDUCING AND METHANOGENIC CONDITIONS

5.1 Introduction

The sulfate-reducing and methanogenic (methane-producing) microbial redox levels are the most reducing redox levels in environmental systems. In terms of formal reduction potentials (E_H, all potentials are referenced to SHE), sulfate-reduction (at pH 7) occurs at about -220 mV (1) and methanogenesis (at pH 7) at about -240 mV (2). These low redox levels are attained in environmental systems when conditions are completely anoxic and the terminal electron acceptors (TEAs) NO_3^-, Mn(IV) and Fe(III) have been depleted (3). Sulfate-reducers use sulfate as the TEA in the process of creating ATP, producing sulfide (1, 3). Methanogens use CO_2 as a TEA, producing methane as a byproduct (1, 3).

As obligate anaerobes, sulfate-reducers and methanogens have a symbiotic relationship with fermentative microbes (3). Fermentative microbes break down larger organic molecules (e.g., carbohydrates), which sulfate-reducers and methanogens cannot use directly, to smaller organic acids (e.g., acetate, lactate) which sulfate-reducers and methanogens can utilize as electron donors (1). Details of microbial processes are described in Appendix G.

Currently, there is considerable interest in the development of a simple and accurate method for determination of redox conditions in environmental systems (4, 5). Furthermore, a variety of chlorinated organic contaminants are degraded under very

reducing conditions (e.g., sulfate-reduction and methanogenesis). For instance, in anaerobic groundwater aquifers, microbial dechlorination of the organic contaminant trichloroethylene (TCE) to *cis*-dichloroethylene (*cis*-DCE), has been shown to occur under sulfate-reducing conditions (6). In microbial cultures, partial transformations of tetrachloroethylene (PCE) and TCE to *cis*-DCE occur as conditions change from aerobic to anaerobic, accompanied by the release of sulfide (7). Anaerobic dechlorination of *cis*-DCE to the less halogenated (and more toxic) compound vinyl chloride (VC) and of VC to ethene occur under the more reducing, methanogenic redox level (6, 7).

Some pure microbial cultures, under sulfate-reducing or methanogenic conditions, can quantitatively dechlorinate carbon tetrachloride to chloroform (7). There is evidence that di- and trichlorofluoromethane are degraded under methanogenic conditions in freshwater sediments (7) and that PCB's may be partially degraded under methanogenic conditions (2). In addition, the non-halogenated organic compounds toluene and benzene have shown to degrade under methanogenic conditions (3).

Sulfate-reducing bacteria (e.g., *Desulfovibrio*) are commonly found in groundwater systems and were the first kind of bacteria isolated from deep environments such as oil reservoirs and aquifers (3). They commonly use H_2, lactate and acetate as electron donors. With sulfate as the TEA, sulfide is produced as hydrogen sulfide (2):

$$SO_4^{2-} + 8e^- + 10H^+ \rightleftharpoons H_2S(g) + 4H_2O \qquad (5\text{-}1)$$

Lactic acid is a common electron donor for sulfate-reducers. When coupled to the sulfate reduction half-reaction above, the overall reaction becomes (8)

$$2\ CH_3CHOHCOOH + SO_4^{2-} \rightarrow 2\ CH_3COOH + HS^- + H_2CO_3 + HCO_3^- \qquad (5\text{-}2)$$

The appearance of sulfide in environmental systems (e.g., groundwater aquifers) can have important consequences for the geochemistry of the local environment. Sulfide precipitates many divalent metal species including Fe(II), Cu(II), Hg(II) and Cd(II). Although this process reduces the solubility and mobility of these ions, it also tends to concentrate these precipitates in localized areas (2). This is particularly a problem when the system becomes re-oxidized, releasing Hg(II) and Cd(II) back into the environment (1). The re-oxidation of HgS also promotes methyl mercury production (1).

Sulfide is toxic to many organisms, as it combines with iron in cytochromes and other essential iron compounds in the cell (1). In water treatment processes, in addition to its toxicological properties, sulfide causes corrosion problems in concrete sewers and has claimed the lives of numerous workers (9). Sulfide also causes corrosion in stone and concrete, pumps and sewage distribution systems (8). In oil reserves and coal fields, sulfate-reduction over time has given rise to high concentrations of sulfur in these deposits, which leads to major pollution problems from the burning of these fuels (8).

Sulfate-reducing conditions in environmental systems are normally determined by monitoring decreases in sulfate concentration or the appearance or increase of sulfide in the system. Common means of measuring sulfate include ion chromatography with a conductivity detector and gravimetric or turbidimetric methods based on Ba(II) as a precipitating agent (9). Sulfide is commonly measured with the colorimetric methylene blue method, iodometric titrimetry (Appendix D), or potentiometry with a Ag/Ag_2S electrode (9).

Because of the nature of the analytical methods for sulfate, analysis in the field is often difficult. Ion chromatographs are relatively expensive and bulky, time-consuming to calibrate, and not particularly amenable to field use. Furthermore, gravimetric methods require filtering and drying of the precipitate, while turbidimetric methods, although simple to use in the field, are unselective and subject to interferences by particulates in the sample, and the detection limit is only about 1 mg SO_4^{2-}/L (~10 μM) (9). In addition to these problems, there is always the risk of oxidizing reduced sulfur species (e.g., HS^-, SO_3^{2-}) to sulfate upon sampling or during analysis.

Methods for determination of sulfide are somewhat less problematic than those for sulfate. The methylene blue method is a colorimetric method specific for total sulfide (S^{2-}, HS^- and H_2S) (9, 10). It is used for sulfide (field) testing kits from CHEMetrics based on vacuum-sealed, glass ampules filled with necessary reagents (i.e., dimethyl-*p*-phenylenediamine, ammonium phosphate), with a detection limit of about 0.06 mg/L (0.6 μM) (10). The use of Ag/Ag_2S electrodes in the field are also common and allow direct, *in situ* measurements of S^{2-} (DL ~ 3 μM *total* sulfide (11)). Iodometric methods (9), on the other hand, are not selective for sulfide, and also respond to sulfite and other reduced sulfur species (Appendix D).

However, both the methylene blue and Ag/Ag_2S potentiometric methods have some limitations. Reducing agents such as SO_3^{2-} can interfere with the color development with the methylene blue method. In fact, Frevert (11) found that the Ag/Ag_2S electrode was more suited for making sulfide measurements under conditions of varying ionic strength than the methylene blue method. However, for quantitative measurements, the Ag/Ag_2S electrode requires calibration (9) which is time consuming

and nearly impossible in *in situ* analysis in the field. Furthermore, Jeroschewski (12) points out that the Ag/Ag_2S electrode can respond to other species (i.e., a *mixed* potential is observed), and the response deviates from Nernstian below 10 μM total sulfide.

Misleading results can be obtained in the determination of sulfate-reducing conditions due to oxidation of sulfide to sulfate upon sampling or transport of sulfate or sulfide to regions where there is actually no sulfate reduction. Oxygen gas rapidly oxidizes sulfide, making measurements difficult (13). Also, sulfide commonly precipitates with many divalent metal ions, removing it from solution (14). Furthermore, sulfide as H_2S gas is highly volatile and can be lost upon sampling. Sulfate can often leach into aquifer systems and wells from mineral sources or move through the water column to areas depleted of sulfate (14). Therefore, a decrease in sulfate concentration over time in a given system or constant sulfate or sulfide concentrations in a system can be misinterpreted (14).

As sulfate is depleted in anaerobic environments, microbial activity shifts to using carbon dioxide as the terminal electron acceptor, and conditions become methanogenic and more reducing. The half-reaction for the conversion of CO_2 to CH_4 is (2)

$$CO_2(g) + 8H^+ + 8e^- \rightleftharpoons CH_4(g) + 2H_2O \qquad (5\text{-}3)$$

When coupled to H_2 as the electron donor, the overall reaction becomes (1)

$$4H_2(g) + H^+ + HCO_3^- \rightarrow CH_4(g) + 3H_2O \qquad (5\text{-}4)$$

Methane, unlike sulfide, is generally unreactive and its appearance in environmental systems does not significantly alter the local geochemistry. However, methanogenesis has significant effects on the carbon cycle (1). Methanogens are responsible for depletion of CO_2 and occasionally acetate (by acetate fermentation (1)) and commonly use H_2 as an electron donor. A symbiotic relationship exists between methanogens and H_2-producing, fermentative microbes which can oxidize complex organic molecules such as cellulose, proteins and fats to obtain energy. Removal of H_2 by methanogens (and sulfate-reducers) promotes this process and, ultimately, the degradation of complex organic molecules to CO_2, CH_4 and simple carbon species (e.g., acetate).

Methods for determination of methanogenic conditions are generally limited to analysis of CH_4 by gas chromatography with an FID or TCD detector (15) or titrimetric analysis for CO_2 (9). In controlled laboratory experiments with microbial cultures, $^{13}CO_2$ is often added to the system and $^{13}CH_4$ is quantified by isotopic analysis (1). Like H_2S, CH_4 is volatile and prone to transport to regions where conditions are not methanogenic. Therefore, determination of methanogenic conditions based solely on CH_4 analysis may be misleading.

There is some evidence that the Pt electrode potential (E_{Pt}) can be used to determine when sulfate-reducing and methanogenic conditions exist. Patrick (16), using a soil slurry in an anaerobic bioreactor in which E_{Pt} could be maintained constant (statted) by addition of O_2, found that the onset of sulfate reduction occurred at an E_{Pt} of approximately -150 mV. Furthermore, in studies of anaerobic marine sediments under sulfate-reducing conditions, Berner (17) reports E_{Pt} values between -150 and -250 mV.

A plot of E_{Pt} values versus the log of S^{2-} concentration calculated from Ag/Ag_2S electrode measurements was reasonably linear from 10^{-8} to 10^{-11} M S^{2-} and experimental E_{Pt} values were close to those predicted with the Nernst equation based on rhombic sulfur as the oxidized sulfur species. Lovley (18), summarizing the work of other researchers, presented results indicating that methanogenic conditions occurred at Pt electrode potentials of -200 to -250 mV.

There are, however, serious limitations to the use of E_{Pt} to determining sulfate-reducing and methanogenic conditions. Under sulfate-reducing conditions, E_{Pt} values have been reported to vary between 0 and -300 mV by different researchers (18). Fetzer (19), in studies of pure methanogenic cultures, found that E_{Pt} could be adjusted between -420 and +100 mV by addition of various oxidants (not O_2) and reductants without a substantial effect on the rate of methane production. Furthermore, it is well documented that the CO_2/CH_4 couple has no effect on E_{Pt} (20) and what redox species might be affecting E_{Pt} at this redox level have not been identified. Overall, the E_{Pt} values observed by many researchers for both redox conditions do not differ enough (or even overlap) to delineate between the two levels.

Compared to other methods, redox indicators present a possible means of determining when sulfate-reducing and/or methanogenic conditions exist. Normally, colored in their oxidized form and colorless when reduced, the absorbance of the redox indicator can be monitored with a spectrophotometer. As the oxidized species reacts with a reductant (e.g., S(-II)), the absorbance decreases and the "reducing power" of the sample can be estimated. The redox half-reaction of a redox indicator is described by

$$Ind_{ox} + ne^- + mH^+ \rightleftharpoons Ind_{red} \qquad (5\text{-}5)$$

where n, the number of electrons transferred, is typically 1 or 2, and m, the number of protons transferred, is typically 0, 1 or 2 and dependent on the pH (21).

Many redox indicators are reversible and couple to the Pt electrode (22-24). The redox potential for an indicator (E_{ind}) is determined by the relative concentrations (activities) of the oxidized and reduced species and the Nernst equation,

$$E_{ind} = E^{0'}_{ind,m} - \frac{RT}{nF} \ln \left(\frac{[Ind_{red}]}{[Ind_{ox}]} \right) \qquad (5\text{-}6)$$

where $E_{ind,m}{}^{0'}$ is the formal potential of the indicator and m indicates the pH. This formal potential is different for different indicators and is often a complex function of pH because many indicators have groups such as amines which can be protonated or unprotonated. Experimentally, the concentration ratio in equation 5-6 is evaluated by measuring the absorbance of one of the species, which is usually the colored oxidized form (see Appendix I for details). In this case, the concentration ratio equals $(1 - f_{ox})/f_{ox}$ where f_{ox} is the *fraction of indicator oxidized*, determined from the absorbance of the oxidized form of the indicator. Equation 5-6 can then be rewritten as

$$E_{ind} = E^{0'}_{ind,m} - \frac{RT}{nF} \ln \left(\frac{1 - f_{ox}}{f_{ox}} \right) \qquad (5\text{-}7)$$

In previous work, the immobilized redox indicator thionine (Thi) ($E_7{}^{0'}_{(imm)} = +52$ mV) was found to couple well to the reductant Fe(II) at pH 7 ($E_7{}^{0'} = +54$ mV for 100 μM Fe(II) and ferrihydrite Fe(III) product) (25). Furthermore, evidence supports the hypothesis that Fe(II), the product of the TEA process under Fe(III)-reducing conditions, is a primary reductant of Thi under these conditions (25). These results suggest that a redox indicator with a formal potential close to the formal potential of a

given TEA process may be useful for determining when a given redox level exists.

An indicator for sulfate-reducing conditions might be chosen so that it responds to (is reduced by) a reduced sulfur species such as SO_3^{2-} or S(-II) produced under sulfate-reducing conditions. Of these reduced sulfur species, sulfide (H_2S, HS, or S^{2-}) is the more common and less transitory product of this TEA process. Sulfite, the initial product of sulfate reduction, is rapidly reduced to sulfide by sulfate-reducing microorganisms (1). Furthermore, oxidation of S(-II) (by a given redox indicator) would most likely produce a solid sulfur species (e.g., rhombic sulfur, S^0(s, rhmb)) in a two electron transfer process rather than produce SO_4^{2-} which would require a transfer of eight electrons (1) (redox indicators commonly accept one or two electrons upon reduction (21)). The S^0(s, rhmb)/S^{2-} half-reaction

$$S^0(s, rhmb) + 2e^- \rightleftharpoons S^{2-}(aq) \qquad (5\text{-}8)$$

at 25°C, has a redox potential based on the Nernst equation (17) of

$$E_{S/S2-} = -0.475 - 0.0295 \log [S^{2-}] \qquad (5\text{-}9).$$

At pH 7 and 25°C, the redox potentials for 1, 10 and 100 μM *total* sulfide (see Appendix H for calculations based on $[S^{2-}]$ and $[S(-II)_{(tot)}]$) are -81, -111, and -140 mV, respectively.

Some redox indicators (e.g., Thi, cresyl violet (CV)) couple well to sulfide in solution (26) and may be useful for determining when sulfate-reducing conditions exist. Of the immobilized indicators characterized in previous work (Thi, toluidine blue O (TB), CV, and phenosafranine (PSaf) (22, 23, 25)), CV may be the indicator of choice for determining when sulfate-reducing conditions exist. This immobilized indicator has a

formal potential ($E_7^{0\prime}$ = -81 mV) nearest the $S^0_{(s,\ rhmb)}/S^{2-}$ couple at pH 7 with 1 - 100 μM total sulfide.

Unlike S(-II) produced under sulfate-reducing conditions, the product of methanogenesis, CH_4, is not particularly reactive under most conditions (27) and would not be expected to directly reduce redox indicators. However, the methanogenic redox level is the most reducing redox level (3-5). Various intermediates or byproducts which are strong reductants may be produced during methanogenesis (e.g., perhaps an *intracellular* electron carrier such as cytochromes or ferredoxins (3)) and some may couple to certain redox indicators. An indicator with a lower formal potential (e.g., phenosafranine, $E_7^{0\prime}$(free) = -267 mV, $E_7^{0\prime}$(imm) = -286 mV (22)) might be reduced by one of these reductants under these conditions.

In this chapter, the application of the redox indicators Thi, CV and PSaf to evaluate sulfate-reducing and methanogenic conditions is presented. These indicators were covalently immobilized to agarose affinity beads and packed into spectrophotometer flow cells with procedures developed by Lemmon (22, 23). Filtered solution from a wastewater slurry, under sulfate-reducing or methanogenic conditions (at pH 7), was pumped through the cells. Reduction of the indicators was monitored spectrophotometrically while various relevant parameters of the system (e.g., [S(-II)], partial pressure of CH_4 (P_{CH4}), E_{Pt}) were measured concurrently. All experiments were performed in a 2-L, deaerated, bioreactor system developed by Lemmon (22, 23).

In parallel experiments, the immobilized indicators were titrated with sulfide at pH 6, 7 and 8 to determine the effects of pH and sulfide level on indicator speciation (degree of indicator reduction). The dependence of redox indicator speciation on sulfide

concentration was then compared to that predicted by equilibrium models. Additionally, an experiment was conducted to determine if redox indicator speciation could be used to predict the transformation of trichloroethylene (TCE) to *cis*-dichloroethylene (*cis*-DCE) in a groundwater sample, rich in TCE dechlorinators, from a TCE contaminated site Lawrence Livermore National Laboratory.

5.2 Experimental

5.2.1 Instrumentation

All experiments were conducted in an air-tight bioreactor system, shown schematically in Figure 5.1, which has been described previously in detail (28). The bioreactor was used to achieve and maintain anaerobic conditions for both simple electrolyte solutions or wastewater slurries. A Pt-button electrode (Orion 967800) was used for E_{Pt} measurements and a glass pH electrode (Orion 9101BN) was used to measure the pH. One reference electrode (Orion 900200 Ag/AgCl double junction, modified to give the same potential as an SCE) was used for all indicator electrodes. A sulfide electrode (Orion 9416BN) was used to measure low levels of sulfide or to determine if sulfide was being produced in the bioreactor with wastewater slurries or groundwater samples. Dispensing pumps (FMI Micro II-Petter) were used to add acid or base to control the pH. Readings of E_{Pt}, pH and E_{S2-} (the potential of the sulfide electrode) were taken at operator-chosen time intervals with a 386 PC and a QuickBASIC program developed to take electrode readings automatically, control the pH, and to calculate various parameters associated with control such as the pH buffer capacity. The pH electrode was calibrated with pH buffer solutions made from commercially available METREPAK pH capsules.

To remove O_2 and promote anaerobic conditions, the bioreactor was initially purged with N_2 gas (pre-purified grade, 230 ft^3 tanks) for several hours or overnight (~50 mL/min). Gas flow was maintained by a mass flow controller (Tylan FC280 with a

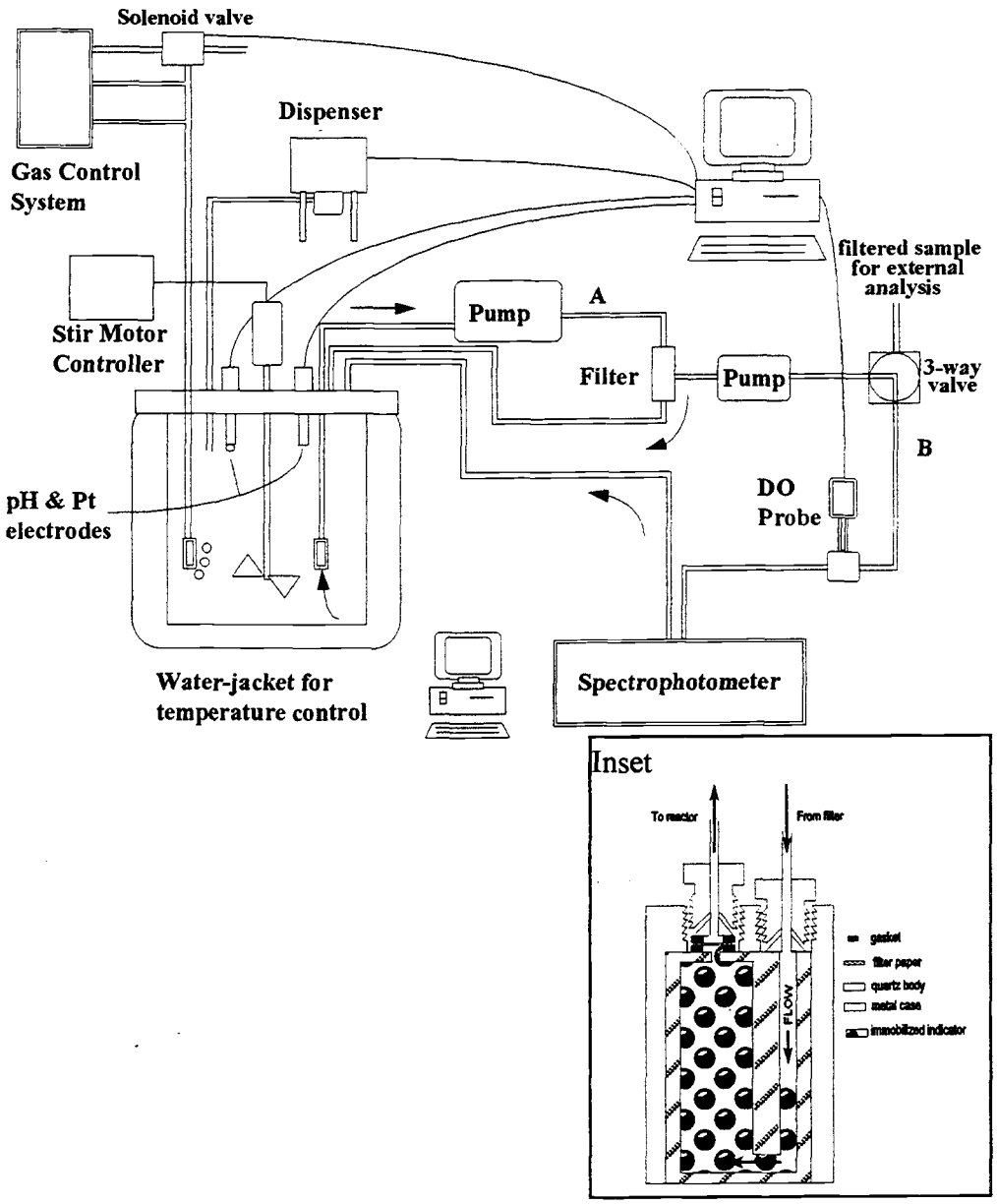

Figure 5.1 Bioreactor system for controlling and maintaining redox conditions, pH and anaerobic integrity. Loop A above refers to the primary loop and loop B above refers to the secondary loop, from which samples are taken for analysis. The bioreactor has a 2-L volume and normally contained 1 L of solution or slurry. The DO probe in loop B was not used for these experiments. The flow cell (inset) is packed with beads containing immobilized indicator, connected in loop B, and placed in the spectrophotometer sample compartment.

Tylan RO-28 readout box). Residual O_2 in the tank was removed with an oxygen trap (Alltech Oxy-Trap 4001). To avoid loss of H_2S, methane or other gases which were produced in experiments, the N_2 flow rate was decreased to very low flow values (a bubble or so every 10 - 20 s), or turned off completely, after anaerobic conditions were achieved (as noted by $E_{Pt} < 0$ mV).

A sophisticated cross-flow filter system provided the continuous separation of liquid from solids in the reactor solution and direct interaction of soluble redox species with the immobilized redox indicator in the packed flow cell (a schematic of the flow cell is shown in the inset in Figure 5.1) (22, 25). The primary loop (A) includes the cross-flow filter and a peristaltic pump (Masterflex speed controller, Easy load pump head 7518-50). A Durapore filter (Millipore, 0.65 μm) was used as the primary filter, which itself was sandwiched between two mesh filters (Spectra-Mesh fluorocarbon, 70 μm). A plastic mesh filter (a particulate filter for a lawn sprinkler with 0.1 - 0.2 mm mesh), attached to the inlet tube in the reactor, was used to filter out large particles. In the secondary loop a persitaltic pump (Pharmacia Peristaltic Pump P-3) pumps filtered solution from the filter through a spectrophotometric flow cell back to the reactor. Filtered bioreactor samples were taken from the external loop. To minimize residual O_2 leakage in the external loop, both pumps were encased in two large, plastic containers (Rubbermaid) which were purged continuously with N_2. With the exception of the tubing used with the two pumps (Tygon tubing size 14, 1.6-mm id, 5-mm od, Masterflex® from Cole-Parmer Instrument Co.), PEEK tubing (UPCHURCH type 1533, 1/16" od, 0.030" id or type 1534, 1/8" od, 0.062" id, which both have low O_2 permeability) was used throughout both primary and secondary loops.

For titration experiments of immobilized indicators with sulfide, the affinity beads with immobilized redox indicators were packed into a flow cell (Hellma 170.700-QS,1-mm pathlength) and allowed to interact with filtered bioreactor solution pumped through the external loop. Absorbance measurements of the immobilized indicators were made with a Hewlett Packard 8452A diode array spectrophotometer. Sulfide injections were made with a 100-μL syringe (Hamilton) through a Chemi-inert septum (VWR) in the reactor lid. The sulfide electrode was calibrated by injecting aliquots of a ~0.1 M total sulfide standard into the reactor solution and measuring the potential (E_{S2-}).

Gas headspace samples (for CH_4, TCE, *cis*-DCE) were withdrawn through the septum in the reactor lid with a 100-μL, gas-tight syringe (Hamilton SampleLock 81056). Methane was quantified with an HP5890 GC with a calibration method developed by Roberts (29). TCE and *cis*-DCE were quantified with an HP 6890 GC with a PID/FID detector, with a calibration method developed by Vancheeswaran (30). Both chromatographs were made available through the Dept. of Environmental Engineering at OSU.

5.2.2 Chemicals

Deionized water, obtained from a Millipore Milli-Q water system, was used for titration experiments of immobilized redox indicators with sulfide and for preparation of all standards. The redox indicators thionine (Thi), cresyl violet acetate (CV), and phenosafranine (PSaf) were obtained from Aldrich. Redox indicators were immobilized on 60-μm, cross-linked agarose (4%), affinity beads (Sterogene ALD beads) with a

procedure developed by Lemmon (22), which is described in detail in Appendix E. The immobilization scheme involves a coupling of the amine groups on the redox indicators to aldehyde groups on the affinity beads (40-50 μmol/mL of gel), forming an imine, which is next reduced to a more stable secondary amine. Lemmon (22) immobilized Thi and PSaf previously. CV, which had not been previously immobilized or even used as a redox indicator, was immobilized to the affinity beads in a similar manner. However, the pH necessary to couple CV was lower than that normally used (in the range of 3-4 rather than 5-7). Ethanolamine (99+%), used to displace any indicator which did not yet formed the stable 2° amine bond, was obtained from Aldrich. NaCl was obtained from EM Science.

Sodium sulfide ($Na_2S•9H_2O$, Mallinckrodt) was used to prepare a ~0.1 M total sulfide standard for sulfide titrations. Total sulfide was quantified with CHEMetrics Vacu-vial® ampoules which employ the colorimetric methylene blue method for sulfide analysis (9, 10). Occasionally, CHEMetrics Vacu-vial® ampoules for sulfate, employing a turbidimetric method with a Ba(II) solution, were used for sulfate analysis. A small, portable spectrophotometer (Multi-Filter Photometer A-1051, CHEMetrics) was used to measure the absorbance. A 0.1 M cupric nitrate ($Cu(NO_3)_2•2.5H_2O$, Mallinckrodt) solution was used as a precipitating agent for sulfide.

Lactic acid (85%, Mallinckrodt), estimated to be 10.9 M, was used as an electron donor for sulfate-reducers. Sodium acetate ($NaC_2H_3O_2•3H_2O$), used as an electron donor for methanogens, was also obtained from Mallinckrodt, Inc. Sodium sulfate ($Na_2HPO_4•7H_2O$, Baker), magnesium sulfate (anhydrous, Baker), and potassium phosphate (KH_2PO_4, Mallinckrodt) were used as nutrients. $CaCl_2•2H_2O$ (Baker) and

NH_4Cl (EM Science) were added to wastewater slurries to increase ionic strength and to provide a microbial nitrogen source, respectively. In titration experiments of immobilized redox indicators with sulfide, 0.05 M KCl (Mallinckrodt) was used as an electrolyte.

For titration experiments, buffers were used to adjust the pH of electrolyte systems in the bioreactor. Phosphate buffer was prepared with $Na_2HPO_4 \cdot 7H_2O$ and sodium phosphate monobasic, NaH_2PO_4 (both from Mallinckrodt, Inc.). In reactor experiments with wastewater slurries, the computerized pH-stat system was used. For sulfate-reducing conditions, 1 M lactic acid (made to pH 1 with HCl (Mallinckrodt, Inc.)) was used with 6 M NaOH to adjust the pH. For methanogenic conditions, 1 M acetic acid (adjusted to pH 1) was used.

A 0.1 M Fe(II) solution in 0.1 M $HClO_4$, was prepared with hydrated ferrous perchlorate crystals ($Fe(ClO_4) \cdot 2H_2O$, G. Frederick Smith Chemical Co.) and 70% $HClO_4$ (Mallinckrodt, Inc.). Hydroxylamine hydrochloride (Aldrich)(10% (w/v) in water), a 0.5% (w/v) 1,10-orthophenanthroline (Mallinckrodt) solution in water, and a 50 mg/L Fe(III) solution in 6 mM HCl (prepared from Fe powder, Aldrich) were obtained from Dean Johnson of the OSU Department of Chemistry. For the TCE/groundwater experiment, trichloroethylene (TCE, Aldrich, 99.5%) was used.

5.2.3 Titrations of immobilized indicators with sulfide

The immobilized redox indicators Thi, CV and PSaf were titrated with sulfide at pH 7. Additionally, immobilized Thi and CV were titrated at pH 6 and 8. A 0.05 M

phosphate buffer was used along with the pH stat system to ensure that there was not a pH difference between solution in the reactor and the external loop.

Each of the immobilized indicators was packed into a separate cell (1-mm path length, Figure 5.1) (22) and an initial absorbance spectrum of each indicator was taken. The three flow cells were placed in series in the external loop and reactor solution was pumped through the cells. After deaeration of the reactor solution, aliquots (10 - 100 μL) of ~0.1 M sulfide were injected into the reactor solution via the Chemi-inert septum and indicator absorbance, total sulfide level, E_{Pt}, and E_{S2-} were measured periodically. In general, 2-3 hr were required between additions for the absorbance of the indicators to reach steady-state.

5.2.4 Wastewater slurry reactor experiments under sulfate-reducing conditions

Wastewater sludge samples were obtained in 1-L plastic bottles from the City of Corvallis Wastewater Reclamation Plant and contained significant numbers of anaerobic, reducing microbes (methanogens and sulfate-reducers). The samples were stored in a refrigerator for subsequent use. Over time, the slurry separated into two phases: an aqueous upper phase with some particulate matter and a thick organic, sludge-like lower phase.

For reactor experiments, approximately 250 mL of the aqueous upper phase was placed in the reactor along with 750 mL of deaerated tap water. Initially to the reactor slurry, 6.8 g of sodium acetate (50 mmol), 1 g each of sodium sulfate, ammonium chloride and calcium chloride (3.7 mmol, 18.7 mmol, and 6.8 mmol, respectively), 2 g

(16.6 mmol) of magnesium sulfate and 0.5 g (3.7 mmol) of potassium phosphate were added. This list of nutrients was adopted from Chapelle for sulfate-reducing conditions (3). The slurry was initially purged with N_2 (3-4 hr) to maintain the anaerobic integrity of the system and prevent unnecessary exposure of the microbes to O_2.

However, as the experiment progressed, no reduction of sulfate was noted (based on sulfide measurements with CHEMetrics vials). It was decided to switch from acetate to lactic acid (lactate) as the electron donor for sulfate-reduction, as suggested by Bottomley (31). Therefore, 4.6 mL (50 mmol) of lactic acid were then added to the slurry.

During initial attempts to pump reactor solution through the primary and secondary loops, significant clogging occurred in the cross-flow filter in the primary loop due to debris in the slurry. To offset this effect, the stirrer controller was turned down to 5 to 10 rpm, allowing larger debris to settle at the bottom of the reactor. The solution pumped through the primary loop was taken from approximately 1-2 in from the top of the wastewater solution rather than near the bottom.

The wastewater experiment was conducted in the same manner as titrations of the immobilized indicators (Thi, CV and PSaf) with sulfide, except sulfide was produced naturally by the microbes (i.e., no sulfide additions to the reactor were made). Also, E_{S2-} was not measured (a sulfide electrode had not yet been acquired). Early in the experiment, an initial measurement of sulfate was taken. Near the end of the experiment, Cu(II) was added to precipitate out the sulfide in the reactor and the indicator speciation was monitored.

5.2.5 Wastewater slurry reactor experiments under methanogenic conditions

Two experiments were conducted with wastewater slurries under methanogenic conditions. Wastewater slurries were obtained and allowed to settle in the same manner as described previously. For the first experiment, approximately 500 mL of the upper aqueous phase of the slurry and 200 mL of the lower phase sludge were added to the reactor along with ~300 mL of deaerated tap water. To this, 7 g of sodium acetate (51 mmol), 1 g of ammonium chloride (18.7 mmol), 1 g of calcium chloride (6.8 mmol) and 0.5 g of potassium phosphate (3.7 mmol) were added as nutrients. The reactor slurry was initially purged with N_2 (after which the N_2-purge system was turned off), and the pH was controlled by addition of 1 M NaOH and 1 M sodium acetate (made to pH 1 by addition of HCl). The immobilized redox indicators Thi, CV and PSaf were packed into flow cells and placed in the secondary loop of the reactor. Filtered reactor solution was pumped through them throughout the day, during which, the absorbances of the indicators were monitored. At night, the pumps for both the primary and secondary loops were turned off to avoid any loss of solution during unsupervised periods. Fe(II) (quantified with the 1,10-orthophenanthroline (OP) method described in Appendix B) and sulfide levels, E_{Pt} and E_{S2-}, and levels of CH_4 in the gas headspace of the reactor were monitored during the experiment.

The second experiment with wastewater slurries under methanogenic conditions was very similar to the first experiment, except for a few details. Only 200 mL of the top phase and 100 mL of the bottom phase were added to the reactor system, along with 700 mL of deaerated tap water. This dilution of the slurry helped to minimize clogging

of the filters which was a problem in the first experiment. Nutrients were added as described in the first experiment. Levels of sulfide and CH_4 were monitored as before, except that all indicator absorbance measurements were taken the morning after the reactor loop pumps had been turned off.

5.2.6 Field studies with immobilized Thi and CV

Immobilized Thi and CV were packed into flow cells and taken to a Lake Creek well in Benton County, Oregon, for testing in the field. The site is located next to a farm, with several wells, which are commonly used for studies by John Baham of the Department of Soil Science at OSU.

At a well described as "the most reducing" (32), the soil pore water in the well was initially drained with a hand pump while the headspace was purged with Ar from a small, portable tank. After draining, the tube supplying Ar to the headspace was removed. Sulfide measurements of the initial well pore water sample were made in the field with CHEMetrics instrumentation (vials and portable spectrometer). An Fe(II) sample was collected and 0.5% (w/v) OP solution was added (approximately 80 µL for a 2-mL sample) for later analysis. Care was taken not to contaminate either sample with O_2. Although the potential of the well was not measured the day of sampling, Pt electrode readings of the soil adjacent to the well measured -50 mV ± 25 mV (vs SHE) over the course of about a month during which the well was sampled (32). Approximately one week before sampling, the well potential was measured to be -119

mV but was measured to be +157 mV a week after sampling (32). This rise in E_{Pt} was attributed to aeration of the soil during this time period (32).

Approximately 45 min after the initial draining, new pore water from the surrounding soil refilled the well. A portion of the new pore water was extracted with the hand pump, from which a sample was taken with a 60-cc syringe (Fisher), through a 1.6-μm filter (Whatman GF/A). Initially, a 0.45-μm filter (Fisherbrand) was used to filter the sample, but it was found to clog easily. The filter was then removed from the syringe and the filtered pore water was injected into both flow cells (connected in series) containing the redox indicators via PEEK tubing (1/16" od, 0.030" id). The inlet and outlet ends of the flow cells were then attached with 1/4•28 standard unions for PEEK tubing (Upchurch P•603) to minimize oxygen leakage into the cells. The cells were then taken back to the laboratory for absorbance measurements. Sulfide was measured in the field and filtered samples were stored in vials or bottles and taken back to the laboratory for Fe(II) and pH measurements. Again, effort was made to minimize oxidation of the samples by O_2.

5.2.7 TCE experiment

For the TCE experiment, a 1-L groundwater sample, rich in TCE-degrading microbes, was obtained from the Dept. of Environmental Engineering at OSU. This sample was originally acquired from a TCE contaminated site at Lawrence Livermore National Laboratory and is described in more detail elsewhere (30). Microbes in the groundwater were shown to dechlorinate TCE to *cis*-DCE at the Livermore site (33).

In a laboratory in the Department of Environmental Engineering at OSU, the groundwater sample was purged with N_2 (the N_2 gas had been heated in a tube furnace to remove residual O_2) to remove volatile background components (TCE, *cis*-DCE, H_2S). The reactor was autoclaved to sterilize the system. Next, ~970 mL of groundwater was then added to the reactor in an anaerobic hood to minimize exposure of the microbes to O_2.

After the reactor was transferred back to the chemistry laboratory, 80 mL of 100% CO_2 was injected into the reactor headspace via the injection port to reduce the pH of the system (which tended to increase over time). The pH-stat system was not used to lower the probability of introducing O_2 into the test solution.

Immobilized Thi and CV were packed into flow cells and placed in the external loop of the reactor. Approximately 50 mg of TCE (34 µL of pure TCE, density = 1.46 g/mL, 378 µmol) was spiked into the reactor. To minimize O_2 leakage into the system, the pumps were turned on for approximately 2-3 hr per day rather than continuously, and absorbance data for the indicators were taken every 1-2 days. Levels of TCE and *cis*-DCE were monitored with GC over time (taking 50-µL gas headspace samples), and occasionally a sample was taken for sulfide determination. E_{Pt} and E_{S2-} were also monitored.

5.3 Results and Discussion

5.3.1 Sulfide titrations of immobilized thionine, cresyl violet and phenosafranine

Lemmon (22) reported that the formal potentials at pH 7 of the immobilized redox indicators Thi and PSaf are +52 and -286 mV, respectively. CV, an indicator which had not been previously tested or immobilized, was measured to have a formal potential between the other two indicators, -75 mV in the free (non-immobilized) form, and -81 mV when immobilized (Appendix I). In terms of formal potentials, Thi (with the highest formal potential) would be expected to be reduced at the lowest sulfide concentration, while PSaf (with the lowest formal potential), would be the most difficult to reduce.

Data for titrations of immobilized Thi and CV with sulfide at pH 7, along with calculated curves, are shown in Figure 5.2. The calculated curves are based equation 5-10.

$$Ind_{ox} + S^{2-}_{(aq)} \rightleftharpoons Ind_{red} + S^{0}_{(s,\ rhumb)} \qquad (5\text{-}10)$$

The fraction of oxidized indicator (f_{ox}) is determined from equation 5-11.

$$f_{ox} = \frac{1}{\left(10^{\left[\frac{2}{0.059}\,(E^{0'}_{ind,m} - E_{S/S2-})\right]} + 1\right)} \qquad (5\text{-}11)$$

This equation is derived by equating the potential of the indicator half-reaction (right side of equation 5-7) to the potential of the sulfide half reaction ($E_{S/S2-}$) and solving for f_{ox}. The value of $E_{S/S2-}$ is calculated from equation 5-12 (based on eq. H-9 in Appendix H) and the total sulfide concentration [$S(-II)_{(tot)}$], measured after steady-state was reached.

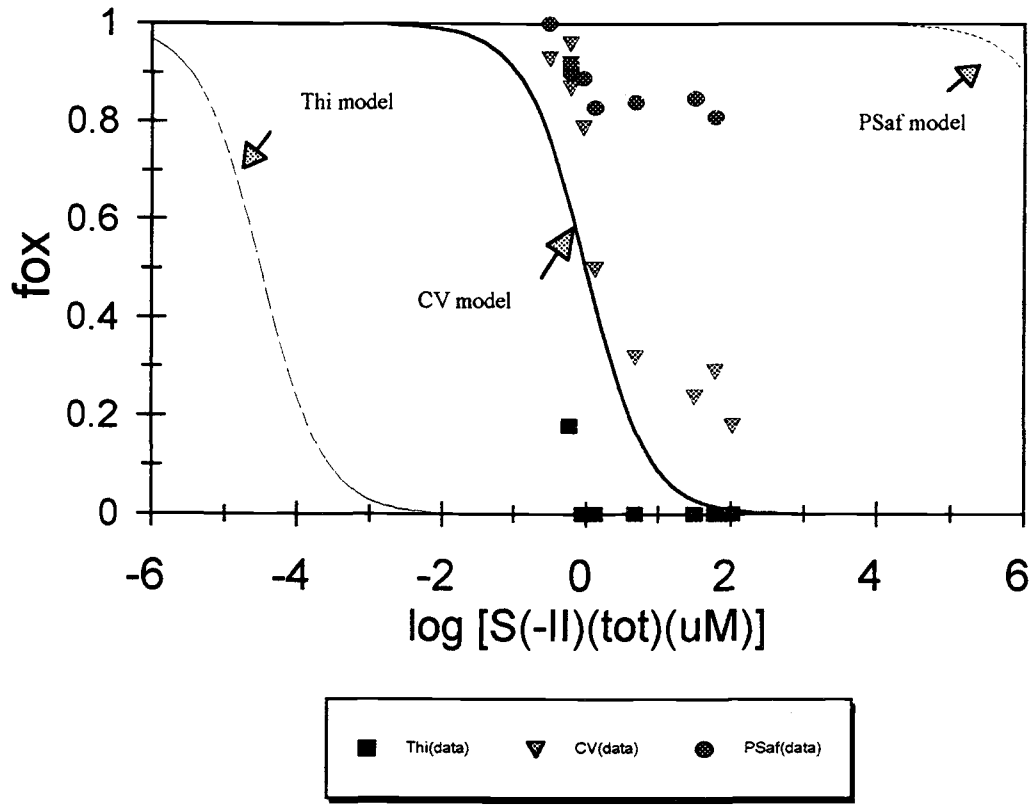

Figure 5.2 Sulfide titration data for thionine (Thi), cresyl violet (CV), and phenosafranine (PSaf) at pH 7. The curves are calculated with eqs. 5-11 and 5-12 and the measured total sulfide concentration.

$$E_{S/S^{2-}} = -0.475 - 0.0295 \log \left[\frac{[S(-II)_{(tot)}]}{1 + \frac{[H^+]}{10^{-14}} + \frac{[H^+]^2}{(10^{-7.1})(10^{-14})}} \right] \quad (5\text{-}12).$$

From the data, CV couples well to sulfide in the range of 1 - 100 μM total sulfide while Thi is useful for low level detection (< 1 μM total sulfide). PSaf appeared slightly reduced (f_{ox} ~ 0.8) at [S(-II)$_{(tot)}$] > 100 μM. However, at these high sulfide levels, buildup of solids in the flow cell (hypothesized to be S^0(s, rhmb) or other solid sulfur species) caused large shifts in baseline absorbance, which might cause error in the calculation of f_{ox}. There was no significant change in the absorbance of PSaf after re-oxidation with DI water saturated with atmospheric O_2. Therefore, PSaf does not appear useful for sulfide detection.

The formal potential of CV (-81 mV at pH 7 and f_{ox} = 0.5) is the same as the value calculated for the S^0(s, rhmb)/S^{2-}(aq) couple at 1 μM total sulfide. Hence, reduction of CV should be observed with total sulfide levels around 1 μM. From Figure 5.2, the experimental values of total sulfide necessary to reduce a given fraction of CV are greater (to the right of the equilibrium curve) than those predicted by the equilibrium model. This discrepancy may be due to non-equilibrium conditions (i.e., slow kinetics of the sulfide/indicator reaction) or an incorrect formal potential for the sulfur half-reaction (e.g., formation of an oxidized or a reduced sulfur species different than $S^0_{(s),\ rhmb}$ or S(-II), respectively, such as mixed sulfur products (polysulfides, S_4^{2-}, S_5^{2-})).

For Thi, the value of f_{ox} for the first data point is unexpected (the value should be less than 0.01 instead of ~0.2). The difference may be due to slow kinetics or the

difficulty in accurately determining low levels of sulfide with CHEMetrics methods (DL ~ 0.6 μM (10)).

In Figure 5.3A, the values of E_{Pt} and E_{S2-}, measured during the course of titration of the three immobilized indicators, are compared. Between 0 and 90 hr, the first two additions of sulfide to the reactor resulted in significant drops in both E_{Pt} and E_{S2-}. The increase in potentials after the first addition is attributed to leakage of O_2 into the reactor solution. The potentials of both electrodes exhibit somewhat similar dynamics. Beyond 90 hr, the sulfide electrode responded more rapidly and directly to sulfide additions than the Pt electrode.

Between 90 and 175 hr, a "saw-tooth" type pattern in the value of E_{S2-} is obvious. After each addition of sulfide, there was a rapid decrease in potential followed by a slow increase in E_{S2-} attributed to oxidation of the sulfide by O_2. A similar pattern is not observed for E_{Pt} over this time period. In fact, in the region between 100 and 120 hr, the Pt electrode does not respond to additions of sulfide (i.e., the potential remains at about -150 mV).

In Figure 5.3B, the same data are plotted to illustrate the dependence of the two potentials on total sulfide concentration. The Ag^0/Ag_2S electrode is believed to respond to sulfide based on the reaction

$$2Ag^0 + S^{2-} \rightleftharpoons Ag_2S + 2e^- \qquad (5\text{-}13)$$

and should exhibit a semi-log slope of -29.5 mV per decade of [S(-II)] at a given pH (17). However, the response is nonlinear with a "best fit" slope of -23 mV per decade of [S(-II)]. The observed behavior may be due to slow response of the electrode (9) or errors in the colorimetric determination of sulfide (methylene blue method). The sulfide

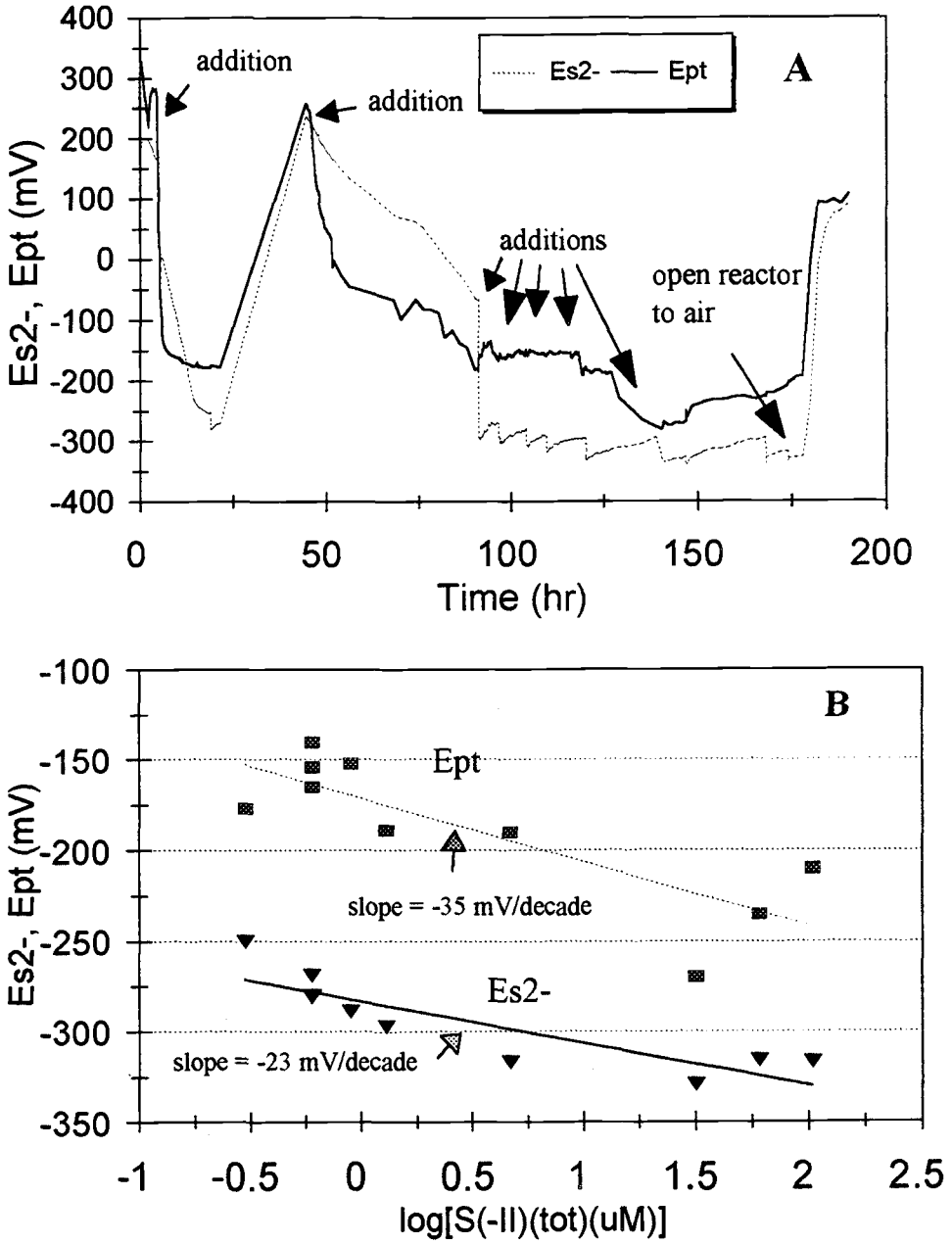

Figure 5.3 Measured values of E_{S2-} and E_{Pt} over the course of titration experiment of immobilized indicators with sulfide at pH 7. Comparison of E_{Pt} and E_{S2-} over time (A) and dependence of E_{S2-} and E_{Pt} on $[S(-II)_{(tot)}]$ (B). Additions of total sulfide were in the 0.1 - 10 µmol range. The standard errors for the slopes are 5 and 9 mV/decade for the E_{S2-} and E_{Pt}, respectively.

electrode appears useful for detecting sulfide ($[S(-II)_{(tot)}] \geq \sim 1$ μM and $E_{S2-} < -280$ mV), although a Nernstian slope was not observed. A plot of the E_{S2-} vs. log $[S(-II)_{(tot)}$ *added*] (not shown) was even more non-linear, perhaps due to oxidation of sulfide over time by O_2 or leakage of $H_2S(g)$ out of the reactor.

The response of the Pt electrode to sulfide concentration (Figure 5.3B) was notably more scattered than that for the sulfide electrode. Clearly E_{Pt} is influenced by sulfide (more apparent from Figure 5.3A) (17, 25). Although the "best fit" slope of -35 mV/decade is not too far from the expected slope of -29.5 mV/decade (based on a Nernstian response and a two electron transfer), the data are too scattered to conclude that the sulfide is poising the Pt electrode in a Nernstian manner.

The response (reduction) of the indicators to sulfide is more comparable to the response of the sulfide electrode than that of the Pt electrode (i.e., both the indicators and the sulfide electrode respond to the initial addition of sulfide to the solution and to all subsequent changes in sulfide concentration). In contrast, the Pt electrode responds primarily to the initial addition of sulfide to the system.

Immobilized Thi and CV were titrated with sulfide at pH 6, 7 and 8. For Thi, changes in pH caused no observable effect on the reduction. Sulfide is a very strong reductant which completely reduces Thi below 1 μM at all these pH values. Titration curves of CV at pH 7 and 8 were similar as shown in Figure 5.4, but more sulfide was necessary to reduce CV at the lowest pH (pH 6 relative to pH 7 or 8).

The observed behavior is consistent with expected changes in redox potential of the two couples with pH as shown in Figure 5.5. The reduction potential of the sulfide couple increases more rapidly below pH 7 (~59 mV per decade) than that of the

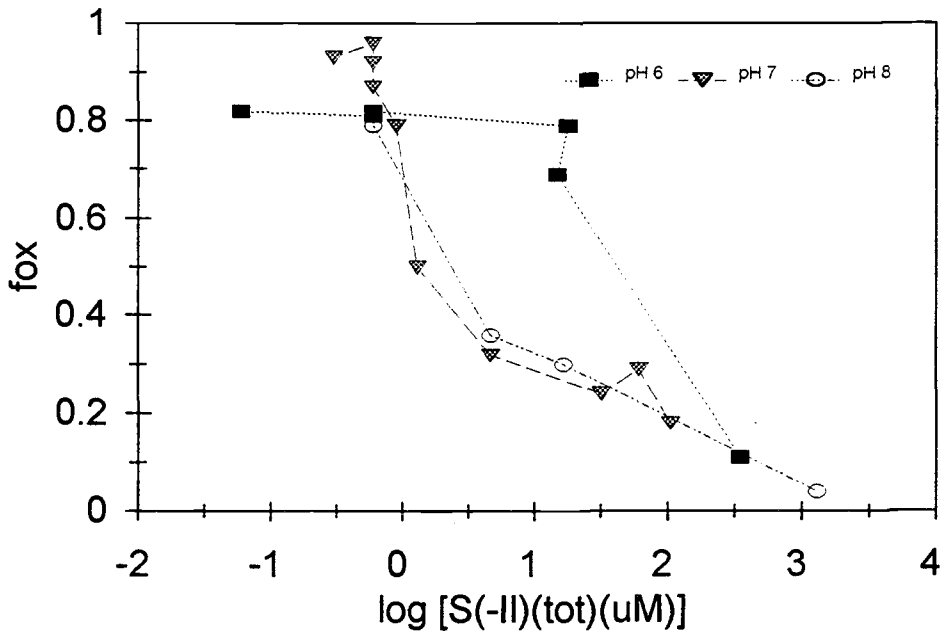

Figure 5.4 Comparison of measured total sulfide concentration ([$S(-II)_{(tot)}$]) necessary to achieve a given level of reduction (f_{ox}) for immobilized CV at pH 6, 7 and 8.

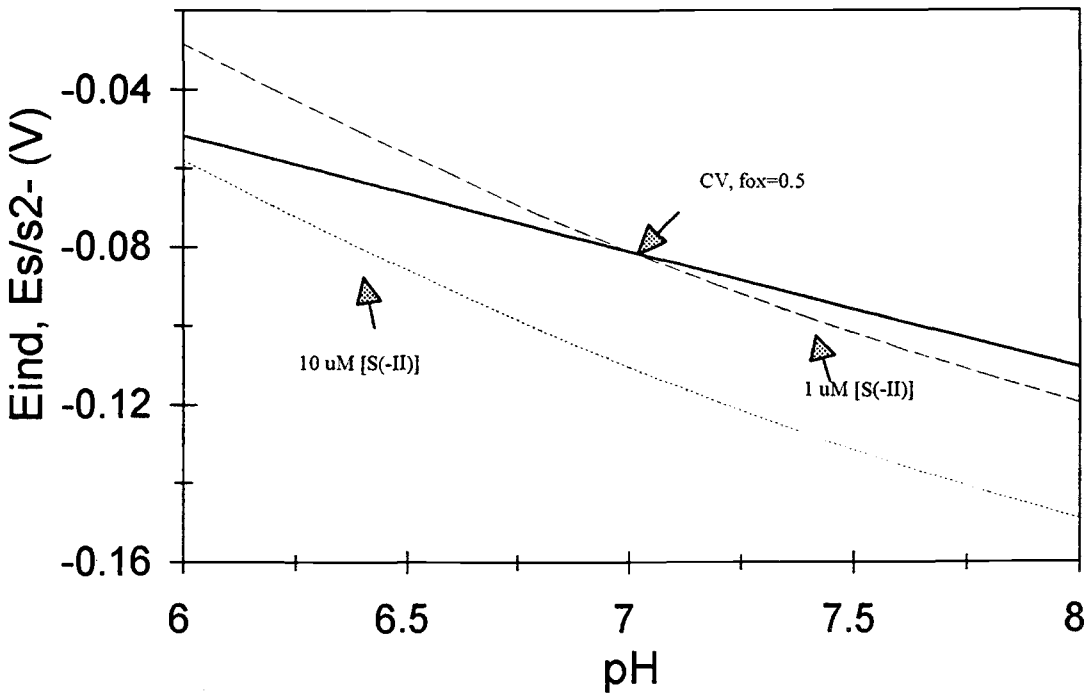

Figure 5.5 Dependence of calculated redox potentials for CV and the S(-II)/S^0 couple on pH. The redox potentials are calculated from equations 5-7 and 5-12, respectively.

indicator (29 mV per decade) as H_2S becomes the dominant form (rather than HS^-). At pH 7 and 8, CV should be half-reduced ($f_{ox} = 0.5$) with 1 μM (or less) $[S(-II)_{(tot)}]$. However, at pH 6, the reduction potential of the $S^0_{(s,\ rhmb)}/S^{2-}$ couple for 1 μM $S(-II)_{(tot)}$ is calculated to be -0.029 V compared to -0.051 V for CV at $f_{ox} = 0.5$. Therefore, a greater total sulfide concentration is necessary to reduce CV to a given f_{ox} at pH 6 than at pH 7 or 8.

For the indicator curve, it is assumed that the pH dependence of the formal potential for CV is the same as that for the redox indicators Thi and TB. A one-proton transfer dependence was observed in the region of pH 6.3 to 7.5 (the slope for a plot of $E_m^{0\prime}$ vs. pH was about -29 and -31 mV, respectively, for Thi and TB over this region (34)). Furthermore, Bishop (21) tabulated $E_m^{0\prime}$ dependencies for many indicators (e.g., Thi, PSaf) which exhibited a single proton transfer dependence in this region.

5.3.2 Evaluation of thionine and cresyl violet in wastewater slurries under sulfate-reducing and methanogenic conditions

The time-dependence of the speciation of immobilized Thi and CV in contact with a wastewater slurry under sulfate-reducing conditions at pH 7 is plotted in Figure 5.6. Thi is completely reduced within minutes by contact with low levels of sulfide (about 195 hr) as predicted by the titration experiment. CV became over half reduced when total sulfide levels reached ~10 μM, and nearly completely reduced when concentrations exceeded 100 μM. The initial concentration of sulfate in the reactor solution was > 885 μM (85 μg/mL), beyond the calibration range of the CHEMetrics method.

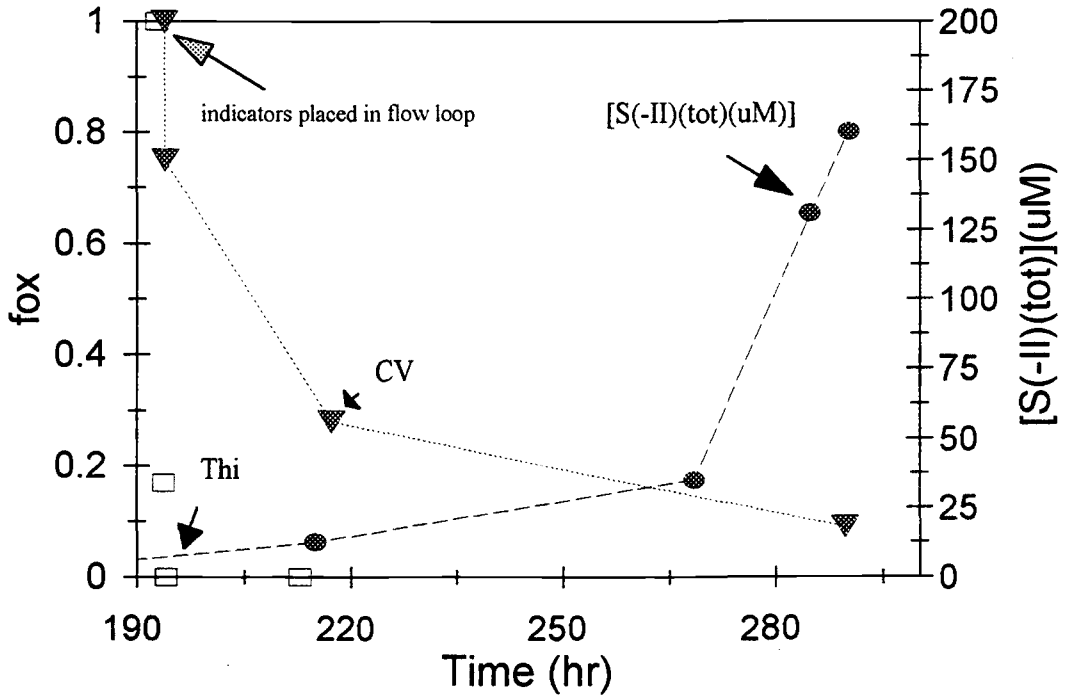

Figure 5.6 Comparison of redox indicator speciation to sulfide levels under sulfate-reducing conditions. During the first 150 hr, acetate was used as the electron donor (substrate) for the sulfate-reducing bacteria, but no sulfide was detected. After this, lactate was added as the substrate. Sulfide was detected (by smell) at 190 hr, at which point Thi and CV were placed in the external loop.

Addition of 200 μmol Cu(II) to the reactor (after 295 hr, not shown in Figure 5.6), when $[S(-II)_{(tot)}]$ was above 100 μM, precipitated the sulfide, as measured with CHEMetrics methods. After complete precipitation of the sulfide (when measured total sulfide was below the DL of the CHEMetrics method), *reoxidized* Thi (reoxidized with O_2-saturated DI water) was placed in the external loop. After several hours, no significant reduction of Thi was observed. Reoxidized CV was not tested. The fact that Thi was no longer reduced after precipitation of the sulfide is consistent with sulfide being the major reductant of the redox indicators under sulfate-reducing conditions.

Tests of redox indicators under methanogenic conditions gave more ambiguous results than tests under sulfate-reducing conditions. In the first experiment under methanogenic conditions, large particles in the slurry tended to coat the plastic mesh filter (inlet of the primary loop) in the bioreactor, occasionally clogging the primary loop or the cross-flow filter. In this situation, the pump in the secondary loop would suck in air visible as bubbles in the secondary loop. This unwanted oxygen re-oxidized the indicators or kept them from becoming reduced. If the cross-flow filter was kept under water, occasionally water from the sonicator bath would be sucked into the secondary loop, contaminating the indicators.

Normally each night, the pumps were turned off, and in the morning, often indicators were reduced. It is hypothesized that some microbes from the reactor slurry passed through the cross-flow filter membrane (0.65 μm), or through holes in the filter membrane, and remained active in the indicator beads. It is not known whether the reduction was a result of sulfide produced by sulfate-reducing microbes (traces of sulfide

were occasionally measured in the slurry) or the production of some unknown reductant produced by methanogens.

In the second experiment, an alternative strategy was utilized. Absorbance measurements were taken in the morning, prior to turning the pumps back on, rather than during pumping. Methane and sulfide levels in the reactor were measured the same day and compared to indicator absorbance taken that morning. To determine if methane was actively being produced (and to purge the reactor of O_2 which tended to seep in over time), the N_2-purge system was turned on to remove methane from the headspace. The accumulation of methane in the headspace over time indicated active methanogenic conditions. In general, 1 - 3 days were allowed between methane and sulfide measurements.

As shown in Figure 5.7, early in the experiment (75 - 250 hr), methane was actively produced. Beyond 250 hr, methane production ceased almost completely when a low level of sulfide ($\leq$ 2 μM) was detected and Thi and CV were mostly reduced. Thi remained mostly reduced for the remainder of the experiment. Sulfide levels tended to fluctuate, and after 500 hr, CV became more oxidized. These phenomena may be indicative of an oxygen leak.

Under the experimental conditions and slurry tested, it appears that Thi and CV were not reduced under methanogenic conditions. Methane is inert and does not couple to the redox indicators. However, one might expect that other reductants or mediators would be produced under methanogenic conditions. Apparently, in the experiment performed, a high, *steady-state* level of an extracelluar reductant which reacts with the indicators was apparently not produced. More experiments should be performed under

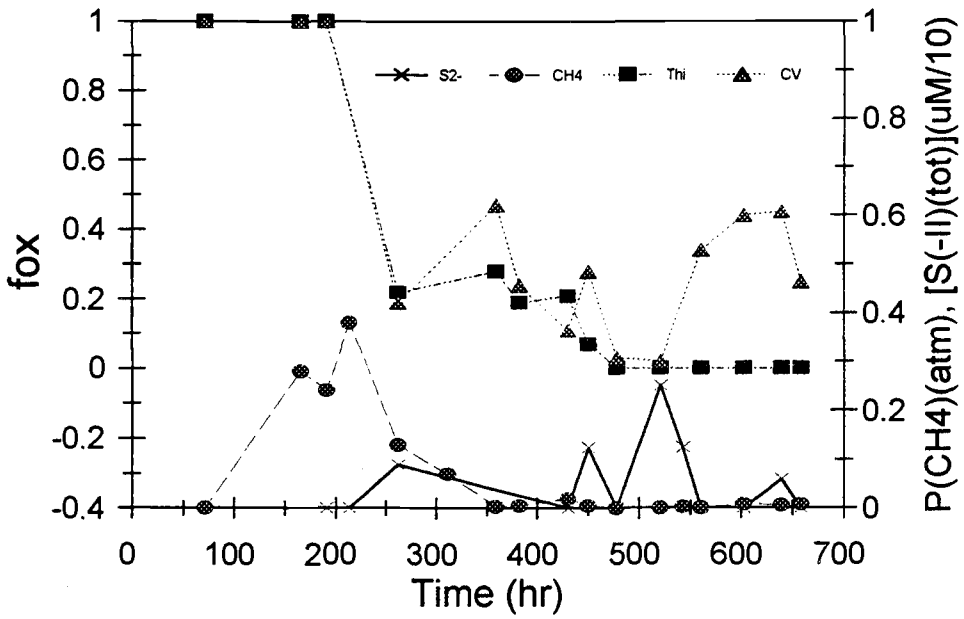

Figure 5.7 Behavior of redox indicator speciation first under methanogenic, and later, sulfate-reducing conditions. After about 250 hr, significant indicator reduction was observed.

conditions that provide higher levels of methane production and that completely eliminate sulfate-reduction (e.g., by addition of an inhibitor such as molybdate (35)) and low levels of sulfide.

5.3.3 Field tests with immobilized redox indicators

Concentrations of Fe(II) and total sulfide in the original well sample were 135 μM and 19 μM, respectively. However, in the second sample (after the well refilled with new ground water), Fe(II) levels were about the same (~130 μM) but no sulfide was detected. It may be that O_2 from the atmosphere contaminated the well (although purged with Ar) and oxidized the sulfide or sulfide production rates were low relative to Fe(II) production rates. The pH was measured (in the lab) to be 7.2.

Filtered well water from the second sampling was injected through the flow cell packed with Thi- and CV-immobilized beads. Only the second well water sample was injected because it was believed to be more representative of the pore water in the soil (32). The experiment was not successful because of clogging in the packed cell which occurred about 50% of the time in subsequent field tests.

Back in the laboratory, the absorbance of Thi was monitored over time. No initial reduction was observed, but after about two days the Thi was completely reduced. This result is consistent with reduction of Thi by moderate Fe(II) levels at a pH of 7.5 or greater (25) or by sulfide. Because measurements of CV speciation were not made, the effective reductant at the site could not be identified. Furthermore, the presence of Fe(II) *and* sulfide in the well water suggest the two reductants can exist simultaneously

in groundwater. This observation is further substantiated by results of a simple bioreactor experiment in which both sulfide ($[S(-II)_{(tot)}] \approx 40$ μM) and Fe(II) ($[Fe(II)] \approx 50$ μM) coexisted for more than a day (data presented in Appendix K).

The field test results illustrate some important lessons and problems. More than one indicator is needed to evaluate redox levels to minimize ambiguity in the results. For some indicators, moderate levels of Fe(II) at neutral pH can give the same result as low levels of sulfide, indicative of two very different redox levels. If both Fe(II) and sulfide are present (e.g., because of a transition between Fe(III)- and sulfate-reducing conditions), the stronger reductant might dominate, resulting in complete reduction of Thi and partial reduction of CV, indicating only sulfate-reducing conditions.

Clogging of the flow cells by particulate matter in the sample must be overcome to use the immobilized indicators in the field. Filtering of samples prior to injection can be difficult and time-consuming and likely will introduce oxygen which subsequently reacts with reductants in the sample. A format for immobilization different from the packed bed configuration (e.g., a film configuration) may be more necessary for field work (36).

In the immobilized form, redox indicators can be placed in intimate contact with microbes in the sample over a period of time without flow. This is a particularly useful quality, making continual pumping of well water into the flow cells unnecessary for qualitative characterization of the redox level.

5.3.4 TCE experiment

Results of the experiment involving microbial reduction of TCE are shown in Figure 5.8. Reduction of Thi occurred from the onset of the experiment and Thi was completely reduced after 400 hr. CV was noticeably reduced after about 600 hr. After 200 hr, *cis*-DCE was detected and its concentration increased rapidly after 400 hr. No sulfide was detected in samples taken at about 100 hr and near the end of the experiment. The value of E_{S2-} remained above -250 mV ($[S(-II)_{(tot)}] < 0.3$ μM) for most of the experiment although it fell to -300 mV (about 1 μM) for a few hours (at about 100 hr). E_{Pt} varied significantly throughout the experiment, reaching as high as +100 mV and as low as -150 mV.

Early in the experiment, TCE levels (not shown) fell rapidly, decreasing by nearly 50% in the first 100 hr, without any obvious production of *cis*-DCE. At first, it was believed that TCE was leaking from the reactor, but later, *cis*-DCE was detected. Similar results were obtained in a later experiment (after re-autoclaving the reactor) conducted with only TCE. It is hypothesized that a significant amount of TCE adsorbed on the surfaces of the reactor (i.e., Delrin lid and stirrer) and made it impossible to obtain a mass balance.

The results obtained suggest that complete reduction of Thi and partial reduction of CV is indicative of the onset of TCE reduction to *cis*-DCE. However, because TCE may have adsorbed to reactor fittings, *cis*-DCE may also have adsorbed, and therefore, the onset of TCE transformation may have started before complete reduction of Thi. The reductant (or reductants) that was (were) responsible for completely reducing Thi

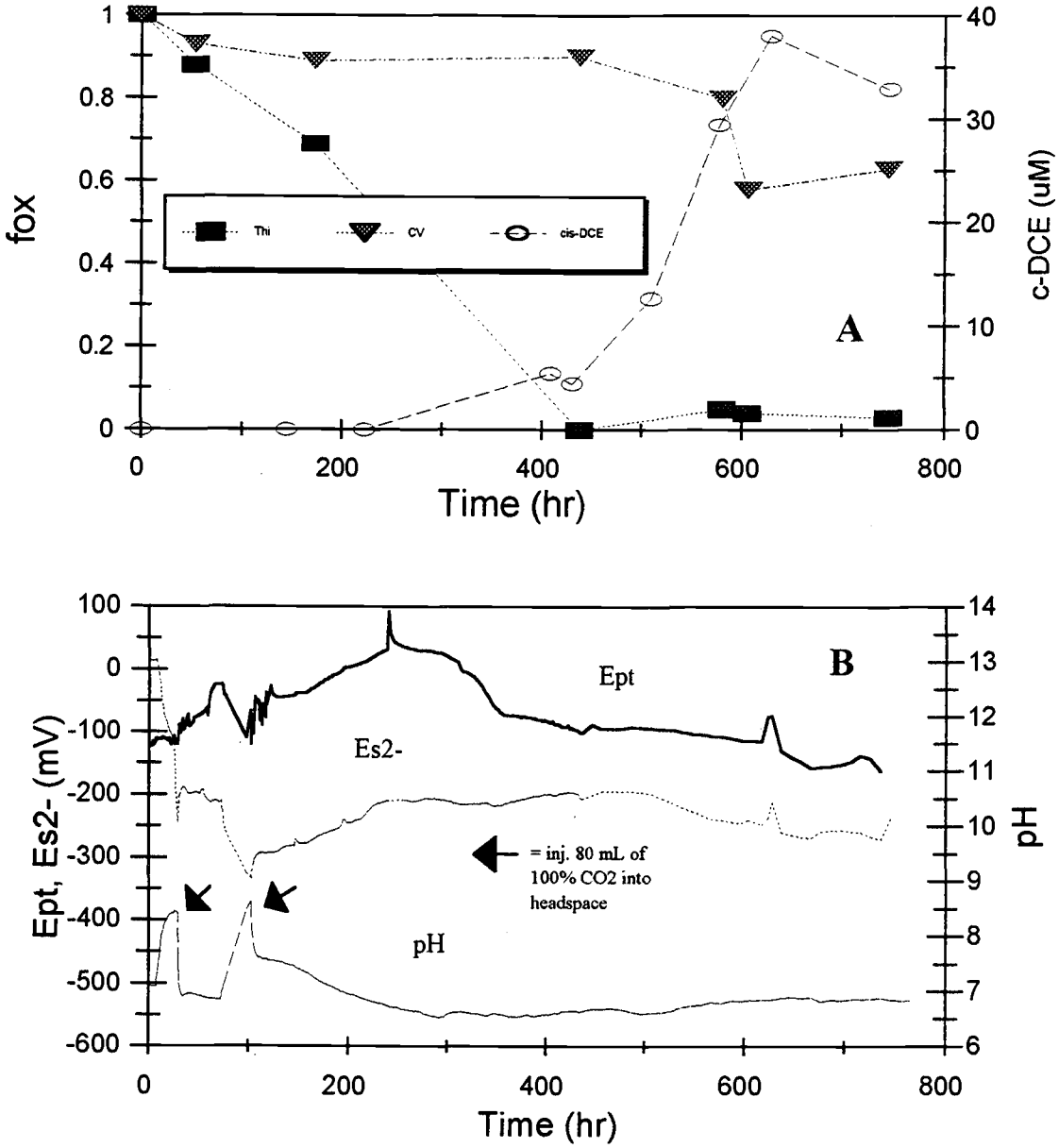

Figure 5.8 Time dependence of redox speciation of thionine and cresyl violet (A) and E_{Pt}, E_{S2-} and pH (B) during transformation of TCE to *cis*-DCE. The unfilled arrows represent when 50 µL of TCE were injected. After the first injection (0 hr), the reactor was purged with N_2 because it was believed that there was an air leak. A second injection of 50 µL TCE was made at ~100 hr. When *cis*-DCE was detected at ~200 hr, Thi was significantly reduced. As *cis*-DCE levels reached about 30 µM, CV was partially reduced ($f_{ox} \approx 0.6$) at 600 hr.

and partially reducing CV was (were) not identified. The reductant could have been sulfide but sulfide levels were below that detectable by the colorimetric method (CHEMetrics test). Reductants of biochemical origin (e.g., ferrodoxins, cytochromes) may be responsible for reduction of the indicators.

5.3.5 Concept of a "redox window" with immobilized redox indicators

Thi couples well to Fe(II) and is the indicator of choice for identifying Fe(III)-reducing conditions (25). In this chapter, CV was shown to couple well to sulfide and is useful as an indicator for sulfate-reducing conditions. Fe(II) titration data and sulfide titration data for immobilized Thi and CV are shown in Figure 5.9. From the figure, levels of reductant (Fe(II) or sulfide) compare fairly well with equilibrium models. Clearly, from the titration data, the redox indicators are reduced by comparably lower levels of total sulfide (0.3 - 100 μM) than by Fe(II) (100 - 100,000 μM).

Ideally, a redox sensor based on immobilized redox indicators would employ a series of redox indicators with redox potentials covering the range of about +400 to -350 mV (at pH 7), which react reversibly with the reductants and oxidants in ground water and can be monitored spectrophotometrically. As a system became more reducing, one of the indicators would be completely reduced, just as the next (in terms of redox potential) started to become reduced. To fully characterize the range of environmental redox potentials, up to 10 - 12 reversible immobilized indicators (each spanning a redox range of about 60 mV) might be necessary. Any two colored, reversible redox indicators define a "redox window" based on the differences in formal potentials.

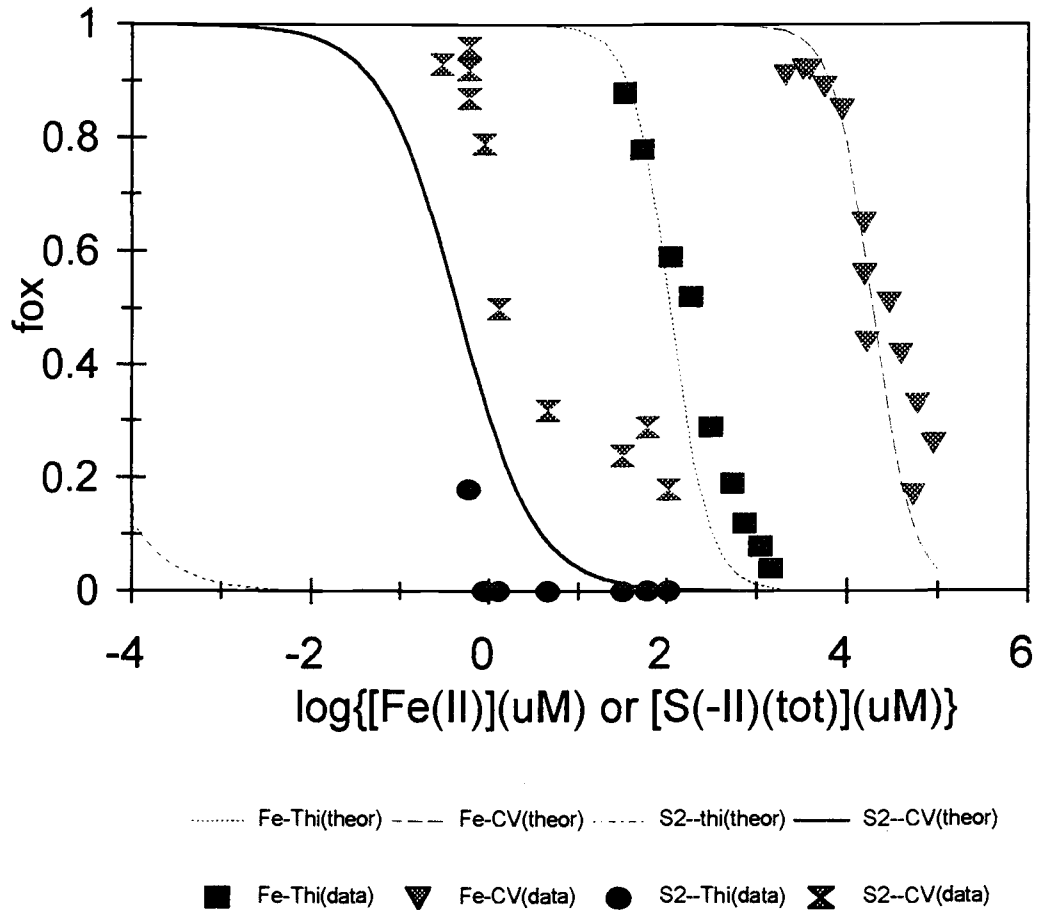

Figure 5.9 Titration curves for immobilized Thi and CV with Fe(II) and sulfide at pH 7. Curves generated for the indicator/S^{2-} and indicator/Fe(II) equilibrium are based on equation 5-11 and equation F-8 in Appendix F, respectively. Data for Fe(II) reduction are obtained from Chapter 4 (Figure 4.11) in this thesis. The curves for CV based on an equilibrium model lie to the right of the corresponding Thi curves for both titration experiments with either Fe(II) or sulfide.

Two useful indicators, Thi and CV, have been identified as useful for this purpose. Other immobilized redox indicators such as toluidine blue O (TB) (25) or PSaf could also be employed. Immobilized TB has a potential very close to that of immobilized Thi ($E_7^{0'}$ = +36 mV (25) vs. +52 mV (22), respectively) and therefore, gives little extra qualitative information (25). Also, PSaf has such a low redox potential ($E_7^{0'}$ = -286 mV (22)) that no reductant has yet been identified in environmental systems which couples to it.

Fortunately, Thi and CV are "well-placed" in terms of where their formal potentials lie and define a large "redox window". Not only do both indicators couple well to important major reductants (Fe(II) and S(-II), respectively), but their "location" in the "redox window" gives important information about transformations of other toxic, redox-active species. This concept is shown schematically in Figure 5.10. The Thi equilibrium curve lies directly over the Fe(III)-reducing potential region *and* overlaps the potential region for transformations of As(V) to As(III). In fact, Thi was previously shown to be reduced as As(V) was transformed to As(III) under Fe(III)-reducing conditions (25). In reactor studies by Lemmon (23), Cr(VI) was reduced completely to Cr(III) by Fe(II) before free (non-immobilized) Thi started to be reduced. In the context of Figure 5.9, Cr transformations (Cr(VI) → Cr(III)) occur in the region from 0.5 - 0.45 V, and Cr(VI) is completely reduced to Cr(III) before the onset of reduction of Thi.

The CV equilibrium curve lies to the left (less negative potential) of region defining sulfate-reducing conditions (-0.18 to -0.25 V) which is based on the formal potential of the SO_4^{2-}/S(-II) couple of about -220 mV (1). Hence, CV is useful for detecting the onset of sulfate reduction. The sulfur couple responsible for reduction of

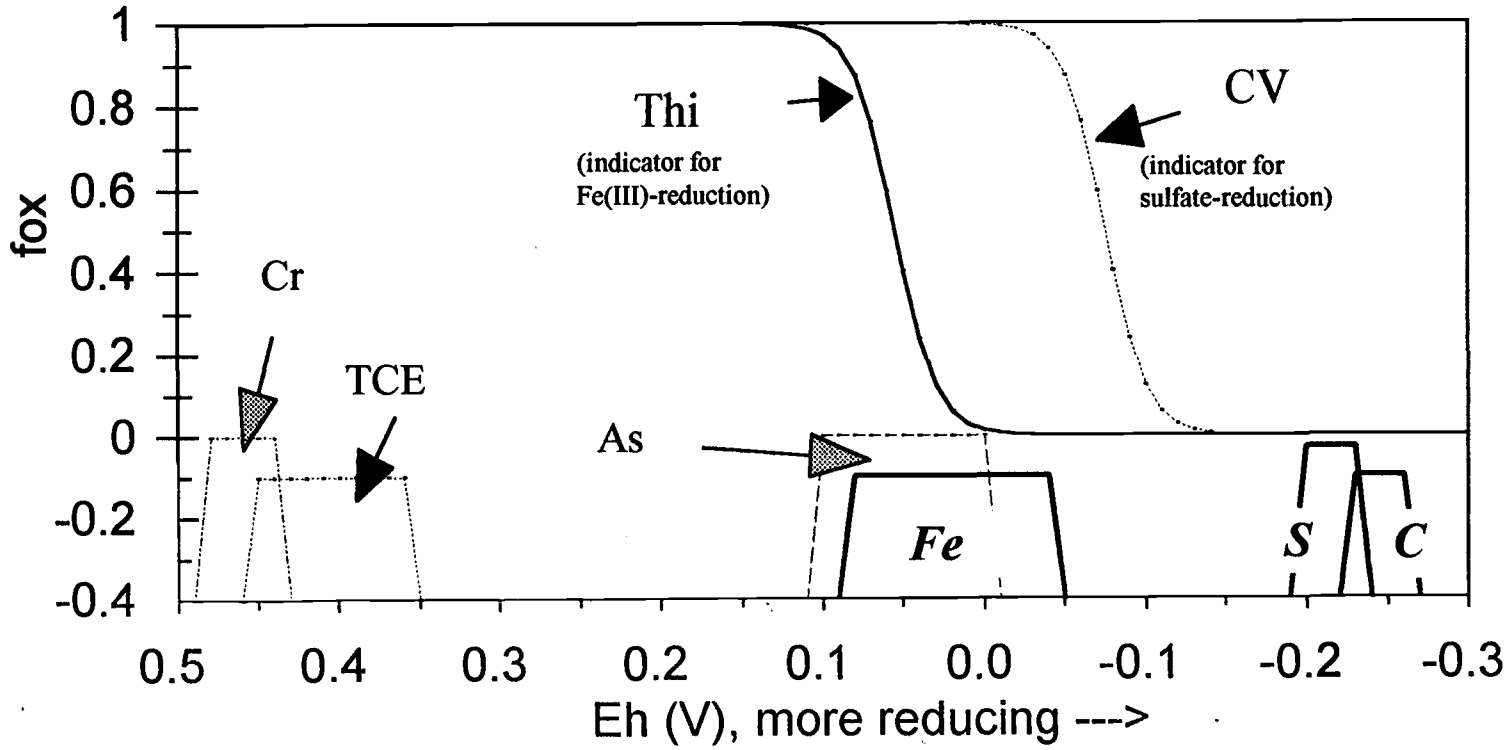

Figure 5.10 "Redox window" concept with immobilized Thi and CV at pH 7. The Fe(II)/$Fe(OH)_3$ region (***Fe***) is based on a ferrihydrite Fe(III)-solid phase and 10 - 1000 µM Fe(II). This potential region is calculated with equation 4-6 with an $E_7^{0\prime}$ value of -0.182 V for the ferrihydrite solid phase. The sulfate-reducing (***S***) region is calculated based on the SO_4^{2-}/HS^- couple ($E_7^{0\prime}$ = -0.22 V (1)) and the methanogenic (***C***) region is based on the $CO_2(g)/CH_4(g)$ couple ($E_7^{0\prime}$ = -0.244 V (2)), based on a ratio of oxidized and reduced species ranging between about 0.01 - 100. The arsenic (**As**) region ($E_7^{0\prime}$ = 0.034 V (37) for the $HAsO_4^{2-}/H_3AsO_3$ (As(V)/As(III)) couple and a 0.01 - 100 ratio of oxidized and reduced species) lies inside the Fe(III)-reducing region. The chromium (**Cr**) region ($E_7^{0\prime}$ = 0.578 V (38) for the $CrO_4^{2-}/Cr(OH)_3$ couple and 0.1 - 10 µM Cr(IV)) is indicative of the Cr(VI)/Cr(III) couple and the TCE region (**TCE**) for the TCE/*cis*-DCE transformation (occurring between 0.35 - 0.45 V at pH 7 (without conditions given (7)).

CV is a different couple, the $S^0/S(-II)$ couple, which as a reduction potential of -81 mV at 1 μM total sulfide) (see Appendix H). In contrast, the same couple ($Fe(OH)_3$/Fe(II)) represents the TEA reduction process and is involved in the reduction of Thi. If the CV reduction potential were in the same potential region as the SO_4^{2-}/S^{2-} couple, far more [S(-II)(tot)] would be required for half-reduction of the indicator (nearly 0.1 M total sulfide at pH 7). Such levels of sulfide are not normally obtained in ground water systems.

Interestingly, TCE, thermodynamically, should be reduced to *cis*-DCE around 0.4 V (7). However, this transformation is normally noted under sulfate-reducing conditions and experimentally was observed to occur after significant reduction of Thi and partial reduction of CV. This fact illustrates the importance of kinetics and microbial mediation in many environmental redox transformations.

As pH increases, the redox potential for most couples illustrated in Figure 5.10 shifts to a lower value but to different extents. For the region of pH 6-8, E_H for Thi changes -30 mV per pH unit, while the potential shift for the $Fe(OH)_3$/Fe(II) couple is more pronounced, -177 mV per pH unit. At pH 6, the center of the redox region for the $Fe(OH)_3$(ferrihydrite)/Fe(II) couple shifts to the left (more positive potentials) about 120 mV more than the redox region for the Thi couple. This difference makes Fe(II) a much poorer reductant for Thi at pH 6 than at pH 7 ([Fe(II)] is ~30 mM rather than ~0.1 mM for $f_{ox} = 0.5$). Because levels of Fe(II) significantly above 1 mM are uncommon in ground water (32), Thi will most likely not be an effective indicator for Fe(III)-reduction at pH 6. However, if lepidocrocite were the Fe(III)-solid phase formed at pH 6, the overlap between $Fe(OH)_3$/Fe(II) and Thi regions would be more similar to that at pH 7

([Fe(II)]≈ 0.9 mM for f_{ox} = 0.5). At pH 8, the Fe redox region is shifted more to the right of the Thi region, and Fe(II) is even a better reductant than at pH 7.

For CV in the region of pH 6-8, a shift of about -30 mV per pH unit is assumed and is the same as that for the $S^0_{(s,\ rhmb)}/HS^-$ couple in the pH region of 7-8 (see Figure 5.4). Therefore, in this region, the relative separation of the two transition regions is constant. At pH 6, however, a two-proton transfer (-60 mV per pH unit) is expected for the $S^0_{(s,\ rhmb)}/H_2S$ couple. Relative to pH 7, both zones shift toward less negative potentials but the $S^0_{(s,rhmb)}/H_2S$ zone moves ~30 mV further to the left relative to the CV reduction zone. Although more total sulfide is required to reduce CV, CV can still be used as an effective indicator of sulfate-reduction in this region (Figure 5.4).

The *S* region (SO_4^{2-}/H_2S couple) shifts ~74 mV higher from pH 7 to 6 (H_2S is the predominant sulfide form below pH 7) but remains considerably below the redox region of the CV couple. At pH 8, the potential of SO_4^{2-}/HS^- couple is even lower than at pH 7. Of the other couples shown, the redox potential over the pH region 6 to 8 decreases with increasing pH by 59 mV per pH unit for the CO_2/CH_4 couple, ~120 mV per pH unit for the As couple (37) and ~100 mV per pH unit for the Cr (38). An E_H/pH dependency for TCE/*cis*-DCE was not given in the reference (7).

5.4 Conclusions

CV has shown to be useful for identifying sulfate-reducing conditions in wastewater slurries. Experimental results support the hypothesis that sulfide is the primary reductant of immobilized redox indicators at this redox level. In reactor experiments at pH 7, CV couples well to total sulfide in the range of 1 - 100 μM while Thi couples well to low levels (< 1 μM) of total sulfide. Phenosafranine, with a formal potential substantially below the other two indicators, does not couple to sulfide.

In agreement with previous research (23, 25), Thi was found to be useful for predicting Fe(III)-reducing conditions. Thi and CV can be used together to define a "redox window" which delineates between Fe(III)-reducing and sulfate-reducing conditions. Furthermore, this concept may be extended to predicting the occurrence of other transformations of other redox species including contaminants. Thi has been shown to be completely reduced only after the complete reduction of Cr(VI) to Cr(III) has already occurred (23). In this chapter, evidence was presented that Thi speciation can be used to determine the onset of transformations of As(V) to As(III) and that redox transformations of TCE to *cis*-DCE occur as Thi is completely reduced and CV partially reduced.

Further studies to be considered include development of indicator technology for determining methanogenic conditions, development of a better physical configuration for immobilized indicators, and determination if reductants other than Fe(II) and sulfide couple to the indicators. So far, there is no evidence that indicators studied couple to reductants formed under methanogenic conditions. This is a major limitation because

redox transformations of many chlorinated compounds occur under methanogenic redox conditions (7). Determination of methanogenic conditions might be possible if *another* substrate, product or intermediate characteristic of methanogenic (and fermentative) conditions, such as H_2 (4, 14, 18), can be quantified and is further discussed in Chapter 7.

In this thesis research, the "apparent" absence of *active* reductants (as opposed to inert but reduced species) under methanogenic conditions might be due to several causes. Possibly low levels of reductants are produced but are oxidized by residual O_2 introduced in the external loop of the reactor before they can reduce the indicators. The development of an *in situ* sensor based on immobilized indicators (e.g., fiber optics) might be more useful to alleviate this potential problem. Also, reductants may be produced that exhibit very slow reduction kinetics with the indicators.

In field studies (and in some instances with the reactor system), the "packed-bed" configuration of immobilized indicators contributed to clogging problems and ultimately oxygen contamination. Immobilization of the indicators in film form that can be placed in a spectrophotometric flow cell (36) and allow solution to flow parallel to the film with less resistance might be advantageous. Such a configuration would allow for greater flow rates through the cell and less stringent filtering of particles (filter pore sizes of 10 - 40 μm rather than the 0.65 μm currently used) and more contact of indicators with larger particles. Alternatively, it has been demonstrated that redox can be used without continual pumping (or with a single injection) and the ensuing problems with oxygen. With filtered wastewater slurries in the reactor or well water in the field, immobilized

indicators were reduced over time by the action of microbes in contact with the indicators.

Determination of whether or not other reductants of redox indicators exist under natural conditions is difficult because conditions must be adjusted to effectively eliminate the production of Fe(II) or S(-II). Inhibitors such as molybdate could be used to eliminate sulfate-reduction (35) and the production of sulfide. It also might be possible to use enriched cultures developed by other researchers in which Fe(III)- and sulfate-reducers have been suppressed.

It might be possible to use immobilized Thi to determine low levels of sulfide. In many cases, reduction of Thi by sulfide was observed to occur before sulfide was detected with methylene blue method.

5.5 References

1. Brock, Thomas D.; Madigan, Michael T.; Martinko, John M.; Parker, Jack, *Biology of Microorganisms, Seventh Edition*, Prentice Hall: Englewood Cliffs, New Jersey, 1994.

2. McBride, Murray B., *Environmental Chemistry of Soils*, Oxford University Press, Inc., 1994.

3. Chapelle, Francis H., *Groundwater Microbiology and Geochemistry*, John Wiley & Sons, Inc., 1993.

4. Lovley, Derek R.; Chapelle, Francis H.; Woodward, Joan C., *Environ. Sci. Technol.*, **1994**, *28*, 1205-1210.

5. Lovley, Derek R.; Goodwin, Steve, *Geochim. Cosmochim. Acta*, **1988**, *52*, 2993-3003.

6. Rifai, Hanadi S.; Borden, Robert C.; Wilson, John T.; Ward, Herb C., *Intrinsic Bioattenuation for Subsurface Restoration*, printed in *Intrinsic Bioremediation*, Hinchee, Robert E.; Wilson, John T.; Downey, Douglas C., Eds., Batelle Press: 1995.

7. Semprini, L., *In Situ Transformation of Halogenated Aliphatic Compounds Under Anaerobic Conditions*, printed in *Subsurface Restoration*, Ward, C. H.; Cherry J. A.; Scalf, M. R., Eds., Ann Arbor Press, Inc.: 1997.

8. Paul, E. A.; Clark, F. E., *Soil Microbiology and Biochemistry*, Academic Press, Inc.: 1989.

9. *Standard Methods for the Examination of Water and Wastewater;* American Public Health Association: Washington, D. C., 1995.

10. *Product Catalog*, CHEMetrics, 1997-1998.

11. Frevert, T., *Schweiz. Z. Hydrol.*, **1980**, *42*, 255-268.

12. Jeroschewski, P.; Steuckart, C.; Kühl M., *Anal. Chem.*, **1996**, *68*, 4351-4357.

13. Jones, Brian, personal research experience, 1993-1999, Oregon State University.

14. Chapelle, Francis H.; McMahon, Peter B.; Dubrovsky, Neil M.; Fujii, Roger F.; Oaksford, Edward T.; Vroblesky, Don A., *Water Resour. Res.*, **1995**, *31*, 359-371.

15. *Chromatography*, Alltech Product Catalog 400, 1997.

16. Patrick, W. H., Jr.; Connell, W. E., *Science*, **1968**, *159*, 86-87.

17. Berner, R. A., *Geochim. Comochim. Acta.*, **1962**, *27*, 563-575.

18. Lovley, Derek R.; Goodwin, Steve, *Geochim. Cosmochim. Acta*, **1988**, *52*, 2993-3003.

19. Fetzer, Silke; Conrad, Ralf, *Arch. Microbiol.*, **1993**, *160*, 108-113.

20. *Equilibrium Concepts in Natural Water Systems,* Stumm, Werner, Ed., Chapter 13, 270-285; American Chemical Society: 1967.

21. *Indicators*, Bishop, E., Ed., Pergamon Press: Oxford, 1972.

22. Lemmon, T. L.; Westall, J. C.; Ingle, J. D. Jr., *Anal. Chem.*, **1996**, *68*, 947-953.

23. Lemmon, Teresa, *Development of Chemostats and Use of Redox Indicators for Studying Transformations in Biogeochemical Matrices,* **1995**, Ph.D. Thesis, Oregon State University.

24. Mobley, James, Oregon State University, unpublished report, **1992**.

25. Jones, Brian; Chapter 4 of this thesis.

26. Jones, Brian, Laboratory notebook #5, 1997, Oregon State University.

27. McMurry, John, *Organic Chemistry*, Brooks/Cole Publishing Company: Monterey, California, 1984.

28. Jones, Brian; Chapter 3 of this thesis.

29. Roberts, David, Laboratory GC/TCD calibration procedure, Oregon State University, 1997.

30. Vancheeswaran, Sanjay, *Abiotic and Biological Transformation of TBOS and TKEBS, and their Role in the Biological Transformation of TCE and c-DCE,* **1998**, M.S. Thesis, Oregon State University.

31. Bottomley, Peter, Private communication, Oregon State University, February 4, 1997.

32. Baham, John, Private communication, Oregon State University, April 29, 1997.

33. Vancheeswaran, Sanjay; Halden, Rolf U.; Semprini, Lewis; Williamson, Kenneth J.; Ingle, James D. Jr., "Abiotic and Biological Transformation of Tetraalkoxysilanes and Trichloroethene/cis-1,2-Dichloroethene Cometabolism Driven by Tetrabutoxysilane-Degrading Microorganisms", *Environ. Sci. Technol.*, in press.

34. Jones, Brian; Laboratory notebook #2, 1995, Oregon State University.

35. Lovley, Derek R.; Dwyer, Daryl F.; Klug, Michael J., *Appl. Environ. Microb.*, **1982**, *43*, 1373-1379.

36. Jones, Brian; Chapter 6 of this thesis.

37. Bos, Mark, *Part I: Development and Application of an Arsenic Speciation Technique Using Ion-Exchange Solid Phase Extraction Coupled with GFAAS, Part II: Investigation of Zinc Amalgam as a Reductant,* **1996**, M.S. Thesis, Oregon State University.

38. *Standard Potentials in Aqueous Solution*, Bard, Allen J.; Parsons, Roger; Jordan, Joseph, Eds., Marcel Dekker, Inc.: 1985.

CHAPTER 6: ALTERNATIVE IMMOBILIZATION METHODS FOR REDOX INDICATORS

6.1 Introduction

In recent years, sensor development based on immobilized "sensor molecules" has been of major interest to researchers, particularly in the fields of environmental and bioanalytical chemistry (1, 2, 3). Sensors, tailored to couple to specific analytes, can be deployed directly into samples, eliminating a separate "sampling" step. Usually, the sensor molecules are covalently bonded to, or "doped" into, a chemical matrix, often in a film form, at the surface of an electrode or at the tip of a fiber-optic probe. Chemically modified electrodes (CME's) can preconcentrate the analyte of interest at the sensor surface and can be highly sensitive (1).

One type of sensor commonly developed employs sensor molecules which interact directly with the analyte of interest to produce the signal (current or absorbance). Wier et al. (1) developed amperometric sensors for Cu(I) and Fe(II) based on various ligands (e.g., 4-vinyl-4'-methyl-2,2'-bipyridine, sulfonated bathophenanthroline) polymerized with azobisisobutyronitrile at the surface of electrodes. When placed in a sample, the analyte ions formed complexes with the immobilized ligands and the electrochemical response (current) was measured. Lev et al. (2) developed disposable sensors for Fe(II) based on 1,10-phenanthroline (OP) doped into silicon sol-gel glasses. The doped glasses could be placed in Fe(II) solutions, allowing diffusion of the Fe(II) into the structure and subsequent

complexation by the OP. The Fe(II)-$(OP)_3$ complex (with a wavelength maximum at 510 nm) could then be monitored spectrophotometrically. Because of the ability to concentrate the Fe(II) in the sol-gel, detection limits were below 100 parts per trillion (2). Furthermore, Anvir et al. (3) reports that the pH indicators thymolphthaleine and phenolphthaleine have been doped into Si sol-gels, producing pH sensors with response times on the order of 1 s.

A second type of sensor involves the immobilization of an enzyme to a sensor surface, allowing the catalysis of the reaction of specific analytes (which themselves do not produce a detectable signal (absorbance, fluorescence, or current)) to form detectable products. In many cases, these sensors were developed for bioanalytical purposes. Zhujun et al. (4) developed a fiber optic sensor for determination of H_2O_2 based on its reaction with thiamine. The reaction, catalyzed by horseradish peroxidase immobilized at the sensor surface on a bovine albumin matrix with glutaraldehyde, formed a fluorescent product, thiochrome, which was monitored spectrophotometrically. Arnold (5) developed a fiber optic sensor for *p*-nitrophenyl phosphate based on the enzyme alkaline phosphatase, immobilized on nylon, which catalyzed the hydrolysis of *p*-nitrophenyl phosphate to *p*-nitrophenoxide, a colored product. The response of the fiber optic to *p*-nitrophenyl phosphate was linear up to 0.4 mM.

Sensor development based on immobilized redox indicators for environmental redox monitoring is currently being developed and investigated. Lemmon et al. (6, 7) managed to immobilize the redox indicators thionine and phenosafranine to agarose affinity beads. More recently, the redox indicators toluidine blue O, azure A and cresyl

violet have been immobilized to the same affinity beads (8, 9). The immobilization reaction involves the coupling of amine groups on the redox indicators to aldehyde groups on the 40 - 60 μm agarose beads via a reductive amination reaction.

Normally colored in their oxidized form and colorless when reduced, redox indicators immobilized on agarose affinity beads can then be packed into a flow cell for spectrophotometric monitoring. Filtered sample solution (e.g., soil or wastewater slurry) was pumped through the flow cell, allowing contact between the immobilized indicator and soluble reductants or oxidants in the sample. As the oxidized indicator reacts with a reductant (e.g., Fe(II), S(-II)), the absorbance decreases and the "reducing power" of the sample can be estimated. The redox half-reaction of a redox indicator is

$$Ind_{ox} + ne^- + mH^+ \rightleftharpoons Ind_{red} \qquad (6\text{-}1)$$

where n, the number of electrons transferred, is typically 1 or 2, and m, the number of protons transferred, is typically 0, 1 or 2 and dependent on the pH (10).

Many redox indicators are reversible and couple to the Pt electrode (6, 11). The redox potential for an indicator (E_{ind}) is determined by the relative concentrations (activities) of the oxidized and reduced species and the Nernst equation,

$$E_{ind} = E^{0'}_{ind,m} - \frac{RT}{nF} \ln\left(\frac{[Ind_{red}]}{[Ind_{ox}]}\right) \qquad (6\text{-}2)$$

where $E^{0'}_{ind,m}$ is the formal potential of the indicator and m indicates the pH. This formal potential is different for different indicators and is often a complex function of pH because many indicators have groups such as amines which can be protonated or unprotonated. Experimentally, the concentration ratio in equation 6-2 is evaluated by measuring the absorbance of one of the species, which is usually the colored oxidized

form (see Appendix I for details). In this case, the concentration ratio equals $(1 - f_{ox})/f_{ox}$ where f_{ox} is the *fraction of indicator oxidized*, determined from the absorbance of the oxidized form of the indicator. Equation 6-2 can then be rewritten as

$$E_{ind} = E^{0'}_{ind,m} - \frac{RT}{nF} \ln \left(\frac{1 - f_{ox}}{f_{ox}}\right) \qquad (6\text{-}3)$$

Laboratory studies of applications of immobilized redox indicators to environmental analysis showed that immobilized redox indicators can be useful in determining when Fe(III)-reducing or sulfate-reducing conditions exist in soil and wastewater slurries (8, 12). They have also proved useful for determining when the redox transformation of Cr(VI) to Cr(III) has occurred (7) and when the onset of redox transformation of As(V) to As(III) (8) or TCE to *cis*-DCE is occurring (12).

Use of redox indicators immobilized on beads in field applications proved problematic, however. In recent field studies (12), well water was injected with a syringe into a packed flow cell containing redox indicators immobilized on agarose beads. Clogging occurred due to particulate matter in the water. Attempts to pre-filter the sample did not help much (a 1.6-μm filter placed between the syringe and flow cell tended to clog) and ultimately resulted in introduction of oxygen into the sample. Although the immobilized redox indicators responded to reductants for some samples (12), it was obvious that another configuration for immobilized indicators (i.e., a film form) would be more useful for field analysis.

In this chapter, three methodologies (silicon sol-gels, polyacrylamide and agarose gels) for immobilizing redox indicators in a film form are described. Agarose films provided the best results in terms of strength, immobilization efficiency and

reproducibility. Immobilization of redox indicators to aldehyde-coated cellulose membrane filters is also described. The response of Pt electrodes in contact with these membranes was investigated. Also a unique flow cell was developed specifically for spectrophotometric measurements of film immobilized indicators.

Indicators immobilized in agarose films were titrated with Fe(II) and sulfide at pH 7 in a chemostat reactor system (6, 8, 12, 13). Reductant levels required to reduce a given fraction of indicator and formal potentials of immobilized indicators were compared to those previously determined from titrations of the same indicators immobilized on beads (8, 12). Indicators immobilized to filter membranes were fitted to the tip of a Pt electrode and also tested in the bioreactor to determine the degree of poising of the Pt electrode and formal potentials. The behavior of the indicators immobilized on agarose films were evaluated with wastewater slurries under sulfate-reducing and methanogenic conditions.

6.2 Experimental

6.2.1 Chemicals

Deionized water, obtained from a Millipore Milli-Q water system, was used for titration experiments of immobilized redox indicators with Fe(II) and sulfide and for preparations of all standards and immobilization matrices. The redox indicators thionine (Thi), azure A (AA), cresyl violet acetate (CV), nile blue (NB) and phenosafranine (PSaf) were obtained from Aldrich. Their structures are shown in Figure 6.1.

For preparing silicon sol-gels, tetramethyl orthosilicate (TMOS), tetramethylammonium hydroxide solution (TMAOH, 25%(w/w) solution in methanol), poly(dimethylsiloxane), hydroxy terminated (PDMS), 3-aminopropyltriethoxysilane (APTES), 3-glycidoxypropyltrimethoxysilane (GPTMS), and formamide were all obtained from Aldrich. Glutaraldehyde (50%(w/w) in water) was also obtained from Aldrich. Sodium acetate ($NaC_2H_3O_2 \bullet 3H_2O$, Mallinckrodt) was used to prepare buffers for coupling of APTES with glutaraldehyde. Acetone was obtained from Fisher. Methanol and ethanol were obtained from Mallinckrodt and Midwest Solvents Co., respectively. Palladium powder, (99.9%, submicron) was obtained from Aldrich. Hydrogen gas (pre-purified, 100%) was obtained from Industrial Welding Supply, Inc.

For making polyacrylamide gels, a 40% acrylamide/N,N'-methylenebisacrylamide (Bis) solution (19:1), N,N,N',N'-tetramethylenediamine (TEMED) and ammonium persulfate, used as a radical initiator, were obtained from

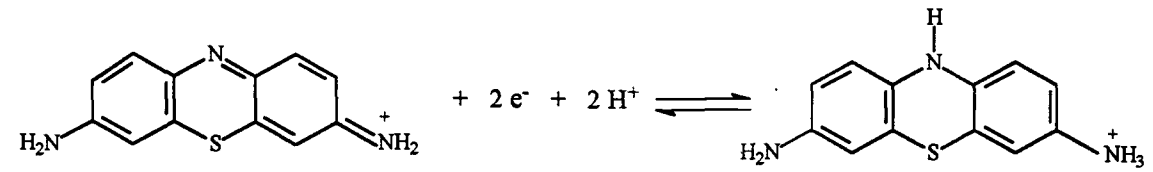

Thionine

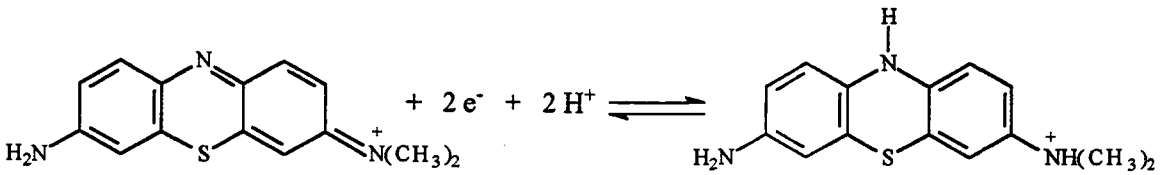

Azure A

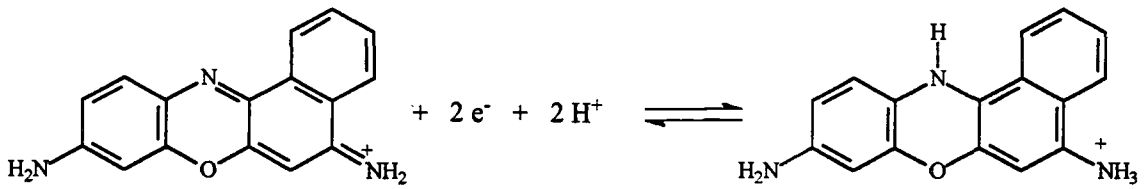

Cresyl violet

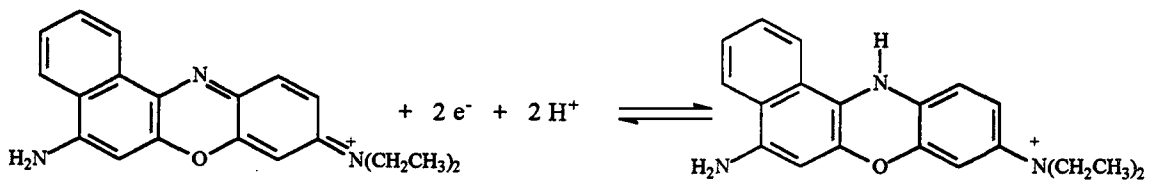

Nile blue

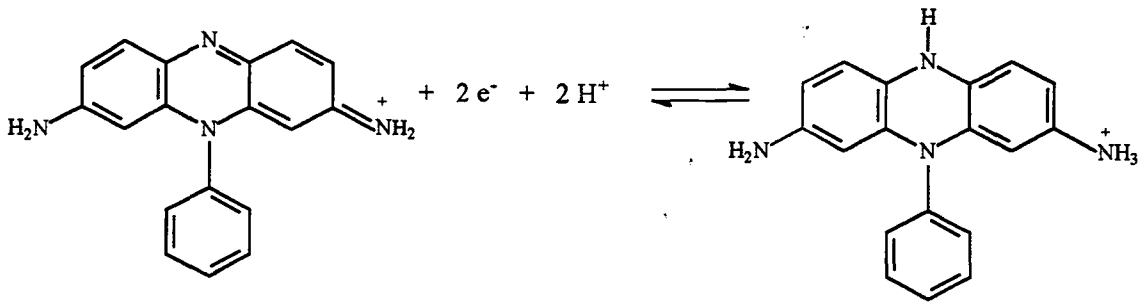

Phenosafranine

Figure 6.1 Redox indicators used in this study.

Bio-Rad. Methylene bis- acrylamide, used as a crosslinker, was obtained from Pharmacia Biotech. N-(3-aminopropyl) methacrylamide hydrochloride (APMA) was obtained from Polysciences, Inc. Dimethyl pimelimidate (DMP) and dimethyl succinimide (DSS), used as chemical crosslinkers for species with amine functional groups, were obtained from Pierce Chemical Co. Boric acid, H_3BO_3, obtained from Mallinckrodt, was used to make a borate buffer. Dimethyl sulfoxide (DMSO) was obtained from Fisherbrand. Coomassie® Brilliant Blue R (CBB) was obtained from Aldrich. For making agarose films, agarose powder, sodium cyanoborohydride ($NaCNBH_3$) and sodium periodate ($NaIO_4$) were all obtained from Aldrich.

For titration experiments, a 0.1 M Fe(II) solution in 0.1 M $HClO_4$ was prepared from hydrated ferrous perchlorate crystals ($Fe(ClO_4)\bullet 2H_2O$, G. Frederick Smith Chemical Co.) and 70% $HClO_4$ (Mallinckrodt, Inc.). Hydroxylamine hydrochloride (10% (w/v) in water), a 0.5% (w/v) OP solution in water, and a 50 mg/L Fe(III) solution in 0.6 mM HCl were obtained from Dean Johnson of the OSU Department of Chemistry. Sodium sulfide ($Na_2S\bullet 9H_2O$), used to prepare a ~0.1 M total sulfide standard for sulfide titrations, was obtained from Mallinckrodt. For the Ti(III) citrate solution, titanium trichloride solution (13% w/w in ~20% hydrochloric acid, Fluka), sodium citrate dihydrate (Mallinckrodt) and TRIZMA® hydrochloride (Sigma) were used.

Lactic acid (85% w/w in water, Mallinckrodt), estimated to be 10.9 M, was used as an electron donor for sulfate-reducers. Sodium acetate ($NaC_2H_3O_2\bullet 3H_2O$, Mallinckrodt), used as an electron donor for methanogens, and sodium molybdate (Na_2MoO_4, Aldrich) was also used to inhibit sulfate-reduction. Sodium sulfate (Na_2SO_4,

anhydrous, Baker), magnesium sulfate (anhydrous, Baker) and potassium phosphate (KH_2PO_4, Mallinckrodt), were used as nutrients. Also, $CaCl_2 \cdot 2H_2O$ (Baker) and NH_4Cl (EM Science) were added to wastewater slurries to increase ionic strength and to provide a microbial nitrogen source, respectively. NaCl was obtained from EM Science. $Na_2HPO_4 \cdot 7H_2O$, KCl and sodium phosphate monobasic, NaH_2PO_4, were all obtained from Mallinckrodt. N_2 gas (pre-purified) in 230 ft^3 tanks was used.

6.2.2 Immobilization of redox indicators in silicon sol-gels

Silicon sol-gels form transparent glass-like structures in which reagent molecules can be "doped" directly, without the necessity for covalent immobilization. In general, they are formed by the reaction of silicon alkoxides and water, with acid or base as the catalyst (14). The general reaction mechanism is shown in Figure 6.2.

Three approaches were used to develop sol-gel immobilized redox indicators: 1) production of flat, ~ 0.5 - 1 mm thick sol-gels (monoliths) with redox indicator incorporated into the structure, with NaOH as the catalyst, 2) immobilization of redox indicator/sol-gel on glass plates with PDMS and TMAOH as a catalyst, and 3) immobilization of sol-gels on glass plates with subsequent immobilization of indicators to the sol-gel structure by covalent means with glutaraldehyde.

Method 1: Follow general procedure given by Anvir et al. (15). In a small beaker, the following solutions were added and mixed:

2.5 mL of tetramethyl orthosilicate (TMOS)

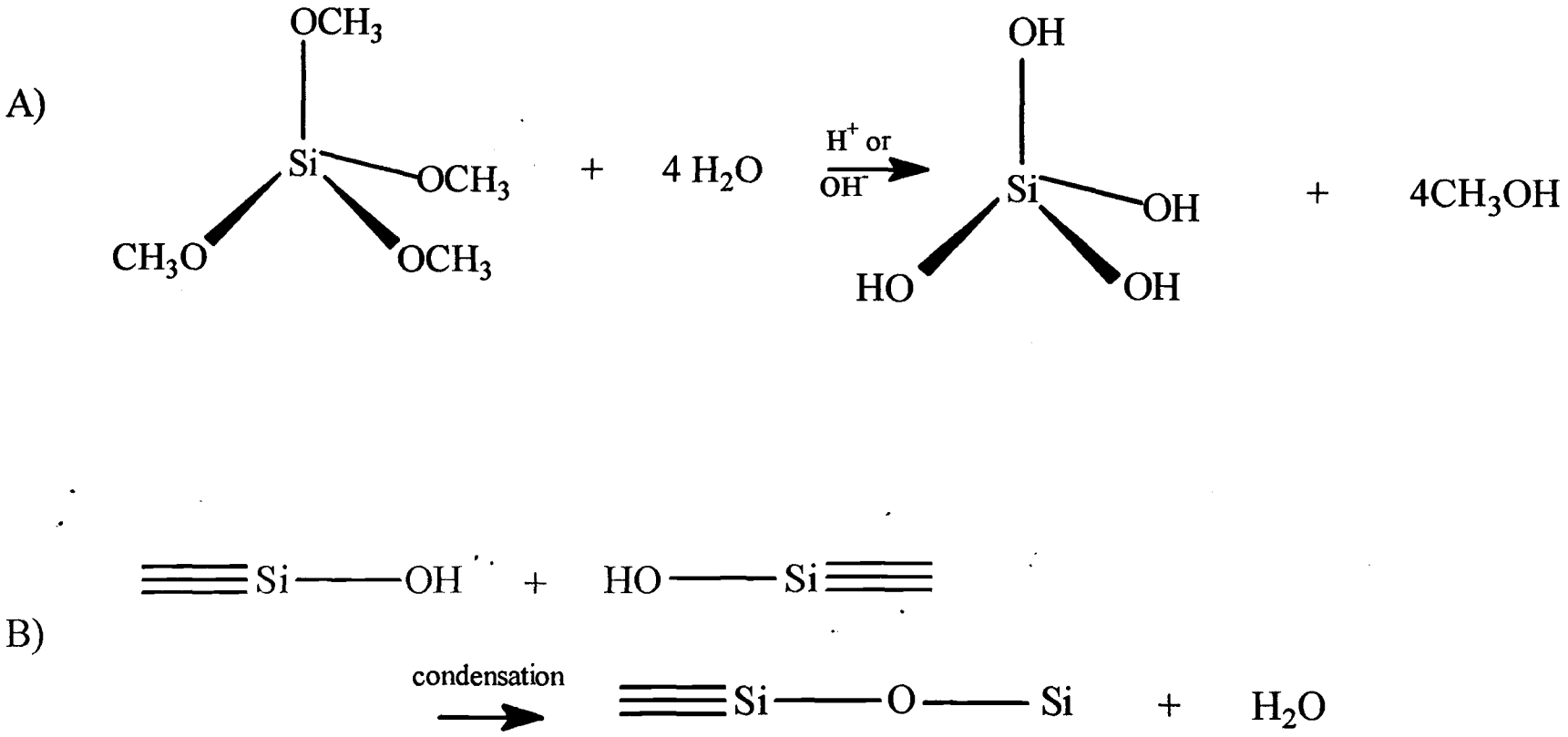

Figure 6.2 Mechanism for the formation of silicon sol-gels. The formation of Si sol-gels begins with hydrolysis of the silicon alkoxide under acidic or basic conditions (A). After hydrolysis, the -OH bonds condense (B) to form a glass-like, SiO_2 structure. Analyte molecules (e.g., redox indicator) are entrapped in the matrix.

3.0 mL of reagent (3 mL of 2 mM redox indicator (Thi or PSaf) with 30 μL of 0.1 M NaOH added, diluted to 10 mL).

2.0 - 3.0 mL of methanol (less methanol gives faster reaction time)

In some cases, 1 mL of formamide (to help prevent cracking) was added to the mixture. Also in some cases, Pd powder (~10 - 20 mg) was added to the mixture.

The mixture was allowed to sit 2 - 3 hr until it became viscous (syrup-like). It was then poured onto an acetone-cleaned Teflon sheet affixed to a glass plate. The mixture was then covered with a Petri culture dish and allowed to solidify for 1 - 2 days.

Method 2: Follow the general procedure adopted from Angel et al. (16). In a cooled 50-mL flask placed in an ice bath, 0.4 mL of tetramethyl ammonium hydroxide (TMAOH, 25%) and 1.5 mL of ethanol were added. This solution was allowed to cool for approximately 30 min. At this time, in a test tube, 0.6 mL of TMOS, 0.4 mL of poly(dimethyl siloxane), hydroxy-terminated (PDMS), 0.3 mL of 3-amino propyl triethoxysilane (APTES), and 0.3 mL of glycidoxypropyl trimethoxysilane (GPTMS) were mixed with a stirring rod and place in the ice bath. A small amount (~5 mg) of *dry* indicator (no H_2O) was then added to the test tube solution and stirred well. Both cooled solutions were then mixed together and stirred for 30 s. The mixture was then allowed to sit in the ice bath for 2 - 3 hr until a syrupy consistency was reached. In the mean time, glass slides (VWR 22-mm micro cover glasses) were soaked in a 1:1 NaOH/DI water solution for 0.5 - 2 hr to facilitate -OH bonding. The glass slides were rinsed well with DI water at least 30 min before use and allowed to dry completely.

When the sol-gel/indicator mixture was the proper consistency, portions of the mixture were pipetted onto the Teflon plate and covered with the pre-soaked glass

slides. The slides were then pressed down to increase contact with the mixture and decrease the film thickness. The coated slides were then covered with a Petri dish and allowed to solidify for 1-3 days.

Method 3: This method was chemically similar to method 2, except that no indicator was added to the initial sol-gel mixture and immobilization of glutaraldehyde to the amine groups on the APTES was attempted. The intent was to immobilize the redox indicator to aldehyde groups after the sol-gels were formed. The steps after mixing were similar to those in Method 1, forming slabs (monoliths) rather than glass-coated films.

The solidified sol-gels were placed in 7.4-mL vials (Fisherbrand) along with 1 mL of 1 M glutaraldehyde, 1 mL of 0.1 M $NaCNBH_3$ solution and 1 mL of 1 M acetate buffer (in pH range of 3.5 to 4.5). The vial was then placed in a rotator for several hours or overnight.

6.2.3 Immobilization of redox indicators in polyacrylamide gels

Polyacrylamide gels are commonly used in electrophoresis. They are formed by the addition of a catalyst (TEMED) and a radical initiator (ammonium persulfate) to a solution of acrylamide monomer and a cross linker. Once formed, they are highly hydrophilic (17). The general mechanism of polyacrylamide gel formation is shown in Figure 6.3.

Several attempts were made to dope redox indicators into the polyacrylamide structure directly without covalent immobilization. In these cases, the solution of 40%

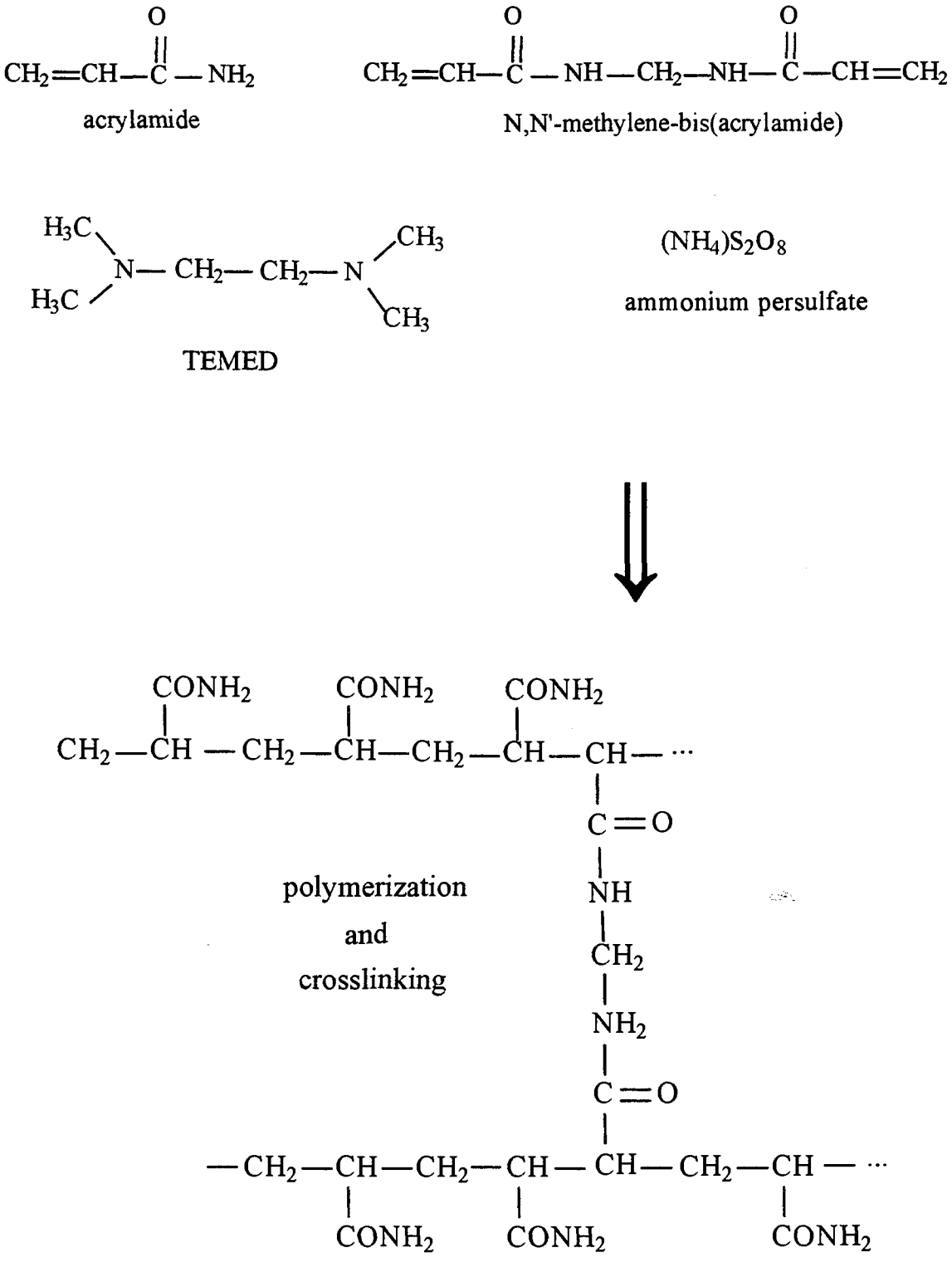

Figure 6.3 Mechanism for polymerization reaction of acrylamide with N,N'-methylene-bis(acrylamide). TEMED acts as a catalyst and ammonium persulfate as a radical initiator.

acrylamide monomer/Bis crosslinker (19:1) in DI water was mixed (at different ratios) with a 2-mM solution of indicator (Thi or PSaf), catalyst TEMED (4 μL), and the radical initiator (80 μL of a 10%(w/w) ammonium persulfate solution in DI water). The volume of acrylamide/Bis solution was varied between 2 and 6 mL, the difference (to a total of 10 mL) made up with the indicator solution. In some experiments, to increase the crosslinking and decrease the pore size of the gel, between 0.1 and 0.3 g of methylene bisacrylamide monomer was added to the solution (making ~10:1 and ~5:1 acrylamide/Bis solutions, respectively).

Once the solution was prepared, it was shaken and aliquots (0.5 - 1 mL) were pipetted on the Teflon board, allowed to react for ~30 min, and then covered with a glass slide. After the gel had partially solidified (~20 min), the glass slides were removed from the gels. The gels were then left to solidify for ~2 - 3 hr, at which time they were placed in DI water to soak.

To covalently immobilize the redox indicators, two different amine-amine chemical crosslinkers were employed: dimethyl pimelimidate (DMP) and dimethyl succinimide (DSS). These crosslinkers, available from Pierce Chemical, were used to covalently bond the amine group of the redox indicator with the amine group of N-(3-aminopropyl) methacrylamide hydrochloride (APMA), which could then be polymerized into the polyacrylamide structure. The reactions of DMP and DSS with APMA and the redox indicators are shown in Figures 6.4 and 6.5, respectively.

To chemically link the redox indicator (Thi or CV) with APMA, indicator, APMA and the crosslinker were mixed together (generally in a 1:~5-20:1 ratio) and allowed to react directly in buffered solution. The general methods for crosslinking the

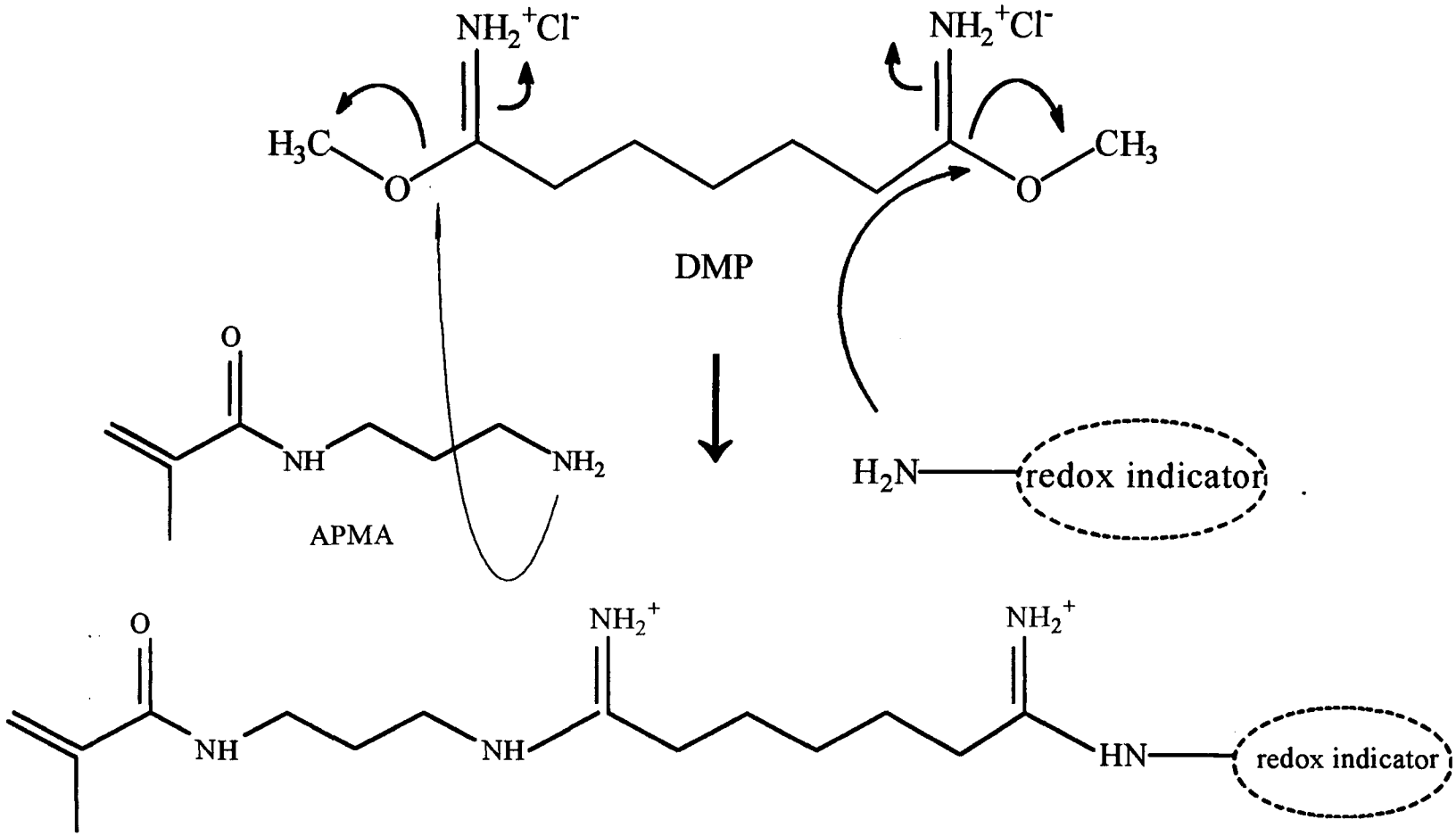

Figure 6.4 General reaction mechanism for crosslinking of N-(3-aminopropyl)methacrylamide (APMA) and redox indicator with dimethyl pimelimidate (DMP). After crosslinking, the acrylamide functional group on the APMA can be polymerized into a polyacrylamide gel.

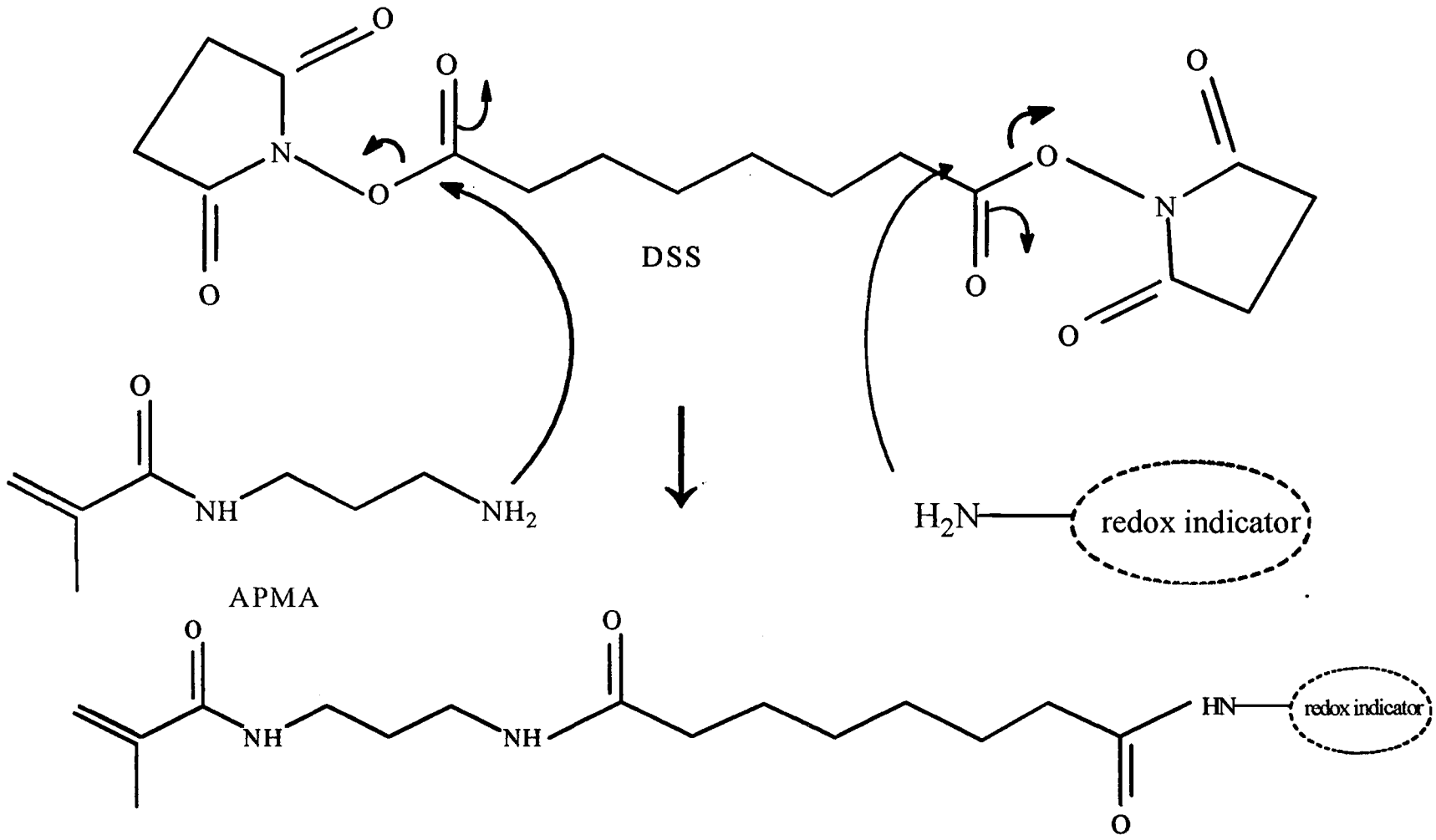

Figure 6.5 General reaction mechanism of APMA and redox indicator, crosslinked with disuccinimidyl suberate (DSS).

molecules with the two crosslinkers are described separately and were adopted from procedures described by Pierce Chemical (18).

Cross linking with DMP: First, 25 mL of a 0.2 - 0.5 M borate buffer was prepared and adjusted to pH 8.3 by addition of HCl and NaOH. Next, 5 mL of this buffer was placed in a 25-mL beaker along with the redox indicator (7 mg (22 μmol) Thi or 32 mg (66 μmol) CV) and APMA (4 mg (22 μmol) for Thi or 12 mg (66 μmol) for CV). Then, 3 mL of ethanol were added to enhance indicator solubility. Finally, 0.1295 g (500 μmol) DMP was added in two portions, half initially and the other half 30 min later. The solution was then covered with a Petri dish and allowed to react for 4 - 5 hr. The solution was well-stirred throughout the reaction.

Crosslinking with DSS: To 45 mL of a stirred, pH 7, 20-mM phosphate buffer, 0.15 M in NaCl, indicator (8.35 mg (26 μmol) Thi or 12 mg CV (25 μmol)) was added along with 4.45 mg (25 μmol) of APMA. In 5 mL of DMSO, 0.184 g (500 μmol) of DSS was dissolved. This solution was then poured into the indicator/APMA solution, covered, and allowed to react for 1 - 2 hr. In some cases, approximately 5 - 10 mL of ethanol were added to increase the solubility of the DSS or indicator.

For preparation of the indicator immobilized polyacrylamide gels, the procedure for making the gels was the same as before, except that crosslinker solution was substituted for the 2 mM indicator solution. In general, for Thi-polyacrylamide films, 4 mL of Thi-crosslinked solution were added while 6 mL of CV-crosslinked solution were added to produce CV-polyacrylamide films.

6.2.4 Immobilization of redox indicators in agarose gels

Agarose is a polysaccharide which forms a gel in water after heating. Used as an electrophoresis gel, it is highly hydrophilic (19) and is also commonly formed into beads (ranging from 40 - 300 μm) with added functionalities for affinity chromatography (20). In fact, redox indicators were originally immobilized by Lemmon (6) on 60-μm, cross-linked agarose (4%) affinity beads (Sterogene ALD beads) which had been modified with an aldehyde functionality (40-50 μmol/mL of gel). The details of this immobilization procedure are described in Appendix E.

The overall reaction scheme, including the formation of aldehydes on the agarose films and immobilization of the indicators, is shown in Figure 6.6, and was modified from instructions given from Pierce Chemical Co. (21). In 50 mL of DI water, ~1 g of agarose was added, stirred and heated in a microwave oven to just below the boiling point. After cooling slightly, 2.3 g (11 mmol) of sodium periodate were added and the solution was stirred for approximately 1 min. At this point, 2 - 4 mL portions of the agarose/periodate solution were pipetted onto the Teflon sheet and pressed down with Petri dishes to form films approximately 0.3 - 0.5 mm in thickness. The film set rapidly (about 2-3 min) and after about half an hour, the Petri dishes were removed. The agarose was allowed to react with the periodate for 60 - 90 min more. The films were then rinsed well with tap water for about 15 min and placed in DI water to soak overnight. This step ensures that unreacted periodate is washed from the film so that it does not continue to oxidize and break down the agarose structure.

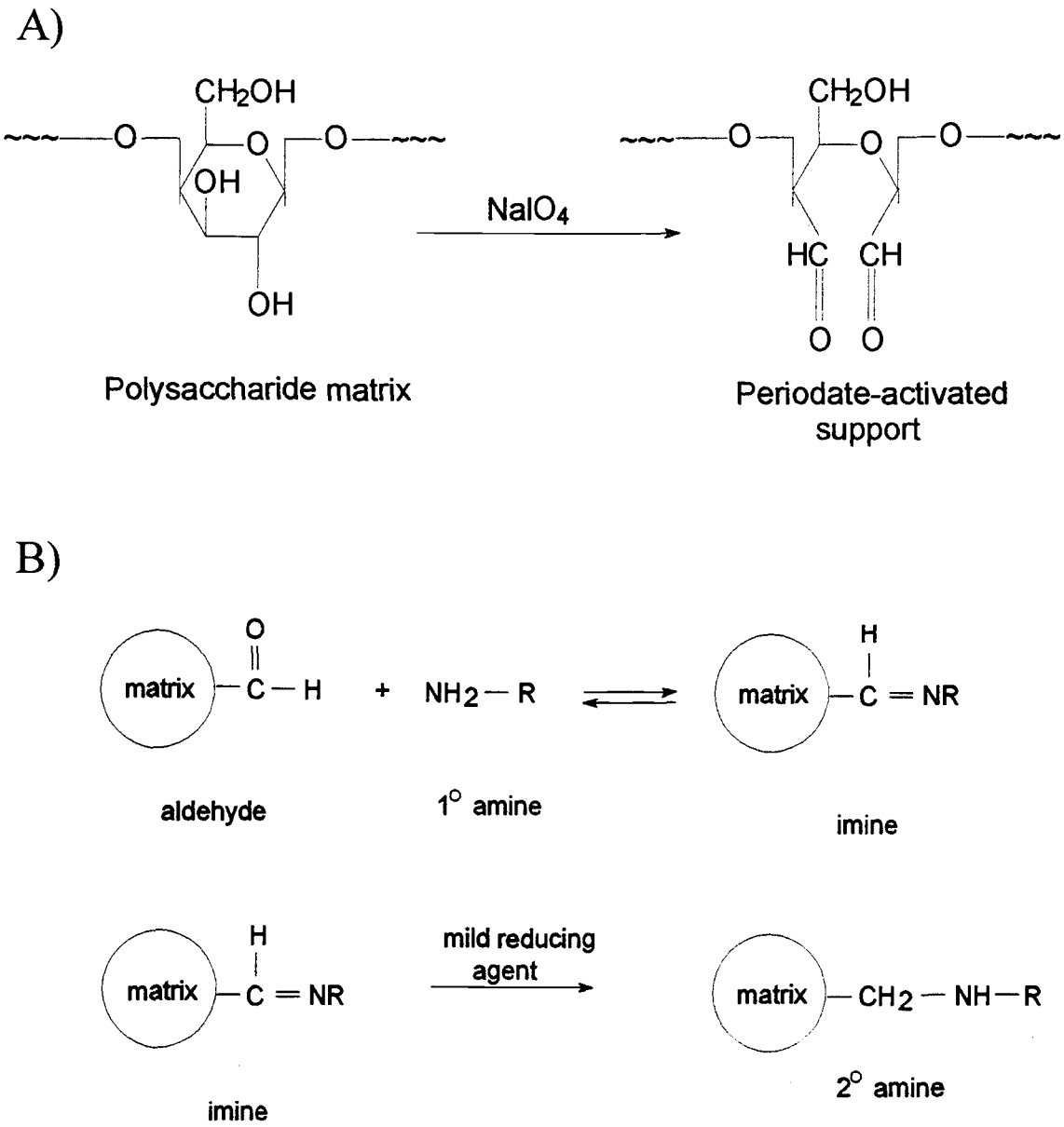

Figure 6.6 Immobilization scheme for redox indicators on agarose. In step A, the agarose matrix is oxidized with periodate, forming aldehyde groups. In step B, the amine group of the redox indicator couples to the aldehyde, forming an imine. The double bond is subsequently reduced with a mild reducing agent (e.g., $NaCNBH_3$) to form a 2° amine.

To immobilize the redox indicators, aldehyde-prepared agarose films were first soaked 1 - 2 days in ~50 mL of 2 - 5 mM indicator solutions (in a 0.1 M sodium acetate adjusted with strong acid to a pH between 3.5 and 2.5 or lower, depending on the indicator) along with 10 - 20 mL of ethanol to enhance the solubility of the indicator in the film. This soaking procedure was found to promote complete diffusion of the indicator into the porous structure and also it is believed to enhance imine formation (Figure 6.6B) of the indicator with the aldehyde groups (a step not necessary for agarose beads).

The next step in the immobilization process was the coupling procedure. In general, soaking and coupling solutions were prepared separately to vary the pH or indicator concentration, or simply to have a "fresh" solution. After sitting in the soaking solution, the films were cut into ~2" x 2" pieces and placed in a 50-mL I-Chem bottle (Fisherbrand) along with ~20 mL of the 2 - 5 mM indicator/buffer coupling solution. For AA, CV and NB, ~10 mL of DI water and ~10 mL ethanol were added to enhance solubility of the indicator. For these indicators, dry indicator was added to the coupling solution to maintain the indicator concentration at about the same concentration as the soaking solution. Also, the pH was maintained at the same value (typically pH 2.5 - 3.2). For Thi and PSaf, dilution of the original indicator soaking solution (from ~2 to ~0.5 mM) was necessary for coupling to prevent too much indicator from being immobilized on the agarose. Occasionally, ~10 mL ethanol were also added. For Thi and PSaf, the pH of the coupling solution was readjusted to higher values (pH 3.6 - 4) to ensure reduction of the imine bond by $NaCNBH_3$ (rapid hydrolysis of $NaCNBH_3$ occurs at low pH (22)).

For Thi and PSaf, ~0.2 g of $NaCNBH_3$ were added to the solution (for a final concentration of ~0.1 M) to reduce the imine formed to a secondary amine. The vial was then capped and allowed to rotate on a mechanical rotator for 3-4 hr, at which point the films were taken out and allowed to soak in a 1:1 DI water/ethanol solution overnight to remove uncoupled indicator. The films were then stored in DI water in a refrigerator for further use.

At the lower pH values required for coupling AA, CV and NB, $NaCNBH_3$ was not useful, and the indicator leached out. Instead, a ~50 mM Na_2S solution served as the reducing agent. Typically, 2 to 5 mL of the de-aerated sulfide solution was injected with a syringe into a de-aerated I-Chem vial containing the indicator/buffer/film solution. The solution was allowed to react for 1 - 2 hr, at which point the films were removed and treated as described for the Thi and PSaf coupled films.

6.2.5 Immobilization of redox indicators to filter membranes and cellulose filter paper

The Sartorious membrane filters used (Sartobind®) were 25 mm in diameter with a 0.45-μm pore size. The density of aldehyde groups on the membrane was not listed, although information about the product stated that the "covalent binding capacity (of the membrane) to γ-globulin is about 25 - 35 $\mu g/cm^2$" (23).

The coupling scheme employed previously for the agarose films was also used to bind redox indicators (Thi, AA, CV, NB and PSaf) to the membrane (step B in Figure 6.6). However, no aldehyde-formation step was necessary and no pre-soaking step was used. The time for the coupling reaction was generally about 1 - 2 hr and less

concentrated indicator solutions were used (ranging from 0.2 - 1 mM). In some cases, the buffer pH values were higher (by 0.5 - 1 pH unit) than those used with agarose as the substrate.

For immobilization of redox indicators to cellulose filters, two types of Whatman filter paper were tested: 1) filter type 1, with a diameter of 42.5 mm and an exclusion limit of 11 μm, and 2) ashless filter type 540 with a diameter of 5.5 cm and an exclusion limit of 8 μm. The reaction scheme was essentially identical to that shown in Figure 6.6.

To form aldehyde groups on both types of cellulose filters, the filters were placed in 25 mL of DI water in an I-Chem vial along with 2.3 g (11 μmol) of sodium periodate (0.44 mM). The vial was placed in a mechanical rotator for 2 hr, at which point the filters were taken out and soaked in DI water for several hours to remove the periodate. For indicator immobilization, the reaction conditions were identical to those employed for the Sartorious membranes.

6.2.6 Flow cell for film immobilized indicators

In previous work, indicators, immobilized on 60-μm affinity beads, were packed into a 1-mm pathlength cell (Hellma 170.700-QS) for spectrophotometric analysis (6, 8) as schematically shown in Figure 6.7A. Filtered reactor solution (6, 8, 12) or well water sample (12) was pumped through or injected into the flow cell. This "packed bed" configuration, although suitable for reactor experiments in a laboratory with well-filtered reactor solution, was not particularly amenable for field analysis due to clogging

A

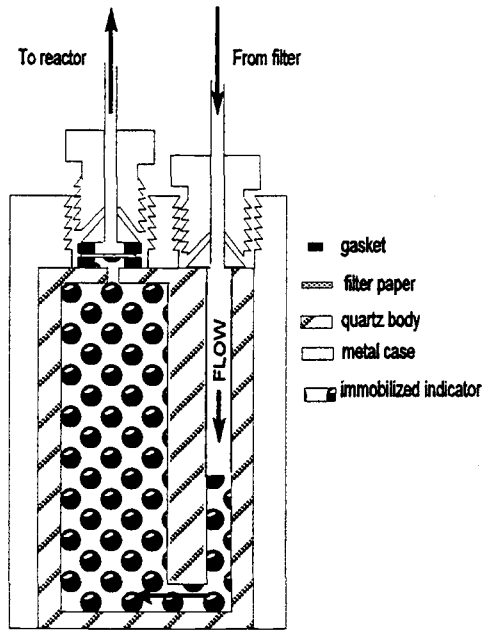

B

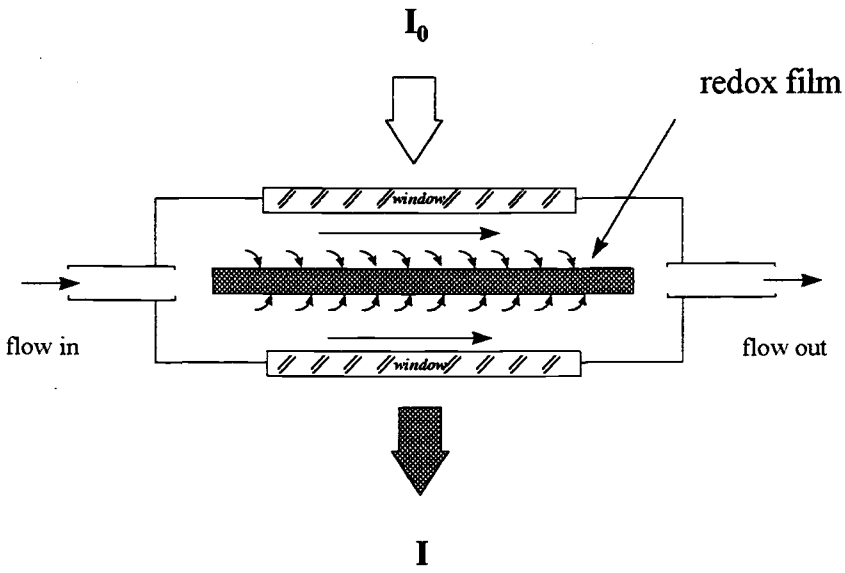

Figure 6.7 Schematics of flow cells. (A) Original Hellma flow cell (170.700-QS, 1-mm pathlength) packed with immobilized indicator beads. (B) Conceptual design of the new removable-window flow cell for indicator films.

of the flow cell during sampling (12). This factor was a major reason for the development of film-immobilized indicators.

To accommodate indicators immobilized in films, a special spectrophotometer flow cell (denoted the removable-window flow cell) was developed and is shown schematically in Figure 6.7B. The cylindrical body of the flow cell was made from black Delrin with an outer diameter of 1.5 in and length of 1 1/8 in. The interior of the flow cell consists of a 3-mm by 5-mm by 5-mm cavity in which the redox film is placed. Inlet and outlet female ports (1/4"-28 threads) are opposite each other and oriented parallel to the 5-mm x 5-mm plane of the cavity, allowing solution to flow parallel to the film. The holes into the cavity are 0.030-in id and the cell is connected to 0.030-in id, 1/16-in od PEEK tubing with Delrin nuts (P•252, Upchurch). The cell windows are made of sapphire (Rolyn Optics) with a diameter of 0.5 in and a thickness of 0.5 mm. Each window is press fit into a custom-made Delrin fitting which screws (5/8"•28 thread) into the body of the cell which seals the window against one side of the cavity.

The flow cell was positioned in the light path of the spectrophotometer (Hewlett Packard 8452A diode array) by a special holder which was designed to screw directly into the original base of the spectrophotometer. The cell is placed rotated in the holder until pins set into the flow cell mated with holes drilled into the holder. The base of the holder is 1.75 in by 2.75 in with a height of 1.9 in. The centerline (parallel to the light path) is 1.444-in high.

6.2.7 Instrumentation

Titration and wastewater slurry experiments were conducted in an air-tight bioreactor system which is schematically shown in Figure 6.8 and which has been described previously in detail (13). A Pt-button electrode (Orion 967800) was used for E_{Pt} measurements and a glass pH electrode (Orion 9101BN) was used to measure the pH. One reference electrode (Orion 900200 Ag/AgCl double junction, modified to give the same potential as an SCE) was used for all indicator electrodes. A sulfide electrode (Orion 9416BN) was used to measure or determine if sulfide was being produced in the bioreactor when wastewater slurries were present, and for low-level sulfide measurements. For wastewater slurry experiments, dispensing pumps (FMI Micro II-Petter) were used to add acid or base to control the pH. Readings of E_{Pt}, pH and E_{S2-} (the potential of the sulfide electrode) were taken at operator-chosen time intervals with a 386 PC and a QuickBASIC program developed to take electrode readings automatically, control the pH, and to calculate various parameters associated with control such as the pH buffer capacity. The pH electrode was calibrated with pH buffer solutions made from commercially available METREPAK pH capsules.

To remove O_2 and promote anaerobic conditions, the bioreactor was initially purged with N_2 gas (pre-purified grade) for several hours or overnight. Gas flow was maintained by a mass flow controller (Tylan FC280 with a Tylan RO-28 readout box). Residual O_2 in the tank was removed with an oxygen trap (Alltech Oxy-Trap 4001). To avoid loss of H_2S, methane or other gases which were produced in experiments, the N_2 purge was turned off after anaerobic conditions were achieved (typically $E_{Pt} < 0$ mV).

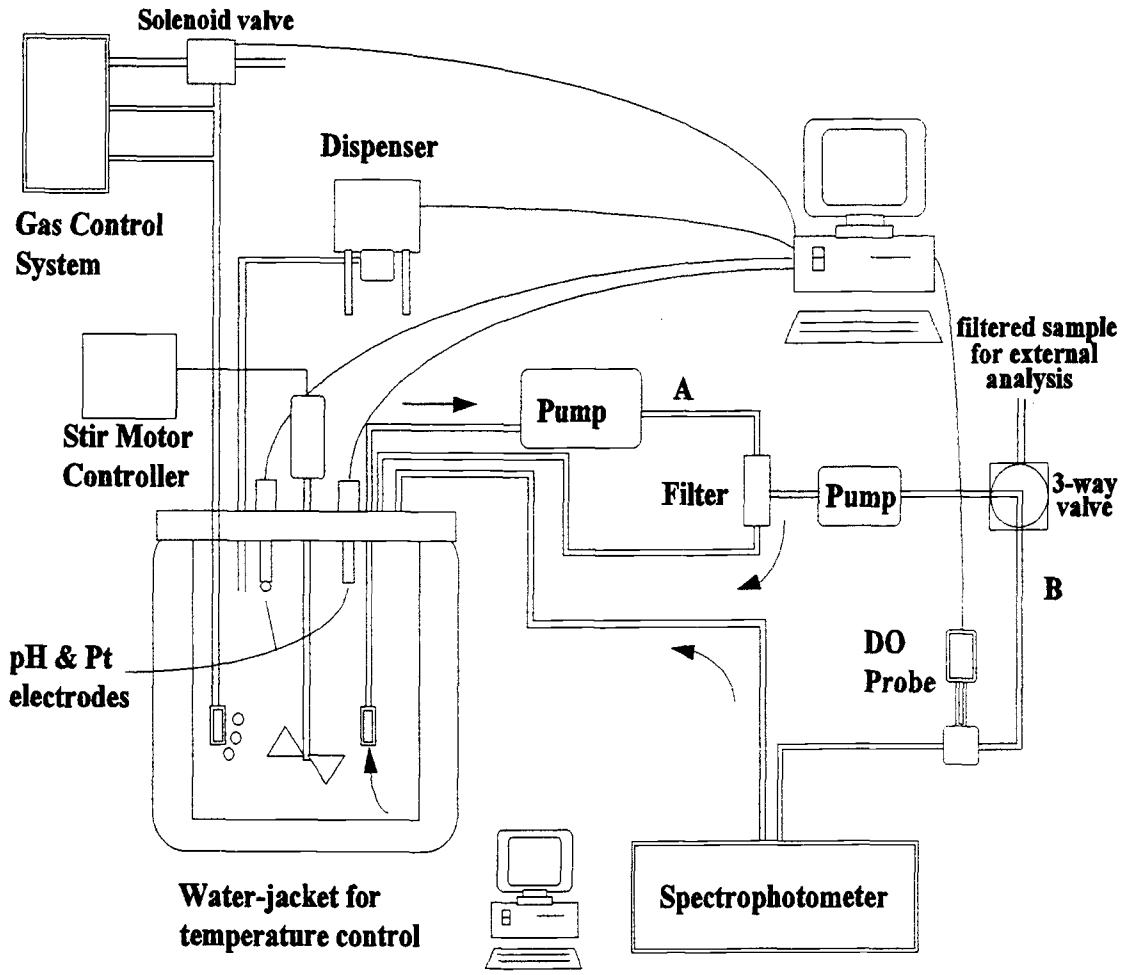

Figure 6.8 Bioreactor system for controlling and maintaining redox conditions, pH and anaerobic integrity. Loop A above refers to the primary external loop and loop B above refers to the secondary external loop, from which samples are taken for analysis. The bioreactor has a 2-L volume and normally contained 1 L of solution or slurry. The DO probe shown in Loop B, which had been used in previous experiments, was not used for these experiments.

A cross-flow filter system provided the continuous separation of liquid from solids in the reactor solution and direct interaction of soluble redox species with the immobilized redox indicator (6, 13). The primary loop (A in Figure 6.8) includes the cross-flow filter and a peristaltic pump (Masterflex speed controller, Easy load pump head 7518-50). In the secondary loop a peristaltic pump (Pharmacia Peristaltic Pump P-3) pumps filtered solution from the filter through the spectrophotometric flow cell back to the reactor. Because larger particles can pass through the removable-window flow cell for film-immobilized indicators than through the previously used "packed flow cell", the mesh size of the primary filter was increased from 0.45 μm (6, 8, 12) to 40 μm (Nylon mesh, CMN-40-A, Small Parts, Inc.). The primary mesh filter was sandwiched between two 70-μm mesh filters (Spectra-Mesh fluorocarbon). A plastic mesh filter (a particulate filter for a lawn sprinkler with 0.1 - 0.2-mm mesh), attached to the inlet tube of the primary loop, was used to filter out large particles. Filtered bioreactor samples were taken from the external loop. To minimize residual O_2 leakage in the external loop, both pumps were encased in two large, plastic containers (Rubbermaid) which were purged continuously with N_2. With the exception of the tubing used with the two pumps (Tygon tubing size 14, 1.6-mm id, 5-mm od, Masterflex® from Cole-Parmer Instrument Co.), PEEK tubing (UPCHURCH type 1533, 1/16-in od, 0.030-in id and type 1534, 1/8-in od, 0.062-in id, which both have low O_2 permeability) was used throughout both primary and secondary loops.

For titration experiments, Fe(II) and sulfide injections were made with a 100-μL syringe (Hamilton) through a Chemi-inert septum (VWR) in the reactor lid. Gas headspace samples were withdrawn with a Hamilton SampleLock 81056 100-μL, gas-

tight syringe. Methane was quantified with an HP5890 GC/TCD with a calibration method developed by Vancheeswaran (24). The chromatograph was made available through the Department of Environmental Engineering at OSU.

6.2.8 Determination of formal potentials of immobilized indicators

The formal potentials of indicators immobilized in agarose films and in cellulose filters were determined by a procedure originally devised by Lemmon et al. (6, 7). This procedure involves the concurrent titration of both the free and immobilized redox indicator with Ti(III) citrate and is described in more detail in Appendix I. The free indicator poises the Pt electrode while the absorbances of both the free and immobilized forms of the indicator are monitored. In this way, the Pt electrode potential can be measured while the both the free and immobilized indicator are reduced.

The titrant was a ~240 mM Ti(III) citrate solution prepared as described in Appendix I. It was injected into the reactor solution with a 100-µL syringe as 10-µL (2.5 µmol) aliquots.

6.2.9 Titration of immobilized indicators with Fe(II) and sulfide

To determine the Fe(II) levels necessary for reducing indicators immobilized in agarose films, portions of immobilized indicator (~4- x 4-mm slabs, cut from larger films with an X-acto® knife) were first placed in the removable-window flow cell (Figure 6.7B). The reactor solution consisted of a deaerated, 0.05 M TRIZMA® buffer (in DI water) along with 0.05 mol KCl, made to pH 7 by additions of HCl and NaOH

and was pumped through the flow cell. After an initial absorbance measurement of the indicator (Thi or CV) was taken, aliquots (10 -100 μL) of 0.1 M Fe(II) were injected into the reactor system via the Chemi-inert septum. The absorbance of the indicator was measured and aliquots of sample were removed from the external loop to determine Fe(II) (OP method, Appendix B) only after the absorbance of the indicator reached steady-state (typically 2-3 hr after an addition).

Immobilized Thi and CV were titrated with sulfide in a similar fashion. The reactor buffer was a 0.05-M phosphate buffer adjusted to pH 7 and the titrant was a ~0.1 M sulfide solution. After initial deaeration of the reactor solution with N_2 gas for 2-3 hr, the flow rate was decreased to a low value (a N_2 bubble every 10 s or so) to minimize the loss of sulfide (as $H_2S(g)$). Some N_2 was needed to minimize O_2 leakage into the reactor. Total sulfide concentration in samples withdrawn from the external loop was quantified by the colorimetric methylene blue method (25, 26). Pre-prepared reagents (CHEMetrics Vacu-vial® ampules) and a small, portable spectrophotometer (Multi-Filter Photometer A-1051, CHEMetrics) were used.

Titration experiments were also conducted with "Pt/indicator" electrodes constructed as shown in Figure 6.9. Thi immobilized on a Sartorious membrane filter was pressure-fitted to the Pt electrode with a small, Delrin electrode tip machined by Ted Hinke (machine shop, Dept. of Chemistry, OSU). The tip, 2-mm thick, 8-mm long, was drilled to fit the diameter of the Pt electrode (1.2 cm) with a 6-mm diameter opening. This opening (approximately the same diameter as the Pt surface) allows interaction of the membrane-bound indicator with both the sample solution and the Pt

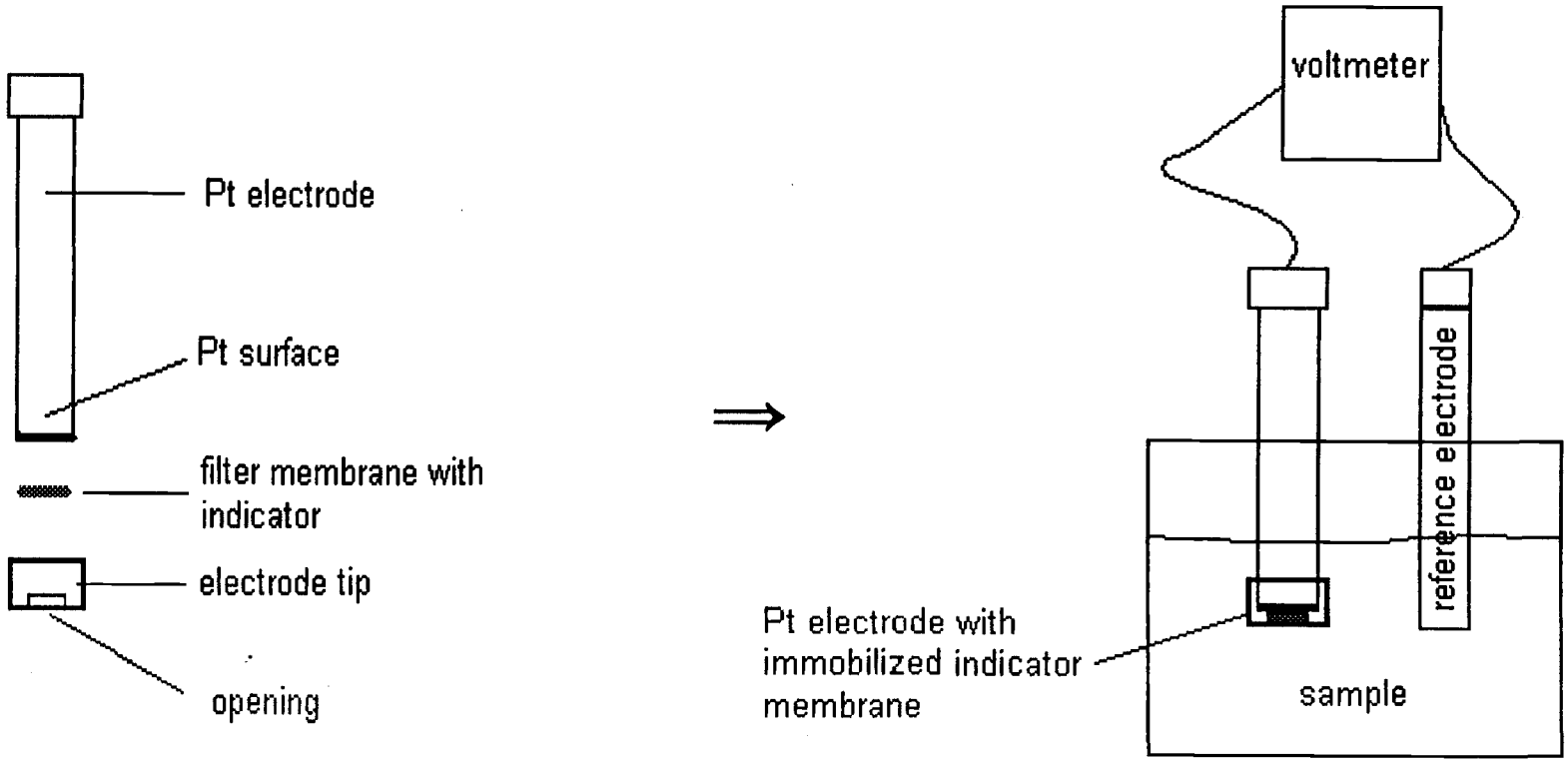

Figure 6.9 Schematic diagram of Pt/indicator electrode for environmental analysis. When placed in a sample, the potential of the Pt/indicator membrane electrode (E_{ind}) can be measured relative to a reference electrode.

surface. For the titration, the Pt/indicator (Thi) electrode was inserted into a reactor solution (pH 7) with the same composition as previously used for titration of immobilized indicator in the flow cell. During the period of sulfide additions to the reactor, the potential of the Pt/indicator electrode ($E_{Pt/ind}$) and of the sulfide electrode (E_{S2-}) were monitored and the total sulfide concentration was determined colorimetrically.

6.2.10 Evaluation of immobilized indicators in wastewater slurries under sulfate-reducing and methanogenic conditions

Wastewater sludge samples were obtained in 1-L plastic bottles from the City of Corvallis Wastewater Reclamation Plant and contained significant numbers of anaerobic, reducing microbes (methanogens and sulfate-reducers). The samples were stored in a refrigerator for subsequent use. Over time, the slurry separated into two phases: an aqueous upper phase with some particulate matter and a thick organic, sludge-like lower phase.

For reactor experiments, approximately 250 mL of the aqueous upper phase was placed in the reactor along with 750 mL of DI water and purged immediately with N_2 to remove O_2. To achieve sulfate-reducing conditions, 4.6 mL (50 mmol) of lactic acid (as the substrate), 1 g each of sodium sulfate, ammonium chloride and calcium chloride (3.7 mmol, 18.7 mmol, and 6.8 mmol, respectively), 2 g (16.6 mmol) of magnesium sulfate, and 0.5 g (3.7 mmol) of potassium phosphate were added. This list of nutrients was adopted from Chapelle (27) for sulfate-reducing conditions. To achieve methanogenic conditions, the nutrient mixture was the same except 6.8 g (50 mmol) of sodium acetate

were added as the substrate rather than lactate and no sulfate containing species were added. To inhibit any sulfate-reduction under methanogenic conditions and to stop the process of sulfate-reduction after a significant amount of sulfide had accumulated under sulfate-reducing conditions, 10.3 g (~50 mmol sodium molybdate) were added to the soil slurry.

In reactor experiments with wastewater slurries, the computerized pH-stat system was used. For sulfate-reducing conditions, a solution that was 1 M each in lactic acid and HCl was used as the acid source and 6 M NaOH (after dilution to 1 M) was added to increase the pH. For methanogenic conditions, a solution that was 1 M each in acetic acid and HCl was used to maintain the slurry at pH 7.

For sulfate-reducing conditions, the potentials of a single Pt/indicator (Thi or CV) membrane electrode and a sulfide electrode were measured over the duration of the experiment. Sulfide levels and the absorbance of agarose film-immobilized indicator (Thi or CV) were monitored as for the titration experiments with sulfide. For methanogenic conditions, two Pt/indicator membrane electrodes were used simultaneously, each with a different indicator (Thi, AA, CV, NB or PSaf immobilized on Whatman filter paper rather than the Sartorious membranes). No sulfide potential measurements were taken. Electrode potentials, indicator absorbance, methane and occasionally Fe(II) and sulfide levels were monitored. For either reactor experiment, only a single agarose-immobilized indicator was used in the flow cell at any one time.

For the second experiment (under methanogenic conditions), ~25 g of solids and 45 mL of water from a methanogenic groundwater/sediment sample, obtained from Semprini (28) of the Department of Environmental Engineering at OSU, were spiked

into the reactor slurry at about 175 hr to enhance production of methane. This sample was originally from Site 24 of Naval Weapons Station, Point Mugu, CA.

6.3 Results and Discussion

6.3.1 Redox indicator immobilization in silicon sol-gels

Si sol-gel preparation Method 1 produced monolithic slabs of 0.5 - 1 mm in thickness with areas of ~1 cm^2 (after substantial cracking). The slabs could be formed reproducibly and doped redox indicator did not leach out significantly, even after several weeks. Formamide, known to help prevent cracking in Si sol-gels (14) did help when added to the Si alkoxide/indicator mixture, allowing preparation of sol-gels monoliths with greater area (~3 x 3 cm^2). However, after reduction of the doped indicator in the presence of formamide in the sol-gel, the indicator could not be re-oxidized. It is believed that the formamide reacted with the reduced indicator, forming a non-colored product.

Indicators doped into the sol-gels without formamide were reduced by a variety of reductants and re-oxidized by O_2. Thi doped into the Si sol-gel was reduced by Fe(II), S(-II), ascorbic acid and Ti(III) citrate. Phenosafranine doped in the structure was reduced by Ti(III) citrate (PSaf, with an $E_7^{0'}$ = -267 mV, requires a much stronger reductant than Thi ($E_7^{0'}$ = +66 mV) (6, 8)); Ti(III) citrate ($E_7^{0'}$ = - 480 mV) is the strongest reductant in the group (29)).

Although this method was adequate for immobilizing redox indicators, many problems were apparent. In general, the length of time for complete reduction of the doped indicator was approximately 1 - 2 hr, regardless of the type of reductant, suggesting a diffusion limited reaction. A slow response is a disadvantage for rapid field

measurements. Also, the reduction of Thi with Fe(II) produced solid Fe(III) hydroxides (8), which caused the sol-gel to crack (particularly after re-oxidation). For these reasons, alternative methods for preparing Si sol-gels were pursued.

Method 2 was used to prepare films (5 - 10 μm thickness) on glass, but these cracked badly. Redox indicators doped into the structure were reduced more rapidly (10 - 20 min), but when placed in water, sol-gel coated on glass slides rapidly peeled off.

Attempts to couple glutaraldehyde to the amine functional groups (Method 3) proved problematic. Sol-gel monoliths placed in glutaraldehyde coupling solution rapidly turned dark brown which would interfere with the spectrophotometric measurements of the indicator. Walt (30) suggested that the brown color was due to polymerization of the glutaraldehyde and this probably could not be avoided.

Because of the problems mentioned with the Si sol-gels, attempts to immobilize redox indicators in this matrix were abandoned. However, interesting results were obtained when Pd powder, along with redox indicator (Thi or PSaf), were incorporated into the sol-gel structure (monoliths prepared with Method 1). Previously, H_2 gas had been shown to reduce redox indicators in de-aerated buffers or DI water when Pd is present (31, 32). When sol-gels doped with redox indicator and Pd powder (~0.6 μm) were placed in vials with DI water or buffer and purged with 100% H_2 gas, the redox indicator was (mostly) rapidly reduced (within ~10 min). With 1% H_2 gas reduction took over 30 min. The indicators could then be re-oxidized with O_2.

Pd catalyst is necessary because H_2 must first dissociate on the Pd catalyst (33) to produce H^- (and H^+), or $H\cdot$ radicals, which can reduce the indicator. For this

mechanism, the indicator must contact the H^- or $H\cdot$ radical at the Pd surface. Interestingly, the majority of the indicator (based on nearly complete de-colorization of the sol-gel to the eye) was reduced in the sol-gel. Since the Pd catalyst was dispersed only intermittently throughout the sol-gel, redox indicator must have been able to diffuse through the sol-gel to the Pd surface. It may be that the Pd powder increases the pore size of the sol-gel significantly, allowing the doped indicator to move throughout the interior (or at least in the vicinity of a Pd powder pellet). However, electrostatic interactions in the gel or smaller pore size at the edges kept the indicator from leaching out. The Pd powder greatly lessened the cracking of the sol-gels, allowing formation of significantly larger (~3 x 3 cm^2) monoliths than without the Pd.

6.3.2 Redox indicator immobilization in polyacrylamide gels

Attempts to entrap redox indicators into polyacrylamide gels failed because the "doped" indicators rapidly leached out when the gels were placed in DI water. Increasing the bisacrylamide/acrylamide monomer ratio (from 1:19 to as high as 1:5) did not significantly reduce leaching and the gels formed under these conditions were nearly opaque.

Results from attempts to achieve covalent bonding of redox indicators to polyacrylamide gels were inconsistent and unsatisfactory. In many experiments, all the indicator rapidly leached out of the gels when placed in DI water. To determine if the acrylamido functional group of N-(3- aminopropyl) methacrylamide hydrochloride (APMA) was or was not polymerizing with the acrylamide, the gels (from which the

indicator had leached out), were soaked in ~1 mM Coomasie® brilliant blue (CBB) (which rapidly binds to materials containing amine functional groups (34)) solution. Polyacrylamide gels which had been formed without the APMA/crosslinker/indicator mixture (and to which no APMA was added) rapidly leached the CBB, but those formed with the mixture (which contained APMA) retained the blue compound. This result suggests that APMA did polymerize with the acrylamide and that failure of the immobilization procedure most likely occurred at some point in the crosslinking scheme.

Some aspects of the chemistry of both crosslinkers may have affected the success of the reaction. Protonation of the imido ester functional group in DMP (Figure 6.4) withdraws electron density from the carbon atom, making it more electrophilic and reactive to amines. If the N atom is deprotonated, the carbon is less electrophilic and less reactive to amines (35). Therefore, DMP reactivity is sensitive to pH conditions and coupling above pH 10 is not recommended (this also increases the rate of hydrolysis of the imidoester) (20). For DSS (Figure 6.5), the reactivity of the carbon atom attached to the NHS ester leaving group is less affected by pH (35). However, for both crosslinkers, hydrolysis is a competing reaction (18, 35) and water molecules can attack the reactive carbon atom of the crosslinkers, forming a methyl ester in the case of unreacted DMP (36) or a carboxylic acid in the case of unreacted DSS. Furthermore, the imidoamine formed by reaction of the amine group of the redox indicator or APMA with the imidoester of DMP can further be hydrolyzed, in some cases removing the bonded redox indicator or APMA (i.e., they act as leaving groups in the hydrolysis reaction) (35). Because of the multiple step nature of the coupling scheme, an unsuccessful overall reaction could be due to the failure of any one of many steps in the

crosslinking scheme (bonding between APMA/crosslinker/indicator and the APMA to acrylamide/Bis must occur). Finally, the final products of the crosslinking schemes are rather hydrophobic and tended to leach from the polyacrylamide as the gel was forming.

Not all attempts to immobilize redox indicators in polyacrylamide gels failed. Gels containing Thi or CV (immobilized covalently or, possibly, by electrostatic interaction) were tested for leaching by placing sections approximately 3 mm x 3 mm in the removable-window flow cell and reactor solution (~50 mM KCl in DI water) was pumped through the cell (~20 mL/min). Figure 6.10 shows how the absorbance of the gel varies over time. Interestingly, Thi was retained in polyacrylamide gels when DSS but not DMP was used as the crosslinker, while the opposite behavior was observed with CV (retained in polyacrylamide gels in which DMP was used as the crosslinker). For CV/DMP-immobilized gels, the absorption maximum shifted to the blue (~525 nm compared to 582 nm for the free indicator and ~570 nm for the agarose-bead immobilized CV (37)). For Thi/DSS (~610 nm), the absorbance was generally greater than that for CV/DMP and the wavelength shift less dramatic (600 nm in the free form and ~620 nm immobilized to agarose beads) than for CV.

Thi immobilized in the polyacrylamide could be reduced easily and rapidly with both Fe(II) and HS^-. However, CV immobilized in the gel was difficult to reduce with HS^-, and only high levels of sulfide ($[S(-II)_{(tot)}] > 1$ mM) partially reduced the indicator (as apparent to the eye). Previously, in experiments with CV immobilized on agarose beads, $S(-II)_{(tot)}$ levels of 1 - 10 μM reduced CV (12). This change in redox behavior for CV may be due to formation of an imido (or, if hydrolysis of the imido product occurs, an amide) bond linkage during immobilization rather than the secondary amine

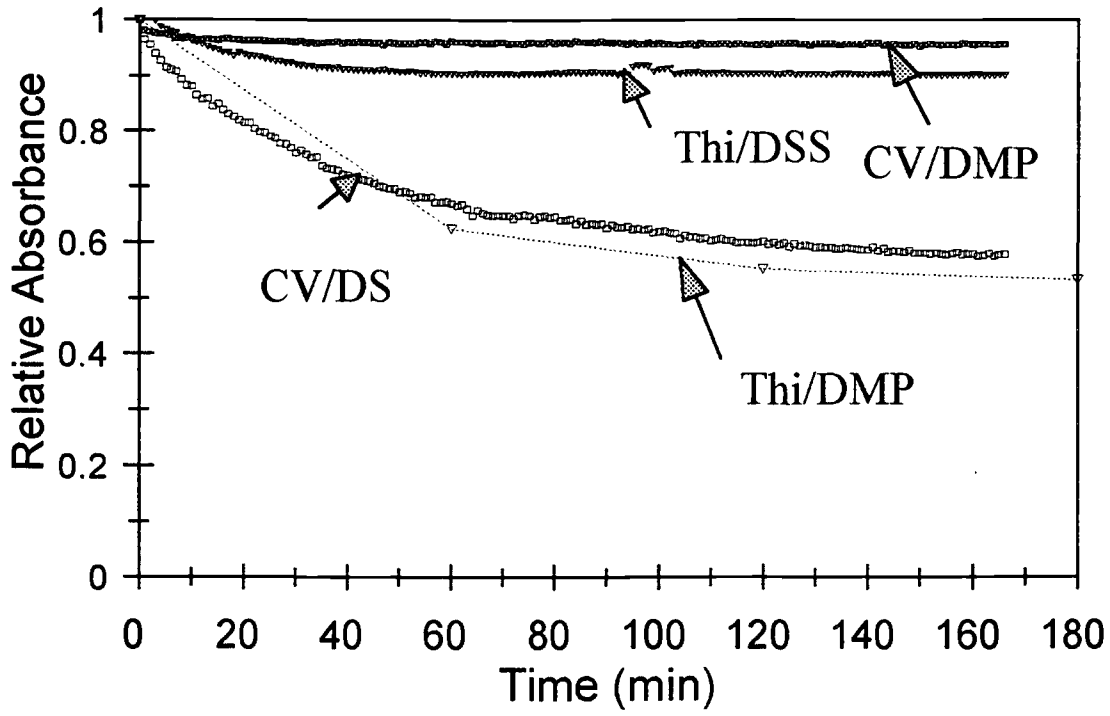

Figure 6.10 Time dependence of leaching of Thi and CV from polyacrylamide gels. The relative absorbance is the ratio of the measured absorbance at the band maximum above the baseline to the initial absorbance (0.6 - 0.8 A.U. for Thi/DSS and Thi/DMP, 0.2 - 0.3 A. U. for CV/DMP and CV/DSS).

formed when reacted with an aldehyde (6). Furthermore, this imido (or amide) linkage may contribute to the large wavelength shift.

The slight change in the redox properties or the absorption maximum of Thi immobilized in polyacrylamide suggests that immobilization may have been partially or completely electrostatic rather than covalent. It is possible that a carboxylic acid group on immobilized DSS (formed after hydrolysis) could interact electrostatically with the positively-charged Thi molecule. Moreover, failure of the Thi/DMP immobilization scheme (if successful immobilization with DSS was due to electrostatic interactions) may have been due to electrostatic repulsion from a positively-charged, protonated imide, or, due to lack of any electrostatic interaction after methyl ester formation by hydrolysis of immobilized DMP. Although there was some (small) success in immobilization of redox indicators in polyacrylamide gels, concerns about the redox properties of immobilized CV, lack of convincing evidence that Thi was covalently immobilized, the expense of reagents, and poor yields and poor reproducibility of the immobilization procedure were convincing evidence that an alternative immobilization procedure should be pursued.

6.3.3 Redox indicator immobilization in agarose gels and filters

Immobilization of redox indicators in agarose films proved successful and films with a thickness of 0.3 - 0.5 mm could be prepared in which the redox indicators could be rapidly reduced and re-oxidized. From leaching experiments with Thi or CV immobilized in agarose films (Figure 6.11), the immobilization was effective.

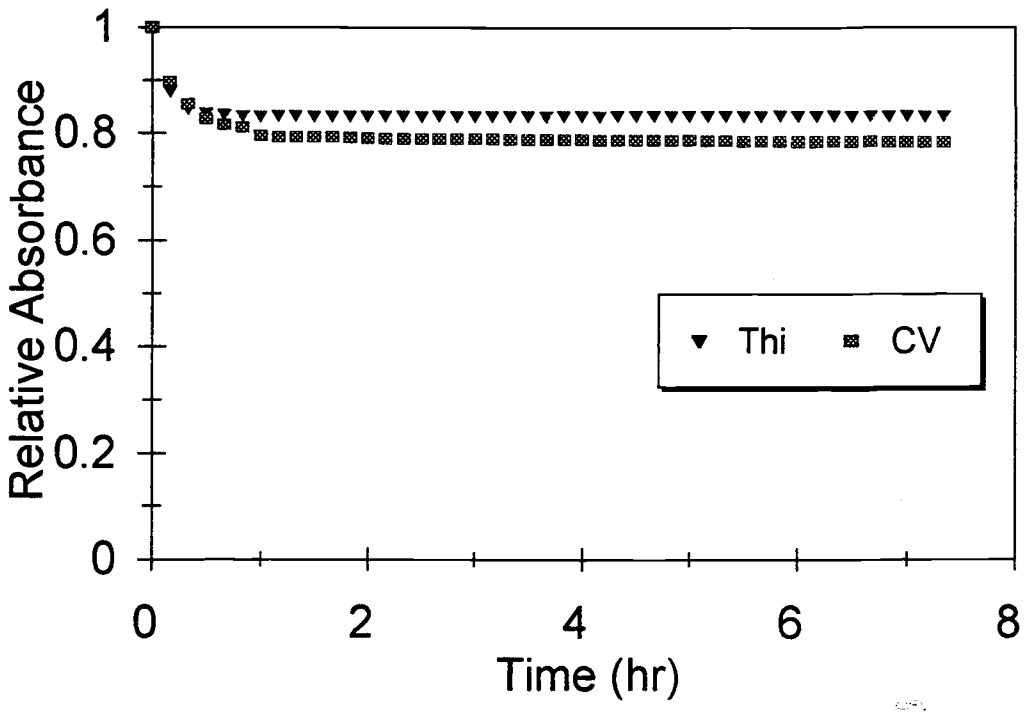

Figure 6.11 Examples of leaching of Thi and CV from agarose films.

The redox indicators Thi, AA, CV, NB and PSaf were covalently bonded to groups in agarose gel. The reaction conditions varied as summarized in Table 6.1, along with the wavelength of maximum absorption (λ_m). A pre-soaking step with indicator solution (for 1 - 2 days) at relatively low pH (2.5 - 3.5) was necessary for successful immobilization (adequate absorbance) of redox indicators in agarose films, but was unnecessary with agarose affinity beads. Soaking may be important for the films because diffusion times required to saturate the films are longer (0.5-mm thickness compared to 50-μm bead diameter) or the effective concentration of aldehyde groups in the films may be less than in the beads. Also for films, ethanol (10 - 30% of soaking solution) enhanced the solubility of indicators in the films and was particularly important for successful immobilization of more hydrophobic indicators, CV and NB.

The initial attempt to immobilize Thi in the Sartorious filter membrane was successful. In fact, the same indicator/coupling solution used to immobilize Thi to agarose films (A of ~0.6 for a thickness of ~0.5 mm) produced a very dark blue membrane (A > 3 with the HP8452 diode array spectrophotometer relative to a filter blank). This behavior suggests that the concentration of aldehyde groups in the Sartorious filter is significantly higher than that in the agarose films. Very little leaching was observed, even in solutions of 1:1 DI H_2O/ethanol. The redox indicators AA, CV, and PSaf were also immobilized to the Sartorious membranes.

For the Whatman filter paper, the same coupling procedure proved successful for Thi, AA, CV, NB and PSaf (after forming aldehyde groups on the cellulose with periodate). The reaction conditions for immobilization (identical to Sartorious

Table 6.1 Optimal reaction conditions and absorbance maxima for redox indicators immobilized to agarose films.

redox indicator	pH of indicator /buffer[e]	[indicator] (mM)	reducing agent	λ_m (nm) immobilized to agarose films	λ_m (nm) free indicator[a]	λ_m (nm) immobilized to agarose beads
Thi	3.3/3.8	~0.5	$NaCNBH_3$	624	598	640[b]
AA	3.2/3.2	~1	S(-II)	642	633	658[c]
CV	2.5/2.5	~3	S(-II)	554	582[c]	568[c]
NB	3/3	~5	S(-II)	650	634	ND[d]
PSaf	3.3/3.8	~0.5	$NaCNBH_3$	516	520	544[b]

[a] From Green (37)
[b] From Lemmon (6).
[c] From Jones (9).
[d] ND = not determined in this work.
[e] pH of soaking solution/pH of coupling solution.

Table 6.2 Optimal reaction conditions and absorbance maxima for redox indicators immobilized to Sartorious membranes and Whatman filter paper.

redox indicator	pH of indicator/ buffer	[indicator] (mM)	reducing agent	λ_m (nm)
Thi	4.2	~0.2	$NaCNBH_3$	630
AA	3.5	~0.2	S(-II)	641
CV	3.3	~1.0	S(-II)	573
NB	3	~3.0	S(-II)	652
PSaf	4	~0.2	$NaCNBH_3$	543

membranes) are summarized in Table 6.2. To promote better homogeneity of the indicator on the filter, ethanol was added to the indicator buffer solution (to a final volume of 30-50% ethanol). This step was particularly important for the more hydrophobic indicators (AA, CV and NB). In general, immobilization of indicators to filter paper proved simpler and more reproducible than that to agarose. Absorption maxima for a given indicator differ by typically 10 to 20 nm with the immobilization medium. Precise determination of the maximum is difficult because the absorption band is broad and on a sloping baseline.

6.3.4 Determination of formal potentials of immobilized redox indicators

Formal potentials determined for redox indicators immobilized to agarose films and cellulose filters are listed in Table 6.3. In most cases, the formal potentials with agarose films or agarose affinity beads are within 6 mV. However, for PSaf, the formal potential is 19 mV less negative when immobilized on the agarose film relative to agarose beads. For AA, CV and PSaf, the formal potential for the agarose film-immobilized indicator is nearly identical to that of the corresponding free indicator. The formal potential for CV or PSaf immobilized on the cellulose filter paper is significantly more negative (over 10 mV) than the formal potential determined for the same indicator immobilized on the agarose film. Some uncertainty in values of formal potentials determined is expected due to variability in pH of the reactor solution or non-equilibrium.

Table 6.3 Formal potentials of free and immobilized indicators at pH 7 determined by titration with Ti(III).

redox indicator	$E_7^{0'}$ (mV) (free)	$E_7^{0'}$(mV) (immobilized on agarose beads)	$E_7^{0'}$(mV) (immobilized on agarose film)	$E_7^{0'}$(mV) (immobilized on cellulose filters)
Thi	+66[a]	+52[a]	+55	+53
AA	+18[b]	+13[b]	+19	+9
CV	-75[b]	-81[b]	-75	-98
NB	-119[a]	ND[c]	-131	-137
PSaf	-267[a]	-286[a]	-267	-286

[a] From Lemmon (6, 7).
[b] Determined previously (Appendix I).
[c] ND = not determined in this work.

6.3.5 Titrations of immobilized redox indicators with Fe(II) and sulfide.

Results from titrations of Thi and CV immobilized on agarose with Fe(II) and sulfide (at pH 7) are shown in Figure 6.12A and 6.12B, respectively. For each indicator data are shown for the film form (this work) and the bead form (8, 12). The curves represent the calculated value of the fraction of indicator oxidized (f_{ox}) based on an equilibrium between the indicator and titrant (reductant) couples. For this model, the potential of the indicator half-reaction (right side of equation 6-3) is set equal to the potential of the reductant half-reaction (Nernst equation) and solved for f_{ox}.

The Fe(II)/indicator reaction is hypothesized to be (8)

$$Ind_{(ox)} + 2\ Fe(II) + 6H_2O \rightleftharpoons Ind_{(red)} + 2\ Fe(OH)_3 + 4H^+ \qquad (6\text{-}4)$$

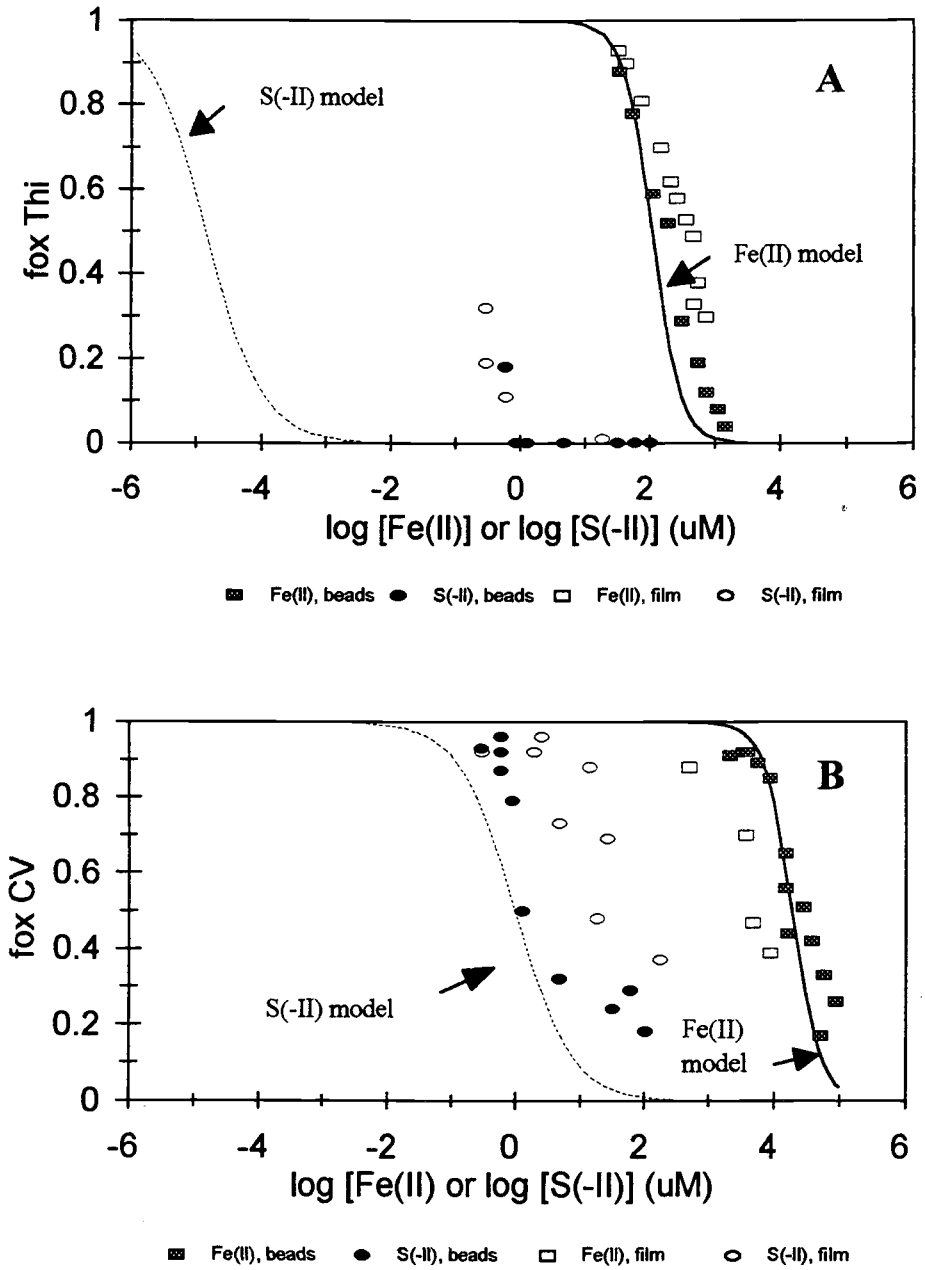

Figure 6.12 Titrations of immobilized Thi and CV with Fe(II) and sulfide at pH 7. In A (Thi) and B (CV), data are shown for both agarose film and bead supports. The curves represent calculated values of fraction oxidized based on an equilibrium between the indicator and reductant couples.

with a Fe(III)-solid phase of ferrihydrite ($E_7^{0\prime}$ = -0.182 mV (38)). The $Fe(OH)_3$/Fe(II) potential is given by

$$E_{Fe(OH)_3/Fe(II)} = E_m^{0'} - \frac{RT}{nF} \ln [Fe(II)] \tag{6-5}$$

For this reaction, the calculated curves in Figure 6.12 are based on the equation 6-6 (see Appendix F for derivation)

$$f_{ox} = \frac{1}{(10^{\left[\frac{2}{0.059}(E_7^{0'} + 0.182\ V) + \log [Fe(II)]^2\right]} + 1)} \tag{6-6}$$

where $E_7^{0\prime}$ is the formal potential of the immobilized redox indicator at pH 7 and [Fe(II)] is the measured Fe(II) concentration.

The S(-II)/indicator reaction is hypothesized to be (12)

$$Ind_{ox} + S^{2-}(aq) \rightleftharpoons Ind_{red} + S^0(s, rhmb) \tag{6-7}$$

The calculated curves for S(-II)/indicator equilibrium are based on (12)

$$f_{ox} = \frac{1}{(10^{\left[\frac{2}{0.059}(E_7^{0'} - E_{S/S2-})\right]} + 1)} \tag{6-8}$$

where $E_{S/S2-}$, the potential of the $S^{2-}(aq)/S^0(s, rhmb)$ couple, is calculated from (see Appendix H for derivation):

$$E_{S/S^{2-}} = -0.475 - 0.0295 \log \left[\frac{[S(-II)_{(tot)}]}{1 + \frac{[H^+]}{10^{-14}} + \frac{[H^+]^2}{(10^{-7.1})(10^{-14})}} \right] \tag{6-9}$$

where $[S(-II)_{(tot)}]$ is the equilibrium total sulfide concentration.

For titrations of Thi (Fig. 6-12A), data for film-immobilized Thi are quite comparable to that for bead-immobilized Thi. With Fe(II) as the titrant, the data lie

somewhat to the right of the equilibrium line (i.e., more Fe(II) is required to titrate the indicator than predicted by the model). This behavior may be due slow kinetics (i.e., measurements were made before equilibrium had been reached) or the formal potential used in the model for the Fe(III) hydroxide may be inappropriate. There is a wide disparity between experimental and calculated values with sulfide as the titrant. A primary difficulty is that the theoretical levels of total sulfide necessary to reduce Thi are considerably less than 1 μM which is below the practical detection limit for sulfide with conventional methods (12).

With titrations of immobilized CV (Figure 6.12B), there are greater differences between data obtained for films compared to beads and between experimental results and predictions from an equilibrium model. For a CV-film, *less* Fe(II) was required to reduce a given fraction of indicator than predicted by the equilibrium model (by about a factor of 2.5 for $f_{ox} = 0.5$). One possibility is that the pH value is not correct. An increase of 0.2 pH units from pH 7 decreases the level of Fe(II) necessary (based on equation 6-7 with ferrihydrite as the solid phase) to achieve half-reduction ($f_{ox} = 0.5$) of CV from ~18 to ~6 mM. Another possibility is that the effective concentration of CV immobilized in the film is lower. In previous studies (8), it was found that the steady-state Fe(II) level necessary to achieve a given f_{ox} increased with the concentration of the immobilized indicator. This behavior is not predicted by the simple model. From the observed absorbances and film thicknesses, it appears the effective concentration of the more hydrophobic indicators was less in the agarose films than in the beads. For the beads, the absorbance of immobilized CV with the 1-mm pathlength cell was about 0.6 (32). For the CV-immobilized film, the absorbance was generally 0.3 - 0.4 for a film

thickness of 0.8 - 1 mm (two films were generally used for CV titrations due to the relatively low absorbance of the CV in the single films). Therefore, the effective concentration of CV in the immobilized films was about half that in the beads.

For the sulfide titration of CV, there is considerable scatter in the data. A higher level of $[S(-II)_{(tot)}]$ was required to reduce CV in the film form than in the bead form or than that predicted by the equilibrium model. Much of this behavior is attributed to the experimental difficulties of measuring low levels of sulfide for which even a small O_2 leak into the reactor provides enough O_2 to oxidize some of the sulfide or partially oxidize the indicator. Possibly a higher sulfide concentration is required to offset these effects. With Fe(II) as the titrant, the Fe(II) levels necessary are much greater ([Fe(II)] >> 0.1 mM, total Fe(II) >> 0.1 mmol)) so enough Fe(II) is present to act as a reductant for O_2. The level of sulfide in the reactor solution is much lower (($[S(-II)_{(tot)}]$ ~ 1 - 100 μM or 1 - 100 μmol total sulfide).

The response of the Pt/indicator (Thi) electrode to additions of sulfide is shown in Figure 6.13. After each sulfide addition, the potential ($E_{Pt/Thi}$) decreased to a new, lower value that was relatively constant (Fig. 6.13A). When enough sulfide was added to completely reduce the Thi immobilized to the membrane (~27.5 hr), the potential rapidly fell, the electrode was no longer poised, and the measured total sulfide increased above 10 μM. The formal potential for immobilized Thi (on cellulose) is 53 mV so that poising is expected to occur from about 90 to 15 mV.

In Figure 6.13B, the potentials of the Pt/indicator electrode and sulfide electrode (E_{S2-}) are compared and they track each other fairly well. After each sulfide addition, both potentials dropped rapidly, but only E_{S2-} increased (at about a constant rate)

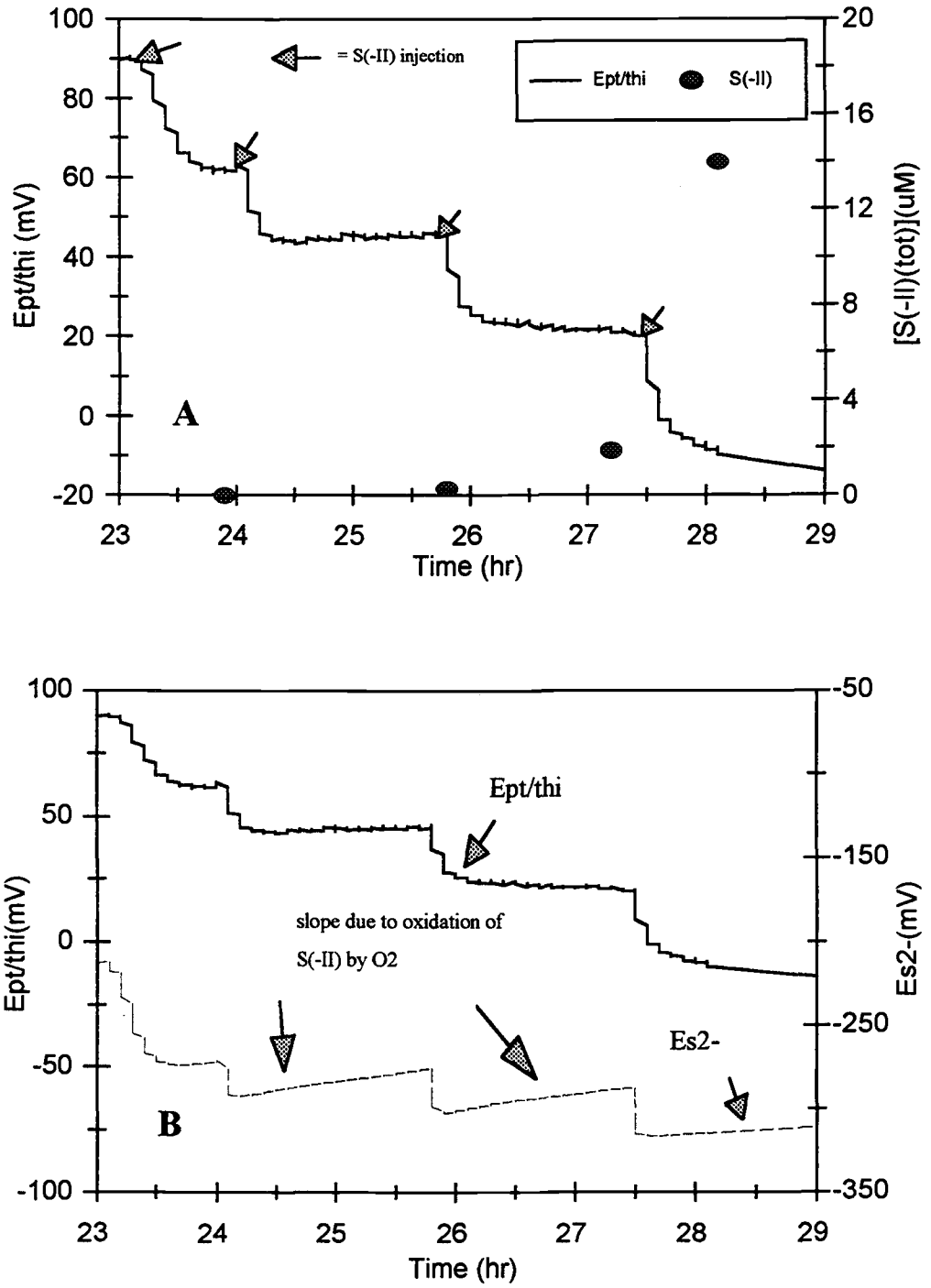

Figure 6.13 Effect of addition of sulfide at pH 7 on the potential ($E_{Pt/Thi}$) of a Pt electrode in contact with Thi immobilized on a Sartorious membrane. The potential is plotted with measured levels of total sulfide (A) and with the potential of a sulfide electrode (E_{S2-}) (B).

following the addition. This increase is attributed to the O_2 leak discussed previously. It is hypothesized that 1) all the O_2 reacted with the sulfide in solution before it could re-oxidize the immobilized Thi, or 2) the Thi immobilized to the membrane at the Pt surface is relatively protected from changes in the bulk solution. The sulfide electrode responds directly to the solution concentration of sulfide. For the Pt/indicator electrode to respond, the O_2 must diffuse completely through the membrane to oxidize the immobilized Thi in contact with the Pt. Over a few hours, little O_2 might have diffused through the entire membrane because most of it was reduced by sulfide or by reduced Thi immobilized throughout the membrane. If the time between additions had been longer (4 hr or more), re-oxidation of the Thi may have occurred. Note that Thi on the membrane was not completely reduced until the measured level of sulfide was much higher than that observed with Thi immobilized to agarose beads or films ($[S(-II)_{(tot)}] < 1$ μM, (12)). The diffusion effects combined with the high concentration of Thi on the membrane used in this experiment ($A > 3$) may have contributed to the differences noted.

6.3.6 Response of indicators in wastewater slurries under sulfate-reducing

In Figure 6.14, the time dependence of the response of indicators immobilized on agarose films, Pt/indicator electrodes, and a sulfide electrode in contact with an anaerobic wastewater slurry is shown. Attempts to measure sulfide levels with CHEMetrics® vials (employing the methylene blue method) failed because of the high levels of particulate matter in the samples acquired from the external loop of the reactor.

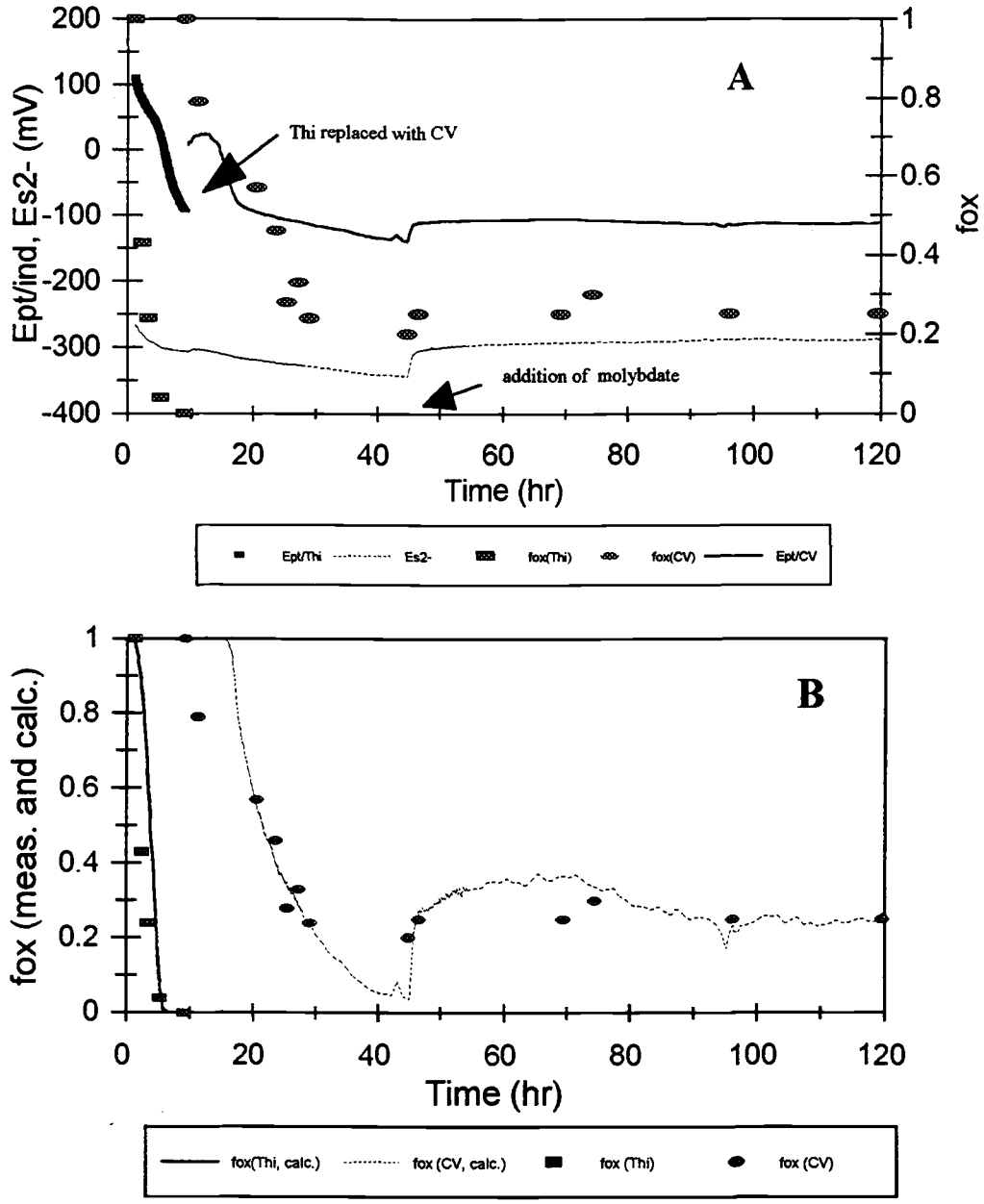

Figure 6.14 Time dependence of reduction of redox indicators in reactor under sulfate-reducing conditions at pH 7. In A, f_{ox} values with agarose films and Pt/indicator electrode potentials ($E_{Pt/ind}$) for immobilized Thi and CV are plotted along with E_{S2-}. In B, the f_{ox} values of the agarose films and the calculated f_{ox} values (based on $E_{Pt/ind}$ data and eq. 6-3) over time are compared. At about 45 hr, 50 mmol of sodium molybdate were added to inhibit sulfate reduction. Notably, both E_{S2-} and $E_{Pt/CV}$ increase abruptly (but concurrently) to new, steady-state levels. Comparatively, there is little change in f_{ox}(CV). Based on previous experiments (12), E_{S2-} values between about -280 and -340 mV indicate sulfide levels between about 1 and 100 μM.

The use of a larger pore filter (40-μm filter) with the film format allowed high flow rates but proved a limitation for quantitative sulfide measurements. Sulfate-reducing conditions were clearly reached from the smell of $H_2S(g)$ detected during the experiment.

The reduction of Thi immobilized in the film form or on the filter began immediately after being placed in contact with the anaerobic wastewater slurry. This is clear in Fig. 6.14A from the decrease in f_{ox}(Thi) for the agarose-immobilized indicator (placed in the spectrophotometric flow cell in the external loop of the reactor at ~0 hr) or in the potential of the Pt electrode in contact with the membrane-immobilized indicator. Within less than 10 hr, the Thi in the agarose was completely reduced ($f_{ox} \approx 0$), and the the potential of the Pt/Thi electrode fell nearly 150 mV below the formal potential of Thi (+55 mV at pH 7). The final potential is well below the "redox range" expected for electrode poising (see Table 6.4).

Table 6.4 Calculated redox potentials of cellulose-immobilized indicators at pH 7 as a function of f_{ox}.[a]

Indicator	potential (mV) for $f_{ox} = 0.95$	potential (mV) for $f_{ox} = 0.75$	potential (mV) for $f_{ox} = 0.50$	potential (mV) for $f_{ox} = 0.25$	potential (mV) for $f_{ox} = 0.05$	potential range (mV)
Thi	+91	+67	+53	+39	+15	+90 ⇔ +15
AA	+47	+23	+9	-5	-29	+50 ⇔ -30
CV	-60	-84	-98	-112	-136	-60 ⇔ -135
NB	-99	-123	-137	-151	-175	-100 ⇔ -175
PSaf	-248	-272	-286	-300	-324	-250 ⇔ -325

[a] calculated redox potential based on eq. 6-3 and an assumed value of f_{ox}.
[b] potential range over which poising of the Pt/indicator electrode is expected based on f_{ox} values between 0.95 and 0.05 (ratio of oxidized to reduced Thi ($f_{ox}/(1 - f_{ox})$ from 19 to 0.053).

When the Thi membrane was removed from the electrode surface (at ~10 hr and replaced with a CV membrane) and inspected, the circular region in contact with the Pt (and the reactor solution) was completely white (i.e., all the immobilized Thi was reduced in this region). The outer annular region of the membrane (the region physically blocked and not in contact with the reactor solution) was still blue (i.e., Thi remained oxidized in this region). This observation supports the hypothesis that the Pt/Thi electrode responded to the Thi couple rather than another redox couple(s) in the solution (i.e., the Pt/Thi electrode was not simply responding to species in the solution as a normal Pt electrode).

After Thi was replaced with CV (in both the potentiometric and spectrophotometric configurations), the potential of the modified Pt/indicator electrode increased at first but soon decreased over time. The reduction of CV immobilized in agarose began soon after it was placed in the flow cell and f_{ox} stabilized at ~0.25 after ~30 hr. The total sulfide concentration at this point (estimated from E_{S2-}) was ~50 μM.

The response of the Pt/indicators and the film-immobilized indicators are compared in more detail and in *terms of f_{ox} values* in Figure 6.14B. Clearly, the f_{ox} values for the agarose films and the f_{ox} (calc) values calculated based on $E_{Pt/ind}$ values track each other well and are comparable through the duration of the experiment.

A similar comparison is shown in Figure 6.15 but in *terms of the redox potential*. After the addition of molybdate at 45 hr (to inhibit the production of more sulfide), $E_{Pt/CV}$ stabilized at a value around -110 mV (between -105 and -112 mV); whereas calculated values ranged 15 - 20 mV greater. Overall there is reasonable agreement between the

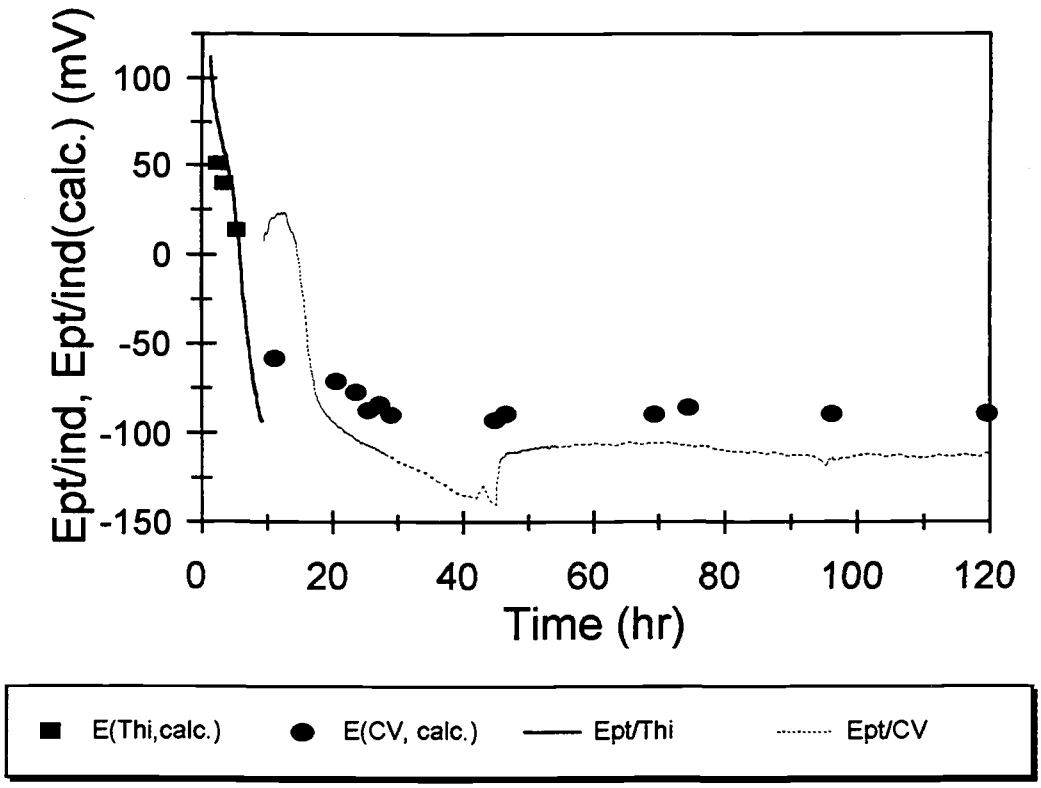

Figure 6.15 Measured potentials ($E_{Pt/ind}$) under sulfate-reducing conditions compared to calculated potentials (E(ind,calc.)). The calculated potentials are based on eq. 6-3 and measured values of f_{ox} for agarose films. For CV immobilized in agarose, $E_7^{0\prime} = -75$ mV, from Table 6.3

two measurement schemes. The indicator electrode responds more slowly and previous data (Table 6.3) do indicate that the formal potential of an indicator can vary with the type of immobilization.

6.3.7 Response of indicators in wastewater slurries under methanogenic conditions

The indicators Thi, AA, CV, NB and PSaf (in the agarose film and Pt/indicator electrode configurations) were all tested in the slurry under methanogenic conditions and the results are shown in Figure 6.16. For the Pt/indicator electrodes, when one immobilized indicator was reduced (after its potential decreased ~30 mV below its formal potential), the membrane was replaced with the next indicator with a lower formal potential.

In Figure 6.16A, measured f_{ox} values are compared with f_{ox} values calculated with the Pt/indicator potentials (eq.6-3). Thi, the first indicator tested and the indicator with the highest formal potential ($E_7^{0\prime}$ = +55 mV), was rapidly reduced within 20 hr when placed in contact with the slurry. Furthermore, AA ($E_7^{0\prime}$ = +19 mV) and CV ($E_7^{0\prime}$ = -75 mV) were also reduced (in succession) within about 20 hr after being placed in contact with the wastewater slurry. The reduction of NB ($E_7^{0\prime}$ = -131 mV) occurred over a longer time period. NB was only half-reduced after ~30 hr (at which point, it was removed from the flow cell and replaced with PSaf).

It is clear in Figure 6.16A that the reduction of a given indicator associated with the Pt electrode lagged behind that of the same indicator immobilized in the agarose. After about 4 hr, f_{ox} was ~0.4 for Thi immobilized in the agarose, but was calculated to

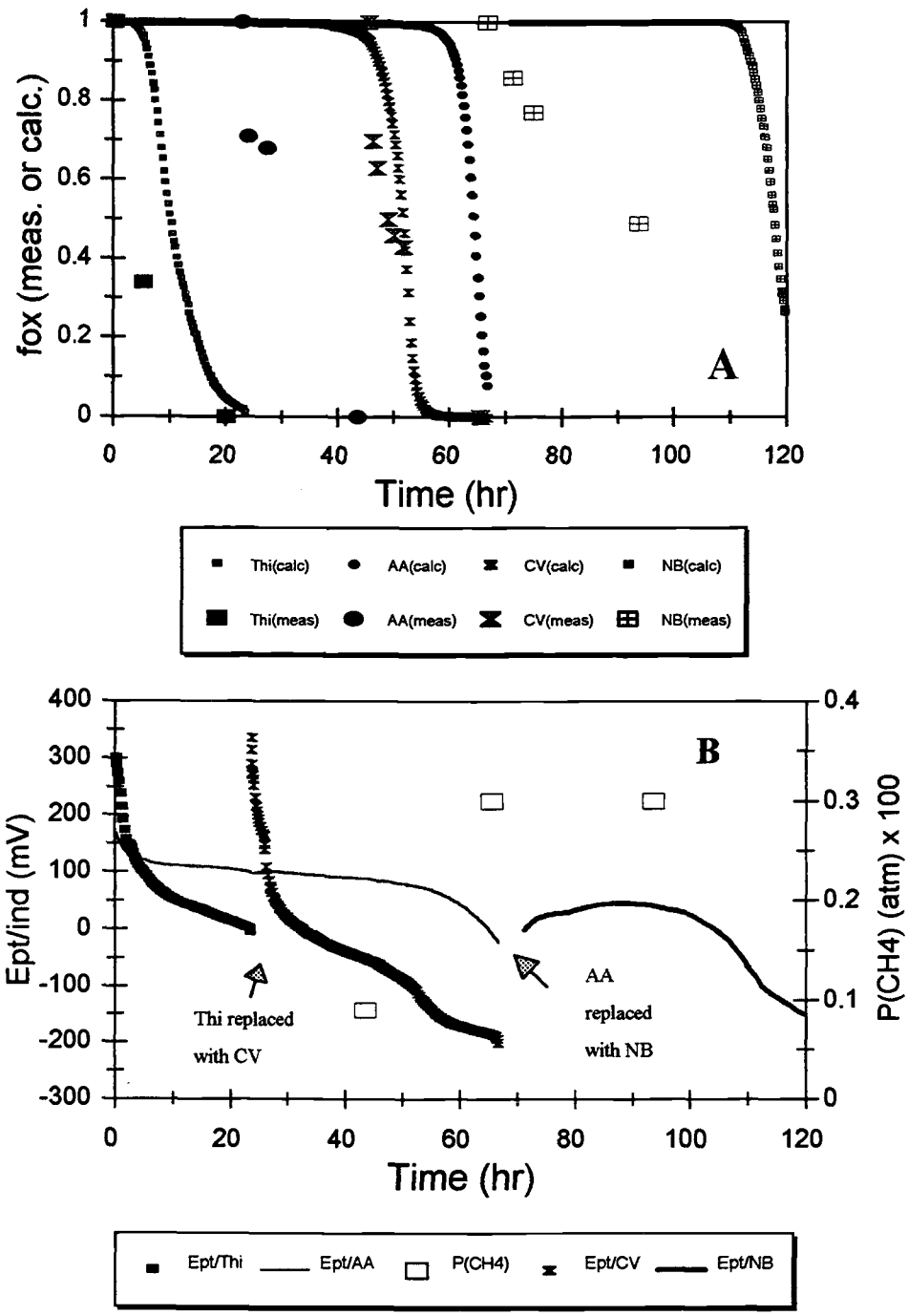

Figure 6.16 Redox behavior of immobilized Thi, AA, CV and NB in contact with a methanogenic wastewater slurry maintained at pH 7 in the reactor. In A, f_{ox} data for indicators immobilized on agarose film (spectrophotometrically determined and on cellulose paper (calculated from potentials) are shown. In B, the measured potentials of the Pt/indicator electrodes along with measured headspace methane levels are shown.

be near 1 from the electrode data ($E_{Pt/Thi}$ above the range for which poising is expected (Table 6-4)). Within 20 hr, $E_{Pt/Thi}$ had fallen below 0 mV (Fig. 6.16B), indicating complete reduction in agreement with the spectrophotometric measurement.

The Pt/CV electrode was placed in contact with slurry about 20 hr before the agarose-immobilized CV (~25 hr and ~45 hr, respectively). Although the potential of the Pt/CV electrode decreased rapidly, it did not assume a potential indicative of the CV couple until ~45 hr (Table 6.4). After 45 hr, the measured and calculated values of f_{ox} are fairly similar, although the calculated value is higher due the slower response of the Pt/CV electrode. Half-reduction ($f_{ox} = 0.5$) of the agarose-immobilized CV occurred when $E_{Pt/CV} \approx -90$ mV (at ~50 hr).

For AA and NB, the indicators immobilized in the agarose films responded much more quickly (were reduced sooner) than the indicators immobilized on the filter paper. For agarose-immobilized AA, complete reduction occurred by ~43 hr, but for the Pt/AA electrode, poising was lost ($E_{Pt/AA} < -15$ mV) only at about 68 hr. Similarly, agarose-immobilized NB was half-reduced ($f_{ox} \approx 0.5$) at 94 hr, but $E_{Pt/NB}$ was about +40 mV (far above its formal potential of -137 mV) at this time. The Pt/NB electrode appeared poised even after about 120 hr (when $E_{Pt/NB} < -140$ mV) .

The differences in response times for the two configurations could be due to several factors and similar behavior was previously noted for the sulfide reduction of Thi immobilized to a Sartorious membrane (Figure 6.14). The indicator immobilized in the filter paper may be more difficult to reduce because its effective concentration is greater than that in the agarose (for AA, $A > 4$ at λ_m). This effect was noted previously for

indicators immobilized to agarose beads (8). Furthermore, it may take longer to reduce the greater concentration of indicator with a given concentration of reductant.

Another important factor influencing the time of response is the nature of the detection method. For spectrophotometric measurements of the indicators immobilized in agarose, changes in absorbance due to reduction at any depth in the film (at the edges and throughout the structure) are monitored; whereas, the Pt/indicator electrode only responds to reduction of indicator at the Pt surface, which is somewhat protected.

Finally, the diffusion coefficients of reductants may be less in cellulose and affected by the hydrophobicity of the immobilized indicators. Overall, agarose appears to be an excellent immobilization support because diffusion is rapid (diffusion coefficients for species in agarose are about half those measured in electrolyte solutions (39)). Nile blue and AA (to a lesser extent) are the most hydrophobic indicators. This hydrophobic nature, enhanced by the higher effective concentration in the filter (visually less colored than AA with $A \approx 2.5$) may have contributed to the especially slow response of the Pt/NB and Pt/AA electrode.

Results for PSaf immobilized in agarose and in contact with the same methanogenic slurry are shown in Figure 6.17A. Placed in the spectrophotometer flow cell in the external loop of the reactor at 100 hr, PSaf was ~70% reduced by about 225 hr as methane levels rose to about 0.012 atm (1.2% of the reactor headspace as methane), after having been purged with N_2 at ~150 hr. In contrast to results with Thi and CV, there is not good agreement between the measured and calculated f_{ox} values for PSaf. The measured value of f_{ox} for the agarose film was much lower than the value calculated from the potential of the indicator electrode.

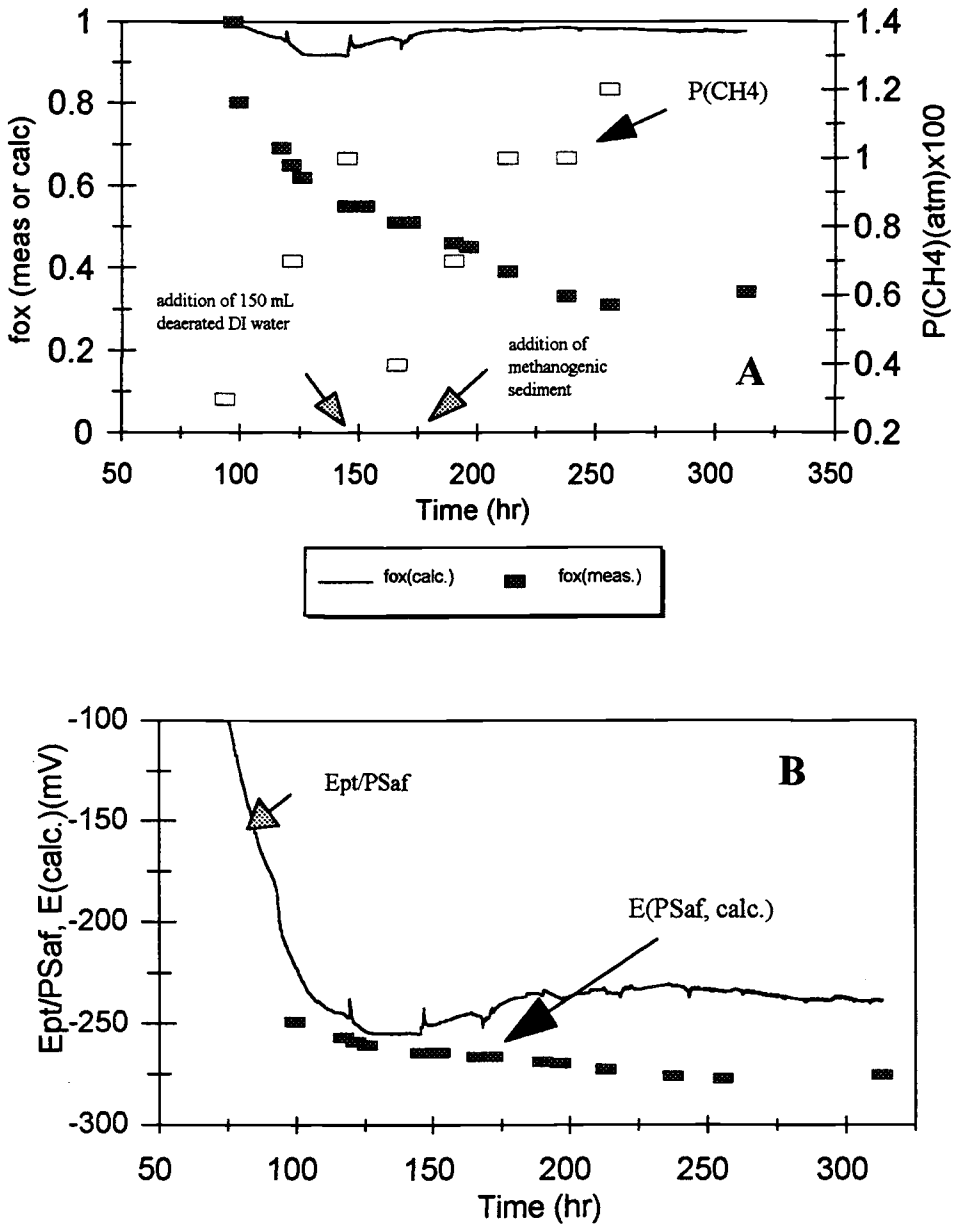

Figure 6.17 Spectrophotometric and potentiometric behavior of phenosafranine with a methanogenic slurry in the reactor at pH 7 (same slurry as discussed in Figure 6.16). In A, f_{ox} values for agarose film-immobilized PSaf, the calculated f_{ox} values based on the Pt/PSaf electrode potentials and eq. 6-3, and the partial pressure of methane in the reactor headspace are plotted. In B, the potentials of the Pt/PSaf electrode are compared to calculated potentials based on the f_{ox} values for the agarose film and eq. 6-3.

Notably, the measured potentials ($E_{Pt/PSaf}$) and calculated potentials based on the agarose f_{ox} data agree more closely (between 100 and 150 hr), as shown in Figure 6.17B. However, the values of f_{ox} calculated from $E_{Pt/PSaf}$ (0.92 to 0.98, Figure 16A) would suggest that poising is unlikely. After 200 hr, the agarose form of PSaf indicated a lower "redox potential" than the electrode/cellulose form of the indicator.

The measured potentials of the Pt/PSaf electrode and of an uncovered Pt electrode (E_{Pt}) over the course of the experiment with the same slurry are shown in Figure 6.18. $E_{Pt/PSaf}$ decreased to ~-255 mV by 150 hr while E_{Pt} remained above 0 V. As detailed in the experimental section, sediment slurry, known to be methanogenic, was added at ~175 hr to enhance methane production. During the next 25 hr, the value of E_{Pt} dropped sharply to -240 mV, while $E_{Pt/PSaf}$ increased about 20 mV (to -235 mV). For the remainder of the experiment, $E_{Pt/PSaf}$ closely tracked E_{Pt} which remained relatively constant. There was no obvious change in the rate of methane production in the reactor after addition of the sediment or 50 mmol of acetate (the substrate) at about 220 hr.

The difference in the two "redox levels" (after 150 hr) and increase in $E_{Pt/PSaf}$ upon addition of the methanogenic sediment were unexpected. Possibly, the Pt/PSaf electrode was weakly poised by the PSaf couple before the addition of the sediment and became poised by a different couple (e.g., biochemical) after addition by species in the methanogenic sediment. This hypothesis is consistent with the rapid drop in E_{Pt} of the bare Pt electrode and the convergence of E_{Pt} and $E_{Pt/PSaf}$ after addition of the sediment. Previously, it has been noted that the potentials of two "equivalent" Pt electrodes placed in the same sample (soil or wastewater slurry) tend to converge as the system becomes very reducing (-250 mV or less) (13). It appears that the methanogens, or the chemical

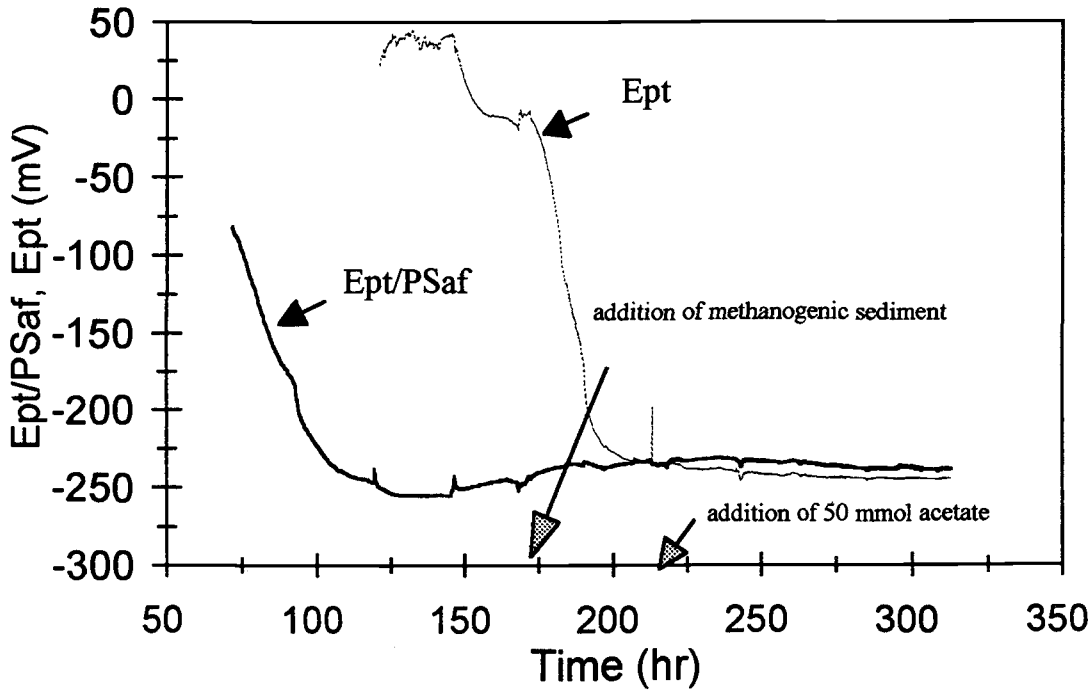

Figure 6.18 Time dependence of the potentials of a Pt/PSaf electrode and a bare Pt electrode in contact with a methanogenic wastewater slurry at pH 7 (same slurry as discussed in Figures 6.16 and 6.17). After addition of the methanogenic sediment at ~175 hr, E_{Pt} rapidly decreased and the potentials of the two electrodes converged. Addition of the substrate acetate at ~220 hr had little effect on the potentials or on rates of methane production (Figure 6.17A).

byproducts of the methanogens, in the wastewater slurry differed from those in the added sediment and species in the sediment may have dominated over PSaf in poising the Pt/indicator electrode. Furthermore, these redox species may have coupled to the Pt electrode but not to PSaf.

At the conclusion of the experiment, inspection of the PSaf cellulose filter revealed that the filter was still rather red (and therefore, PSaf was at least partially oxidized). It is possible that the PSaf was rapidly oxidized by O_2 when the electrode was taken out of the reactor.

In previous studies with methanogenic wastewater slurries (12), more negative values of E_{Pt} ($\leq$ -275 mV) and significantly greater methane production ($P_{CH4} \geq 0.2$ atm) were observed. It would be instructive to evaluate immobilized PSaf under such methanogenic conditions to determine if it could be more reduced and if $E_{Pt/PSaf}$ would assume lower values.

Presently, spectrophotometric monitoring of redox indicators immobilized in agarose (in a film form) is preferable to monitoring of the redox potential based on Pt/indicator electrodes. With the spectrophotometric method, response times are faster. Formal potentials of indicators immobilized to agarose appear somewhat lower than those for indicators immobilized on cellulose. Certainly, Pt/indicators deserve more study because they offer a potentially simple means to monitor redox conditions without the need for a spectrophotometer.

6.3.7 Phenosafranine as an indicator for methanogenic conditions

In previous studies, it was shown that Thi, which couples well to Fe(II), is useful for identifying Fe(III)-reducing conditions (8) and that CV couples well to sulfide and is suitable for identifying sulfate-reducing conditions (12). In the current study, the applicability of CV for evaluating sulfate-reducing conditions has been reconfirmed. Also PSaf was shown to couple well to reductants produced under methanogenic conditions which allows for expansion of the "redox window" concept that was previously proposed (12).

As a biologically-active sample (soil, groundwater) becomes more reducing, reduction of Thi, AA, CV, NB and PSaf will occur (theoretically) in the order illustrated in Figure 6.19. The redox regions for Fe(III)-reducing, sulfate-reducing, and methanogenic conditions, and for redox transformations of As, Cr and TCE are also illustrated in the figure.

In previous experiments with methanogenic soil slurries (12) and Thi and CV immobilized on agarose beads, little or no reduction of the indicators was observed, in contrast to the results obtained here. This difference is hypothesized to be due to the substantial change in configuration of the immobilized indicators. The agarose film form (and cellulose membrane filters placed directly in the sample) allows for more contact of indicators with larger particles and microbes and results in less contamination from O_2 in the pumping/filtering process.

The pH dependence of Thi and CV in terms of the "redox window" concept and relevant environmental couples was discussed previously (12). For PSaf, the redox

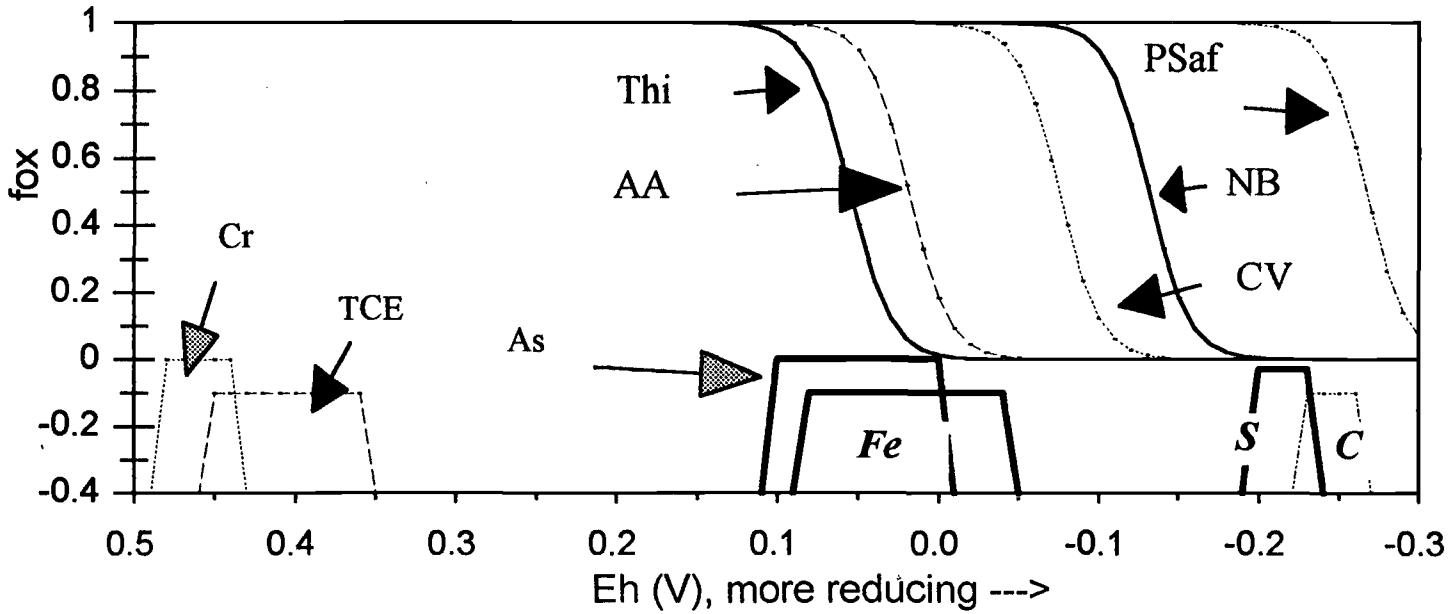

Figure 6.19 "Redox window" concept with immobilized Thi, AA, CV, NB and PSaf at pH 7. The indicator potentials are calculated with eq. 6-3. The Fe(II)/$Fe(OH)_3$ region (***Fe***) is based on a ferrihydrite Fe(III)-solid phase and 10 - 1000 µM Fe(II). This potential region is calculated with equation 6-5 with an $E_7^{0\prime}$ value of -0.182 V for the ferrihydrite solid phase at pH 7. The sulfate-reducing (***S***) region is calculated based on the SO_4^{2-}/HS^- couple ($E_7^{0\prime}$ = -0.22 V (1)) and the methanogenic (***C***) region is based on the $CO_2(g)/CH_4(g)$ couple ($E_7^{0\prime}$ = -0.244 V (2)), with a ratio of oxidized and reduced species varying between about 0.01 - 100. The arsenic (**As**) region ($E_7^{0\prime}$ = 0.034 V (37) for the $HAsO_4^{2-}/H_3AsO_3$ (As(V)/As(III)) couple and 0.01 - 100 ratios of oxidized and reduced species) lies inside the Fe(III)-reducing region. The chromium (**Cr**) region ($E_7^{0\prime}$ = 0.578 V (38) for the $CrO_4^{2-}/Cr(OH)_3$ couple and 0.1 - 10 µM Cr(IV)) is indicative of the Cr(VI)/Cr(III) couple and the TCE region (**TCE**) for the TCE/*cis*-DCE transformation (occurring between 0.35 - 0.45 V at pH 7 (without conditions given (7)).

transition zone is expected to shift -29 mV per pH unit over the region of pH 6-8 (one H^+ transfer in the reduction (10)). For the CO_2/CH_4 couple, the expected pH dependency of redox potential over this region is -59 mV per pH unit. Because the reductants actually responsible for reducing PSaf under methanogenic conditions are not known, it is not possible to predict how pH will affect the use of PSaf as an indicator of methanogenic conditions from pH 6 to 8. If the pH dependency of the redox potential of the reductant(s) is the same as for PSaf (-29 mV per pH unit), changes in pH will not affect the concentration of reductant(s) necessary to reduce a given fraction of PSaf. However, if the redox potential shift is -59 mV per pH unit (or greater), a *higher* level of reductant (compared to the level at pH 7) will be required below pH 7 to reduce a given fraction of PSaf. Above pH 7, this trend is reversed and a *lower* reductant concentration would be required. Clearly, to fully evaluate the effect of pH on PSaf speciation, the reductant(s) of PSaf under methanogenic conditions must be identified.

6.4 Conclusions

Several attempts were made to immobilize redox indicators in a variety of different chemical matrices. Silicon sol-gels proved to be simple to make and any indicator could be immobilized (no covalent bonding scheme was necessary). However, diffusion rates of reductants into the structures were slow and the sol-gels cracked. The redox indicators, Thi and CV, were successfully immobilized to polyacrylamide gels in some cases, but the immobilization scheme was complex and results were inconsistent. Furthermore, CV immobilized in the gels was difficult to reduce and evidence suggests that Thi may have been bound electrostatically to the gel, rather than bonded covalently.

Agarose films proved to be an excellent matrix for immobilization of redox indicators and provide good response times. Preparation of the films is simple. The immobilization procedure is straightforward but limited for use with redox indicators containing amine groups that do not take part in the redox reaction.

The redox indicators Thi, AA, CV, NB and PSaf were successfully immobilized to agarose films and were shown to have redox properties similar to those indicators previously immobilized to agarose beads (Thi, CV, PSaf). These immobilized indicators can be reduced with Fe(II), S(-II), and Ti(III), respectively, and re-oxidized with O_2. The extent of reduction of Thi or CV with Fe(II) at pH 7 compares reasonably well to that predicted with equilibrium models or previous data from titrations of Thi and CV immobilized on agarose beads. With S(-II) as the reductant, the fraction of CV in the film form that was oxidized at pH 7 was significantly greater than that observed with agarose beads) or that predicted by equilibrium models. The experimental difficulties of

measuring micromolar levels of sulfide and totally eliminating small O_2 leaks into the reactor contributed to the difficulties.

A significant advantage of the film configuration for immobilization of the redox indicators, relative to the "packed-bead" cell configuration, is that it is less subject to clogging by particles in samples. Hence, films (in the appropriate flow cell) present less back pressure to pumps and syringes which allows higher solution flow rates to be used (an order of magnitude greater) and less or (conceivably) no filtering. With the film format, interaction of the indicators with solid particles and microbes, and, potentially, reductants which are adsorbed to solid particles, is greater. In bioreactor experiments, the new film configuration allowed the filter pore size in the external loop to be increased from 0.6 μm (for experiments with bead-immobilized indicators) to 40 μm with a corresponding increase in flow rate from ~0.5 mL/min to as high as ~50 mL/min. Exposure to residual O_2 is also minimized which allows low levels of reductants to reduce the immobilized indicator. These advantages may explain why the film indicator configuration was applicable to methanogenic conditions when the bead configuration was not.

The first known demonstration that the indicator PSaf is reduced under methanogenic conditions is quite significant. Reduction of the indicator can only occur at very negative redox potentials (~ -0.25 V at pH 7). This indicator complements the use of Thi for sensing Fe(III)-reduction (8) and CV for evaluating sulfate-reduction (12).

The immobilization of redox indicators to cellulose filter membranes is also an important and unique accomplishment of this research. For some indicators, the formal potential is more negative when immobilized to cellulose relative to agarose beads or

films. To obtain comparable absorbances with filters, which are thinner than agarose films, the effective indicator concentration is higher. This situation may have contributed to the shift in the measured formal potential.

In the filter paper format, redox indicators can be used in different configurations including a Pt/indicator electrode (an indicator filter pressure-fitted to the surface of a Pt electrode). Furthermore, Pt/indicator electrodes could be deployed *in situ* in ground water (wells) or in a bioreactor without any need for pumping. These Pt/indicator electrodes have proven useful in sulfate-reducing wastewater slurries, and generally, the redox levels predicted by immobilized indicators measured potentiometrically or spectrophotometrically are similar.

Instrumentally, redox sensors based on Pt/indicator electrodes are conceptually simpler because a voltage is measured rather than an absorbance which requires a spectrophotometer (e.g., source, photodetector). It may be possible to construct a "redox indicator array" for monitoring redox conditions based on a number of small Pt/indicator electrodes. Pairs of electrodes would define a "redox window", a concept previously defined for spectrophotometric measurement of immobilized redox indicators (12).

With Pt/indicator electrodes, reversible redox-active couples (one or both redox states) need not be colored at all, as is required for spectrophotometric monitoring. Redox-active couples might include quinones, which are not colored, can poise the Pt electrode in soluble forms, and possess formal potentials ranging from +250 to -200 mV (37). Currently, only quinones which contain amine groups can be immobilized. There is a need to synthesize new indicators for this application such as quinones with amine

groups to fill in gaps in potential ranges or "redox windows" not covered by the indicators currently available.

Redox status can best be predicted with the use of redox indicators if the pH of the system is known. In this regard, spectrophotometric measurement of indicator speciation may be preferable to potentiometric measurement with a Pt/indicator electrode. For spectrophotometric measurements, there is no question of the *degree* of reduction of the indicator. With potentiometric measurements, pH affects the measured potential and therefore, the actual degree of reduction cannot be known (unless the pH is also measured). Because pH is a major variable in any environmental system (e.g., groundwater, soil), it should also be measured to relate with more certainty the degree of reduction of an indicator (f_{ox}) or the measured potential ($E_{Pt/ind}$) to the microbial redox level.

Measurable reduction of an indicator signals the presence of one or more reductants which in turn can be indicative of certain types of microbial processes. The sample pH determines the reductant concentration that is necessary to observe significant reduction and to identify the onset of a particular microbial process. Overall, multiple indicators should be used to define redox conditions. pH information is especially critical for thionine in order to differentiate between Fe(III)-reducing and sulfate-reducing conditions (i.e., both Fe(II) and sulfide can serve as reductants). Also Fe(III)-reducing conditions may not be detected with thionine when the pH below 6.5 because the levels of Fe(II) are relatively high (>> 1 mM).

6.5 References

1. Guadalupe, Ana R.; Wier, Larry M.; Abruna, Hector D., *Amer. Lab.*, **1986**, August, 102-107.

2. Lev, Ovadia; Anvir, David; Iosefzon-Kuyavskaya, Berta; Gigozin, Ida; Ottonleghi, Michael,, *Fresenius J. Anal. Chem.*, **1992**, *343*, 370-372.

3. Anvir, David; Zusman, Rivka; Rottman, Claudio; Ottolenghi, *J. Non-Cryst. Solids*, **1990**, *122*, 107-109.

4. Zhujun, Zhang; Jianzhong, Li; Ling, Li, *Talanta*, **1994**, *41*, 1999-2002.

5. Arnold, Mark A., *Anal. Chem.*, **1985**, *57*, 565-566.

6. Lemmon, T. L.; Westall, J. C.; Ingle, J. D. Jr., *Anal. Chem.*, **1996**, *68*, 947-953.

7. Lemmon, Teresa, *Development of Chemostats and Use of Redox Indicators for Studying Transformations in Biogeochemical Matrices*, **1995**, Ph.D. Thesis, Oregon State University.

8. Jones, Brian; Chapter 4 of this thesis.

9. Jones, Brian, Laboratory notebook #2, 1995, Oregon State University.

10. *Indicators*, Bishop, E., Ed., Pergamon Press: Oxford, 1972.

11. Mobley, James, Oregon State University, unpublished report, **1992**.

12. Jones, Brian; Chapter 5 of this thesis.

13. Jones, Brian; Chapter 3 of this thesis.

14. Brinker, C. Jeffrey; Scherer, George W., *Sol-Gel Science*, Academic Press, Inc.: 1990.

15. Avnir, David; Lev, Ovadia; Iosefzon-Kuyavskaya, Berta; Gigozin, Ida; Ottonleghi, Michael, *J. Non-Cryst. Solids*, **1992**, *147 & 148*, 808-812.

16. Angel, Michael S.; Zhang, Yunke; Nivens, Delana A., *Anal. Chim. Acta*, **1998**, *376*, 235-245.

17. *Acrylamide Polymerization - A Practical Approach*, US/EG Bulletin 1156, BIO-RAD.

18. Hermanson, Greg T., *Bioconjugate Techniques*, Academic Press, Inc., 1996.

19. Tercier, M.-L.; Buffle, J., *Anal. Chem.*, **1996**, *68*, 3670-3678.

20. Hermanson, Greg T.; Mallia, A. Krishna; Smith, Paul K., *Immobilized Affinity Ligand Techniques*, Academic Press, Inc.: 1992.

21. O'Sullivan, Valerie, Private communication, PIERCE Chemical Co., May 6, 1998.

22. *Merck Index*, Budavari, S., Ed., Merck & Co., Inc.: Rahway, N.J., 1989.

23. *Instructions for covalent binding of ligands to Sartobind Membranes with Aldehyde Groups*, Sartorius.

24. Vancheeswaran, Sanjay, instructions for GC use, Private communication, Oregon State University, June 28, 1998.

25. *Product Catalog*, CHEMetrics, 1997-1998.

26. *Standard Methods for the Examination of Water and Wastewater;* American Public Health Association: Washington, D. C., 1995.

27. Chapelle, Francis H., *Groundwater Microbiology and Geochemistry,* John Wiley & Sons, Inc.: 1993.

28. Semprini, Lew, Private communication, Oregon State University, August 24, 1998.

29. Bos, Mark, *Part I: Development and Application of an Arsenic Speciation Technique Using Ion-Exchange Solid Phase Extraction Coupled with GFAAS, Part II: Investigation of Zinc Amalgam as a Reductant,* **1996**, M.S. Thesis, Oregon State University.

30. Walt, David R., Private communication, Tufts University, November 18, 1997.

31. Jones, Brian; Chapter 7 of this thesis.

32. Jones, Brian, Laboratory notebook #4, 1996, Oregon State University.

33. Shriver, Duward F.; Atkins, Peter; Langford, Cooper H., *Inorganic Chemistry, Second Edition*, W.H. Freeman and Co.: 1994.

34. Firpo, Emile, Private communication, Oregon State University, December 11, 1997.

35. Gable, Kevin, Private communication, Oregon State University, November 19, 1997.

36. Robarge, Lonnie, Private communication, Oregon State University, August 16, 1998.

37. Green, Floyd J., *The Sigma Aldrich Handbook of Stains, Dyes and Indicators*, Aldrich Chemical Company, Inc.: Milwaukee, WI, 1990.

38. McBride, Murray B., *Environmental Chemistry of Soils*, Oxford University Press, Inc., 1994.

39. Belmont-Hébert, C.; Tercier, M. L.; Buffle, J., *Anal. Chem.*, **1998**, *70*, 2949-2956.

40. Clark, W. Mansfield, *Oxidation-Reduction Potentials of Organic Systems*, Williams & Wilkins Company: Baltimore, 1960.

CHAPTER 7: APPLICATIONS OF REDOX INDICATORS TO H_2 ANALYSIS

7.1 Introduction

The importance of H_2 level in ground water and soil systems has recently been realized (1 - 5). As a major product of microbial fermentation, H_2 is utilized by a variety of non-fermentative microbes (methanogens, dechlorinators) as a substrate (6). The steady-state H_2 level in an environmental/microbial sample is indicative of several important factors including the redox status of a soil or groundwater sample (1 - 4) and the rate or extent of dechlorination in dechlorinating cultures (5, 6). Because current methods of measuring H_2 levels are expensive, complicated and time consuming, a simple, inexpensive H_2 sensor for field applications would be useful for environmental field monitoring.

Chapelle, Lovley and others (1 - 4) propose that H_2 levels in environmental systems are indicative of the dominance of the given terminal electron acceptor (TEA) process of a system, and therefore, the redox level of the system. H_2 is an important intermediate in the microbial oxidation of organic matter along with the concurrent reduction of TEA's (3) and a primary substrate for methanogens, sulfate-reducing and Fe(III)-reducing bacteria, and many dechlorinating microbes (6). According to Lovley et al. (3), different typical levels of H_2 are found in groundwater and sediments in which metabolism is coupled with different TEA processes because different types of microorganisms exhibit different efficiencies for utilizing H_2. For CH_4 production (methanogenesis), a H_2 level of 7 - 10 nM has been reported in groundwater aquifers

while H_2 in the range of 1 - 4 nM has typically been measured in groundwater exhibiting sulfate-reduction. In groundwater systems exhibiting Fe(III)-reduction and nitrate-reduction, the steady-state H_2 level is significantly lower, 0.1 - 0.8 nM and less than 0.05 nM H_2, respectively.

Rates of H_2 production (by fermentative microbes) and consumption (by methanogens, sulfate- and Fe(III)-reducers, and dechlorinators) are rapid compared to the overall consumption rates of the TEA, resulting in relatively stable, steady-state concentrations of H_2 in regions in which a dominant TEA process is occurring. These rapid rates of production and consumption give rise to more regionalized and constant levels of H_2 compared to concentrations of TEA's (or products of TEA's). Less transitory species such as CH_4 or HS^- might diffuse into other zones and not further react. Hence, the detection of these species may give misleading results if these species alone were being used to determine the dominant TEA process in a given region (3, 4). Furthermore, these steady-state levels of H_2 do not appear to be influenced by the rate of organic matter decomposition, pH or salinity of the system (4), as long as the dominant TEA process remains the same in that region.

Recent evidence suggests that H_2 is also an important substrate for dechlorinating microbes (5, 6). In studies of TCE dechlorination to cis-DCE in groundwater, H_2 levels in the range of 10^{-2} to 10^{-4} atm (8000 to 80 nM) were consistently measured during dechlorination (7). Furthermore, dechlorination of TCE ceased when H_2 levels fell outside of this range. In studies of PCP dechlorination in media containing dechlorinating microbes in a chemostat reactor system, significant rates of dechlorination were observed if H_2 headspace levels were maintained in the range of 10^{-2} - 10^{-4} atm (8).

These results suggest that monitoring H_2 levels during bioremediation/dechlorination processes can provide critical information about the rates of dechlorination of a given compound or whether dechlorination is likely to be occurring or not.

A major limitation with using H_2 as a measure of redox status or as an indicator of dechlorination in the field is the difficulty and expense of the analysis. Determination of very low levels of H_2 in groundwater aquifers requires both a gas sampling system (to attain sufficient H_2 for analysis) and a sensitive detection system. Lovley et al. (3) describe a "bubble strip method" to collect enough H_2 for analysis. Aquifer groundwater is pumped (at about 0.6 L/min) through a sampling tube containing a bulb with a gas headspace. The analyst then injects 20 mL of H_2-free N_2 gas into this headspace and waits at least 5 min for equilibration of the sample with the gas headspace. A gas sample is then taken and injected into a GC with a specialized gas detector (based on Hg_2^{2+} reduction by H_2 to Hg^0 and subsequent AA determination of Hg vapor). Overall, this sampling/analysis procedure requires special equipment, access to a pumping system, and an expensive GC detection system which can cost over $20,000 (9). It is apparent that a simpler, more convenient, and less expensive method for H_2 analysis would be well received by microbiologists, soil and environmental scientists and engineers.

Redox indicators, which have been studied extensively in this research (10 - 12) and in previous research (13 - 15), present the basis for a colorimetric method for quantifying H_2. In recent studies, 100% H_2 gas, when bubbled into a solution of the redox indicator thionine in the presence of Pd catalyst, rapidly and completely reduces the thionine (which can easily be reoxidized with O_2) (16). Traytnik (9) uses H_2 gas to obtain solutions of completely reduced redox indicators without having to add a

reductant (in excess) which would otherwise remain in solution after the reduction (H_2 gas can subsequently be removed from the solution with an inert gas such as N_2).

The majority of well-characterized organic redox indicators are colored in their oxidized form and colorless when reduced (17) and contact of the oxidized form of the indicator with H_2 (a very strong reductant) in solution (and in the presence of a catalyst) will decolorize these solutions. Potentially, H_2 gas samples acquired in the field (perhaps acquired with a "bubble strip method" as employed by Lovley (3)) could be bubbled into a solution of redox indicator containing Pd catalyst. The reduction rate of the indicator (as measured as a decrease in absorbance) could then be used to estimate the partial pressure of H_2 in the gas. This concept is the basis for an H_2 sensor based on reduction of redox indicators.

This concept has been proposed and demonstrated in principle with immobilized redox indicators. Silicon sol-gels slabs were doped with Thi or PSaf and Pd powder (12) and placed in de-aerated water. Both immobilized indicators were rapidly reduced when 100% H_2 was bubbled through the water. With 100% H_2, it took over 30 min to reduce the indicators.

In some cases, redox indicators, such as the organic indicators methyl and benzyl viologen, are colorless in their oxidized form and colored when reduced and therefore, would become *colored* when placed in contact with H_2 gas. Furthermore, tris-chelated Fe(III) and Cu(II) (chelated with certain organic, nitrogen-containing ligands) are somewhat colored in their oxidized forms but become more colored (with a significant wavelength shift) when reduced (17). In this case, reduction of these particular chelates would result in an increase in color (absorbance) compared to the oxidized species. The

option of using redox indicators which become colored upon reduction is very important and will be discussed further.

In this chapter, application of redox indicators to low-level H_2 determination is discussed. Different levels of H_2 gas (ranging from 100% H_2 (1 atm) to 0.01% H_2 (10^{-4} atm) in N_2) were bubbled into solutions of oxidized redox indicator containing Pd (or another catalyst). The effect of H_2 level, pH, amount and type of catalyst used, and indicator concentration on the rate and degree of reduction of the indicator were evaluated to improve the detection limit for H_2. Redox indicators tested for this purpose included organic redox indicators such as thionine (Thi), phenosafranine (PSaf), benzyl viologen (BV), and methyl viologen (MV). Several Fe(III) and Cu(II) chelates (with ligands such as 1,10-orthophenanthroline (OP), dipyridyl (DP), etc.) were also evaluated.

7.2 Experimental

7.2.1 Chemicals

The redox indicators thionine (Thi), phenosafranine (PSaf), benzyl viologen (BV) and methyl viologen (MV) were obtained in the oxidized form from Aldrich. These structures are shown in Figure 7.1. Palladium powder (99.9%, submicron), palladium/ alumina pellets (palladium powder coated on alumina, 0.5% w/w Pd), and platinum/ alumina pellets (0.5% w/w Pt) were also obtained from Aldrich. A 50 μg/mL (895 μM) Fe(III) standard (prepared by dissolving solid Fe in solution in 6 mM HCl) was obtained from the Department of Chemistry at OSU, as was a 100 μg/mL (1574 μM) Cu(II) solution in 0.03 M HNO_3 (prepared from a 1000 mg/L Cu AA solution (VWR)). Hydroxylamine hydrochloride (10% (w/v) in water, prepared from Mallinckrodt), used as a reductant for Fe(III) species, was obtained premade from the OSU Department of Chemistry. L-ascorbic acid AR®, used as a reductant for Cu(II) species, was obtained from Mallinckrodt.

A variety of organic ligands were obtained for testing with the Fe(III) and Cu(II) species. These chemicals are listed in Table 7.1.

Sodium acetate ($NaC_2H_3O_2 \cdot 3H_2O$, Mallinckrodt), potassium phosphate monobasic (KH_2PO_4, Mallinckrodt), sodium bicarbonate ($NaHCO_3$, Mallinckrodt), HCl (concentrated, Mallinckrodt) and NaOH (6 M, obtained pre-made from OSU Chemistry) were used to prepare pH buffers (~0.05 M at pH 4 (acetate) and pH 7 (phosphate)). Also, a pH 10 buffer, prepared from METREPAK pHydrion buffer capsules (containing

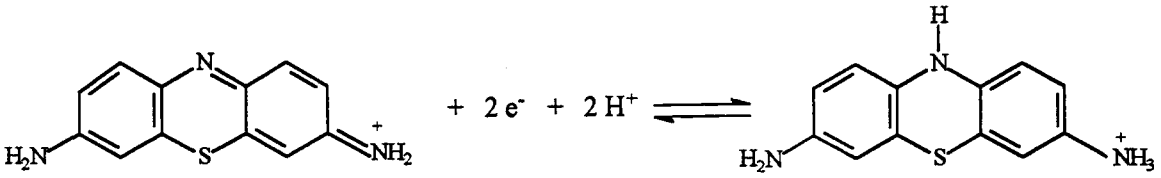

Thionine

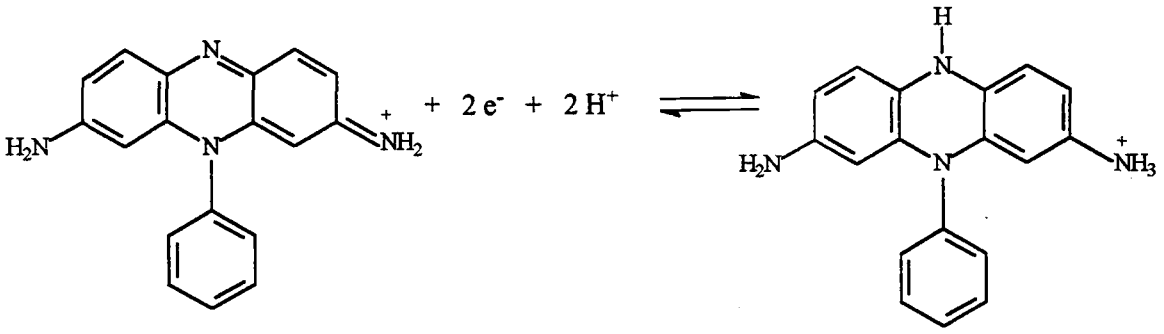

Phenosafranine

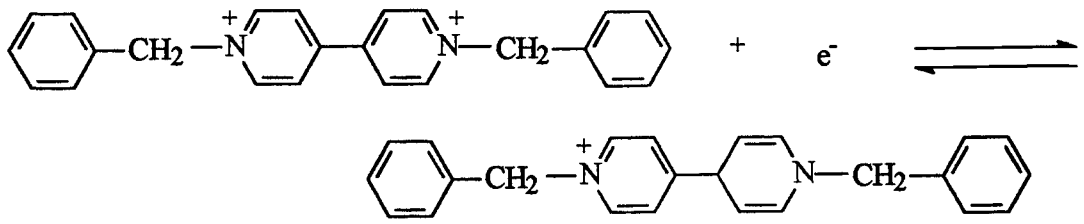

Benzyl Viologen

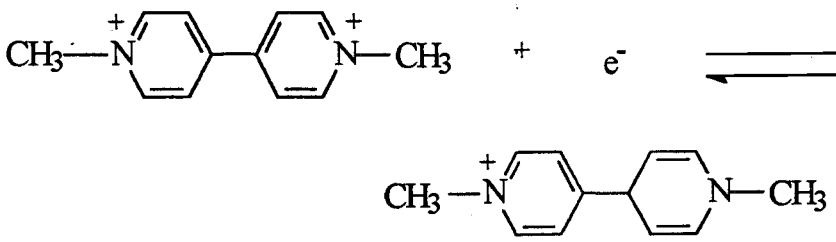

Figure 7.1 Redox reactions of organic indicators evaluated for reactions with H_2.

Table 7.1 Chelating ligands for Fe(III) and Cu(II) tested for H_2 analysis.

chemical	source
1,10-phenanthroline	Mallinckrodt[a]
dicyano-bis(1,10-phenanthroline) iron(II) complex	Sigma
4,7-dimethyl-1,10-phenanthroline, 98%	Aldrich
3,4,7,8-tetramethyl-1,10-phenanthroline, 99+%	Aldrich
neocuproine hydrochloride hydrate, 98%	Aldrich
2,2'-dipyridyl, 99+%	Aldrich
4,4'-dimethyl-2,2'-dipyridyl, 99%	Aldrich
syn-2-pyridinealdoxime, 99+%	Aldrich
di-2-pyridyl ketone oxime, 99+%	Aldrich
2-mercaptopyridine, 99%	Aldrich
dimethylglyoxime, 99+%	Aldrich
4-amino-5-isopropylsulphonyl-2-(pyrid-2-yl) pyrimidine	Maybridge Chemical Co. LTD.

[a] pre-made as 0.5% (w/v) solution from OSU Department of Chemistry.

sodium carbonate and sodium bicarbonate), was used with some experiments. Sulfuric acid (H_2SO_4, 3 M) was obtained premade from OSU chemistry department (Mallinckrodt). Hydrogen gas (pre-purified, 100%) and N_2-H_2 mixtures (pre-purified 1%, 0.01% in H_2 (molar)) were obtained in tanks from Industrial Welding Supply, Inc., as were tanks of pre-purified N_2.

7.2.2 Instrumentation

For gas control, a Tylan RO-28 readout and control box and three Tylan FC280 mass flow controllers (10 sccm, 50 sccm and 100 sccm full range) were used. An O_2 trap (Alltech Oxy-Trap 4001) and an indicating oxygen trap (Alltech 4004) were placed in the N_2 flow line between the gas cylinder and the mass flow controller to eliminate any residual O_2. No oxygen trap was used at the H_2 source line. To measure gas flow rates, a J&W Scientific ADM 1000 Intelligent Flowmeter was used.

Copper tubing (1/8" o.d.) connected the N_2 and N_2-H_2 gas lines (with Swagelok fittings) to the mass flow controllers (MFC's). From the MFC's, polyetheretherketone (PEEK) tubing (0.030" i.d., 1/16" o.d., Upchurch) connected the outlets of the MFC's to a flangeless Delrin nut (P•202, Upchurch) which was coupled to a syringe needle (Perfektum®) with a luer adapter (Small Parts, Inc.) and standard union (1/4•28, P•603 Upchurch).

For absorbance measurements of indicators in solution, a UV-Vis spectrophotometer cuvette with a septum screw cap was used (Spectrocell RF-0010-T, 10-mm, vol., 3.7 mL). The syringe needle of the gas outlet was pushed into the cuvette

through the septum, and a second syringe needle was poked into the cuvette septum for gas outflow. All absorbance measurements were made with a Hewlett Packard 8452A diode array spectrophotometer.

7.2.3 Titrations of organic indicators with H_2

Thionine was chosen to evaluate the effects of different variables such as H_2 partial pressure, pH, indicator concentration, and amount and type of Pd catalyst used on the extent of reduction and the reaction rate kinetics. A 2 mM stock solution of (oxidized) Thi was initially prepared.

For each experiment, 2 mL of total solution (indicator plus buffer solution) were pipetted into the cuvette into which the gas mixture (H_2/N_2) was bubbled. Early in these experiments, it was determined that absorbance measurements could be acquired with the syringe needle left in solution and bubbles present without affecting the precision. Absorbance measurements were taken at the wavelength maximum (600 nm) of the primary visible band and at 798 nm (for background correction) at time intervals ranging from 10 s to 10 min, depending on the rate of reduction of the oxidized Thi, until reduction was complete (if possible). The total gas flow rate was set and measured to be 50 mL/min. No temperature control was used in these experiments, and the temperature was assumed to be constant at 25 °C for subsequent calculations.

To determine the effect of Thi concentration on reaction rate, Thi concentrations were tested in the range of 5 - 40 μM with an H_2 partial pressure of 0.01 atm (1% H_2 gas). To test the effects of H_2 partial pressure on reaction rate, H_2 partial pressures were

varied between 1 atm (100% H_2) and 0.0001 atm (0.01% H_2) with [Thi] = 40 μM. For all these experiments, the pH of the solution was 7 and two Pd/alumina pellets were used as the catalyst.

In tests to determine the effect of pH (at values of 4, 7 and 10) on reaction rate, total Thi concentration was maintained at 50 μM while H_2 partial pressure was maintained at 0.01 atm. Two Pd/alumina pellets were used for each case.

To determine if the amount of Pd catalyst affected the reaction rate, several separate experiments were conducted at pH 7 with one, two, four and eight Pd/alumina pellets at a Thi concentration and H_2 partial pressure of 50 μM and 0.01 atm, respectively. Pd powder (2 - 4 mg) was also tested as the catalyst under the same conditions.

Titration experiments of the indicator PSaf with H_2 were also conducted with only visual monitoring of color changes. As previously in the Thi experiments, these titrations were conducted in the spectrophotometer cuvette with 2 mL portions of a 40 μM PSaf solution in pH 10 buffer. In this case, Pd powder (2 - 4 mg) was employed as the catalyst. The H_2 partial pressure was varied between 1 and 0.001 atm.

H_2 titrations of the indicators BV and MV were conducted at pH values in the range of 11.5 to 14. For experiments in the pH range of 11.5 - 12, 1 mM solutions of BV and MV were prepared (separately) in ~0.05 M sodium bicarbonate (made to the desired pH by additions of HCl and NaOH). For pH values greater than 12, only 1 M NaOH was used to adjust the pH of the indicator solutions. In each case, ~25 mL of the indicator solutions were prepared and placed in a 50-mL vial (with a septum cap, I-CHEM) along with 5 - 6 Pd/alumina pellets. These solutions were then tested by

bubbling 100% (1 atm), 1% (0.01 atm) and 0.1% (0.001 atm) H_2 gas into the solutions as the color formation (on reduction these indicators become colored dark blue) was observed visually.

7.2.4 Titrations of Fe(III)-(OP)$_3$ complex with H_2

In most experiments, 250 µL of the 50 µg/mL Fe(III) standard, 250 µL of the 0.5% (w/v) (0.028 M) 1,10-phenanthroline (OP) solution and 1.5 mL of pH buffer were pipetted into the spectrophotometer cuvette yielding a total volume of 2.0 mL. The resulting total Fe(III) concentration was 112 µM and it was assumed that all the Fe(III) was chelated with the OP (three OP molecules chelate Fe(III) (or Fe(II), as described in Appendix B)). In some cases, H_2SO_4 was added to the solution (instead of a buffer) to evaluate the effect of very low pH (in a (calculated) pH range of 0.6 to -0.3). In most cases, two Pd/alumina pellets were used as the catalyst, although in some experiments two Pt/alumina pellets were employed. These Fe(III)-(OP)$_3$ solutions were then titrated with H_2 at partial pressures ranging from 1 to 0.0001 atm H_2. Absorbance measurements were taken at 510 nm (the wavelength maximum of the Fe(II)-(OP)$_3$ complex) and at 798 nm (background). For the blank, the initial Fe(III)-(OP)$_3$ solution was used. Absorbance measurements were taken over time at intervals ranging from 10 s to 10 min, depending on the rate of reduction.

7.2.5 Evaluations of various chelating agents with Fe(III) and Cu(II)

The ligands listed in Table 7.1 (with the exception of the dicyano-bis(1,10-phenanthroline) iron(II) complex (Fe(II)-DCOP)) were evaluated with Fe(III) and Cu(II) to determine if they formed stable complexes with the metal ions which could subsequently be reduced. Each complexant was mixed with a solution of Fe(III) and Cu(II) at pH 4. The Fe(II) in the Fe(II)-DCOP complex could not be oxidized to the Fe(III) state with O_2 or H_2O_2 and thus was not considered for further studies.

In two separate 4-mL vials (Fisherbrand) for each chemical, ~5 mg of each ligand (~20 times the molar amount necessary for chelation of all Fe(III) and Cu(II) based on a 3:1 complex), 300 μL of the 50 μg/mL Fe(III) solution or 200 μL of the 100 μg/mL Cu(II) solution, 1 mL of pH 4 buffer, and sufficient DI water to bring the total volume up to 2 mL were mixed. The final total concentrations of Fe(III) and Cu(II) were 134 and 157 μM, respectively. In some cases, the vial solution was heated in a microwave to solubilize the chelating agent. A reductant was added to one vial (400 μL of 10% (w/v) hydroxylamine for Fe(III)-complexes or ~10 mg of ascorbic acid, for the Cu(II)-complexes). To the other vial with a given metal Fe(III)- or Cu(II)-complex, one Pd/alumina pellet was added. The absorption spectra of both the oxidized and reduced form of the chelate were acquired. The color of both forms of the complexes were compared after 12 - 24 hr to determine if the oxidized form of the complex was stable in the presence of the Pd.

7.3 Background Considerations

The extent and rate of reduction of redox indicators with H_2 is dependent on thermodynamics, reaction kinetics, and kinetics of mass transfer. The Henry's law constant for H_2 is 0.00079 M/atm at 25°C (18) such that partitioning in the gas phase is strongly favored. Typical levels in aqueous systems (e.g., groundwater) are only 0.1 to 10 nM (or 1.3×10^{-7} to 1.3×10^{-5} atm in the vapor phase in contact with the liquid) (3). All these factors must be considered in the development of an H_2 sensor based on the reaction of H_2 with redox indicators.

Two basic configurations were considered for the development of a H_2 sensor based on redox indicators. These two methods are distinguished based on the mode of sampling (mass-transfer) used to transfer the H_2 from the sample to the redox indicator.

For gas sampling, the sample would be continuously bubbled (or the headspace gas from an aqueous sample would be pumped) into a spectrometer sample cell containing a solution of the indicator, a pH buffer, and some solid catalyst. The indicator could be immobilized if the method provides contact with the catalyst. For liquid sampling, the sample would be directly pumped into a spectrometer cell that contained immobilized indicator in contact with the catalyst. In either case, the concept is that quantitation of the H_2 would be based on the *rate* of reduction of the indicator rather than the extent of reduction. The two sampling approaches are now compared.

First consider the rate of transfer of H_2 to the sample cell. Based on Henry's law and $PV = nRT$ at 25°C, the molar concentration of H_2 is ~50 times greater in the gas phase than in the aqueous phase. For example, if the concentration of aqueous H_2 in the

sample is 8 nM, the equilibrium gas H_2 concentration is 10^{-5} atm or 0.4 μM. Hence, for a given flow rate (gas or liquid), the mass flow rate of H_2 to the cell is greater for gas mass transfer than for liquid mass transfer. With gas bubbling, the transfer rate from the gas into the indicator solution must also be considered. The H_2 concentration in the indicator solution cannot be higher than in the original sample solution.

A distinct advantage of gas sampling is the elimination of many potential interferents because most species in the sample are not volatile. In the aqueous phase, reductants such as Fe(II), HS^-, and ascorbic acid reduce redox indicators (9, 10, 13, 14). With solution mass transfer, these reductants would compete with H_2 in the reduction of the redox indicator and cause a positive interference. Fe(II) or HS^- are the most likely interferants in environmental systems (e.g., groundwater) because Fe(II) levels can be as high as 1 mM or more (14, 19, 20) and HS^- levels can approach 0.1 mM (20). These reductant concentrations are much higher than normal environmental H_2 concentrations.

$H_2S(g)$ would be the most likely interfering reductant in the gas-phase sampling of highly anaerobic environmental samples (21). However, H_2S gas could be removed from gas samples by bubbling through a scrubber specific for H_2S (9, 11).

Because of the difficulty of immobilizing redox indicator in contact with a catalyst and the desire to minimize interferences, it was decided to pursue development of an H_2 sensor based only on gas transfer. This type of transfer can be easily simulated by bubbling solutions of indicator with mixtures of N_2/H_2 with a varying H_2 content.

7.3.1 Equilibrium considerations

The oxidation-reduction (redox) reaction between a redox indicator and H_2 in the presence of a catalyst (e.g., Pd) is based on two half-reactions. The half-reaction for H_2 (the reducing agent) is

$$H_2 \rightleftharpoons 2H^+ + 2e^- \tag{7-1}$$

and that for a redox indicator (the oxidizing agent) is

$$Ind_{ox} + ne^- + mH^+ \rightleftharpoons Ind_{red} \tag{7-2}$$

where n, the number of electrons transferred, is typically 1 or 2, and m, the number of protons transferred, is typically 0, 1 or 2 (17). The overall reaction with n = 2 is given by equation 7-3.

$$H_2 + Ind_{ox} \rightleftharpoons Ind_{red} + (2\text{-}m)H^+ \tag{7-3}$$

where the actual stoichiometry for H^+ varies with the indicator and pH.

Thermodynamics can be used to predict under what conditions the reaction could occur. The reduction potentials of the half-reactions are determined from the Nernst equation:

$$E_{H_2/H^+} = E^{0'}_{H_2/H^+} - \frac{RT}{2F} \ln \frac{P_{H2}}{[H^+]^2} = -0.0295 \log \frac{P_{H2}}{[H^+]^2} \tag{7-4}$$

$$E_{ind} = E^{0'}_{ind,m} - \frac{RT}{nF} \ln \left(\frac{[Ind_{red}]}{[Ind_{ox}]} \right) \tag{7-5}$$

where P_{H2} is the partial pressure of H_2(g), $E^{0'}_{H_0/H^+}$ is the formal potential for the H_2 couple and is *defined* as 0 V, and $E^{0'}_{ind,m}$ is the formal potential for the indicator at pH m.

For thiazine type indicators (e.g., Thi) and safranine type indicators (e.g., PSaf),

$$E_m^{0'} = E^{0'} + \frac{RT}{nF}\ln\left(\frac{[H^+]^4 + K_{r1}[H^+]^3 + K_{r1}K_{r2}[H^+]^2}{[H^+] + K_{O1}}\right) \qquad (7\text{-}6)$$

where K_{r1} and K_{r2} are acid dissociation constants of the reduced form of the indicator and K_{O1} is the acid dissociation constant for the oxidized form of the indicator (17). For Thi, K_{r1}, K_{r2} and K_{O1} are $10^{-4.38}$, $10^{-5.3}$ and $10^{-11.0}$, respectively (16), and $E^{0\prime} = 0.563$ V (17). For PSaf, K_{r1} and K_{r2} are $10^{-4.86}$ and $10^{-5.78}$, respectively (17) (no value for K_{O1} is given in the reference) and $E^{0\prime} = 0.280$ V (17).

The pH dependence of the redox potential of the H_2 couple and of the two indicator couples are shown in Figure 7.2A. Thermodynamically, H_2 (for the H_2 levels shown) should completely reduce Thi at any pH because the H_2 redox potential is significantly below that of the indicator couple. In contrast, PSaf would be completely reduced at the lowest level of H_2 (10^{-6} atm or 0.8 nM) only for pH values below ~3 or above ~8.

In Figure 7.2B, the pH dependence of the redox potentials of two more indicators, BV and MV, are shown along with H_2 redox potentials. The equilibrium lines for BV and MV are not pH dependent with formal potentials of -359 mV and -446 mV, respectively (17), while the H_2/H^+ redox potential has a slope of -59 mV/pH unit. Reduction of BV at low levels of H_2 can occur only above pH ~9, while reduction of MV can occur only above pH ~11.

In general, conditions such as pH should be chosen such that the formal potential of the redox indicator is much greater than the reduction potential calculated for H_2.

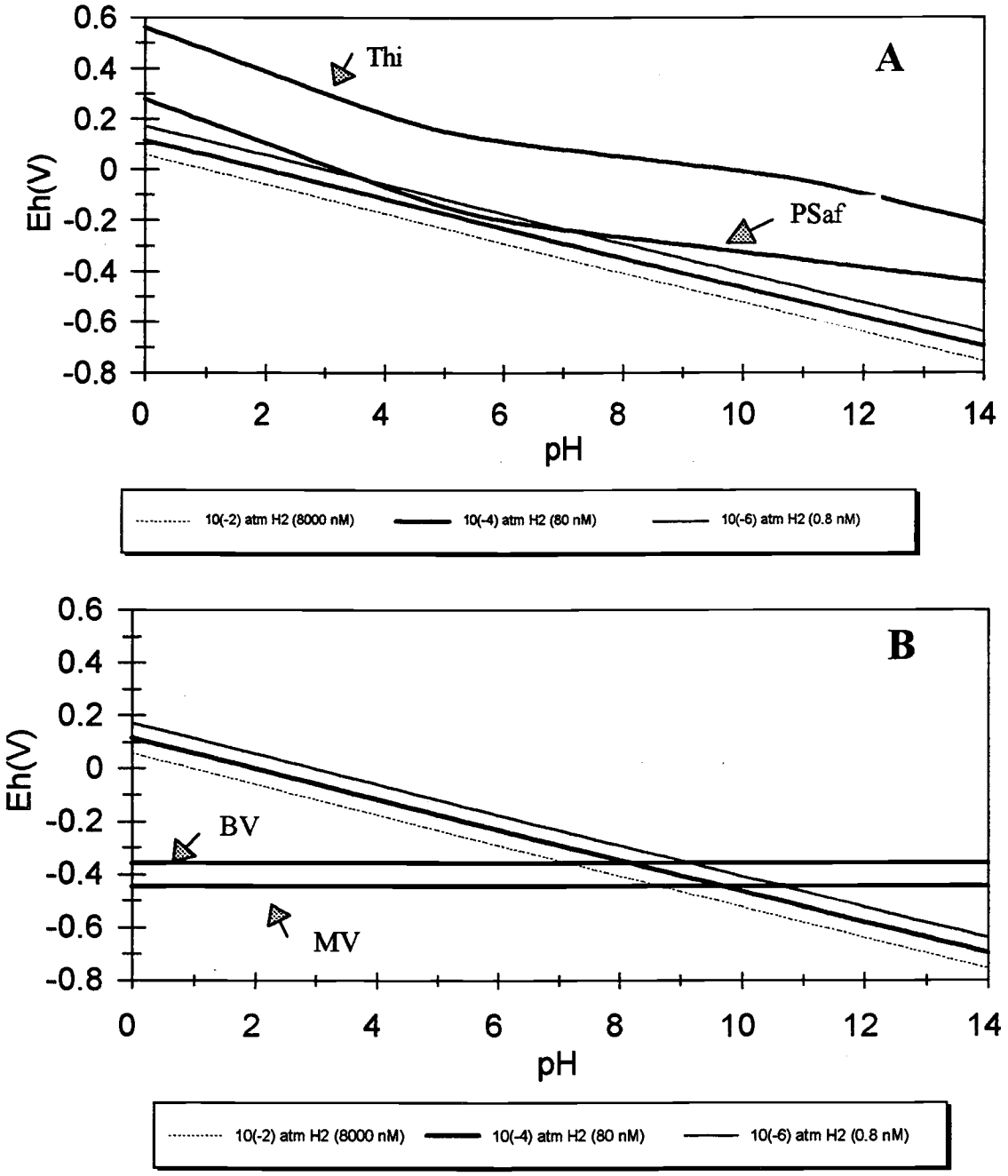

Figure 7.2 Dependence on pH of theoretical redox potential of redox indicators and the H^+/H_2 couple. E_H for the H_2 couple is based on equation 7-4. For the indicators, the line represents the redox potential where the indicator is half-reduced and is based on eq. 7-5 with the formal potential given by eq. 7-6 for Thi and PSaf. For Thi ($E_7^{0\prime}$ = +66 mV (17)) and PSaf ($E_7^{0\prime}$ = -244 mV (17)).

Often the rate of a redox reaction increases if the separation of the redox potentials of the two half-reactions is greater (19, 22).

7.3.2 Kinetic Considerations

Ideally the kinetics of the indicator/H_2 reaction should be rapid to provide a rapid response time and maximize the amount of indicator reduced per unit time for a given H_2 level. The rate of reduction of the oxidized form of the indicator (Ind_{ox}) with H_2 is hypothesized to be of the form

$$\text{Rate} = -d[Ind_{ox}]/dt = k_{obs}\,[Ind_{ox}]^a(P_{H2})^b[H^+]^c \qquad (7\text{-}7)$$

where k_{obs} is the observed rate constant (units dependent on overall form), P_{H2} is the partial pressure of H_2 (atm), $[H^+]$ is the hydrogen ion concentration (M), and a, b and c are the reaction orders with respect to $[Ind_{ox}]$, P_{H2} and $[H^+]$, respectively. For further discussion, the reaction is assumed to be first order in indicator. The value of k_{obs} is expected to depend on the nature of the particular indicator, the type of catalyst, and the surface area of the catalyst. Equation 7-7 serves as a guide for studies in which k_{obs}, a, b and c are determined experimentally. The rate of reduction of a given indicator is directly related to the H_2 partial pressure and (by Henry's law) the concentration of $H_2(aq)$ in the sample. It will be assumed that the sample volume is large enough that the input gas phase H_2 concentration is constant.

Experimentally, the rate of reduction will be evaluated in terms of the rate of decrease or increase in the *fraction of oxidized indicator*, f_{ox}. Measurements are made at the wavelength maximum of the primary visible absorption band of the indicator. For

redox indicators that are colored in the oxidized form, f_{ox} is based on the ratio of the absorbance at any time to the absorbance of the fully oxidized indicator (see Appendix I for more discussion). If both sides of equation 7-7 are divided by the total indicator concentration (oxidized and reduced) with the assumption that a = 1,

$$\text{Rate} = df_{ox}/dt = -k_{obs} f_{ox} (P_{H2})^b [H^+]^c \tag{7-8}$$

The integrated form of equation 7-8 is

$$-\ln (f_{ox}) = k_{obs}(P_{H2})^b [H^+]^c t \tag{7-9}$$

where t is time. Therefore, for the first-order reaction of the indicator with constant H_2 partial pressure and pH, a plot of $-\ln (f_{ox})$ vs t should be linear with a slope related to k_{obs}, P_{H2} and $[H^+]$.

The rate and observed rate constant depend both on the rate of chemical reaction between the indicator and H_2 and the rate of H_2 mass transfer. If the chemical reaction rate is low, the concentration of dissolved H_2(aq) in the indicator solution would approach the value determined by Henry's law constant and P_{H2} ($[H_2(aq)]_{eq}$). If the chemical reaction rate is sufficiently large, then $[H_2(aq)] < [H_2(aq)]_{eq}$ such that the rate of transfer limits the overall rate of reduction and the response time.

7.4 Results and Discussion

7.4.1 Titrations of Thi with H_2

The effect of the concentration of indicator on titration of Thi with 1% H_2 (0.01 atm H_2) is shown in Figure 7.3. The initial slow change in f_{ox} (and -ln (f_{ox})) before 2 min is hypothesized to be due to the finite time required to saturate the solution and Pd with H_2 or to reduce or remove any residual O_2. The initial absorbance of the test solutions varied from 0.3 to 1.8 A.U. It is clear the relative noise was greater with the lowest indicator concentration.

The linearity of the curves (after 2 min) in the semi-log graph (Fig. 7.3B) suggest first-order kinetics for reduction of Thi (23). The slopes vary slightly over a factor of 2 for a range of indicator concentration (varying over a factor of 8) and the order of slopes does not montonically increase with concentration. The differences in the slopes (and k_{obs}) are attributed to differences in the condition or area of the Pd surface in the Pd/alumina pellets in the cuvette. Repetitive measurements were not made to evaluate precision.

Results of titrations of 40 μM Thi with different levels of H_2 are shown in Figure 7.4A. The reduction of the Thi is (generally) rapid and the shape of the titration curve is sigmoidal for H_2 levels down to 0.1% H_2. Below 0.1% (0.001 atm H_2), the shape of the titration curves is less sigmoidal and the curves for 0.01% H_2 and blank (N_2 only) cannot be distinguished. This result suggests that the effective detection limit is around 0.02 % H_2 for this configuration (Thi, Pd/alumina pellets as the catalyst). Unfortunately, this

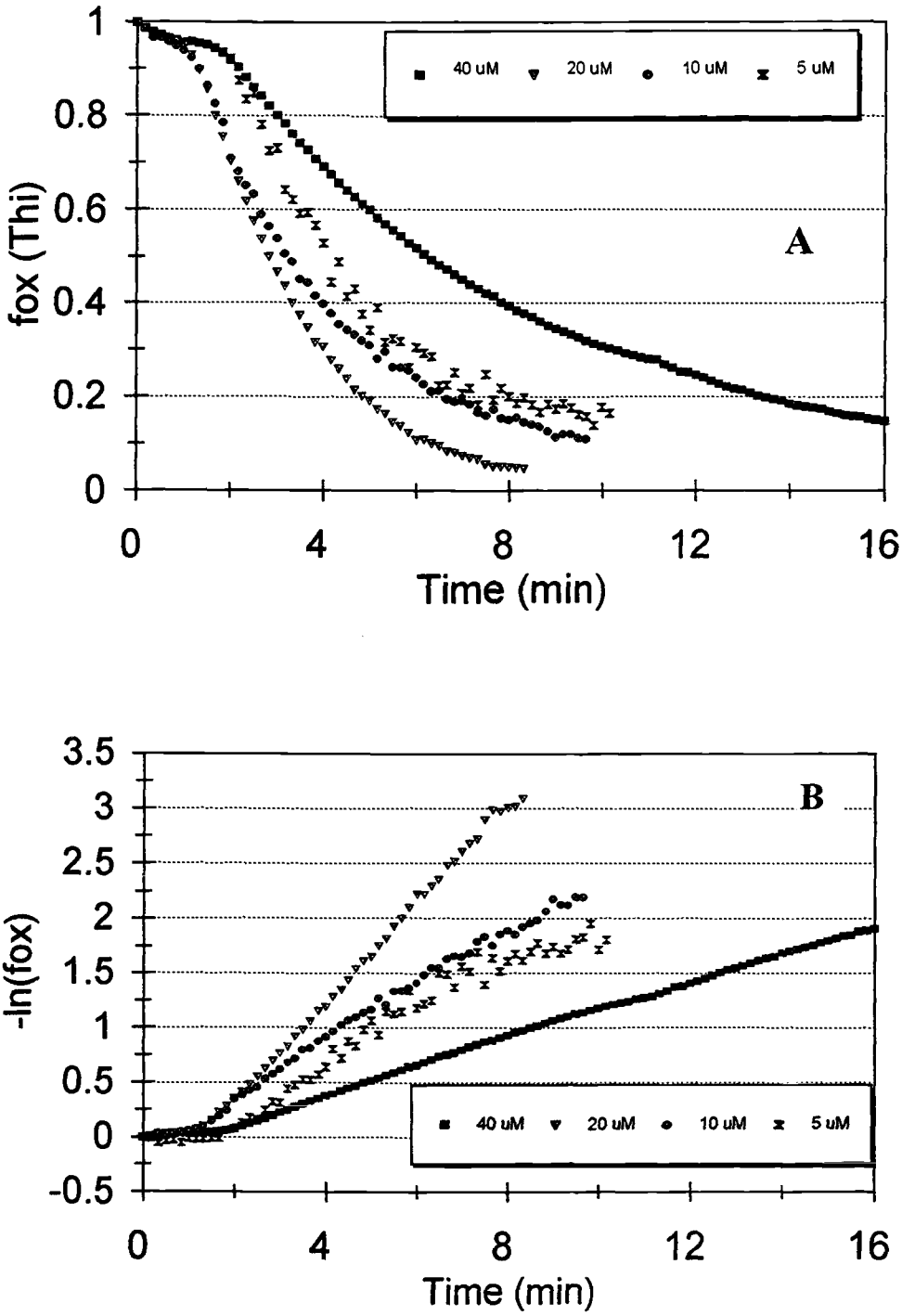

Figure 7.3 Time dependence of reduction of Thi with 1% H_2 on Thi concentration at pH 7. In A, a linear plot is shown, while in B, the data are plotted in a semi-log fashion to illustrate first-order kinetics. The slopes in B (calculated with linear regression) are 0.13 and 0.45 min^{-1} for 40 and 20 μM Thi, respectively.

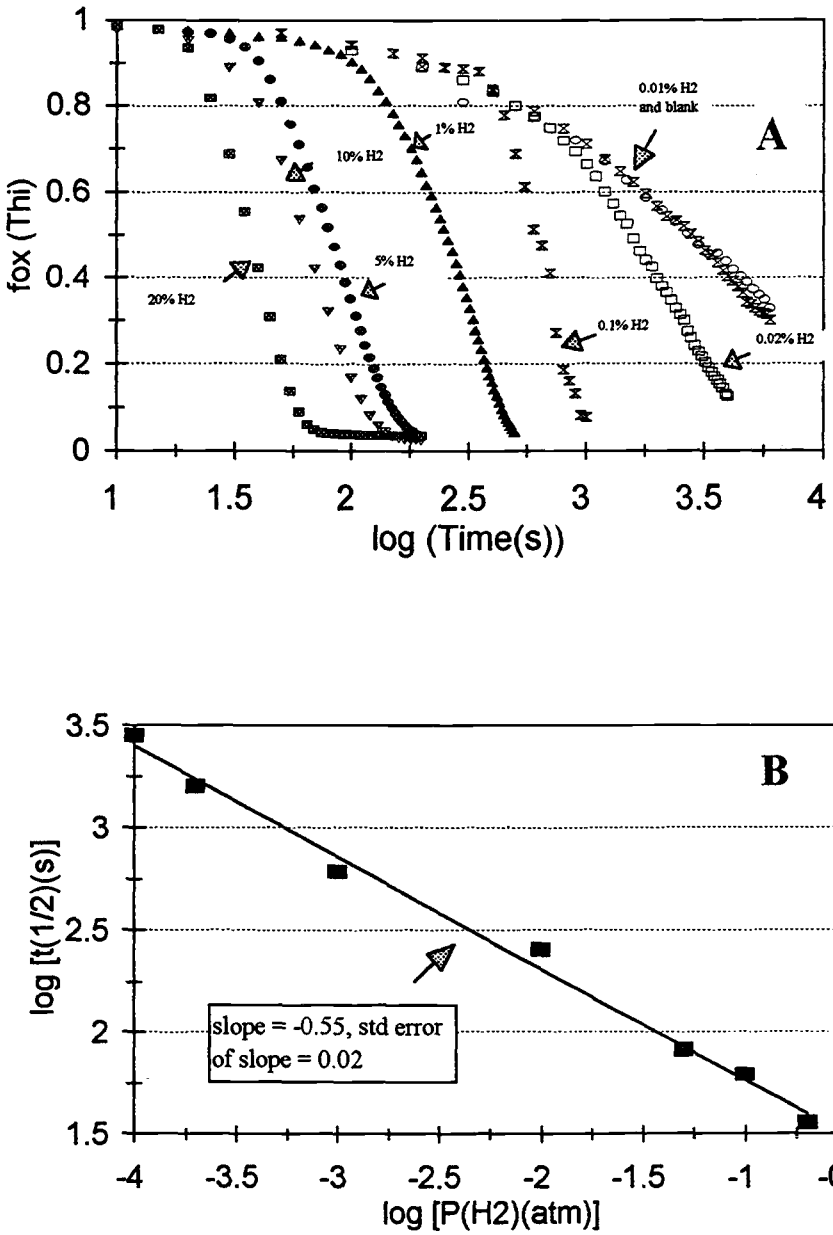

Figure 7.4 Time dependence of reduction of 40 μM Thi on H_2 level at pH 7. In A, a linear plot is shown. In B, the same data are shown in terms of dependence of the *time for half-reduction* ($t_{1/2}$) on H_2 partial pressure. Here, $t_{1/2}$ is the time required to reduce half the indicator ($f_{ox} = 0.5$).

detection limit is two to three orders of magnitude higher than required for determination of H_2 in environmental samples.

The reaction order of $H_2(g)$ can be evaluated from equation 7-9 by finding the dependence of the time necessary for the indicator to reach half-reduction ($f_{ox} = 0.5$) on H_2 partial pressure. Taking the log of both sides, substituting $f_{ox} = 0.5$, and solving for the time yields:

$$\log t_{1/2} = -b \log P_{H2} + K \qquad (7\text{-}10)$$

where $t_{1/2}$ is the *time for half-reduction* and $K = \log (\ln 0.5) + \log k_{obs} + c \log [H^+]$. It is assumed that K, $[H^+]$, and P_{H2} are constant (only the concentration of the oxidized indicator varies during a given experiment).

The plot shown in Figure 7.4B is reasonably linear and the slope of the curve is -0.55. Based on eq. 7-10, the reaction order is 0.5 for P_{H2}. This non-integral order would arise if molecular H_2 splits into a hydride H^- and H^+ ion, or H· radicals, at the Pd surface (22). The rate limiting step would likely be reduction of a Thi molecule by the hydride H^- or the initial one electron reduction by the radical H· (forming a very reactive Thi· species which would quickly react with the adjacent H· radical).

The effect of pH and amount of Pd/alumina catalyst on Thi reduction by H_2 are shown in Figures 7.5A and 7.5B, respectively. The indicator reduction is fastest at pH 7, but the time for complete reduction is within a factor of 2 over the studied pH range. Clearly, there is no strong dependence of the reaction rate on $[H^+]$ which was varied over six orders of magnitude. It appears that the order of the reaction with respect to H^+ (c in equation 7-9) is very near 0.

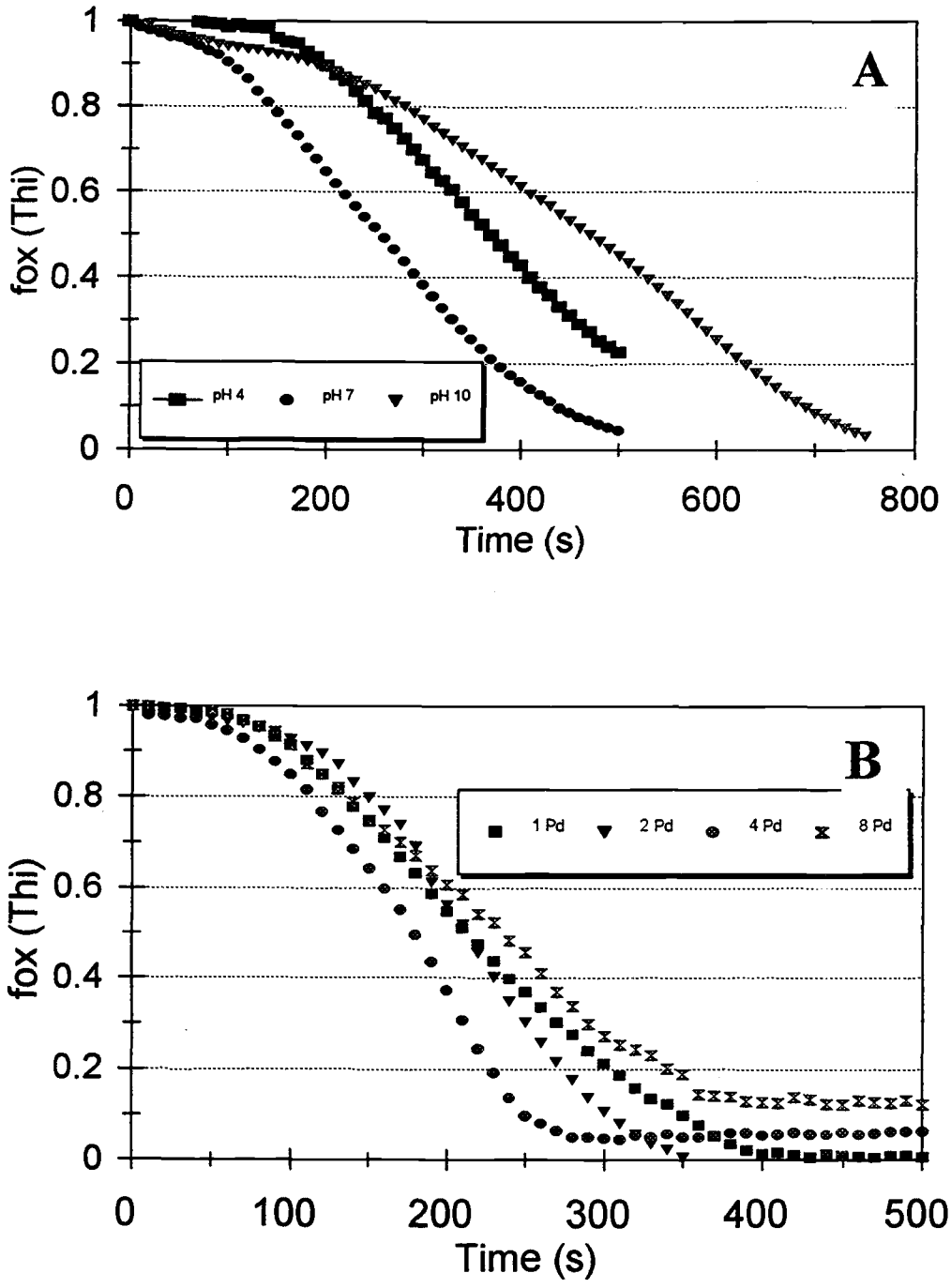

Figure 7.5 Time dependence of reduction of 50 μM Thi (with 2 Pd/alumina pellets as catalyst) with 1% H_2 as a function of pH and total amount of Pd catalyst. In A, pH is varied and in B, the number of Pd/alumina pellets is varied (at pH 7).

The data presented in Figure 7.5B provide no evidence that changing the amount of Pd catalyst affects the reaction rate significantly. This result suggests that there is a sufficient surface area of catalyst for this reaction and that this surface area is not limiting under the conditions studied. Furthermore, with Pd powder as the catalyst (not shown), reductions with 1% and 0.1% H_2 took about the same amount of time as with the alumina form of the catalyst. The surface area of the Pd of the powder form is expected to be considerably greater than that of the pellet form because of the greater total mass of Pd in the powder form. Pd/alumina pellets are estimated to contain ~0.2 mg Pd/pellet (0.5% w/w Pd on each pellet); whereas, 2 - 4 mg of Pd powder was used (5 - 10 times more Pd). This result, along with tests with the pellets, suggests that the surface area of Pd is not limiting. Below 0.1% H_2 with Pd powder, it was difficult to distinguish reduction of Thi from adsorption on the catalyst.

From these results, the integrated forms of the proposed reaction rate equations (7-8 and 7-9) for Thi can be simplified to

$$\text{Rate} = -d[\text{Thi}_{ox}]/dt = k_{obs}\,[\text{Thi}_{ox}](P_{H2})^{1/2} \qquad (7\text{-}11)$$

$$-\ln f_{ox} = k_{obs}(P_{H2})^{1/2}t \qquad (7\text{-}12)$$

Calculated k_{obs} values (based on $t_{1/2}$ data at $f_{ox} = 0.5$ and equation 7-12) for the studies presented in Figures 7-3 to 7-5 are summarized in Table 7.2. The range of values for k_{obs} was 0.014 to 0.045 $atm^{-1/2}\,s^{-1}$ with a pooled average of 0.030 $atm^{-1/2}\,s^{-1}$ and standard deviation of 0.01 $atm^{-1/2}\,s^{-1}$. The values of the rate constant obtained during the pH study were about 50% lower than the values in the other studies. There are not enough data to judge the significance of this difference. It is possible that the type of pH buffer has a modest effect on the rate of reduction.

Table 7.2 Calculated k_{obs} values.[a]

method	condition	k_{obs} [$atm^{-1/2} s^{-1}$]	mean ± std dev [$atm^{-1/2} s^{-1}$]
Dependence on [Thi]	5 μM Thi	0.030	
(Figure 7.3)	10 μM Thi	0.036	
	20 μM Thi	0.043	
	40 μM Thi	0.020	0.032 ± 0.01
Dependence on P_{H2}	0.2 atm H_2	0.046	
(Figure 7.4)	0.1 atm H_2	0.037	
	0.05 atm H_2	0.039	
	0.01 atm H_2	0.028	
	10^{-3} atm H_2	0.037	
	2×10^{-4} atm H_2	0.030	
	1×10^{-4} atm H_2	0.025	0.035 ± 0.007
Dependence on pH	pH 4	0.023	
(Figure 7.5A)	pH 4'[b]	0.015	
	pH 7	0.026	
	pH 7'	0.026	
	pH 10	0.017	
	pH 10'	0.014	0.020 ± 0.006
Dependence on Pd mass/	1 Pd pellet	0.033	
surface area	2 Pd pellets	0.033	
(Figure 7.5B)	4 Pd pellets	0.039	
	8 Pd pellets	0.028	0.033 ± 0.006

[a] These values were calculated with eq. 7-12.
[b] A prime indicates a duplicate run.

In Figure 7.6, results of blank titrations (with pure N_2 gas) of Thi with two Pd/alumina pellets at pH values of 4, 7 and 10 and with Pd powder at pH 7 are presented. These data make it clear that the adsorption of Thi, particularly with the Pd/alumina pellets, limits the measurement of low levels of H_2. The rate of reduction appears somewhat lower at pH 4 for the Pd/alumina pellets and for the pure Pd. After ~350 hr, the cuvettes were opened to the atmosphere (and atmospheric O_2) and no re-oxidation of the Thi was noted (adsorption continued until the solutions were colorless ($f_{ox} = 0$)). This result confirms that the decrease in f_{ox} was not due to reduction by residual H^- or $H\cdot$ radicals adsorbed on the Pd surface.

Pd can chemically interact with S atoms (24, 25). Hence, it is expected that the sulfur atom in the Thi molecule chemisorbs on the Pd surface. An indicator without a S atom in its structure (e.g., PSaf, BV, MV in Figure 7.1) may not adsorb as strongly as Thi and potentially may provide a lower detection limit for H_2 determination.

Overall, the results suggest that the rate of reduction of thionine observed is limited by the reaction kinetics between Thi and H_2 at the surface of Pd, the reaction is first order in indicator and one-half order in H_2, and the detection limit is limited by the adsorption of indicator on the Pd surface. The mass transfer rate of H_2 to the indicator solution is not limiting. For example, the time to reduce 90% of 40 μM Thi (0.080 μmol in 2 mL) with 0.1% H_2 is ~15 min (Fig. 7.4A). With the gas bubbling rate used (50 mL/min), the molar delivery rate is ~2 μmol/min or ~30 μmol in 15 min which greatly exceeds the total amount of Thi in the cuvette. Clearly, the efficiency of utilization of the delivered H_2 to reduce Thi is very low.

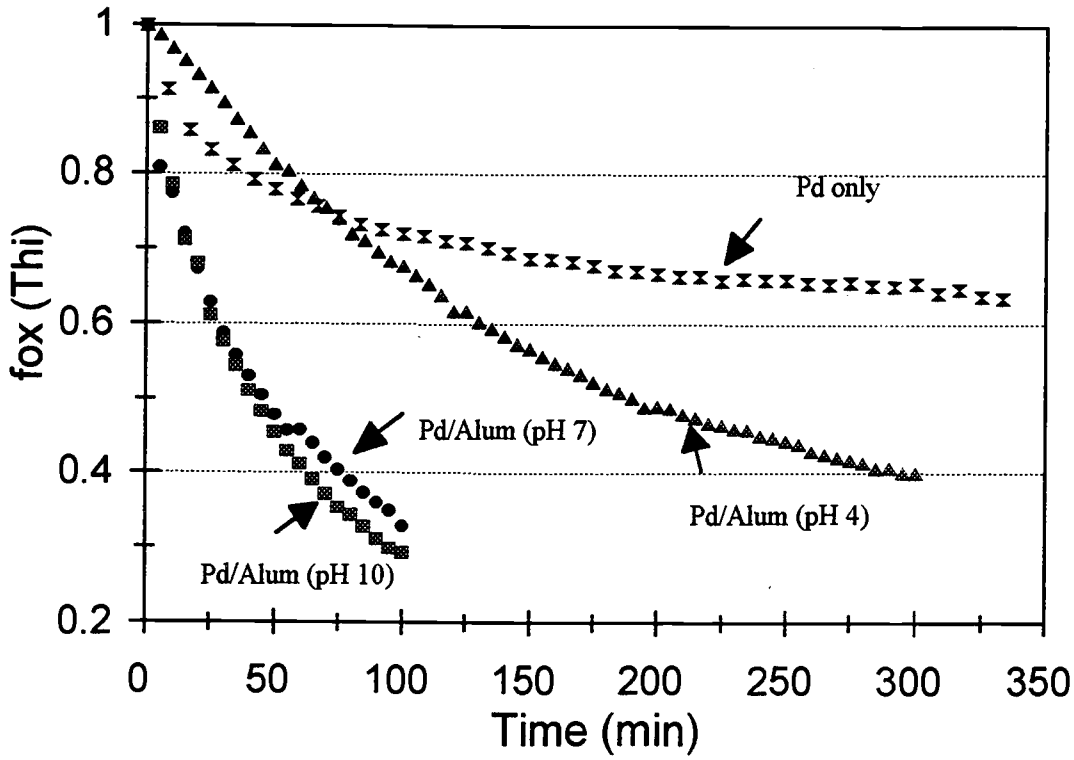

Figure 7.6 Blank titrations of Thi with Pd/alumina pellets at pH values of 4, 7 and 10 and with Pd powder at pH 7. Two Pd/alumina pellets (~0.4 mg Pd) were used at each pH and ~3 mg Pd powder was used in one experiment (at pH 7).

7.4.2 Titrations of PSaf, BV and MV with H_2

Although PSaf did not adsorb as readily on Pd at pH 10 as Thi, the rate of reduction of PSaf with H_2 was significantly lower than that with Thi and no reduction of 40 μM PSaf with 0.1% H_2 was observed (decrease in the color intensity) after 2 - 3 hr. The lower rate of reduction of PSaf may be related to its lower formal potential ($E_7^{0\prime}$ = -244 mV) relative to Thi ($E_7^{0\prime}$ = +66 mV).

A PSaf solution was first reduced with 1% H_2 and then bubbled with 0.1% H_2 for over 6 hr. No coloration (oxidation) of the PSaf in solution was observed which suggests that the slow reduction of PSaf was not limited by residual O_2 in the N_2 or H_2 tanks. Because of the poorer detection limit for H_2 and slower reaction rates with PSaf, no more studies were conducted with this indicator.

For H_2 determination, one has the choice of using an indicator that is colored in the oxidized form (case 1) or in the reduced form (case 2). For organic indicators such as Thi and PSaf, equation 7-11 applies and the reaction is first order in the indicator. The rate of reaction (μmol/min) and rate of increase in absorbance (dA/dt) are also proportional to indicator concentration. The length of time to *achieve a given level (fraction) of reduction* is independent of the indicator concentration (eq. 7-12).

For indicators that are colored when oxidized but become colorless when reduced, the maximum indicator concentration is limited by the maximum absorbance that can be accurately monitored with the spectrophotometer at a given wavelength and cell pathlength. In general, this maximum absorbance is about 2 because at high absorbance non-linearity due to factors such as stray light become important and the noise in the

absorbance, σ_A, increases (26). For indicators with a molar absorptivity of about 5 x 10^4 AU/M-cm the maximum concentration is 40 μM.

With an indicator that is colorless when oxidized but that becomes colored when reduced, the indicator concentration can be much higher because the initial absorbance is zero. For case 2 (relative to case 1), the detection limit can be improved because the noise (σ_A) is often less at lower absorbances and the reaction rate and dA/dt are higher (if the molar absorptivity of the monitored species is the same). If the indicator concentration is increased by a factor of 10, then the same rate (dA/dt or ΔA in a given measurement period) is obtained with 1/100 the H_2 concentration yielding a factor of 100 improvement in detection limit. This calculation is based on equation 7-11 for ½ order in H_2. Here it is assumed that the rate of reduction is limited by reaction kinetics and not mass transfer and that the aqueous H_2 concentration remains at the equilibrium value predicted by Henry's law.

For very low levels of H_2, the fraction of indicator reduced is essentially small and 7-11 simplifies to

$$\text{Rate} = -d[\text{Ind}_{ox}]/dt \approx -k'_{obs}(P_{H2})^{½} \qquad (7\text{-}13)$$

where $k'_{obs} = k_{obs}\,[\text{Ind}_{ox}]_o$ and $[\text{Ind}_{ox}]_o$ denotes the initial concentration of the indicator (fully oxidized). With a higher concentration of an indicator which is colored only in the reduced form, it should be possible to measure this initial rate. With an indicator that is colored only in the oxidized form, it may be necessary to reduce a larger fraction of the indicator to obtain a large enough absorbance difference to measure accurately and the reaction rate would decrease over the measurement period.

At a very high concentration of indicator and low H_2 partial pressure, the rate of reduction would become limited by the absolute mass transfer rate of H_2 into the indicator solution. For example, with 1 mM indicator in 2 mL of solution (2 μmol), 10^{-4} % H_2, and a gas bubbling rate of 50 mL/min, the mass delivery rate of H_2 is ~0.002 μmol/min and it would take ~2 min to deliver enough H_2 to reduce 4 nmol of indicator (2 μM of reduced indicator or 0.2% of the total amount of indicator). For this case and a reduced indicator with a molar absorptivity of 5 x 10^4 AU/M-cm (in a 1-cm pathlength cuvette), the solution absorbance would be 0.1 AU. From equation 7-12 with the k_{obs} for Thi (0.033 $atm^{-½}$ s^{-1}, Table 7.2) the time to reduce 4 nmol of indicator is calculated to be 60 s. Under these conditions, both chemical kinetics and mass transfer affect the rate of reduction of the indicator. It appears detection of H_2 at low levels (0.8 nM in ground water samples) is feasible (in terms of the length of time for analysis) only if the rate constant and molar absorptivity of the reduced species are high enough. Analysis times in excess of 10 min or so may be inconvenient for many field applications.

Titrations of BV ($E^{0'}$ = -359 mV) and MV ($E^{0'}$ = -446 mV) with 100% H_2 at pH 11.5 - 12 were rapid, producing dark violet and blue solutions (values for λ_{max} for BV and MV are 548 nm and 624, respectively (14)). With 1% H_2, the rate of reduction was considerably slower and neither indicator was significantly reduced (i.e., no color was observed) after 1 hr of contact with 0.1% H_2.

At pH 13, where the difference in reduction potentials between the H_2 and the indicators is greater (see Figure 7.2), no reduction of BV or MV was observed within 2 hr with 0.1% H_2. At pH 14 (and greater), the oxidized forms of both indicators

precipitated as a bluish solid and therefore could not be used. No further experiments with BV or MV were conducted.

7.4.3 Titration of Fe(III)-$(OP)_3$ with H_2

The Fe(III)-$(OP)_3$ complex is very slightly colored (λ_{max} = 590 nm, ϵ = 600 M^{-1} cm^{-1} (16)) compared to the highly colored reduced complex (Fe(II)-$(OP)_3$, λ_{max} = 510 nm, ϵ = 11,100 M^{-1} cm^{-1} (17)). Because the initial absorbance is low, [Ind_{ox}] can be adjusted to relatively high concentrations to increase the rate of the reaction of the indicator with H_2 (Figure 7.7). Thermodynamically, H_2 should be an effective reductant of Fe(III)-$(OP)_3$ at any pH because the reduction potential for the half-reaction of Fe(III)/Fe(II)-$(OP)_3$ is very high ($E^{0\prime}$ = 1.12 V (17)) and not pH dependent.

Results of titrations of Fe(III)-$(OP)_3$ with different levels of H_2 at pH 4 are shown in Figure 7.8A. For 0.1% H_2 and lower, the rate of reduction was relatively constant. With 1% H_2, the rate first increases and then tapers off when the reduction reaction nears completion. The slower increase in absorbance after ~1.2 AU is attributed to increased scattering over time by Pd particles that desorb from the alumina. No tendency of the Fe(II)$(OP)_3$ complex to adsorb on the Pd was observed even after 2 days.

A primary limitation of the use of Fe(III)-$(OP)_3$ as the redox indicator is the large blank rate which is greater when Pd is present suggesting that Pd is a catalyst. The signal and slope of the curve with 0.01% H_2 are only slightly greater than that of the curve of the blank (w/Pd) (0.21 AU/hr compared to 0.18 AU/hr). Therefore, ~0.01% H_2 is the lower limit for H_2 detection.

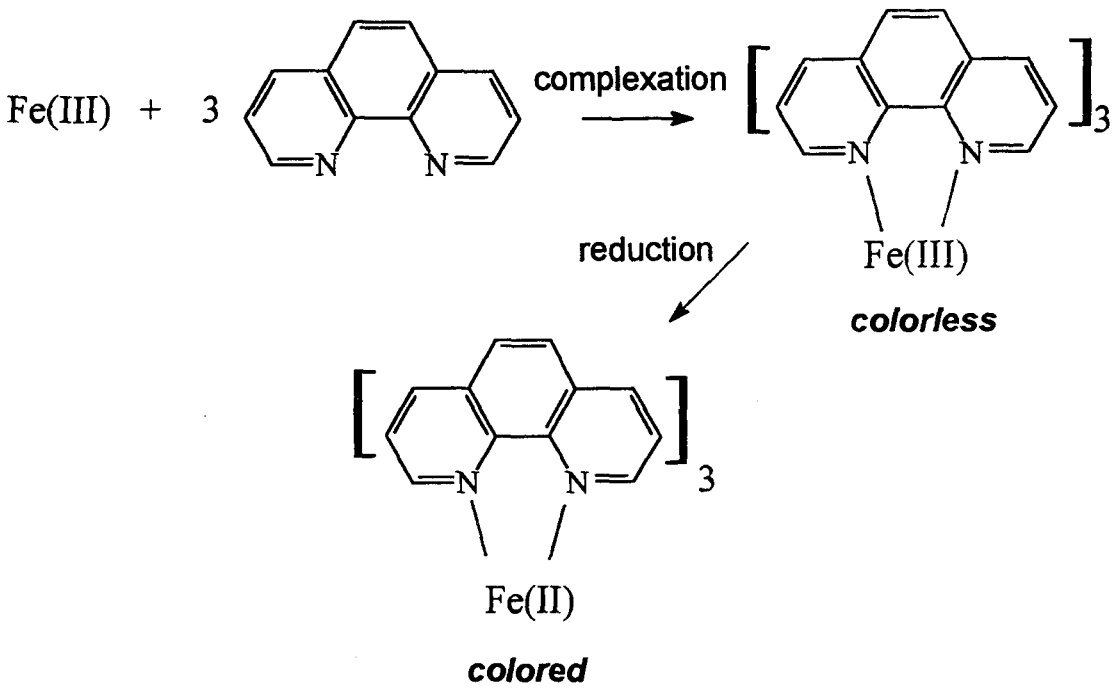

Figure 7.7 Chelation of Fe(III) with OP to form a tris-chelate. The Fe(III)-$(OP)_3$ can subsequently be reduced to form the highly colored Fe(II)-$(OP)_3$ complex.

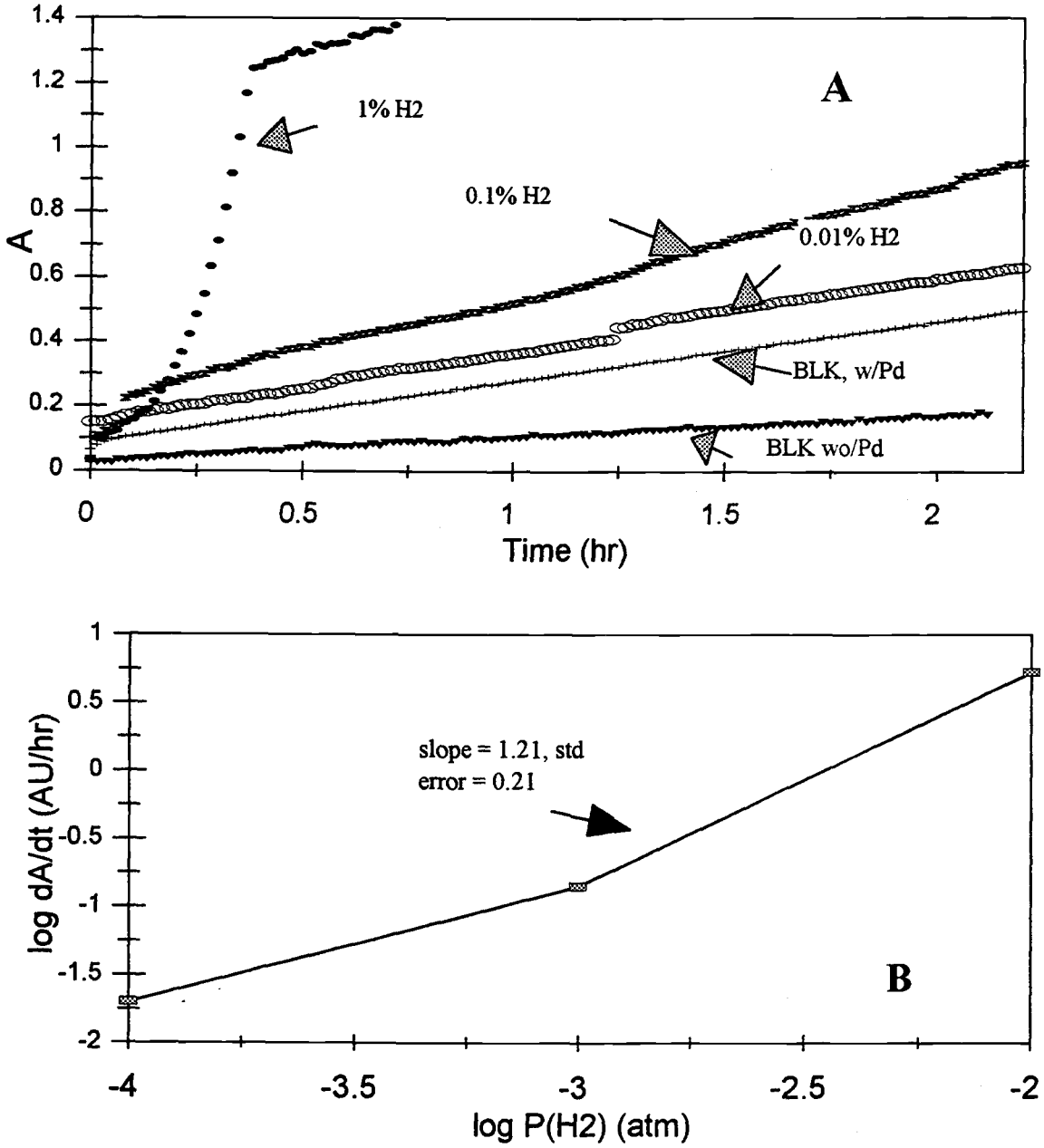

Figure 7.8 Time dependence of reduction of Fe(III)-$(OP)_3$ with H_2 at pH 4. In A, the absorbance of the Fe(II)-$(OP)_3$ complex is shown over time. The total initial concentration of Fe(III)-$(OP)_3$ was estimated to be 0.11 mM. The blank rate (for BLK w/Pd) is 0.19 AU/hr. The slopes of the 1%, 0.1% and 0.01% H_2 titration curves (5.5, 0.33, and 0.21 AU/hr, respectively) are calculated from data in the linear portions of the curves. For 1% H_2, the slope was calculated based on data between 0.25 and 0.36 hr. The blank corrected rates are 5.31, 0.14 and 0.02 AU/hr, respectively. In B, the log values of the rate and P_{H2} are plotted.

The log-log plot (Figure 7.8B) suggests that there is no consistent reaction order with respect to H_2. The order appears to change from below 1 to greater than one as H_2 partial pressure increases. There is great uncertainty in the point for 0.01% H_2 because it is so similar to the blank rate. The dependence of the rate on H_2 partial pressure should be established with more experiments.

It is hypothesized that the blank rate is due to the Fe(III)-$(OP)_3$ complex oxidizing H_2O. The formal potential of the complex ($E^{0\prime}$ = 1.12 V (17)) is above the E_H/pH line for the O_2/H_2O couple ($E^{0\prime}$ = 1.229 V (27)) for pH values above 1 with P_{O2} = 0.001 atm and $P_{O2} = 1 \times 10^{-7}$ atm as shown in Figure 7.9. The wavelength maximum and width of the visible absorption band formed in the blank reaction appeared identical to the band formed with reduction by H_2. Interestingly, the formal potential of the Fe complex couple is also greater than that of Pd^{2+}/Pd couple ($E^{0\prime}$ = 0.83 V (27)) and therefore, the complex could (theoretically) oxidize the Pd catalyst. Comparatively, the formal potential for Pt ($E^{0\prime}$ = ~1.2 V (27)), another catalyst for the reaction (16) is greater than the Fe(III)-$(OP)_3$ couple such that Pt should therefore remain inert.

The effect of pH on the blank rate and analyte rate (H_2 present) was evaluated. Titrations of Fe(III)-$(OP)_3$ at pH values of 7 and 10 yielded rates and detection limits similar to those obtained at pH 4, except that the titration at pH 10 took ~30% longer. With 1% H_2 and 0.1 and 0.2 M H_2SO_4 (estimated as pH 0.7 and 0.4, respectively), the blank and analyte rates of reduction were slightly greater than those at pH 4. At 0.5 M H_2SO_4, no complexation of the Fe(III) was observed and is attributed to protonation of one (or both) of the N atoms in the OP at this low pH. Overall, there was no advantage

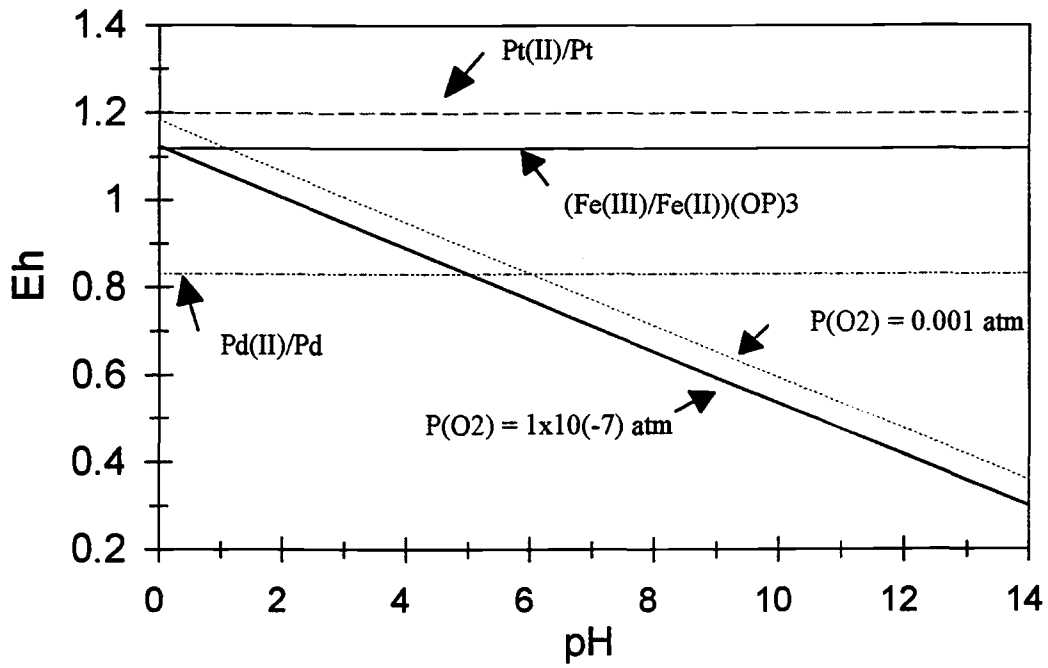

Figure 7.9 Dependence of reduction potential on pH for indicator, water and catalysts. The potential curves for water were calculated based on an O_2 partial pressure of 0.001 atm (arbitrary) and $1x10^{-7}$ atm (calculated from purity level of O_2 in H_2 tank). The E_H/pH equation for O_2/H_2O at 25°C is $E_H = 1.229 - (0.059/4) \log (1/P_{O2}) - 0.059$ pH (27).

to performing the reaction at any particular pH because the blank and analyte rates track each other.

Different catalysts were tested. With Pt/alumina pellets, blank and analyte rates were slightly slower than for Pd. When Pd powder was added directly to a solution of the Fe(III)-$(OP)_3$ complex, the color turned orange (indicative of the maximum absorbance at 510 nm) within seconds. This behavior suggests that most of the Fe(III)-$(OP)_3$ complex was rapidly reduced to the Fe(II) complex in the presence of large amounts of Pd (relative to the experiments with Pd/alumina). Furthermore, this (hypothesized) oxidation of water by the Fe(III) complex may be photocatalyzed (25, 28). The absorbance of a solution of Fe(III)-$(OP)_3$ stored overnight, without Pd or Pt and in a dark place, changed little. Upon exposure to light, the solution turned colored within a couple of hours. Because of the blank rate, no further tests with Fe(III)-$(OP)_3$ as an indicator for H_2 were conducted.

7.4.4 Tests of other chelated Fe(III) and Cu(II) species

Several different chelating agents were evaluated to determine if any Fe(III)-organic chelate indicator complexes could be identified which are not spontaneously reduced in the presence of a catalyst. In general, chelating agents were chosen which formed Fe(III)/Fe(II) complexes with a lower formal potential than that of OP to minimize reduction of the indicator by H_2O. This search was expanded to include Cu(II)/Cu(I)-chelates which normally have a formal potential 0.3 - 0.4 V lower than that

of the corresponding Fe(III)/Fe(II) complex and is not pH dependent (17). Spectral information about the chelates is summarized in Table 7-3.

None of the Fe(III)-complexes formed with the chelating agents listed in Table 7.1 remained in the oxidized state in the presence of Pd for longer than 2 hr. Two of the compounds, 2-mercaptopyridine and dimethylglyoxime, did not chelate either the Fe(III) or Fe(II) ions (tested at pH 4 and 7). For Cu(II), only neocuproine hydrochloride hydrate, *syn*-2-pyridinealdoxime and di-2-pyridyl ketone oxime chelated the metal ion.

Of all the chemical species tested, only the Cu(II) complexes formed with *syn*-2-pyridinealdoxime and di-2-pyridyl ketone oxime were not reduced to the Cu(I) forms in the presence of Pd powder, even after 2 days. These complexes were reduced by 100 and 1% H_2, but not with 0.1% H_2.

Table 7.3 Wavelength maxima and molar absorptivities of Fe and Cu complexes.[a]

chelating agent	λ_{max} (nm) and ϵ Fe(III) species	λ_{max} (nm) and ϵ Fe(II) species	λ_{max} (nm) and ϵ Cu(II) species	λ_{max} (nm) and ϵ Cu(I) species
1,10-phenanthroline	590[b], 600[b]	510[b], 1.1×10^4[b]	no chelation	no chelation
dicyano-bis(1,10-phenanthroline) iron(II) complex	could not oxidize	516, 8.2×10^3	NA	NA
4,7-dimethyl-1,10-phenanthroline	510, 1.9×10^3[c]	512, 1.4×10^4	no chelation	no chelation
3,4,7,8-tetramethyl-1,10-phenanthroline	502, 3.4×10^3[c]	502, 1.6×10^4	no chelation	no chelation
neocuproine hydrochloride hydrate	no chelation	no chelation	454, 3.2×10^3[c]	452, 5.6×10^3
2,2'-dipyridyl	524, 3.8×10^3[c]	524, 8.8×10^3	no chelation	no chelation
4,4'-dimethyl-2,2'-dipyridyl	528, 1.9×10^3[c]	528, 1.2×10^4	no chelation	no chelation
syn-2-pyridinealdoxime	518, 5.4×10^3	490, 8.5×10^3	none detected	410, 6.6×10^3
di-2-pyridyl ketone oxime	530, 4.8×10^3	582, 1.3×10^4[d]	none detected	428, 4.4×10^3
2-mercaptopyridine	no chelation	no chelation	no chelation	no chelation
dimethylglyoxime	no chelation	no chelation	no chelation	no chelation
4-amino-5-isopropylsulphonyl-2-(pyrid-2-yl) pyrimidine	398, 2.0×10^3	370, 6.1×10^3	442, 1.0×10^3	414, 1.5×10^3

[a] Wavelength in nm and ϵ in AU cm^{-1} M^{-1}
[b] Data from Bishop (16).
[c] Oxidized form rapidly reduced such that the measured λ_{max} and ϵ values may actually be for the reduced form.
[d] Oxidized form cloudy.

7.5 Conclusions

The design of sensors based on redox indicators for low-level H_2 determination was considered in terms of the mode of transfer of H_2 from the sample to the indicator solution (gas or solution mass transfer) and the characteristics of the redox indicator. Gas transfer was chosen for experimental studies because of the potential for higher selectivity and higher mass transfer rates. A variety of redox indicators were investigated as to their suitability for this application. The reduction reactions between H_2 and the indicators Thi and Fe(III)-$(OP)_3$ were studied in the greatest detail.

Although none of the indicators tested were found to be suitable for determining H_2 at the low levels expected in environmental samples, insight was gained as to what characteristics of a redox indicator are critical in this application and include:

1) a formal potential significantly above ($\geq$ 0.5 V) the calculated potential for the H^+/H_2 couple at a given H_2 partial pressure and pH;

2) a reaction rate high enough to generate enough reduced indicator to detect in a reasonable time (e.g., 10 min);

3) high molar absorptivity for the monitored form ($> 10^4$ M^{-1} cm^{-1});

4) no sorption to surface of the catalyst (Pd or Pt);

5) no blank reaction (indicator reduction in the absence of H_2); and

6) colored in its reduced form rather than its oxidized form

With an indicator that is initially colorless, the indicator concentration can be higher which increases the rate of reduction of the indicator.

If Thi could be used at a 1 mM concentration (the absorbance would be far greater than 2), the *initial* rate of reduction of Thi, calculated from equation 7-11 with 10^{-6} atm H_2 and a k_{obs} of 0.033 $atm^{-1/2}$ s^{-1} (from Table 7.2), would be ~33 nM/s. It would take only ~60 s to reduce 2 μM Thi and yield an absorbance change of ~0.1 AU. The total concentration of oxidized Thi would be effectively constant. In contrast, with 1/25 the Thi concentration (40 μM) and all other conditions identical, the initial (calculated) reduction rate is 1.3 nM/s and it would take ~25 min to reduce 2 μM Thi (to $f_{ox} = 0.95$). Thi would begin to adsorb to the Pd/alumina pellets or the Pd catalyst long before this condition was reached (Figures 7.4A and 7.6). From this example, clearly the kinetics of reduction of Thi are rapid enough for the purpose of H_2 detection. However, the fact that Thi is colored when oxidized and that Thi adsorbs to Pd prevents its use for low H_2 level determination.

Organic indicators colored in the oxidized form (Thi and PSaf) and in the reduced form (BV and MV) were tested. Of all the indicators evaluated, Thi gave the best results with an effective detection limit for H_2 of ~0.02% (0.0002 atm or 0.16 μM in solution). The rate of reduction was first order in indicator and half order in hydrogen. Low-level H_2 determination was limited by chemisorption of Thi on the Pd catalyst. PSaf did not adsorb on Pd to the same extent as Thi, but the rate of reduction was much lower yielding a detection limit of about ~1% H_2 gas.

Although BV and MV are colored only in their reduced form and were tested at concentrations about a factor of 25 higher than that used for Thi, the effective detection limit was only ~1% H_2. Thermodynamically, the reduction of these indicators by H_2 is favorable, but the rate of reduction was low relative to Thi.

Several redox-active Fe and Cu chelates were evaluated. It was thought that these types of indicators would be well suited for this application because they are colored only in the reduced form and have very high formal potentials (i.e., the reaction with H_2 is thermodynamically favorable). However, the high formal potential appears to be a disadvantage because a blank rate is observed and is attributed to the oxidation of water by the complex. Furthermore, this "blank reaction" appears to be photochemical in nature. With the Fe(III)-$(OP)_3$ complex, the effective lower limit of detection was between 0.1 and 0.01% H_2, in the range observed with Thi. With complexes of Fe(III) or Cu(II) with many other chelating agents, a "blank reaction" was observed in most cases.

Clearly, the development of a H_2 sensor suitable for environmental assessment is dependent on finding an indicator (and conditions) that better meets the criteria established than do the indicators tested to date. In particular, a higher rate of reduction for a given level of H_2, with a stable baseline in the absence of H_2 (e.g., no sorption of the indicator or reduction of the indicator by water), is desired.

Future studies might include exploration of homogenous catalysts (generally organometallic complexes (29)) which may speed up the reaction rate (25). Also, it may be possible to couple a colorless redox-active species with a redox indicator. One redox species at high concentration which is colorless in both states (such as a quinone) would be chosen to react rapidly with H_2. An indicator species (e.g., Thi) in the same spectrophotometric cell would be reduced by the reduced form of the first species and the colored form of the indicator would be monitored spectrophotometrically to determine the rate of reduction.

7.6 References

1. Chapelle, Francis H.; McMahon, Peter B.; Dubrovsky, Neil M.; Fujii, Roger F.; Oaksford, Edward T.; Vroblesky, Don A., *Water Resour. Res.*, **1995**, *31*, 359-371.

2. Chapelle, Francis H.; Haak, Sheridan K.; Adriaens, Peter; Henry, Mark A.; Bradley, Paul M., *Environ. Sci. Technol.*, **1996**, *30*, 3565-3569.

3. Lovley, Derek R.; Chapelle, Francis H.; Woodward, Joan C., *Environ. Sci. Technol.*, **1994**, *28*, 1205-1210.

4. Lovley, Derek R.; Goodwin, Steve, *Geochim. Cosmochim. Acta*, **1988**, *52*, 2993-3003.

5. Vancheeswaran, Sanjay; Halden, Rolf U.; Semprini, Lewis; Williamson, Kenneth J.; Ingle, James D. Jr., "Abiotic and Biological Transformation of Tetraalkoxysilanes and Trichloroethene/cis-1,2-Dichloroethene Cometabolism Driven by Tetrabutoxysilane-Degrading Microorganisms", *Environ. Sci. Technol.*, in press.

6. Fennell, Donna E.; Gosset, James A.; Zinder, Stephen H., *Environ. Sci. Technol.*, **1997**, *31*, 918-926.

7. Vancheeswaran, Sanjay, Private communication, Oregon State University, July 18, 1998.

8. Lotrario, Joe, Private communication, Oregon State University, August 3, 1998.

9. Ingle, James D. Jr., Private communication, Oregon State University, January 11, 1997.

10. Jones, Brian, Chapter 4 in this thesis.

11. Jones, Brian, Chapter 5 in this thesis.

12. Jones, Brian, Chapter 6 in this thesis.

13. Lemmon, T. L.; Westall, J. C.; Ingle, J. D. Jr., *Anal. Chem.*, **1996**, *68*, 947-953.

14. Lemmon, Teresa, *Development of Chemostats and Use of Redox Indicators for Studying Transformations in Biogeochemical Matrices*, **1995**, Ph.D. thesis, Oregon State University.

15. Mobley, James, Oregon State University, unpublished report, **1992**.

16. Jones, Brian, Laboratory notebook #4, 1996, Oregon State University.

17. *Indicators*, Bishop, E., Ed., Pergamon Press: Oxford, 1972.

18. Hand, Clifford W., *General Chemistry*, Saunders College Publishing, 1996.

19. Jones, Brian, personal research experience, Oregon State University, 1993-1998.

20. Baham, John, Private communication, Oregon State University, June 3, 1994.

21. McBride, Murray B., *Environmental Chemistry of Soils*, Oxford University Press, Inc., 1994.

22. Shriver, Duward F.; Atkins, Peter; Langford, Cooper H., *Inorganic Chemistry*, Second Edition, W.H. Freeman and Co.: 1994.

23. Levenspiel, Octave, *Chemical Reaction Engineering, 2nd Ed.*, John Wiley & Sons, Inc.: 1972.

24. Westall, John C., Private communication, Oregon State University, December 10, 1997.

25. Lerner, Michael M., Private communication, Oregon State University, December 13, 1997.

26. Ingle, James D. Jr.; Crouch, Stanley R., *Spectrochemical Analysis*, Prentice Hall, Englewood Cliffs, New Jersey: 1988.

27. Bard, Allen J.; Faulkner, Larry R., *Electrochemical Methods: Fundamentals and Applications*, John Wiley & Sons: 1980.

28. Turner, Gary, Private communication, Oregon State University, March 16, 1998.

29. Chaloner, Penny A., *Hydrogenous Hydrogenation: Catalysis by Metal Complexes, Vol. 15*, Kluwer Academic Publishers, Dordrecht: 1994.

CHAPTER 8: CONCLUSIONS AND FURTHER STUDIES

In this thesis, studies of three major topics relating to evaluation of the redox status of environmental samples have been presented:

1) environmental redox species and factors affecting the response of the Pt electrode

2) applications of redox indicators to evaluate redox status

3) applications of redox indicators for determination of H_2.

These three topics are interrelated and results in each area have been helpful in gaining insight into the other areas.

8.1 Redox measurements with Pt electrodes

Due to its ease of use, the Pt electrode is a convenient sensor for measuring the redox status of environmental systems. However, the absolute value of its potential (E_{Pt}) cannot generally be correlated to concentrations of specific redox-active species or the dominance of a particular microbial process. The value of E_{Pt} is a function of a number of different factors including certain redox-active species (and their concentrations), pH, the history and condition of the particular Pt electrode (oxide coatings, biofilms, cleaning of the Pt surface), factors affecting transport of species to the Pt surface (sample stirring, covering the electrode with a membrane), and ionic strength. Due to this variety of factors, it is not surprising that we and other researchers (1) have observed many inconsistencies in the use of E_{Pt} to evaluate redox status.

The response of the Pt electrode to many redox-active species was evaluated in simple electrolyte solutions and by addition of species to soil or wastewater slurries under anaerobic conditions. Of all the common inorganic redox species studied, only O_2, H_2O_2, Fe(II), Fe(III) and S(-II) appear to have some effect (direct or indirect) on E_{Pt}. Both O_2 and H_2O_2 appear to affect E_{Pt} by oxidation of other species affecting E_{Pt} or modification of the surface of the electrode (e.g., PtO formation). Physical or chemical "cleaning" of the electrode surface significantly affects the potential and response time of a Pt electrode, especially for samples with E_{Pt} above 0 V.

Addition of either S(-II) or Fe(II) was found to cause a direct but non-Nernstian effect (decrease in E_{Pt}) in simple electrolyte systems that was reversed when the added species was removed by precipitation or complexed by a complexing agent. In soil or wastewater slurries, addition of Fe(II) or S(-II) decreased E_{Pt} when added at E_{Pt} values greater than about 100 mV or -250 mV, respectively. For Fe(II), the effect appears to be only indirect (by reducing a species currently affecting E_{Pt} or poising the Pt electrode). No evidence was found that E_{Pt} varied as log [Fe(II)] or log [S(-II)] (a Nernstian response) in real systems or was changed if S(-II) was precipitated in wastewater slurries under sulfate-reducing conditions.

In the course of experiments with two Pt electrodes in either soil slurries or electrolyte solutions, the potentials often differed by a relatively constant value (typically 25 - 50 mV), but the *dynamics* of the response were often similar (i.e., the direction and rate of change of potential). The difference between the two potentials became less pronounced as the system became more reducing which suggests that the Pt electrode is better poised under more reducing conditions.

With the reversible ferrous/ferric hexacyano couple, good poising was observed when the concentration of both forms of the redox couple were ~5 μM or greater (in agreement with findings of Kempton (2)) and ionic strength above ~10 mM. These values provide a guideline to assess the potential of a specific redox couple poising the Pt electrode in environmental samples. Clearly, there are some redox species affecting E_{Pt} in environmental systems, but low concentrations of reversible couples and low ionic strength may be a major contributing factor in the many inconsistencies in redox measurements with Pt electrodes.

The observations in this thesis are consistent with the following hypotheses or recommendations:

1) In less reducing samples (E_{Pt} > 0 V at pH 7), the Pt electrode is generally not well poised, responding to mixed potentials; E_{Pt} may be influenced strongly by Pt electrode films (e.g., PtO layers) at the surface.

2) Under more reducing conditions (especially for E_{Pt} < -200 mV at pH 7), the Pt electrode is better poised, but the species controlling the potential are unknown. Because none of the most likely inorganic redox-active species in environmental samples appear to poise the Pt electrode, it is hypothesized that E_{Pt} is influenced by redox-active organic species. These species might include quinones with low reduction potentials (e.g., juglone ($E_7^{0'}$ = -152 mV, (3))) or reversible biochemical couples produced by microbes (e.g., FAD, ferredoxins, cytochrome couples).

3) Two (or more) Pt electrodes should be used routinely when redox potentials are to be determined with a Pt electrode as a type of quality control. The convergence of the two E_{Pt} values is an indication that the redox buffering capacity of the system is

high enough to poise both Pt electrodes and that the potential measured is a better reflection of a property of the system rather than of the particular Pt electrode used.

In further studies, measurement of exchange current densities in environmental systems may help complement these results and help better evaluate the true nature of the Pt electrode potential. An interesting question is if and how the exchange current density changes as E_{Pt} in an environmental system (e.g., groundwater, soil slurry or microbial culture) decreases in the transition from oxidizing to more reducing potentials (from Fe(III)- , sulfate-reducing and methanogenic systems). In real samples, do exchange current densities ever reach the minimum value needed for poising (e.g., ~10 $\mu A/cm^2$ (2))?

Also it would be useful to measure exchange current densities in simple electrolyte solutions of important organic redox-active species (e.g., biochemical couples such as co-enzymes) to identify which couples could realistically affect E_{Pt} or poise the Pt electrode. These results would serve as a guide for targeting the chemical analyses of real systems for specific organic and biochemical couples which may be responsible for poising the Pt electrode.

8.2 Redox indicators as indicators of redox status

The major focus of this research has been to investigate the use of redox indicators for spectrophotometric evaluation of redox conditions in environmental samples. The primary goals were to 1) find useful redox indicators, 2) immobilize the indicators in a manner useful for field measurements, 3) understand how immobilized redox indicators respond to specific redox-active species and in environmental samples exhibiting different microbial redox levels, and 4) to understand what information redox indicators provide about the redox level of the sample.

Three primary redox indicators with quite different formal potentials, Thi, CV, and PSaf, were immobilized, evaluated extensively, and shown to define distinct regions on a redox scale. Thi ($E_7^{0'}$ = +52 mV on agarose beads), is suitable for identifying Fe(III)-reducing conditions, CV ($E_7^{0'}$ = -81 mV on agarose beads) has shown to be useful for identifying sulfate-reducing, and PSaf ($E_7^{0'}$ = - 267 mV on agarose films) is reduced under methanogenic conditions. The indicators must be used in pairs to define a "redox window". Reduction of one indicator such as Thi could be indicative of Fe(III)- or sulfate-reducing conditions or some other state of low redox potential.

The sample pH is critical because redox potentials of most indicators and environmental couples are pH dependent. The pH of the sample usually determines the concentration of a reductant necessary to reduce a given fraction of indicator. Therefore, pH should be measured concurrently with indicator speciation in real samples to interpret better what information about redox status and microbial levels is provided.

In the pH range of 7 to 8, Thi is half-reduced at Fe(II) levels around 0.1 mM, a level often reached or exceeded when Fe(III)-reducing conditions are dominant. In soil and wastewater slurries, there is strong evidence that Fe(II) is a primary reductant of Thi at this redox level (4). At pH values of ~6.5 and lower, Thi will not normally detect Fe(III)-reducing conditions because [Fe(II)] must be relatively high to observe significant reduction (> 1 mM for half reduction of Thi). However, as observed by Lemmon (5) with soil slurries at pH 6, Thi was reduced when Fe(II) levels were in excess of 1 mM. Because Thi is reduced by S(-II) at concentrations below 1 μM and possibly by other reductants, reduction of Thi does not necessarily indicate Fe(III)-reducing conditions, but clearly indicates a maximum "redox potential" (~50 mV).

The experimental Fe(II) level necessary to reduce a given fraction of free Thi was usually between the values predicted by an equilibrium model with an Fe(III)-solid phase of ferrihydrite or lepidocrocite, respectively. For Thi immobilized on agarose beads, the Fe(II)/ferrihydrite model fit the data most closely. The sample pH and other factors influence the nature of the actual Fe(III) product(s) formed. A more sophisticated model applicable to real systems would have to consider both soluble Fe(II) and Fe(II) adsorbed on the Fe(III)-hydroxides as reductants. This uncertainty in nature of the Fe(III)-solid phase (e.g. formal potential) leads to difficulties in estimating Fe(II) levels with an Fe(II) sensor based on immobilized redox indicators.

CV coupled well to total sulfide in the range of 1 - 100 μM from pH 6 to 8. Sulfide appears to be the primary reductant of CV under sulfate-reducing conditions in wastewater slurries. Although the reducing power of S(-II) decreases at lower pH values, S(-II) is an effective reductant of CV down to pH 6 (half-reduction with ~10 μM

S(-II)). It is unlikely that CV would be reduced by Fe(II) in environmental samples because its formal (immobilized) potential is too low (-81 mV).

The fraction of CV reduced with S(-II) was qualitatively predicted with an equilibrium model. The experimental S(-II) level necessary to reduce a given fraction of CV was greater than that predicted by the equilibrium model and complete reduction is difficult to achieve.

Thi and CV can be used together to define a "redox window" which delineates between Fe(III)-reducing and sulfate-reducing conditions and predicts the transformations of redox-active contaminants. Thi has been shown to be completely reduced only after the complete reduction of Cr(VI) to Cr(III) has already occurred (5). Evidence was presented that Thi speciation can be used to determine the onset of transformations of As(V) to As(III) and that redox transformations of TCE to *cis*-DCE occurs only after Thi is completely reduced and partial reduction of CV ($f_{ox} < 0.8$) is observed.

PSaf is reduced under methanogenic conditions although the reductant(s) is not known. Reduction of the indicator can only occur at very negative redox potentials (~-0.25 V at pH 7). The reduction is not do to Fe(II) or sulfide (even at levels as high as 0.1 mM).

Three secondary indicators have been identified for evaluating different redox levels. TB with a formal potential ~15 mV below that of Thi ($E^{0'}_7$ = +36 mV on agarose beads), coupled well to Fe(II) although the level of Fe(II) necessary to reduce a given fraction of TB was a factor of 2 or 3 greater than for Thi and its formal potential is not different enough from Thi to be particularly useful. AA ($E^{0'}_7$ = +19 mV on agarose

films) became reduced after Thi but before CV when tested in a methanogenic wastewater slurry. In the same methanogenic slurry, NB ($E^{0'}_7$ = -131 mV on agarose films) became reduced after CV but before PSaf. These two indicators (and possibly TB) may be useful as indicators of "transition regions" between redox levels (i.e., to help differentiate between high levels of Fe(II) produced under active Fe(III)-reducing conditions and low level sulfide produced at the onset of sulfate-reducing conditions).

It was found that the level of reductant necessary to reduce a given fraction of an indicator depends on the concentration of immobilized indicator. This effect is not predicted by simple equilibrium models and requires further study. As a practical matter for field sensors based on immobilized indicators, the concentration of immobilized indicator should be maintained at about the same level so that the laboratory calibration applies to the field measurements.

Some of the most important aspects of this research are the investigation and successful development of new immobilization techniques and physical formats for redox indicators. Initially indicators were immobilized to commercially available agarose beads as first shown by Lemmon et al. (6). The amine substitute on the indicator is coupled to the aldehyde groups on the beads. Several attempts were made to immobilize redox indicators in a variety of different chemical matrices (Si-sol gels, polyacrylamide gels and agarose gels). Agarose films (0.5 to 2 mm thickness) proved to be an excellent matrix for immobilization of redox indicators and provide good response times. Preparation of the films is simple. The immobilization procedure is straightforward and identical to the one initially used with the agarose beads. Furthermore, procedures were developed to immobilize indicators on cellulose filter membranes which were found to have

applicability for potentiometric methods. Overall, formal potentials of redox indicators did not shift by more than 10 to 20 mV with different forms of immobilization.

The development of a method to immobilize redox indicators in a film configuration and a new flow cell with removable windows are very critical because this physical form is more amenable to field analysis than indicators immobilized on beads and packed in a flow cell (7). In the "packed-bead" cell configuration, the sample must be highly filtered (pore size less than 1 μm) to prevent clogging which restricts the flow rate and sometimes results in oxygen leaking into the sample solution. With the film configuration, less or no filtering is required, flow rates are higher, clogging is unlikely, and there is more interaction of the immobilized redox indicators with solid-particles and microbes. In fact, it was not possible to use immobilized redox indicators such as PSaf to detect methanogenic conditions in wastewater slurries until the film configuration was employed. With the film configuration, it is also possible to use indicators such as Nile Blue which are too hydrophobic for use in the packed flow cell configuration.

The immobilization of redox indicators to cellulose filter papers has made possible the construction of Pt/indicator electrodes (cellulose filter membranes pressure-fitted to the Pt electrode surfaces) for redox measurements. Instrumentally, redox sensors based on Pt/indicator electrodes are conceptually simpler than optically-based indicator systems because a voltage is measured rather than an absorbance which requires a spectrophotometer (e.g., source, photodetector). Electrodes can be deployed *in situ* in groundwater (wells) or in a bioreactor without any need for pumping. These Pt/indicator electrodes were evaluated in sulfate-reducing and methanogenic wastewater

slurries, and generally, the redox levels predicted by immobilized indicators measured potentiometrically or spectrophotometrically were similar.

It may be possible to construct a "redox indicator array" for monitoring redox conditions based on a number of small Pt/indicator electrodes. Pairs of electrodes would define a "redox window", as previously defined for spectrophotometric measurement of immobilized redox indicators (7). An additional advantage of this technology is that reversible redox-active couples (one or both redox states) need not be colored at all, as is required with spectrophotometric monitoring. Redox-active couples might include quinones (with amine groups for immobilization), which are not colored but can poise the Pt electrode in soluble forms, and possess formal potentials ranging from +250 to -200 mV (8).

Many further studies of redox indicators and how they interact with environmental samples are warranted. One clear need is to find or synthesize redox indicators with amine groups which would fill in gaps in the redox scale. In particular, one or more indicators with a formal potential well above Thi ($E_7^{0'}$ of 100 - 200 mV) are needed for detection of very low levels (sub-μM) of Fe(II), the early onset of Fe(III)-reducing conditions, or perhaps the detection of nitrate-reducing conditions. One or two indicators with formal potentials between -150 and -250 mV would be useful to fill in the gap between NB and PSaf. One indicator with $E_7^{0'} \approx$ -30 mV would bridge the gap between AA and CV. Ideally, the redox scale would eventually be extended across the entire environmental redox range (+350 and -350 mV) with redox indicators with formal potentials differing by about 50 mV each.

Several avenues can be pursued for synthesizing new, amine-containing redox indicators. These approaches include incorporating an amine functional group into an existing redox indicator which does not have this group or to add a different functional group to an existing indicator with an amine-functional group (such as Thi and PSaf) which significantly alters the formal potential. For instance, a Cl atom (an electron withdrawing functional group) added to a position on a ring of the Thi structure might *increase* the formal potential (make the indicator easier to reduce).

Also, new indicators with amine groups for immobilization could be synthesized by combining smaller molecules which already have amine and/or different functional groups which might alter the formal potential. For example, methylene blue (MB) is a commonly used redox indicator very similar in structure to Thi, except that each of the amine groups on MB are fully alkylated with methyl groups (9). MB can be produced by the reaction of N,N'-dimethyl-*p*-phenylenediamine with H_2S in the presence of a Lewis acid (e.g., $FeCl_3$) (10, 11). Therefore, a redox indicator similar to Thi with a Cl substituent might be synthesized from the reaction a phenylenediamine derivative containing a Cl group and an non-alkylated amine with H_2S and $FeCl_3$.

A critical question is what are the reductants of redox indicators under methanogenic conditions? The major product of methanogenesis (CO_2) is not a reductant as is the product of Fe(III)-reducing and sulfate-reducing conditions (Fe(II) and S(-II), respectively). One hypothesis is that intracellular biochemical reductants are released into solution from methanogenic microbes. Common biochemical couples with very low formal potentials (at pH 7) include cytochrome c_3 ox/red ($E_7^{0'}$ = -0.29 V), NAD^+/NADH and $NADP^+$/NADPH ($E_7^{0'}$ = -0.32 V), FMN/$FMNH_2$ ($E_7^{0'}$ = -0.22 V), and

ferredoxin ox/red ($E_7^{0'}$ = -0.38 V) (12). The reduced species of each of these couples should be tested individually as a potential reductant of the redox indicators such as Thi, CV, and PSaf. The concentration of any reductant that reduces one of these indicators should be determined in cultures or slurries under methanogenic conditions. It is conceivable that biochemical or organic couples responsible for reducing redox indicators may also influence E_{Pt}.

Overall it would be useful to know the nature and steady-state level of the natural reductants produced by organisms and how they actually interact with indicators. In experiments in the bioreactor, it appeared in some cases that composition of filtered solution in the external loop was different from that in the bioreactor or that microbial growth in the flow cell on the agarose beads or films might be important. Do some of these reductants have short half-lives in solution? Does filtering change the 'reducing power' of the sample because the reductants are found only near microbes or adsorbed on particulate matter that are removed by filtering? Studies should be conducted with a methanogenic sample to compare the absorbances of two similar redox indicators immobilized in a agarose films: one in contact with filtered solution and the other in contact with the unfiltered solution.

Most importantly, more studies should be conducted with immobilized redox indicators in contact with a variety of microbial cultures (such as dechlorinating cultures) and groundwater systems. It is critical to correlate the fraction oxidized of various indicators to other types of measurements including concentrations of species such as H_2, CH_4, sulfide, and acetate and the redox transformations of important contaminants. This approach has already demonstrated that transformations of Cr, As

and TCE can be predicted from the state of redox indicators. Further studies should be conducted with transformations of redox-active contaminants such as Se, *cis*-DCE ,and VC in various types of microbial systems. Collaboration with environmental engineers and soil scientists who monitor redox transformations of toxic species, both in the laboratory and in the field, will help define the role of redox indicators for field use.

8.3 Redox indicators for use in H_2 analysis

The design of sensors for low-level H_2 determination based on reduction of redox indicators in the presence of a Pd or Pt catalyst was considered in terms of the mode of transfer of H_2 from the sample to the indicator solution (gas or solution mass transfer) and the characteristics of the redox indicator. Gas transfer was chosen for experimental studies because of the potential for higher selectivity and higher mass transfer rates. A variety of redox indicators of organic and organometallic (Fe and Cu chelates) were investigated as to their suitability for this application. The reduction reactions between H_2 and the indicators Thi and Fe(III)-$(OP)_3$ were studied in the greatest detail.

Although none of the indicators tested were found to be suitable for determining H_2 at the low levels expected in environmental samples ($P_{H2} < 0.0001$ atm), insight was gained as to what characteristics of a redox indicator are critical in this application. An indicator must be found for which the reaction rate is high enough to generate enough reduced indicator to detect in a reasonable time (e.g., 10 min) but for which there is no blank reaction. It is recommended that the indicator 1) have a high molar absorptivity in its monitored form ($> 10^4$ M^{-1} cm^{-1}), 2) have a formal potential significantly above the H_2 couple, and 3) be colored only in its reduced form which enables a high indicator concentration to be used to increase the rate of reduction.

The sorption of organic indicators such as Thi on the surface of the catalyst (Pd or Pt) limited the detection limit for H_2 to ~0.0002 atm at best. For organometallic indicators, spontaneous reduction of the indicator occurred in the absence of H_2.

Clearly more indicators must be tested for their suitability for H_2 determination. Most organic indicators (e.g., indophenols, variamine blues, thiazines) are colored in the oxidized form and colorless when reduced (9). The viologens are colored only in the reduced form but the reaction rate observed with two indicators of this type was very low (9).

Some alternatives deserve further study. It may be possible to couple a colorless redox-active species with a redox indicator. One redox species at high concentration which is colorless in both states (such as a quinone) would be chosen to react rapidly with H_2. An indicator species (e.g., Thi) in the same spectrophotometric cell would be reduced by the reduced form of the first species and the colored form of the indicator would be monitored spectrophotometrically to determine the rate of reduction.

A second approach involves employing an homogenous catalyst rather than the solid Pd which would eliminate adsorption of redox indicators such as Thi. Commonly used homogenous catalysts include rhodium and ruthenium complexes which are useful for hydrogenation reactions (13). However, many of these catalysts cannot be used in the aqueous phase, and reduction of redox indicators with H_2 may only be possible in some organic solvent (e.g., methanol).

Electrochemical approaches for H_2 determination might also be pursued. It is possible that a potentiometric method for H_2 could be based on the Pt/indicator electrode (indicators immobilized to cellulose filter membranes) and a reference electrode. If the indicator molecules next to the electrode surface were reduced by H_2 with Pt as the catalyst, the electrode might become poised after some time interval related to the level

of H_2. Bubbling H_2 into a solution of free indicator with Pt and reference electrodes is also a possibility.

A coulometric H_2 sensor is also conceivable. H_2 gas could be bubbled into the cell with a redox indicator in solution, Pd or Pt catalyst, and two or three electrodes. After a specified time, the electrodes would be biased and the charge necessary to oxidize the indicator that was reduced would be measured. For this application, the redox-active species need not be an indicator (neither form colored) because spectrophotometric detection is not involved. Coulometric approaches might also be possible with immobilized indicators. The challenge is to provide sufficient contact between indicator, catalyst, and electrode.

8.4 References

1. Lovley, Derek R.; Chapelle, Francis H.; Woodward, Joan C., *Environ. Sci. Technol.*, **1994**, *28*, 1205-1210.

2. Kempton, J. H., *Heterogenous Electron Transfer Kinetics and Measurement of* E_H, **1982**, M.S. Thesis, University of Colorado.

3. Schwarzenbach, René P.; Gschwend, Philip M.; Imboden, Dieter, M., *Environmental Organic Chemistry*, John Wiley & Sons, Inc., New York: 1993.

4. Jones, Brian, Chapter 4 in this thesis.

5. Lemmon, Teresa, *Development of Chemostats and Use of Redox Indicators for Studying Transformations in Biogeochemical Matrices,* **1995,** Ph.D. Thesis, Oregon State University.

6. Lemmon, T. L.; Westall, J. C.; Ingle, J. D. Jr., *Anal. Chem.*, **1996**, *68*, 947-953.

7. Jones, Brian, Chapter 5 in this thesis.

8. Clark, W. Mansfield, *Oxidation-Reduction Potentials of Organic Systems*; Williams & Wilkins Company: Baltimore, 1960.

9. *Indicators*, Bishop, E., Ed., Pergamon Press: Oxford, 1972.

10. *Standard Methods for the Examination of Water and Wastewater;* American Public Health Association: Washington, D. C., 1995.

11. Ana Barrios, Private communication, Oregon State University, January 22, 1999.

12. Brock, Thomas D.; Madigan, Michael T.; Martinko, John M.; Parker, Jack, *Biology of Microorganisms, Seventh Edition*, Prentice Hall: Englewood Cliffs, New Jersey, 1994.

13. Chaloner, Penny A., *Hydrogenous Hydrogenation: Catalysis by Metal Complexes, Vol. 15*, Kluwer Academic Publishers, Dordrecht: 1994.

BIBLIOGRAPHY

Acrylamide Polymerization - A Practical Approach, US/EG Bulletin 1156, BIO-RAD.

Angel, Michael S.; Zhang, Yunke; Nivens, Delana A., *Anal. Chim. Acta*, **1998**, *376*, 235-245.

Arnold, Mark A., *Anal. Chem.*, **1985**, *57*, 565-566.

Avnir, David; Lev, Ovadia; Iosefzon-Kuyavskaya, Berta; Gigozin, Ida; Ottonleghi, *J. Non-Cryst. Solids*, **1992**, *147 & 148*, 808-812.

Avnir, David; Zusman, Rivka; Rottman, Claudio; Ottolenghi, *J. Non-Cryst. Solids*, **1990**, *122*, 107-109.

Bard, Allen J.; Faulkner, Larry R., *Electrochemical Methods: Fundamentals and Applications*, John Wiley & Sons: 1980.

Belmont-Hébert, C.; Tercier, M. L.; Buffle, J., *Anal. Chem.*, **1998**, *70*, 2949-2956.

Berner, Robert A., *Geochim. Comochim. Acta*, **1962**, *27*, 563-575

Bodek, Itamar, *Environmental Inorganic Chemistry: Properties, Processes, Estimation Methods*, Pergamon Press, Elmsford, N.Y., 1988.

Bohn, Hinrich L., *Soil Science*, **1971**, *112*, 39-45.

Bohn, Hinrick L.; McNeal, Brian L.; O'Connor, George A., *Soil Chemistry, 2nd Ed.*, John Wiley & Sons, 1985.

Bos, Mark, *Part I: Development and Application of an Arsenic Speciation Technique Using Ion-Exchange Solid Phase Extraction Coupled with GFAAS, Part II: Investigation of Zinc Amalgam as a Reductant*, M. S. Thesis, Oregon State University, Corvallis, 1996.

Brett, Christopher M. A., Brett, Ana Maria Oliveira, *Electrochemistry: Principles, Methods and Applications*, Oxford Science Publications, 1993.

Brinker, C. Jeffrey; Scherer, George W., *Sol-Gel Science*, Academic Press, Inc.: 1990.

Brock, Thomas D.; Madigan, Michael T.; Martinko, John M.; Parker, Jack, *Biology of Microorganisms, Seventh Edition*; Prentice Hall: Englewood Cliffs, New Jersey, 1994.

Chaloner, Penny A., *Hydrogenous Hydrogenation: Catalysis by Metal Complexes, Vol. 15*, Kluwer Academic Publishers, Dordrecht: 1994.

Chapelle, Francis H., *Groundwater Microbiology and Geochemistry;* John Wiley & Sons, Inc., 1993.

Chapelle, Francis H.; Haak, Sheridan K.; Adriaens, Peter; Henry, Mark A.; Bradley, Paul M., *Environ. Sci. Technol.*, **1996**, *30*, 3565-3569.

Chapelle, Francis H.; McMahon, Peter B.; Dubrovsky, Neil M.; Fujii, Roger F.; Oaksford, Edward T.; Vroblesky, Don A., *Water Resour. Res.*, **1995**, *31*, 359-371.

Chromatography, Alltech Product Catalog 400, 1997.

Clark, W. Mansfield, *Oxidation-Reduction Potentials of Organic Systems*; Williams & Wilkins Company: Baltimore, 1960.

David, Renate, *Radiat. Environ. Biophys.*, **1986**, *25*, 219-229.

Doyle, Roger W., *American Journal of Sci.*, **1968**, 840-859.

Equilibrium Concepts in Natural Water Systems, Stumm, Werner, Ed., Chapter 13, 270-285, American Chemical Society: 1967.

Fennell, Donna E.; Gosset, James A.; Zinder, Stephen H., *Environ. Sci. Technol.*, **1997**, *31*, 918-926.

Fetzer, Silke; Conrad, Ralf, *Arch. Microbiol.*, **1993**, *160*, 108-113.

Frevert, T., *Schweiz. Z. Hydrol.*, **1980**, *42*, 255-268.

Green, Floyd J., *The Sigma Aldrich Handbook of Stains, Dyes and Indicators*, Aldrich Chemical Company, Inc.: Milwaukee, WI, 1990.

Guadalupe, Ana R.; Wier, Larry M.; Abruna, Hector D., *Amer. Lab.*, **1986**, August, 102-107.

Hand, Clifford W., *General Chemistry*, Saunders College Publishing, 1996.

Hermanson, Greg T., *Bioconjugate Techniques*, Academic Press, Inc., 1996.

Hermanson, Greg T.; Mallia, A. Krishna; Smith, Paul K., *Immobilized Affinity Ligand Techniques*, Academic Press, Inc.: 1992.

Hesse, P. R., *A Textbook of Soil Chemical Analysis*; Chemical Publishing Co., Inc.: 1971.

Indicators, Bishop, E., Ed., Pergamon Press: Oxford, 1972.

Ingle, James D. Jr.; Crouch, Stanley R., *Spectrochemical Analysis*, Prentice Hall, Englewood Cliffs, New Jersey: 1988.

Instructions for covalent binding of ligands to Sartobind Membranes with Aldehyde Groups, Sartorius.

Instructions for ORP Electrode Use, Analytical Sensors, Inc.: Houston.

Jacob, H. E., *Redox Potential*, p. 92-123, from *Methods in Microbiology, Vol. 2*, Norris, J. R.; Ribbons, D. W., Eds., Academic Press, Inc., New York: 1970.

Jeroschewski, P.; Steuckart, C.; Kühl M., *Anal. Chem.*, **1996**, *68*, 4351-4357.

Kempton, J. H., *Heterogenous Electron Transfer Kinetics and Measurement of* E_H, **1982**, M.S. Thesis, University of Colorado.

Laboratory notebook: BASIC computer program for bioreactor.

Lemmon, T. L.; Westall, J. C.; Ingle, J. D., Jr. *Anal. Chem.*, **1996**, *68*, 947-953.

Lemmon, Teresa, *Development of Chemostats and Use of Redox Indicators for Studying Transformations in Biogeochemical Matrices*, **1995**, Ph.D. Thesis, Oregon State University.

Lev, Ovadia; Anvir, David; Iosefzon-Kuyavskaya, Berta; Gigozin, Ida; Ottonleghi, Michael, *Fresenius J. Anal. Chem.*, **1992**, *343*, 370-372.

Levenspiel, Octave, *Chemical Reaction Engineering, 2nd Ed.*, John Wiley & Sons, Inc.: 1972.

Lindberg, R. D.; Runnels, D. D., *Science*, **1984**, *225*, 925-927.

Lovley, Derek R.; Chapelle, Francis H., *Environ. Sci. Technol.*, **1994**, *28*, 1205-1210.

Lovley, Derek R.; Dwyer, Daryl F.; Klug, Michael J., *Appl. Environ. Microb.*, **1982**, *43*, 1373-1379.

Lovley, Derek R.; Goodwin, Steve, *Geochim. Cosmochim. Acta*, **1988**, *52*, 2993-3003.

Lowe, H. J.; Clark, W. Mansfield, *J. Biol. Chem.*, **1956**, *221*, 983-992.

Masscheleyn, Patrick H.; Delaune, Ronald D.; Patrick, William H. Jr., *J. Environ. Qual.*, **1991**, *20*, 522-527.

Masscheleyn, Patrick H.; Delaune, Ronald D.; Patrick, William H. Jr., *Environ. Sci. Technol.*, **1991**, *25*, 1414-1419.

McBride, Murray B., *Environmental Chemistry of Soils*, Oxford University Press, Inc., 1994.

McMurry, John, *Organic Chemistry*, Brooks/Cole Publishing Company: Monterey, California, 1984.

Merck Index, Budarvi, S., Ed., Merck & Co., Inc.: Rahway, N.J. 1989.

Mobley, James, Oregon State University, unpublished report, **1992**.

Pankow, James F., *Aquatic Chemistry Concepts*, Lewis Publishers, Inc.: 1991.

Patrick, W. H., Jr.; Connell, W. E., *Science*, **1968**, *159*, 86-87.

Patrick, W. H., Jr.; Jugsujinda A., *Soil Sci. Soc. Am. J.*, **1992**, *56*, 1071-1073.

Paul, E. A.; Clark, F. E., *Soil Microbiology and Biochemistry*, Academic Press, Inc.: 1989.

Proceedings of Symposium on Paddy Soil, Okazaki, Masanori; Wada, Hidenori; Takai, Yasuo, Science Press, Springer-Verlag: Beijing, China, 1981.

Product Catalog, CHEMetrics, 1997-1998.

Rifai, Hanadi S.; Borden, Robert C.; Wilson, John T.; Ward, Herb C., *Intrinsic Bioattenuation for Subsurface Restoration*, printed in *Intrinsic Bioremediation*, Hinchee, Robert E.; Wilson, John T.; Downey, Douglas C., Eds., Batelle Press: 1995.

Roberts, David, Laboratory GC/TCD calibration procedure, Oregon State University, 1997.

Schwarzenbach, René P.; Gschwend, Philip M.; Imboden, Dieter, M., *Environmental Organic Chemistry*, John Wiley & Sons, Inc., New York: 1993.

Semprini, L., *In Situ Transformation of Halogenated Aliphatic Compounds Under Anaerobic Conditions*, printed in *Subsurface Restoration*, Ward, C. H.; Cherry, J. A.; Scalf, M. R., Ann Arbor Press, Inc.: 1997.

Shriver, Duward F.; Atkins, Peter; Langford, Cooper H., *Inorganic Chemistry,* Second Edition, W.H. Freeman and Co.: 1994.

Snoeyink, Vernon L.; Jenkins, David, *Water Chemistry*; John Wiley & Sons, Inc., 1980.

Standard Methods for the Examination of Water and Wastewater; American Public Health Association: Washington, D. C., 1995.

Standard Potentials in Aqueous Solution, Bard, Allen J.; Parsons, Roger; Jordan, Joseph, Eds., Marcel Dekker, Inc.: 1985.

Stumm, Werner; Morgan, James J., *Aquatic Chemistry*, John Wiley & Sons: 1981.

Tercier, M.-L.; Buffle, J., *Anal. Chem.*, **1996**, *68*, 3670-3678.

Thurman, E. M., *Organic Geochemistry of Natural Waters*, Kluwer Academic, Dordrecht: 1985.

Traytnek, Paul G.; Wolfe, N. Lee, *Environ. Toxicol. Chem.*, **1990**, *9*, 289.

Vancheeswaran, Sanjay, *Abiotic and Biological Transformation of TBOS and TKEBS, and their Role in the Biological Transformation of TCE and c-DCE*, **1998**, M.S. Thesis, Oregon State University.

Vancheeswaran, Sanjay; Halden, Rolf U.; Semprini, Lewis; Williamson, Kenneth J.; Ingle, James D. Jr., "Abiotic and Biological Transformation of Tetraalkoxysilanes and Trichloroethene/cis-1,2-Dichloroethene Cometabolism Driven by Tetrabutoxysilane-Degrading Microorganisms", *Environ. Sci. Technol.*, in press.

Whitfield, M., *Limnol. Oceanogr.*, **1974**, *19*, 857-865.

Zhujun, Zhang; Jianzhong, Li; Ling, Li, *Talanta*, **1994**, *41*, 1999-2002.

Zobell, Claude E., *Bull. Am. Assoc. Petroleum. Geol.*, **1946**, *30*, 477.

APPENDICES

Appendix A

Solid-State Relay for On/Off Control of Sonicator

A switching circuit based on a solid-state relay (SSR) was developed for turning the sonicator (Bransonic 52) on and off. Under computer control, the switch allows the sonicator to be activated periodically at times chosen by the operator (e.g., 15 min every hour) to help minimize clogging of the cross-flow filter by particulate matter in soil or sludge slurries.

The circuit diagram is shown in Figure A.1. Only one of the two available switches was used for the sonicator. The common and ground wires of the single AC input are connected directly to the common and ground of the AC outlets while the "hot" wire of the AC input is connected via a fuse (5 A, 250 V) to pin 1 of both solid-state relays. Pin 2 of the relays is connected to the "hot" wire connectors for the AC outputs. Control pin 3 of each SSR is connected to an inverting output of a 7406 TTL inverter chip. Two of the inputs of the chip are connected to two BNC connectors (TTL input).

In this research, input 1 is connected to an I/O line (Port Bit 0, Pin 10) of a computer interface board (Computer Boards, Inc., CIO-DIO24). The computer program maintains the output of the I/O line at +5 V (high) for OFF and 0 V (low) for ON. When the computer program directs the I/O line to go low, this signal is inverted by the 7406 chip and the SSR is activated allowing AC power to reach the sonicator. The ground and +5 V to power the inverter chip are provided by the interface board in the computer. Connections to these lines are available on the computer interface box (developed by Lemmon (1)).

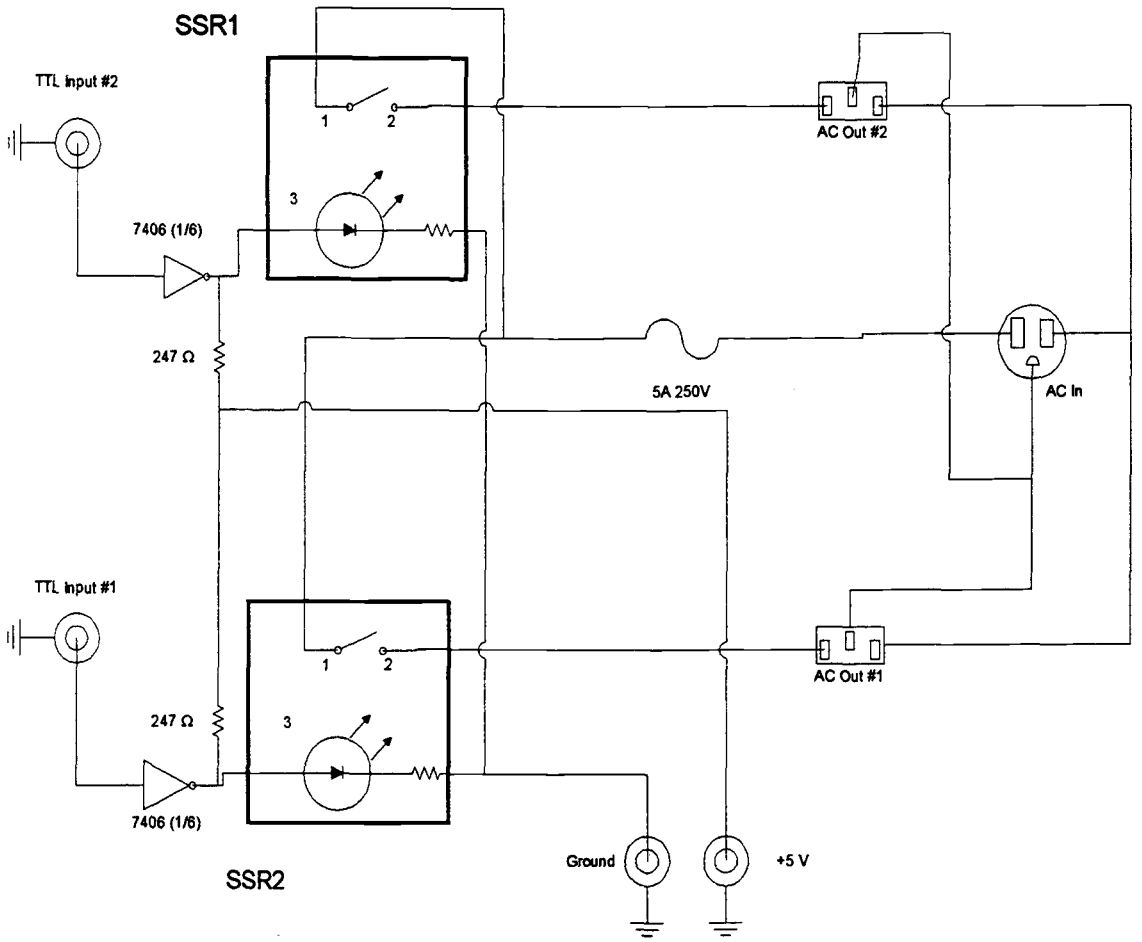

Figure A Schematic of circuit for solid-state relay. The solid-state relay (SSR) is a Teledyne 615-8500.

References

1. Lemmon, Teresa, *Development of Chemostats and Use of Redox Indicators for Studying Transformations in Biogeochemical Matrices,* **1995,** Ph.D. Thesis, Oregon State University.

Appendix B

Determination of Soluble Fe(II) by the 1,10-Phenanthroline Method

Commonly, Fe(II) is measured with a colorimetric method involving the chelation of the Fe(II) ions with a chelating agent, orthophenanthroline (OP). The reaction involves the chelation of one Fe(II) atom with three OP molecules, forming an orange-red complex with a wavelength maxima of 510 nm (1). The calibration curve is typically linear up to a concentration of about 180 μM. The reaction is shown below:

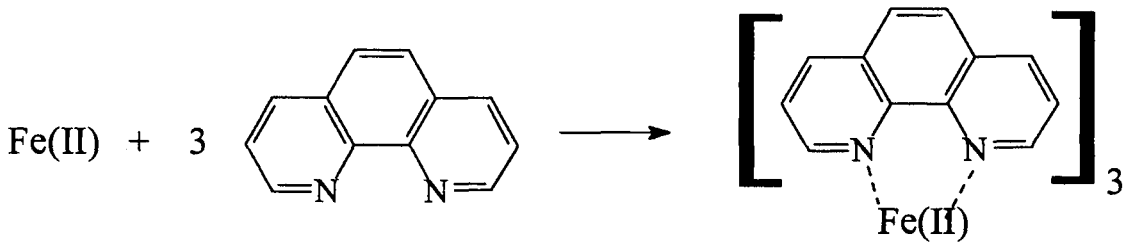

For quantitation in this research, a blank and one Fe(II) standard was used. The following solutions were prepared:

1) Hydroxylamine hydrochloride, 10% (w/v)

2) 1,10-orthophenanthroline, 0.5% (w/v)

3) Sodium acetate/acetic acid buffer, 1 M

4) Fe(III) standard, 50 μg/mL (89 μM) in ~6 mM HCl

To prepare the standard, add 1 mL of 50 μg/mL Fe standard to a 10-mL volumetric flask along with 0.2 mL of hydroxylamine hydrochloride (reduces Fe(III) to Fe(II)), 0.4 mL of acetate buffer, and 0.4 mL of OP solution, and dilute to 10 mL with DI water. Mix well and allow at least 10 min for color development. This makes a 5

μg/mL (89.5 μM) Fe(II) standard that will generally be stable for several weeks. For the blank, use the same solution without the addition of 1 mL Fe.

For samples, generally use 0.2 - 1 mL of sample (in place of the 1 mL of Fe standard) and prepare as before. Again, allow 10 min for color development.

In environmental systems with a pH greater than about 5, soluble iron primarily exists only as Fe(II). This is because Fe(III), the other common Fe ion in most natural systems, forms insoluble precipitates (e.g., am-$Fe(OH)_3$) at these pH values. In most systems, however, the *measured* soluble Fe(II) concentration is not the *total* Fe(II) concentration, since as much as 95 - 98 % of Fe(II) can be adsorbed on soil particulate matter (2).

References

1. *Standard Methods for the Examination of Water and Wastewater;* American Public Health Association: Washington, D. C., 1995.

2. Bodek, Itamar, *Environmental Inorganic Chemistry: Properties, Processes, Estimation Methods*, Pergamon Press, Elmsford, N.Y., 1988.

Appendix C

Preparation of Zobell's Solution

Zobell's solution is commonly used as a reference solution for Pt electrodes. The solution consists of 3 mM potassium ferrocyanide and 3 mM potassium ferricyanide in 0.1 M KCl. Its usefulness as a reference solution for Pt electrodes results from its rapid electron transfer kinetics at the Pt surface. At sufficiently large (and equimolar) concentrations, this redox couple generates large exchange currents and poises the Pt electrode in a Nernstian fashion. This solution was commonly used by Zobell to evaluate the accuracy of Pt electodes. Although not strictly a calibration standard (because it gives only a single potential), Zobell's solution can be used to evaluate the accuracy of a Pt electrode by comparing E_{Pt} measurements of the prepared solution to its tabulated formal potential.

To prepare a Zobell's solution (1):

1. Dissolve 1.4080 g potassium ferrocyanide, $K_4Fe(CN)_6 \cdot 3H_2O$, and 1.0975 g potassium ferricyanide, $K_3Fe(CN)_6$, in 1-L of DI water.
2. Add 7.4555 g potassium chloride, KCl.
3. Stir or shake until completely dissolved.

To use Zobell's solution to determine the accuracy of a Pt electrode, use a reference electrode with a well-known formal potential (e.g., SCE or Ag/AgCl (saturated KCl) with formal potentials of 0.242 and 0.197 V vs SHE at 25°C, respectively (2)) and a voltmeter. Place both electrodes in the Zobell's solution with adequate stirring and measure the potential. Referenced to the standard hydrogen electrode (SHE), this

formal potential is +430 mV at 25°C. Referenced to the standard calomel electrode (SCE) and the Ag/AgCl electrode (saturated KCl), this formal potential at 25°C is +183 and +229 mV, respectively (1). The Pt electrode potential (E_{Pt}) should be no more than ±10 mV from the tabulated potentials (1).

References

1. *Standard Methods for the Examination of Water and Wastewater;* American Public Health Association: Washington, D. C., 1995.

2. Bard, Allen J.; Faulkner, Larry R., *Electrochemical Methods: Fundamentals and Applications*, John Wiley & Sons: 1980.

Appendix D

Determination of Total Sulfide With the Iodometric Method

Total sulfide was determine with a titration method taken from Standard Methods (method 4500-S^{2-} E)(1). The method is summarized below.

First, prepare or obtain the following reagents:

1) HCl solution, 6 M

2) Standard iodine solution, 0.0250 N

Dissolve 1.6 g of I_2 and 12.5 g of KI in 500 mL of DI water.

3) Standard sodium thiosulfate solution, 0.025 N

Dissolve 0.791 g of $Na_2S_2O_3$ in 200 mL of DI water.

4) Starch indicator solution (2%(w/v))

Next, standardize the iodine solution by titration with the sodium thiosulfate solution. The stoichiometry for this reaction is

$$I_2 + 2\ S_2O_3^{2-} \rightarrow 2\ I^- + S_4O_6^{2-} \qquad \text{(D-1)}$$

Place 10.0 mL of iodine solution in a beaker and add 1 mL of 6 M HCl solution. With a buret, add thiosulfate solution incrementally to the iodine solution which will turn from brownish to a cloudy-brown (as $S_2O_3^{2-}$ is oxidized). Stop the titration when the iodine solution turns a tannish color and add 3-5 drops starch indicator yielding a dark brown-black color. Continue titrating with thiosulfate until a blue color forms (near the endpoint) and then in one drop increments until the solution just turns clear (endpoint). The concentration of the iodine solution is calculated from equation D-2.

$$[I_2] = \frac{1}{2}[S_2O_3^{2-}]\frac{(\text{volume thiosulfate added})}{(\text{volume iodine solution})} \qquad \text{(D-2)}$$

For the determination of total sulfide in the sample, pipet 10.0 mL of iodine solution into a beaker and add an aliquot of sulfide sample (1 - 5 mL, but measure precisely). Again, titrate sample with thiosulfate solution as described previously until a clear endpoint is achieved. Calculate the amount of iodine titrated with thiosulfate with Eq. D-2. Finally, calculate the concentration of total sulfide in the sample by finding the difference between the total iodine added to the beaker and the amount reduced with the thiosulfate:

$$\text{total sulfide} = [I_2](0.010\ \text{L}) - \frac{1}{2}[S_2O_3^{2-}]\frac{(\text{volume thiosulfate added})}{(0.010\ \text{L})} \qquad \text{(D-3)}$$

The stoichiometry of the iodine/sulfide reaction is 1:1.

$$I_2 + S^{2-} \rightarrow 2\ I^- + S_0 \qquad \text{(D-4)}$$

Therefore, to find the concentration of total sulfide in the sample, divide the total sulfide calculated with Eq. D-3 by the volume of sulfide sample used in the titration. Thiosulfate ($S_2O_3^{2-}$), dithionite ($S_2O_4^{2-}$) and sulfite (SO_3^{2-}) also are titrated by I_2 and can be interferents in the determination of total sulfide. Therefore, the titration provides an estimate of the "upper limit" for total sulfide.

References

1. *Standard Methods for the Examination of Water and Wastewater;* American Public Health Association: Washington, D. C., 1995.

Appendix E

Covalent Immobilization of Redox Indicators to Agarose Affinity Beads

Affinity beads are commonly used in biochemical applications for the immobilization of proteins and other "target molecules". Lemmon (1) developed a procedure for immobilizing redox indicators via amine groups on the molecule to affinity beads called Spectra/Gel® MAS Beads Macroflow (Spectrum, 121508). The beads are 40 to 60-μm diameter cross-linked agarose (4%) and contain aldehyde groups at a concentration of 40 - 50 μmol/mL of gel (2). More recently, affinity beads with the same properties have been acquired from Sterogene (ALD Beads).

The "reductive amination" reaction involves the coupling of the non-redox-active amine group of the redox indicator to an aldehyde group on the agarose affinity bead. The

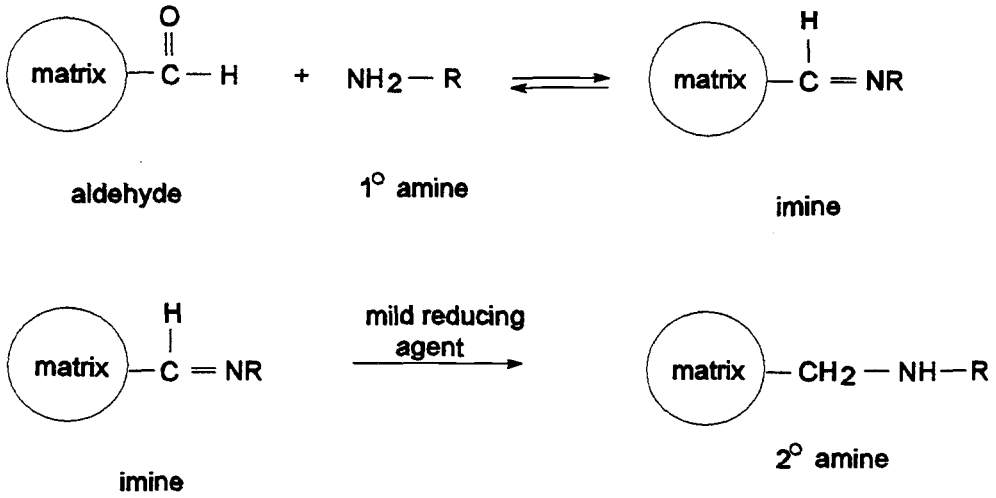

initial product is an imine which is subsequently reduced by sodium cyanoborohydride, a mild reducing agent, to a stable 2° amine.

The step-by-step immobilization procedure follows:

1) Prepare 2 mM solution stock solution of redox indicator in DI water to be immobilized.

2) Prepare pH buffers (~0.1 M) in range of pH 3 - 7. Recommended common buffers include acetic acid buffer (pH 3 - 4.5) and phosphate (pH 5.5 - 7). In general, the lower the pH, the higher the degree of the immobilization. For thionine (1) and toluidine blue O (3), pH 5 - 6 is optimal. For phenosafranine (1) and cresyl violet (3), a pH of 3 - 4 is optimal.

3) Transfer approximately 0.5 mL of the affinity bead gel to a fritted glass funnel (Pyrex® fitted disc funnel, medium (10 - 15 μm), 2 mL) and wash with 3 - 4 volumes of buffer. Transfer washed affinity beads to vial (Fisherbrand® 3-mL vial) and add 0.5 mL of pH buffer, 0.5 mL of 2 mM redox indicator solution, and 0.5 mL of 0.1 M sodium cyanoborohydride solution (prepare from $NaCNBH_3$ solid, Aldrich (95%) in water, prepare day of used).

4) Cap and place vial in rotator (Labquake Shaker, Labindustries, Inc., C400-110) and mix for 3 to 4 hr. The longer mixing is allowed, the greater the degree of immobilization.

5) Transfer contents of vial back to fritted glass funnel and wash with at least 10 volumes of 0.5 M NaCl. This step removes redox indicator which is only adsorbed (electrostatically) on the gel.

6) Transfer gel back to vial and add 1 mL of 0.1 M ethanolamine solution (Aldrich, 99%,) diluted in the same pH buffer as used previously (prepare day of use). Rotate the

vial for 1 hr. This step displaces redox indicator which has coupled as an imine but has not reacted further to form the more stable 2° amine bond.

7) Transfer contents of vial back to fritted glass funnel and rinse gel with immobilized indicator with 3 - 4 volumes of pH buffer. Transfer back to vial with 2-3 mL of buffer and store in refrigerator until use.

8) When needed, the beads can be packed into a flow-cell (Hellma 170.700-QS, 1-mm pathlength, Figure 4.2) as previously described (1,2).

References

1. Lemmon, T. L.; Westall, J. C.; Ingle, J. D., Jr. *Anal. Chem.*, **1996**, *68*, 947-953.

2. Lemmon, Teresa, *Development of Chemostats and Use of Redox Indicators for Studying Transformations in Biogeochemical Matrices,* **1995,** Ph.D. Thesis, Oregon State University.

3. Jones, Brian; Chapter 4 of this thesis.

Appendix F

Fe(II)/Indicator Equilibrium Model

The Nernst equation, when applied to model the reactions of Fe(II) and indicators,

can be rearranged to yield an equation to describe sigmoidal-shaped titration data and a function for which a plot of the molar ratio of the reduced to oxidized indicator vs. $[Fe(II)]^2$ is a straight line. The half-reactions and reduction potentials of the $Fe(II)/Fe(OH)_3$ and redox indicator couples at pH m and 25°C are given below:

$$2Fe(OH)_3(s) + 6H^+ + 2e^- \rightleftharpoons 2Fe^{2+} + 6H_2O \quad \text{(F-1)}$$

$$E_{Fe(OH)3/Fe(II)} = E^{0'}_{Fe(III/II),m} - \frac{0.059}{2} \log [Fe(II)]^2 \quad \text{(F-2)}$$

$$Ind_{ox} + 2H^+ + 2e^- \rightleftharpoons Ind_{red} \quad \text{(F-3)}$$

$$E_{ind} = E^{0'}_{ind,m} - \frac{0.059}{2} \log \frac{[Ind_{red}]}{[Ind_{ox}]} \quad \text{(F-4)}$$

where $E_{Fe(III/II),m}^{0'}$ is the formal potential of the Fe couple at pH m, [Fe(II)] is the Fe(II) concentration, $E_{ind,m}^{0'}$ is the formal potential of the indicator couple at pH m, 0.059 is the Nernstian slope in V (base 10) at 25°C, and $[Ind_{red}]$ and $[Ind_{ox}]$ are the concentrations of reduced and oxidized indicator species, respectively. The value of $E_{Fe(III/II),m}^{0'}$ at pH 7 ($E_{Fe(III/II),7}^{0'}$) is -0.182 V for ferrihydrite and -0.274 for lepidocrocite (calculated from (1) and (2), respectively; it is assumed that standard potentials are equivalent to formal potentials). At pH m, $E_{Fe(III/II),m}^{0'}$ = -0.182 V - 0.177(m - 7) for ferrihydrite and $E_{Fe(III/II),m}^{0'}$ = -0.274V - 0.177(m - 7) for lepidocrocite.

The fraction reduced indicator ($1 - f_{ox}$) and fraction oxidized indicator (f_{ox}) can be substituted into Eq. F-4 for the concentrations of reduced and oxidized indicator species, respectively, yielding equation F-5.

$$E_{ind} = E^{0'}_{ind,m} - \frac{0.059}{2} \log \frac{(1-f_{ox})}{f_{ox}} \qquad \text{(F-5).}$$

At equilibrium, the reduction potentials of the Fe(II)/$Fe(OH)_3$ and Ind_{ox}/Ind_{red} couples are equal. Equating equations F-2 and F-5, multiplying both sides by (2/0.059), and solving for log [$(1 - f_{ox}) / f_{ox}$] gives

$$\log \frac{(1-f_{ox})}{(f_{ox})} = \frac{2}{0.059} (E^{0'}_{ind,m} - E^{0'}_{Fe(III)/Fe(II),m}) + \log [Fe(II)]^2 \qquad \text{(F-6).}$$

Taking the antilogarithm of both sides (base 10) gives

$$\frac{(1-f_{ox})}{(f_{ox})} = \left[10^{\frac{2}{0.059}(E^{0'}_{ind,m} - E^{0'}_{Fe(III)/Fe(II),m})}\right] * [Fe(II)]^2 \qquad \text{(F-7).}$$

Solving for f_{ox} yields equation F-8 which can be used to predict the shape of a titration curve of f_{ox} vs [Fe(II)]

$$f_{ox} = \frac{1}{\left(10^{\left[\frac{2}{0.059}(E^{0'}_{ind,m} - E^{0'}_{Fe(III)/Fe(II),m}) + \log [Fe(II)]^2\right]} + 1\right)} \qquad \text{(F-8).}$$

Equation F-7 can also be written as

$$\frac{(1-f_{ox})}{f_{ox}} = k[Fe(II)]^2 \qquad \text{(F-9)}$$

where

$$k = 10^{\left[\left(\frac{2}{0.059}\right)\left(E^{0'}_{ind,m} - E^{0'}_{Fe(III)/Fe(II),m}\right)\right]} \qquad \text{(F-10)}.$$

When the indicator is half reduced, $[Fe(II)] = k^{-½}$. For a plot of $(1 - f_{ox})/f_{ox}$ (or molar ratio of reduce to oxidized indicator) vs. the square of the Fe(II) concentration, the slope, k, is dependent on the difference between the formal potentials of the indicator couple and the $Fe(II)/Fe(OH)_3$ couple.

References:

1. McBride, Murray B., *Environmental Chemistry of Soils*, Oxford University Press, Inc., 1994.

2. Doyle, Roger W., *American Journal of Sci.*, **1968**, 840-859.

Appendix G

Some Notes on Microbial Transformations in Environmental Systems

The following is a general summary of some facts involving microbes and their transformations in environmental systems which was gleamed from a few estabalished books about soil biology, microbiology, biochemistry and ground-water microbiology. The focus is on processes and information pertinent to anaerobic conditions and microbial oxidative and reductive processes under these conditions. Several biochemical pathways are mentioned in this summary without presentation. These biochemical pathways can be found in several books on microbes and microbial processes, notably, by Brock (1), Chapelle (2) and Paul and Clark (3).

Some definitions:

ATP: adenosine triphosphate; a molecule produced by cells under various pathways used for storing energy; energy is obtained by the cell by breaking the various phosphate bonds

Autotrophs: organisms obtaining growth energy from inorganic sources and cell carbon from CO_2

Chemolithotrophs: organisms which derive their energy from inorganic sources

Chemoorganotrophs: organisms which derive their energy from organic sources

Denitrification: the microbial process by which nitrate is reduced to N_2O and nitrogen gas

Eukaryote: organism with a membrane bound nucleus (e.g., fungi, protozoa, plants)

Facultative anaerobes: organisms normally existing in aerobic environments, but which can adapt to anaerobic environments

Fermentation: microbial use of organic chemicals as both electron acceptors and electron donors

Heterotrophs: organisms obtaining growth energy and most cell carbon from organic material

Lithotrophs: organisms which use CO_2 as a cell carbon source

Nitrogen fixation: the microbial process by which nitrogen gas is used directly as a nitrogen source

Obligate aerobes: organisms which can only exist in an aerobic environment

Obligate anaerobes: organisms which can only exist in anaerobic environments

Organotrophs: organisms which obtain growth energy and cell carbon from organic materials

Phototrophs: organisms using light as an energy source

Prokaryote: organism without a membrane bound nucleus (e.g., bacteria)

Respiration: microbial use of inorganic chemicals (e.g., O_2, Fe(II), etc.) as electron acceptors

Symbiosis: when two or more types of organisms benefit one another, and cannot live without one another

Synergism: when two or more types of organisms benefit one another, but can live without one another

Types of bacteria found in soils:

Arthrobacter - numerically predominant

- uses a wide variety of substrates

- generally aerobic

- poor competitors for easily decomposable substrates (e.g., sugars)

Streptomyces (3 common types)

- Streptomyces: intolerant of waterlogged and acidic soils

  oxidative organotrophs

- Pseudomonas: generally aerobic, but can be anaerobic

  (facultative anaerobes)

  can use NO_3^- as electron acceptor

  very common

  some types can reduce Fe(III)

  uses a variety of organic substrates

- Bacillus: usually organotrophs

  respirative or fermentative

  during glucose fermentation can produce glycerol, 2,3-butanediol, ethanol, H_2, acetone and formic, acetic, lactic and succinic acids

  spore-forming

Clostridium - strictly anaerobic

- always fermentative
- very important in decomposition of organic material under anaerobic conditions
- produce organic acids and reduced gases
- spore-forming

Rhizobium - capable of nitrogen fixation
- usually not located below root zones

Azotobacter - capable of nitrogen fixation
- found throughout soils
- aerobic organotroph

Flavobacterium - widely distributed

Enterobacter - facultative anaerobes
- known for mixed-acid fermentations and butylene-glycol fermentations

Why bacteria break down molecules:

In general, all respirative and fermentative processes by bacteria are used to produce ATP, the high energy compound used to store energy. The pathways used to produce ATP vary, but in general, respirative (external electron acceptor processes) are more efficient (i.e., produce more ATP molecules per cycle) than fermentative pathways.

In fermentative pathways, an organic substrate (e.g., glucose) is oxidized to two molecules of pyruvate through a series of biochemical reactions. This process is called

glycolysis, and has also been called the Embden-Meyerhof pathway, in honor of the scientists who discovered it. In the conversion to pyruvate, the biochemical electron carrier NAD^+ is reduced to NADH. Since the overall process requires available NAD^+ for further oxidation of glucose, the NADH is in turn oxidized by a series of reactions which uses the two molecules of pyruvate as electron acceptors. This leads to a variety of *fermentation products*; for instance lactic acid from some bacteria, or ethanol and CO_2 from yeasts. The overall fermentation process produces two molecules of ATP for every molecule of glucose.

In respiration pathways, an electron transport system involving various enzymes is used to generate a *chemiosmotic potential* across the cellular membrane. Unlike fermentation, the process ultimately relies not only on the availability of a substrate, but also on the availability of an electron acceptor. In *aerobic respiration*, the external electron acceptor is O_2, and in *anaerobic respiration*, the electron acceptor can be an inorganic compound or ion, such as NO_3^-, Mn(IV), Fe(III), SO_4^{2-} or CO_2, or another organic molecule.

In the overall process, a substrate (organic for chemoorganotrophs and inorganic for chemolithotrophs) donates an electron to the transport system, ultimately reducing an electron acceptor (e.g., O_2). As O_2 is reduced to H_2O, H^+ ions are consumed and an excess of OH^- ions accumulate on the inside of the cellular membrane. This accumulation causes a net negative charge inside the membrane, and ultimately a net positive charge of H^+ outside the membrane, creating a pH gradient and an electrical potential across the membrane. This is the chemiosmotic potential described earlier. This potential is capable of doing work, as in the synthesis of ATP from ADP (adenosine

diphosphate) and inorganic phosphate. This reaction is catalyzed by a membrane-bound enzyme known as ATPase, which allows the H^+ ions to move across the membrane, releasing energy.

As with fermentation, the respirative process produces pyruvate as an intermediate, as the first steps in the respirative process are similar to those of glycolysis. However, the pyruvate can be further oxidized to CO_2 in a biochemical pathway known as the *tricarboxylic acid cycle* (TCA; also known as the Kreb's cycle). In contrast to fermentation, in which the substrate (e.g., glucose) is not completely oxidized, the TCA cycle allows complete oxidation of the substrate to CO_2, acquiring the maximum amount of potential energy from the substrate to help produce ATP. In respiration, 1 molecule of glucose can be used to produce as many as 38 molecules of ATP, as compared to 2 molecules of ATP by fermentative pathways. Thus, if available, respirative pathways are far more energy efficient than fermentative pathways.

What makes some bacteria aerobic and others anaerobic:

Normally, O_2 is the preferred electron acceptor for many respirative bacteria, as it has a higher potential than other known microbial electron acceptors. Hence, more ATP can be synthesized using the redox "powered" electron transport mechanism. Also, in surface and subsurface environments, O_2 is generally available, if not abundant. Bacteria which need O_2 to survive are known as *obligate aerobes*. However, there are certain bacteria that normally use O_2 which can function anaerobically, if necessary, and are termed *facultative anaerobes* (i.e., they can use other electron acceptors such as NO_3^- or

Fe(III)). Finally, there are truly anaerobic bacteria, known as *obligate anaerobes*, which either cannot live or cannot reproduce in the presence of oxygen because they lack an enzyme called *catalase* which is used to break down peroxide formed by the reaction of O_2 with water:

$$H_2O + 1/2\ O_2 \rightarrow H_2O_2 \qquad \text{(G-1)}.$$

Hydrogen peroxide is a strong oxidant and can damage cells.

What are some products of bacterial metabolism?

As previously discussed, bacteria produce ATP either through fermentative or respirative processes. Often, bacteria using these different mechanisms are coupled, creating a *synergistic* or *symbiotic* relationship between two or more strains of bacteria. The fermentative bacteria, in general, break down the larger, less accessible organics to a variety of fermentation products (e.g., organic acids such as lactate and acetate) which are further oxidized by respirative bacteria in the presence of an external electron acceptor. The production of simple organic acids, alcohols and H_2 by the fermenters often provide the substrate by which respirative bacteria grow, and, conversely, the respirative bacteria help to remove the unwanted waste created by the fermentation process.

1. Acetate, lactate and organic acid fermentations:

After glycolysis, pyruvic acid is produced and must be used as an electron acceptor in order to oxidize NADH for further ATP synthesis. Many bacterial types in soils produce lactic, acetic and formic acids as fermentative byproducts. A common pathway by which lactate and acetate are formed is the *Bifidum pathway* used by certain bacteria in the oxidation of pyruvic acid to lactate and acetate. In the overall process, 2 moles of glucose are converted to 2 moles of lactate and 3 moles of acetate.

The bacterial family Enterobacteriaceae, which includes the pathogenic members *Salmonella*, *Shigella*, and *Enterobacter*, among others, can grow under aerobic or anaerobic conditions, as they are able to use either O_2 as an electron acceptor during respiration, or ferment organic molecules under anaerobic conditions. Generally, this particular family is well studied because of their relevance in human disease and health (*E. coli* is an example bacterial type from this family), and are often found in soil/groundwater systems which have been contaminated by sewer outflow or introduced through the use of fertilizers. A common means of identifying the different strains of the family is by identifying the fermentation products produced under anaerobic conditions. Two basic fermentation patterns are recognized: *mixed-acid* and *butylene glycol* fermentations. In mixed-acid fermentations, lactic, acetic and succinic acids are produced, along with ethanol, CO_2 and H_2. With butylene glycol fermentation, smaller amounts of these acids are produced, with the main end products being butylene glycol, ethanol, and CO_2 and H_2. With the mixed-acid fermentation, equal amounts of H_2 and

CO_2 are formed, as they are produced only by the decomposition of formate, with the use of a formic hydrogenylase enzyme system:

$$HCOOH \rightarrow H_2 + CO_2 \qquad \text{(G-2)}.$$

With butylene glycol fermentations, CO_2 is produced in greater quantities than H_2, as the CO_2 is also produced directly from the reaction which forms the butylene glycol. As examples, *E. Coli* is a mixed-acid fermenter while the group *Enterobacter* are butylene glycol fermenters.

Some members of the genus *Clostridium* are known to produce butyric acid as a fermentation byproduct. Butyric acid is formed with the reduction of acetoacetyl-CoA by two molecules of $NADH + H^+$. The process also produces butanol, acetone, isopropanol, CO_2 and H_2.

2. Ferredoxins and the production of hydrogen and acetate in fermentation:

Hydrogen gas is used as a substrate by many terminal electron-accepting bacteria including Fe(III)-reducers, sulfate reducers and methanogens. Many of these bacterial types live symbiotically with H_2 producers (notably *Clostridium*). In the production of H_2 during fermentation, microbes employ *ferredoxins*, iron-sulfur proteins as electron carriers in a process known as the *phosphoroclastic reaction*. Interestingly, the ferredoxin couple has a redox potential nearly identical to that of the H_2/H^+ couple, allowing production of H_2 even in environments saturated with H_2 gas.

The ferredoxins are also employed as electron carriers in *acetogenic*, or acetate-producing bacteria. Acetogenic bacteria are considered important in anaerobic systems,

as much of the carbon flow goes through acetate. In addition to acetate formation, formate is often produced by the reaction of CO_2 and H_2, catalyzed by the enzyme formate dehydrogenase. With incubation studies of anaerobic bacteria isolated from deep aquifer systems, acetate, formate and H_2 are found to be the most abundant fermentation products and may be the predominant fermentation products in most anaerobic systems.

3. Methane production:

In methanogenic pathways, CO_2 or acetate serves as the terminal electron acceptor in this respirative process. Methanogenic bacteria must be in close proximity to fermentative bacteria (e.g., *Clostridia*), which supply both the substrate (usually H_2) and the electron acceptor (CO_2 or acetate). The pathways for methane production from CO_2 and acetate are complex, and not fully understood. Methanogenic organisms only exist at significant levels when there is an absence of other electron acceptors. However, in many subsurface environments which *do* lack a significant concentration of electron acceptors, methanogenesis is the predominant respirative process. It should be noted that methanogenic bacteria are obligate anaerobes and cannot survive in the presence of oxygen.

4. Sulfate reduction:

This process is mediated by anaerobic, organotrophic organisms that use organic acids, alcohols and H_2 as substrates. A common type is *Desulfovibrio*, an obligate

anaerobe which is known to exist in anaerobic pockets in aerobic environments. Their existence requires a symbiotic relationship with fermentative bacteria, in turn preventing a buildup of fermentation products in the environment. The most commonly used substrates are formate, acetate, lactate and H_2, with the lactate pathway best understood. The overall stoichiometry for the reduction of sulfate with the oxidation of lactic acid in shown in equation G-3:

$$2\ CH_3CHOHCOOH + SO_4^{2-} \rightarrow 2\ CH_3COOH + HS^- + H_2CO_3 + HCO_3^- \qquad \text{(G-3)}$$

Similarly, the reduction of thiosulfate and tetrathionate ion with H_2 as a substrate is described by the following equations.

$$S_2O_3^{2-} + 4\ H_2 \rightarrow 2\ HS^- + 3\ H_2O \qquad \text{(G-4)}$$

$$S_4O_6^{2-} + 9\ H_2 \rightarrow 2\ HS^- + 2\ H_2S + 6\ H_2O \qquad \text{(G-5)}$$

5. Fe(III)-reduction:

Geochemically, Fe(III)-reduction is one of the most important reactions in soils, although the particular pathway by which it occurs is one of the least well known. GS-15, a bacterial strain isolated by Lovely and Phillips in 1988, has been used to study one possible metabolic pathway, although it is still hypothetical. There are many bacteria which can reduce Fe(III), probably with different pathways. It is known that the GS-15 strain is able to transfer electrons *externally*, directly to the Fe(III) ions contained in Fe(III)-oxyhydroxides. Acetate is a common substrate in the process.

6. Nitrate reduction:

The process of nitrogen reduction has been studied in great detail and is an important part of the nitrogen cycle, which will not be described in detail here. Many nitrogen reducing bacteria are known, and in particular, *Pseudomonas* and *Bacillus* are the most abundant. They are known as *denitrifying* bacteria. They are also facultative anaerobes, and certain strains of *Pseudomonas* are also known to be Fe(III)-reducers. In *denitrification*, the nitrate is reduced to N_2O, or to N_2, as in the reaction

$$5 \text{ glucose} + 24\ NO_3^- + 24\ H^+ \rightarrow 30\ CO_2 + 12\ N_2 + 42\ H_2O \qquad \text{(G-6)}.$$

Denitrification, however, must be distinguished from the use of nitrate as an external electron acceptor in anaerobic environments, which is an example of *dissimilatory reduction*. In this process, nitrate is transformed to ammonium ion or nitrite, rather than N_2 in the pathway

$$2\ HNO_3 \xrightarrow[-2\ H_2O]{+4\ H} 2\ HNO_2 \rightarrow\ ? \rightarrow [2\ NH_2OH] \xrightarrow[-2\ H_2O]{+6H} 2\ NH_4^+ \qquad \text{(G-7)}.$$

Here, the "?" implies an unknown intermediate. This process tends to occur in only very reducing environments, and its importance in soils is not well defined. Some bacteria can only reduce nitrate as far as nitrite, as in the reaction

$$\text{glucose} + 12\ NO_3^- \rightarrow 6\ CO_2 + 6\ H_2O + 12\ NO_2^- \qquad \text{(G-8)}$$

because they lack the enzyme *nitrite reductase*. Nitrite itself is very reactive and can be transformed abiotically to nitrogen gas under aerobic and anaerobic conditions. Interestingly, *nitrite reductase* can be inhibited in soils with the use of acetylene gas.

The enzyme which catalyzes the reaction of nitrate to nitrite, on the other hand, tends to be inhibited by oxygen gas.

Factors affecting bacterial growth:

1) Temperature: most bacteria grow in a range of 10 - 40 °C (*mesophiles)* although rates often increase with temperature.

2) Water: water is important both in terms of its availability to organisms and its affect on diffusion of O_2. In very waterlogged soils, the rate of diffusion of O_2 is much less than

that in air which limits O_2 delivery to aerobic organisms. Similarly, water availability is important for cellular function.

- clayey soils have higher surface areas and tend to adsorb more water, making water less available to organisms. This is one reason that microbes are normally less active in clayey soils compared to sandy soils.

3) Oxygen: dependent on metabolism of organism (aerobic vs. anaerobic). Less available in waterlogged soils. Anaerobic pockets can still exist in highly aerobic soils (and vica versa).

4) pH: can range as much as 4.0 - 9.0

5) Osmotic pressure: important to keep range of total dissolved solids (TDS) in a study sample (e.g., bioreactor sample) similar to that of natural environment.

6) Nutrients:

a) carbon sources

- necessary for *anabolic* metabolism (e.g., building of cell walls)

- usually supplied to growth media as glucose, lactose or organic acids (acetate and formate are *non-fermentable substrates*)

b) nitrogen - needed for protein and nucleic-acid synthesis

- usually supplied as ammonia, nitrate or amino acids

c) phosphorus - needed for synthesis of nucleic acids and ATP

- supplied as potassium salt (e.g., K_2HPO_4)

d) inorganic nutrients

- K: many enzymes specifically activated by potassium

- Mg: used for enzyme activation, production and activity of ribosomes, nucleic acids and cell membranes

- Ca: used for functions of cell walls

- Fe: needed for electron transport

- also Cu, Zn, Co, Mn, and Mo

References

1. Brock, Thomas D.; et al, *Biology of Microorganisms, Seventh Edition*; Prentice Hall: Englewood Cliffs, New Jersey, 1994.

2. Chapelle, Francis H., *Groundwater Microbiology and Geochemistry;* John Wiley & Sons, Inc., 1993.

3. Paul, E. A.; Clark, F. E., *Soil Microbiology and Biochemistry*, Academic Press, Inc.: 1989.

Appendix H

Calculation of E_H for S^0/S^{2-} Couple Based on Total Sulfide Measurements

The S^0/S^{2-} half-reaction

$$S^0(s) + 2e^- \rightleftharpoons S^{2-}(aq) \quad \text{(H-1)}$$

at pH 7 and 25 °C, has a redox potential (V) based on the Nernst equation and a formal potential involving the rhombic form for elemental sulfur which in solution may exist as polysulfide ions such S_4^{2-} (1)

$$E_{S/S2-} = -0.475 - 0.0295 \log [S^{2-}] \quad \text{(H-2)}$$

The total (aqueous) concentration of sulfide is related to its aqueous components $S^{2-}(aq)$, $HS^-(aq)$, and $H_2S(aq)$ by a mass balance:

$$[S(-II)_{(tot)}] = [S^{2-}] + [HS^-] + [H_2S] \quad \text{(H-3)}$$

where the (aq) designation is eliminated for convenience. The speciation of each component is further related to pH by the pK_a values of H_2S and HS^-, 7.1 and 14, respectively (2). The relevant equations are as follows

$$H_2S \rightleftharpoons H^+ + HS^- \quad \text{(H-4)}$$

$$\frac{[H^+][HS^-]}{[H_2S]} = 10^{-7.1} \quad \text{(H-5)}$$

$$HS^- \rightleftharpoons H^+ + S^{2-} \quad \text{(H-6)}$$

$$\frac{[H^+][S^{2-}]}{[HS^-]} = 10^{-14} \quad \text{(H-7)}$$

Solving Eq. H-5 for [H_2S] and Eq. H-7 for [HS^-], substituting the results into Eq. H-3, and solving for [S^{2-}] yields

$$[S^{2-}] = \frac{[S(-II)_{(tot)}]}{1 + \frac{[H^+]}{10^{-14}} + \frac{[H^+]^2}{(10^{-7.1})(10^{-14})}} \qquad \text{(H-8)}$$

Combining Eq. H-8 and Eq. H-2 yields

$$E_{S/S^{2-}} = -0.475 - 0.0295 \log \left[\frac{[S(-II)_{(tot)}]}{1 + \frac{[H^+]}{10^{-14}} + \frac{[H^+]^2}{(10^{-7.1})(10^{-14})}} \right] \qquad \text{(H-9)}$$

For [$S(-II)_{(tot)}$] concentrations of 1, 10 and 100 μM, and at pH 7, application of Eq. H-9 yields potentials of -81, -111, and -140 mV, respectively.

References

1. Berner, Robert A., *Geochim. Comochim. Acta*, **1962**, *27*, 563-575

2. Snoeyink, Vernon L.; Jenkins, David, *Water Chemistry*; John Wiley & Sons, Inc., 1980.

Appendix I

Determination of $E_7^{0'}$ of Free and Immobilized Redox Indicators by Titration with Titanium(III) Citrate

Lemmon (1, 2) devised a scheme to determine the formal potential at pH 7 ($E_7^{0'}$) of both free and immobilized redox indicators with a concurrent titration of the immobilized form of indicator and the free indicator in contact with a Pt electrode. The free indicator poises the Pt electrode while the absorbances of both the free and immobilized forms of the indicator are monitored. In this way, the Pt electrode potential can be measured while the both the free and immobilized indicator are reduced.

For this procedure, the indicator immobilized on agarose affinity beads was packed into the 1-mm pathlength spectrophotometer flow cell (Hellma, 170.700-QS, Figure 4.2 in Chapter 4) and placed in the external loop of the reactor system (Figure 4.1 in Chapter 4). A second, 1-cm pathlength flow cell (Helma, 176.730-QS) for measuring the absorbance of the free indicator was also placed in the external loop. An HP8452A diode array spectrophotometer was used to make absorbance measurements of the indicators. A conceptual diagram of this design is shown in Figure I.1.

A solution of the free (unbound) indicator, phosphate buffer and DI water was added to the reactor system for a final indicator concentration of 5 - 10 μM (an absorbance in the 1-cm path length flow cell of about 0.3 - 0.4 A.U. at λ_{max}), adjusted to pH 7, and deaerated with N_2. Initial absorbance measurements of the free and immobilized indicator were made (it was estimated that the absorbance of the free indicator in the 1-mm pathlength cell accounted for less than 2% of the total absorbance

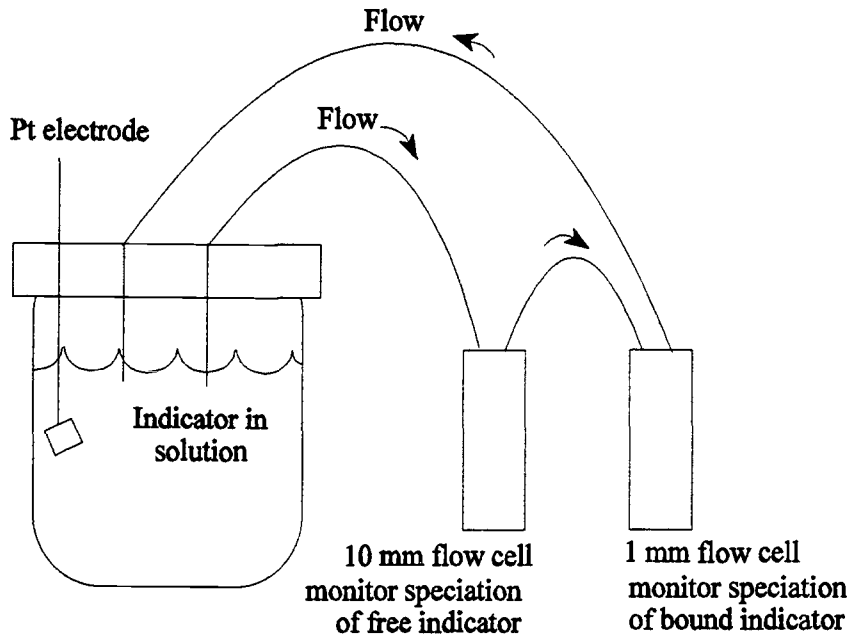

Figure I Conceptual diagram of approach used to determine the formal potentials of indicators immobilized on agarose affinity beads.

so it was neglected). The solution was then titrated with a solution of ~240 mM Ti(III) citrate (with 10-μL (2.4 μmol) injections, ~20% of the indicator was reduced with each addition). Sufficient time was then allowed for the system to equilibrate at which point absorption spectra of the two indicators were taken in succession. The Pt electrode potential and pH were monitored throughout the experiment.

The ~240 mM Ti(III) citrate solution was prepared with a procedure described by Bos (3) which is summarized here:

1) About 4 g of TRIZMA® hydrochloride (Sigma) and 7.4 g of sodium citrate dihydrate (Mallinkrodt) were added to 20 mL of DI water in a 100-mL beaker. The beaker was covered with paraffin and purged with N_2 continually.

2) Approximately 15 mL of $TiCl_3$ (13% w/w in ~20% hydrochloric acid, Fluka) were then added to a beaker which was then placed in an ice bath. The solution was adjusted to pH 7 by addition of NaOH with continuous purging and stirring.

3) The solution was transferred to a 50-mL volumetric flask and brought to volume with DI water. The solution was divided into two parts and the two portions were placed in two 50-mL I-Chem bottles (septum capped). The bottles were then purged with N_2 and stored in the freezer for later use.

The redox potential for a redox indicator, E_{ind}, is given by the Nernst equation

$$E_{ind} = E_{ind}^{0'} - \frac{RT}{nF} \ln \left(\frac{[Ind_{red}]}{[Ind_{ox}]}\right) \qquad \text{(I-1)}$$

where $E_{ind}^{0'}$ is the formal potential of the redox indicator and $[Ind_{red}]$ and $[Ind_{ox}]$ are the concentrations (activities) of the reduced and oxidized forms of the indicator, respectively. Because the free indicator poises the Pt electrode, the Pt electrode potential, E_{Pt}, is a measure of E_{ind}.

The relative concentrations of the reduced and oxidized forms of the redox indicator were measured spectrophotometrically. The fraction of free or immobilized indicator oxidized (f_{ox}) was calculated from the measured absorbance values with equation I-2 for each point in the titration

$$f_{ox} = \frac{A - A_{min}}{A_{max} - A_{min}} \qquad \text{(I-2)}$$

where A is the measured absorbance of the indicator, A_{min} is the absorbance of the indicator at complete reduction, and A_{max} is the absorbance of the indicator when fully oxidized. Normally the absorbance is measured at the wavelength of maximum

absorption of the visible band and is corrected for baseline shifts by subtracting the absorbance at an unabsorbed wavelength (typically 798 nm).

Substitution of $(1 - f_{ox})/f_{ox}$ for $[Ind_{red}]/[Ind_{ox}]$ in equation I-1 yields equation I-3,

$$E_{ind} = E_7^{0'} - \frac{RT}{nF} \ln \left(\frac{1 - f_{ox}}{f_{ox}}\right) \qquad \text{(I-3)}$$

The formal potential at pH 7 ($E_7^{0'}$) was calculated for the free and the immobilized form of indicator for each data point. The results were then averaged to obtain values for $E_7^{0'}$ and $E_{7\,(imm)}^{0'}$. In this thesis, the formal potentials (at pH 7) of the free and immobilized indicators (agarose affinity bead) toluidine blue O (TB), cresyl violet (CV) (4), azure A (AA), and azure C (AC) (5) were obtained in the manner developed by Lemmon (1, 2).

For agarose thin film-immobilized indicators and indicators immobilized on Whatman cellulose filter paper type 540, the formal potentials were obtained in much the same manner except that the thin-film immobilized indicators were placed (separately) in two specially designed flow cells (pathlength 3 mm, Figure 6.8 in Chapter 6) for titration (3). A S2000 fiber optic spectrometer (Ocean Optics, Inc.) was used to monitor the absorption spectrum of the indicators immobilized on the filter papers. For the agarose thin films, DI water was used as the reference while the plain filter paper was used as the reference for the indicators immobilized on the filter paper.

Unlike the titrations of the indicators immobilized on the affinity beads (which were packed into a 1-mm pathlength flow cell), the absorbance of the free indicator could not be neglected. To account for this, the baseline corrected absorbance (vs the background absorbance at 798 nm) of the free indicator in the 1-cm pathlength flow cell

was then subtracted (after multiplying by 0.3 to account for the change in pathlength) from the baseline corrected absorbance of the immobilized indicator.

Formal potentials at pH 7 for the thin film-immobilized indicators were calculated in two ways: 1) directly from the measured E_{Pt} values as outlined above and 2) by calculation of E_{ind} from the measured f_{ox} of the *free* indicator and its previously determined formal potential. In the latter case, the *calculated* E_{ind} (based on the f_{ox} of the free indicator) was substituted into eq. I-3 (rather than E_{Pt}) with f_{ox} data for the immobilized indicator and $E_7^{0\prime}{}_{(imm)}$ (the formal potential at pH 7 of the immobilized indicator) was calculated from this.

The formal potentials of all the free indicators had been determined previously (5) by titrations with Ti(III) citrate, with or without the concurrent titration of the agarose affinity bead-immobilized indicator. In general, the formal potentials for the agarose thin film-immobilized and cellulose-immobilized indicators calculated with methods 1) and 2) differed by 5 - 10 mV and were averaged to obtain the measured potential. These results are given in Table 6.3 (3).

Formal potentials for several redox indicators in solution that had not been characterized by Lemmon (1, 2) were determined by the above procedures (sometimes without immobilized redox indicator). Also, in some cases, Fe(II) was used as the titrant rather than Ti(III) (the procedure for titration with Fe(II) was the same as for titration with Ti(III)). These formal potentials are summarized in Table I.1.

Table I Formal potentials of redox indicators by titration with Ti(III) citrate or Fe(II).

redox indicator	$E_7^{0'}$(mV) free indicator[a] (titrant, Ti(III))	$E_7^{0'}$(mV) immobilized indicator[a,b] (titrant, Ti(III))	$E_7^{0'}$(mV) free indicator (titrant, Fe(II))
Thi	+66[c]	+52[c]	+87, +68, +52[d]
AC	+38	+31	ND[e]
TB	+32	+36	+55, +32, +18[d]
AA	+18	+13	ND
CV	-75	-81	-91, -108[f]

[a] Measured at pH 7 only.
[b] For agarose affinity bead immobilized indicator.
[c] From Lemmon (1, 2).
[d] Measured at pH values of 6.3, 7.0 and 7.5, respectively.
[e] ND = not determined in this work.
[f] Measured at pH values of 7.0 and 8.0, respectively.

References

1. Lemmon, T. L.; Westall, J. C.; Ingle, J. D., Jr. *Anal. Chem.*, **1996**, *68*, 947-953.

2. Lemmon, Teresa, *Development of Chemostats and Use of Redox Indicators for Studying Transformations in Biogeochemical Matrices,* **1995,** Ph.D. Thesis, Oregon State University.

3. Bos, Mark, *Part I: Development and Application of an Arsenic Speciation Technique Using Ion-Exchange Solid Phase Extraction Coupled with GFAAS, Part II: Investigation of Zinc Amalgam as a Reductant,* **1996**, M.S. Thesis, Oregon State University.

4. Jones, Brian; Chapter 4 of this thesis.

5. Jones, Brian, Laboratory notebook #2, 1995, Oregon State University.

Appendix J

Effect of Indicator Concentration on Reduction of Thionine by Fe(II)

The Fe(II) concentration required to reduce a given fraction of indicator is predicted not to depend on the total indicator concentration as shown in equation J-1.

$$\log\frac{(1-f_{ox})}{(f_{ox})} = \frac{2}{0.059}\,(E^{0'}_{ind,7} - E^{0'}_{Fe(OH)3/Fe(II)}) + \log\,[Fe(II)]^2 \qquad \text{(J-1)}$$

This equation is based on the equilibrium model discussed in Appendix F (eq. F-6) for the reaction of the indicator and $Fe(III)(OH)_3$/Fe(II) couples.

However, experimental results show that the Fe(II) concentration required to reduce a given fraction of free thionine *increased* with the total concentration of indicator. Previously (1), when 20 μM of free Thi were titrated with Fe(II) at pH 7, no Fe(II) could be measured in solution until all the Thi was reduced (data shown in Figure 4.6A). However, when the experiment was repeated with twice the concentration of total free Thi, Fe(II) levels were clearly measurable after the second addition as shown in Figure J-1.

There are several possible explanations for this behavior. It may be that the true pH was somewhat lower than the measured pH of 7. In previous experiments (1), the measured [Fe(II)] was about 200 μM at $f_{ox} = 0.5$ for titrations of 20 μM Thi at pH 6.3 (Table for 4.4)). The simple model may not apply because the formal potential of one or both of the couples changes with the total indicator concentration. The titration curve in Figure J-1 is similar to the titration curve for 20 μM TB which has a formal potential ~30 mV below Thi. The value of E_{Pt} at half reduction was 66 and 63 with 20 and 40 μM Thi,

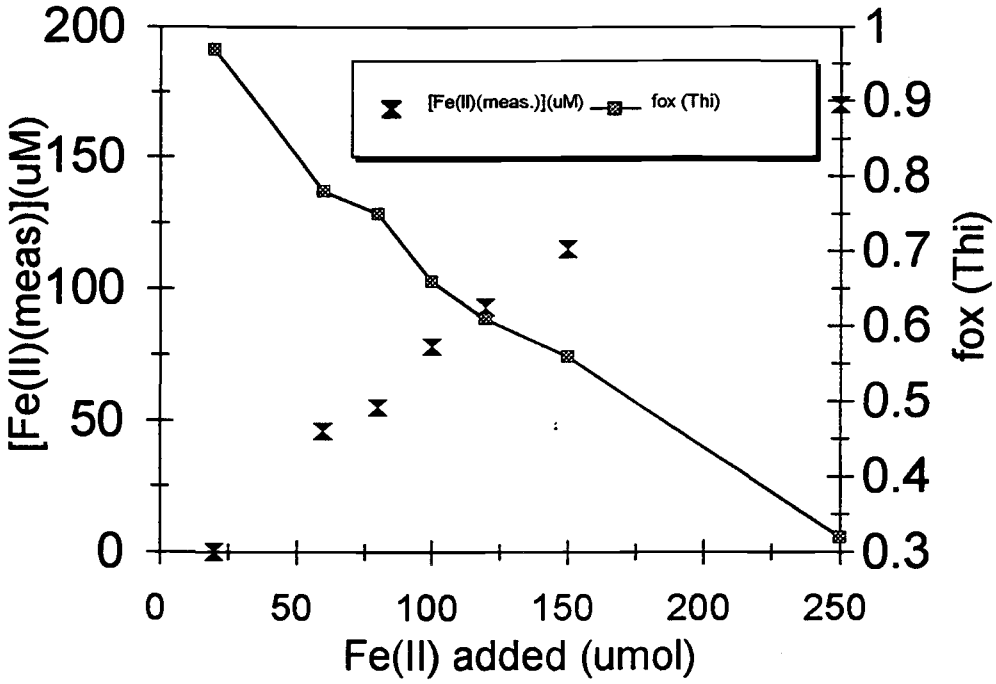

Figure J Titration data of 40 μM free Thi with Fe(II) at pH 7. The solution contained ~50 mM TRIZMA buffer and ~50 mM KCl.

respectively. Finally, the formal potential of the Fe couple may be affected by the adsorption of Fe(II) on the surface of Fe(III) hydroxides and the total amount of Fe(III) hydroxide which increases with indicator concentration (i.e., Thi may be reduced by Fe(II) in solution and sorbed Fe(II)).

In studies of titrations of different concentrations of TB *immobilized* on agarose beads (1), it was also found that the Fe(II) level required to reduce a given fraction of TB increased with the concentration of immobilized TB. These results are discussed in Chapter 4 (1).

References

1. Jones, Brian; Chapter 4 of this thesis.

Appendix K

Coexistence of Fe(II) and S(-II) at pH 7

To determine if Fe(II) could coexist with sulfide in solution for a significant length of time (~day) at typical environmental levels, Fe(II) and S(-II) were mixed in the bioreactor and then monitored. Samples were periodically drawn for determination of Fe(II) with the OP method (Appendix B) and sulfide with the methylene blue method (1). Specifically, 2 mL of a 0.1 M Fe(II) standard (200 μmol) were added to 1 L of de-aerated reactor solution (DI water with 0.05 M KCl) at pH 7 (not buffered, but adjusted with pH stat system). After Fe(II) levels stabilized overnight, ~50 mg of $Na_2S•6H_2O(s)$ (~200 μmol) were added to the reactor solution. Samples were taken intermittently for the determination of Fe(II) and sulfide over the course of about 24 hr.

The results of this experiment are shown in Figure K.1. The calculated (total) sulfide concentration was based on the measured Fe(II) level and the K_{sp} value for FeS of 6×10^{-18} (at 25°C) (2). Upon addition of the sulfide (at 20 hr), ~60 μmol of Fe(II) precipitated. The sulfide level rose to ~35 μM over time. By mass balance, the sulfide concentration should have been 140 μM. Residual O_2 in the reactor may have oxidized some of either species or the initial amounts of the species added many be less than specified due to prior oxidation. Clearly, Fe(II) and S(-II) can coexist at relatively high levels (both species at concentrations greater than 30 μM) for well over a day. Moreover, the calculated equilibrium concentrations of total sulfide are far below (< 1 μM) the measured values. These results suggest that Fe(II) and sulfide may coexist in ground water and other natural systems.

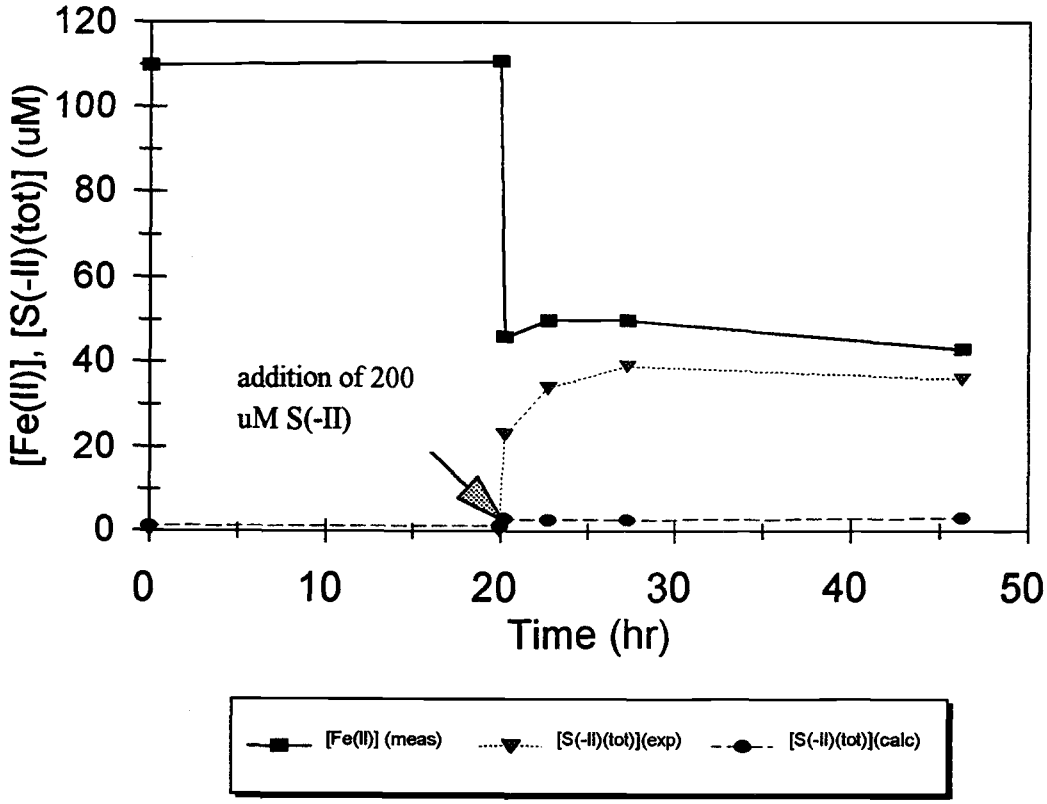

Figure K Time dependence of concentrations of Fe(II) and S(-II) in a deaerated electrolyte in the bioreactor at pH 7. Samples were taken to determine [Fe(II)] after the initial addition of Fe(II) at 0 hr and right before the addition of S(-II) at 20 hr.

References:

1. CHEMetrics, *Product Catalog*, 1997-1998.

2. Ebbing, Darrel D., *General Chemistry*, Houghton Mifflin Company, 1996.